

N 69 39672 49

NASA CR-54572

AUGUST 1969

Allison EDR 5944



Single-Stage Experimental Evaluation of Boundary Layer Bleed Techniques for High Lift Stator Blades

**IV—Data and Performance of
Triple-Slotted 0.75 Hub Diffusion Factor Stator**

CASE FILE COPY

Prepared for

NATIONAL AERONAUTICS AND SPACE ADMINISTRATION

Contract NAS3-7900

Allison Division • General Motors

Indianapolis, Indiana

NOTICE

This report was prepared as an account of Government sponsored work. Neither the United States, nor the National Aeronautics and Space Administration (NASA), nor any person acting on behalf of NASA:

- A. Makes any warranty or representation, expressed or implied, with respect to the accuracy, completeness, or usefulness of the information contained in this report, or that the use of any information, apparatus, method, or process disclosed in this report may not infringe privately owned rights; or
- B. Assumes any liabilities with respect to the use of, or for damages resulting from the use of any information, apparatus, method or process disclosed in this report.

As used above, "person acting on behalf of NASA" includes any employee or contractor of NASA, or employee of such contractor, to the extent that such employee or contractor of NASA, or employee of such contractor prepares, disseminates, or provides access to, any information pursuant to his employment or contract with NASA, or his employment with such contractor.

Requests for copies of this report should be referred to

National Aeronautics and Space Administration
Scientific and Technical Information Facility
P. O. Box 33
College Park, Maryland 20740

NASA CR-54572
AUGUST 1969
Allison EDR 5944



Single-Stage Experimental Evaluation of Boundary Layer Bleed Techniques for High Lift Stator Blades

**IV—Data and Performance of
Triple-Slotted 0.75 Hub Diffusion Factor Stator**

by

R. A. Horn, Jr., G. Seren, and R. H. Carmody

Prepared for

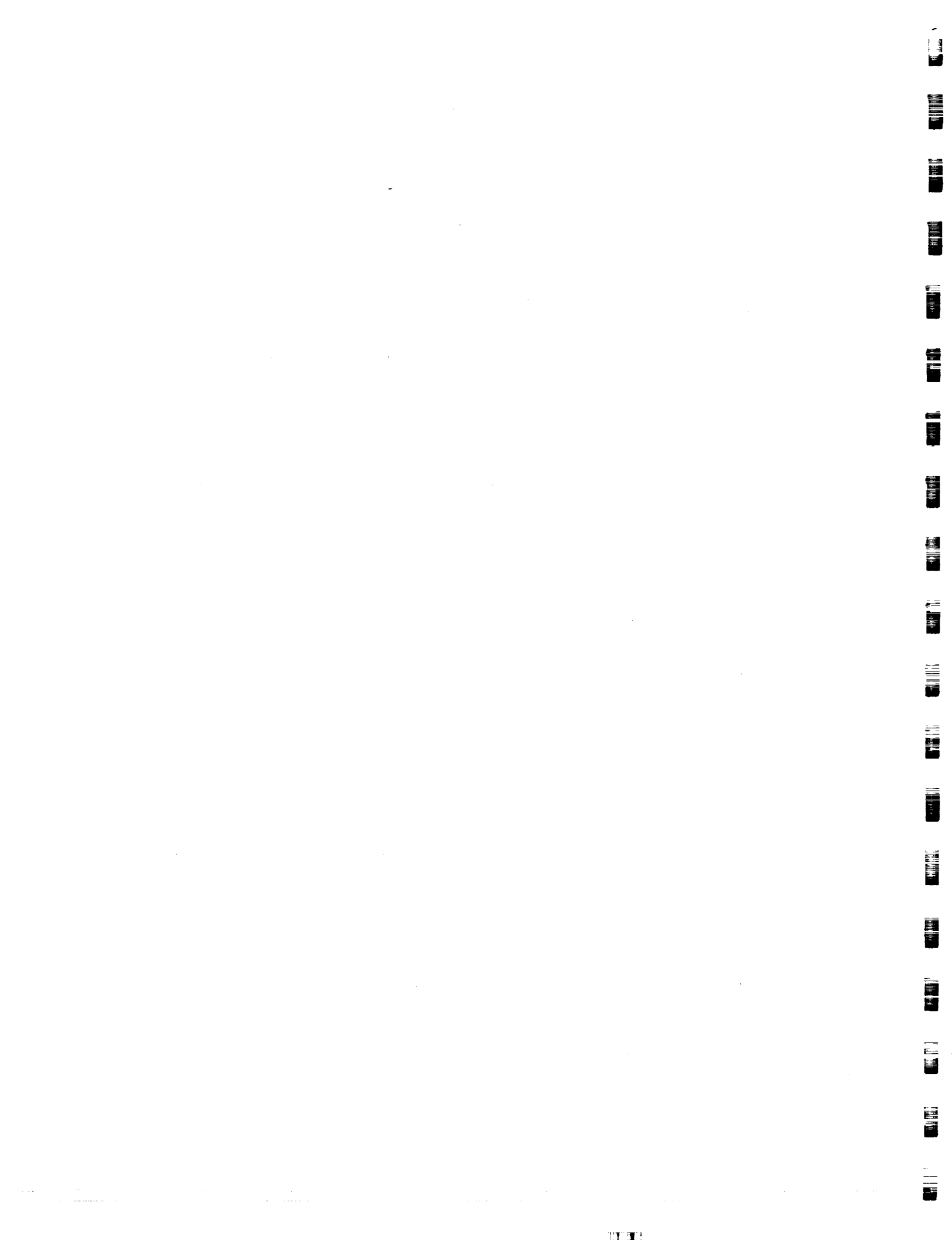
NATIONAL AERONAUTICS AND SPACE ADMINISTRATION

Contract NAS3-7900

Technical Management
NASA-Lewis Research Center
Cleveland, Ohio

Lewis Project Manager: William L. Beede
Lewis Research Advisor: L. Joseph Herrig

Allison Division • General Motors
Indianapolis, Indiana



ABSTRACT

The test described in this report is part of an overall program to establish experimentally the extent to which it is feasible to increase compressor stator loading and stall-free flow margin by employing suction surface boundary layer bleed techniques. A secondary objective was to obtain blade element data for design use.

In this test, overall and blade element performance of a row of triple-slotted 0.75 hub diffusion factor stators with boundary layer bleed was measured. In addition, vane static pressure distributions were obtained at three radial locations. Overall and blade element performance was also obtained for the rotor, at varying rates of vane bleed flow, and compared with data previously obtained for this rotor without stator vanes. Preliminary discussion of test results and correlations of data are presented.



TABLE OF CONTENTS

	<u>Page</u>
Summary	1
Introduction	3
Symbols	4
Apparatus and Procedures	6
Test Facility	6
Compressor Test Rig	7
Blading	7
Instrumentation	8
Determination of Annulus Wall Bleed Flow for Stator Vane Tests	9
Hysteresis Test with Triple-Slotted 0.75 Hub Diffusion Factor Stator	10
Overall and Blade Element Performance Data	10
Data Reduction	10
Presentation of Results	12
Overall Performance of Flow Generation Rotor and Stage	12
Blade Element Performance	12
Discussion of Results	14
Overall Performance	14
Flow Generation Rotor	14
Triple-Slotted Stator Stage	15
Annulus Wall Bleed for Stator Test	15
Hysteresis and Rotating Stall Results—Triple-Slotted Stator Stage	16
Blade Element Performance	17
Rotor	17
Stator	18
Stator Static Pressure Distributions	20
Stator Slot Bleed Flow	20
Concluding Remarks	21
References	21
Appendix—Performance Equations	23

LIST OF ILLUSTRATIONS

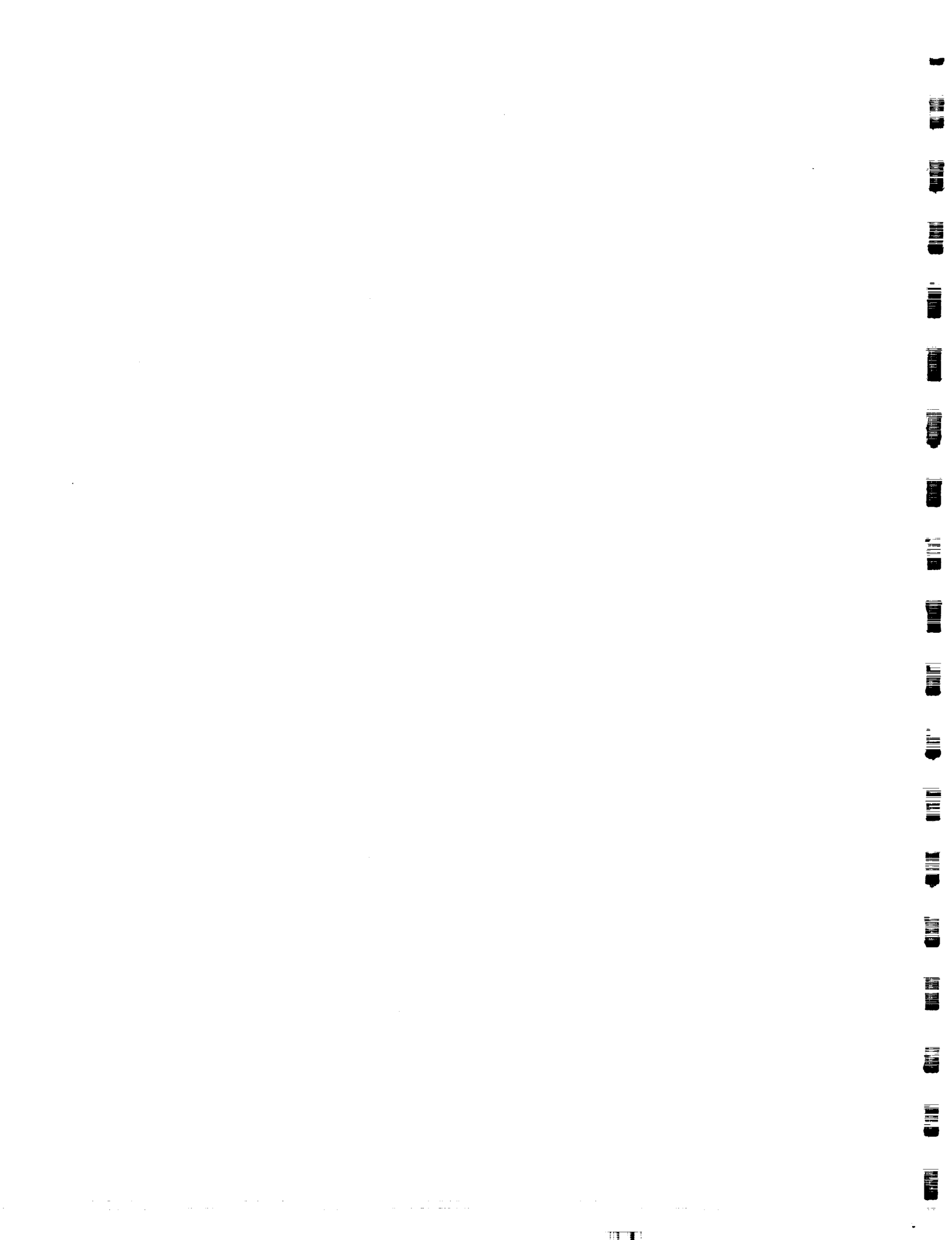
<u>Figure</u>	<u>Title</u>	<u>Page</u>
1	Compressor test facility	27
2	Layout of compressor test rig	27
3	Triple-slotted 0.75 hub diffusion factor stator slot configuration	28
4	Test rig compressor flow path	29
5	Circumferential location of instrumentation viewed downstream	30
6	Radial location of streamlines for instrumentation positions	31
7	Schematics of survey instrumentation	32
8	Triple-slotted stator vane static pressure tap locations at 10, 50, and 90% streamlines	34
9	Flow generation rotor overall performance in stage test with the vane bleed flow at the optimum rate—pressure ratio	35
10	Flow generation rotor overall performance in stage test with the mean vane bleed flow rate—pressure ratio	36
11	Flow generation rotor overall performance in stage test with zero vane bleed flow rate—pressure ratio	37
12	Flow generation rotor overall performance in stage test with the vane bleed flow at the optimum rate—adiabatic efficiency	38
13	Flow generation rotor overall performance in stage test with the mean vane bleed flow rate—adiabatic efficiency	39
14	Flow generation rotor overall performance in stage test with zero vane bleed flow rate—adiabatic efficiency	40
15	Overall stage performance of triple-slotted stator with the vane bleed flow at the optimum rate—pressure ratio	41
16	Overall stage performance of triple-slotted stator with the mean vane bleed flow rate—pressure ratio	42
17	Overall stage performance of triple-slotted stator with zero vane bleed flow rate—pressure ratio	43
18	Overall stage performance of triple-slotted stator with the vane bleed flow at the optimum rate—adiabatic efficiency	44
19	Overall stage performance of triple-slotted stator with the mean vane bleed flow rate—adiabatic efficiency	45
20	Overall stage performance of triple-slotted stator with zero vane bleed flow rate—adiabatic efficiency	46
21	Rotor blade element performance for stage test with the vane bleed flow at the optimum rate	47
22	Rotor blade element performance for stage test with the mean vane bleed flow rate	52

<u>Figure</u>	<u>Title</u>	<u>Page</u>
23	Rotor blade element performance for stage test with zero vane bleed flow rate	57
24	Radial variation of rotor blade element performance with the vane bleed flow at the optimum rate	62
25	Radial variation of rotor blade element performance with the mean vane bleed flow rate	63
26	Radial variation of rotor blade element performance with zero vane bleed flow rate	64
27	Rotor out radial mass flux distribution at design speed with the vane bleed flow at the optimum rate	65
28	Rotor out radial mass flux distribution at design speed with the mean vane bleed flow rate	66
29	Rotor out radial mass flux distribution at design speed with zero vane bleed flow rate	67
30	Rotor loss parameter versus diffusion factor with the vane bleed flow at the optimum rate	68
31	Rotor loss parameter versus diffusion factor with the mean vane bleed flow rate.	69
32	Rotor loss parameter versus diffusion factor with zero vane bleed flow rate	70
33	Triple-slotted stator blade element performance with the vane bleed flow at the optimum rate	71
34	Triple-slotted stator blade element performance with the mean vane bleed flow rate	76
35	Triple-slotted stator blade element performance with zero vane bleed flow rate	81
36	Variation of wall bleed flow with stage pressure ratio and vane bleed flow at the optimum rate	86
37	Variation of wall bleed flow with stage pressure ratio and mean vane bleed flow rate	87
38	Variation of wall bleed flow with stage pressure ratio and zero vane bleed flow rate	88
39	Variation of vane bleed flow at optimum bleed rate with stage pressure ratio	89
40	Variation of vane bleed flow at the mean vane bleed flow rate with stage pressure ratio	90
41	Radial variation of triple-slotted 0.75 D _f stator blade element performance with the vane bleed flow at the optimum rate	91
42	Radial variation of triple-slotted 0.75 D _f stator blade element performance with the mean vane bleed flow rate	92
43	Radial variation of triple-slotted 0.75 D _f stator blade element performance with zero vane bleed flow rate. .	93

<u>Figure</u>	<u>Title</u>	<u>Page</u>
44	Stator loss parameter versus diffusion factor with the vane bleed flow at the optimum rate	94
45	Stator loss parameter versus diffusion factor with the mean vane bleed flow rate.	95
46	Stator loss parameter versus diffusion factor with zero vane bleed flow rate.	96
47	Triple-slotted stator static pressure distribution at 60% speed and vane bleed flow at the optimum rate.	97
48	Triple-slotted stator static pressure distribution at 60% speed and mean vane bleed flow rate	102
49	Triple-slotted stator static pressure distribution at 80% speed and vane bleed flow at the optimum rate.	106
50	Triple-slotted stator static pressure distribution at 80% speed and mean vane bleed flow rate	111
51	Triple-slotted stator static pressure distribution at 90% speed and vane bleed flow at the optimum rate.	115
52	Triple-slotted stator static pressure distribution at 100% speed and vane bleed flow at the optimum rate.	120
53	Triple-slotted stator static pressure distribution at 100% speed and mean vane bleed flow rate	125
54	Triple-slotted stator static pressure distribution at 100% speed and zero vane bleed flow rate	129
55	Triple-slotted stator static pressure distribution at 110% speed and vane bleed flow at the optimum rate.	133
56	Triple-slotted stator wake surveys with the vane bleed flow at the optimum rate	138
57	Triple-slotted stator wake surveys with the mean vane bleed flow rate	143
58	Triple-slotted stator wake surveys with zero vane bleed flow rate	146
59	Variation of stator wake at 10, 50, and 90% streamlines from tip during wall bleed optimization	148

LIST OF TABLES

<u>Table</u>	<u>Title</u>	<u>Page</u>
I	Blade and vane geometry summary	149
II	Rotor incidence at minimum and maximum flow for flow generation rotor and triple-slotted stator stage tests for all three vane bleed flow rates	150
III	Rotating stall results for triple-slotted stator stage test.	151
IV	Blade element performance—triple-slotted stator stage with the vane bleed flow at the optimum rate.	152
V	Blade element performance—triple-slotted stator stage with the mean vane bleed flow rate	176
VI	Blade element performance—triple-slotted stator stage with zero vane bleed flow rate	188



SINGLE-STAGE EXPERIMENTAL EVALUATION OF BOUNDARY LAYER BLEED TECHNIQUES FOR HIGH LIFT STATOR BLADES

IV. DATA AND PERFORMANCE OF TRIPLE-SLOTTED 0.75 HUB DIFFUSION FACTOR STATOR

By

R. A. Horn, Jr., G. Seren, and R. H. Carmody

Allison Division, GM

SUMMARY

To establish the feasibility of increasing compressor stator loading and stall-free flow margin by using a boundary layer bleed technique and determining the extent to which such techniques may be employed, an investigation was made of a single-stage compressor provided with a triple-slotted stator row. The stator was designed with NACA 65-series airfoils and a hub diffusion factor of 0.75. The flow into the stator was generated by a flow generation rotor with prewhirl established by a row of inlet guide vanes.

The triple-bleed slots are designed to keep the suction surface boundary layer attached to a point further downstream of the separation point than would occur under normal conditions. Based on the mid-span suction surface static pressure measurements of an unslotted 0.75 D_f stator as reported in Reference 1, bleed slots were located at the 25, 41, and 61% chord locations. The decision to locate the first bleed slot at the 25% chord position was influenced by experimental surface pressure coefficients which indicated a possible increase in stalling angle of attack. The orientation of the suction slots is 45 degrees to the tangent of the suction surface. To ensure a bleed flow that would prevent separation at the selected slot locations and also remain sensitive to the core total pressure, the slot width was selected as 0.009 in.

Three different bleed rates were applied on the stator. These were classified as the optimum bleed rate, mean bleed rate, and zero bleed rate. The optimum bleed rate is defined as that which analytically removes 1/3 of the local boundary layer thickness at each slot location (Reference 6). To minimize secondary flows and keep the stator end wall boundary layer attached, annulus

wall bleeding from a point upstream of to a point downstream of the stator was employed during all stage tests. The use of wall bleeds aided in the control of the boundary layer flow and had greater influence on the flow at the hub than at the tip.

Surface static pressure distributions and wake surveys were obtained for the triple-slotted stator. The suction surface static pressure distributions do not provide conclusive evidence as to the effectiveness of this bleed technique for controlling separation. A hysteresis test with the acquisition of rotating stall characteristics was also obtained at 60% corrected speed for the triple-slotted stator test. A hysteresis effect was indicated in terms of pressure ratio and flow rate, while recovering from stall. Onset of stall was found to be abrupt at all speeds and bleed flow rates. Stall cells first appeared in the hub region.

The triple-slotted 0.75 hub diffusion factor stator performance was satisfactory at optimum bleed flow rates although design flow turning requirements were exceeded, particularly at the hub. High total pressure losses were encountered at all streamline measuring stations with all the vane bleed rates. The losses tended to increase in the inner half of the blade with decreased vane bleed, whereas the losses were essentially independent of vane bleed in the outer half of the blade. The deviation angle was lower than design at all test conditions; the largest difference from design being at the 10 and 90% streamline positions. Blade element performance loss correlations for these stators provided a fairly good extension to the existing NACA correlations of Reference 2.

The suction surface static pressure distributions indicate that the boundary layer separation was partially attenuated by the influence of suction slots at higher speeds. The data from the pressure distribution plots are inconclusive at lower speeds. The values obtained for the losses also indicate that no extensive flow separation occurred.

INTRODUCTION

Advanced airbreathing propulsion systems require lightweight compact compressors capable of high levels of performance. These compressors should have a broad range of operation and a large stall margin. High reliability and relative insensitivity to inlet flow distortion are generally required of all compressors. In meeting the more demanding compressor design requirements, compromises must be made that are strongly dependent on the particular application. New applications are steadily increasing the range of requirements which the compressor must meet.

Compressor technology has been advanced continuously by extending, among other parameters, the usable rotational speeds; increasing stage loadings or diffusion factors; and reducing stage length through the use of high blade aspect ratios. Whereas further advancements can be made through optimizations and improved combinations of the aforementioned parameters, severe aerodynamic limitations such as increasing losses and decreasing stall margin are being encountered. Significant advancements in compressor technology require the application of advanced concepts in terms of improved blading for high relative Mach numbers and application of high lift devices to extend the stall-free flow range for compressor rotors and stators. Advanced concepts in these areas may result in sizable reductions in the number of compressor stages and improvements in compressor performance.

On airfoils designed to provide high lift, blade surface pressure gradients become steeper as the angle of attack is increased. As a result, the suction surface boundary layer separates and high total pressure losses and a decrease in stall-free flow margin result. To some extent, however, separation of the suction surface boundary layer can be delayed by utilizing boundary layer control. Boundary layer blowing was studied and reported in References 1, 3, and 4. Simple slots were studied in Reference 5. Another approach to boundary layer control is the application of boundary layer bleed. In view of these considerations, an experimental single-stage compressor rig was designed and constructed to test highly loaded stators using suction surface bleed concepts to reduce losses and to improve stall-free flow margin.

The objectives of this program are to establish experimentally the feasibility of increasing blade loading and stall-free flow margin by boundary layer bleeding and to determine the extent to which it may be employed. A secondary objective is to obtain blade element data for design use. The stator designs were to be representative of those for middle and latter stages of highly

loaded axial-flow compressors. Stator inlet flow was to be generated by a state-of-the-art flow generation rotor, described in detail in Reference 6.

This report presents the test results of the triple-slotted 0.75 hub diffusion factor bleed stator performance. Previous test results on the flow generation rotor performance, without stators, are presented in Reference 1. The test results on the performance of a single-slotted 0.65 hub diffusion factor bleed stator are presented in Reference 7.

SYMBOLS

A	Bleed slot cross-section area, in. ²
A _a	Annulus area, ft ²
c	Airfoil chord, in.
D _f	Diffusion factor
g	Gravitational constant, 32.2 ft-lb _m /lb _f -sec ²
H	Hysteresis loop data point
h	Height of bleed slot, in.
i	Incidence angle based on mean camber line, degrees
K _A	Bleed slot aspect ratio coefficient
K _T	Bleed slot flow coefficient
L	Net slot length, in.
M	Mach number
\dot{m}	Bleed mass flow rate in bleed slots per blade, lb _m /sec
n	Number of blades per row
N	Rotational speed, rpm
P _t	Total pressure, psia
p	Static pressure, psia
q	Dynamic pressure, psia

R.	Radius, in.
\mathcal{R}	Gas constant, $53.35 \text{ lb}_f \cdot \text{ft}/\text{lb}_m \cdot {}^\circ\text{R}$
R_c	Pressure ratio
S	Airfoil surface pressure coefficient, Equation (A13)
T_t	Total temperature, ${}^\circ\text{R}$
t	Static temperature, ${}^\circ\text{R}$
t/c	Thickness-to-chord ratio
V	Air velocity, ft/sec
W_a	Compressor airflow, lb_m/sec
W_{BL}	Annulus wall bleed flow, lb_m/sec
x	Distance from blade leading edge, in.
<u>Greek</u>	
β	Air angle measured from axial direction, degrees
γ	Ratio of specific heats
γ°	Blade chord angle, degrees
δ	Ratio of total pressure to standard sea level pressure of 14.7 psia
δ°	Deviation angle, degrees
Δ	Incremental value
η	Efficiency
θ	Ratio of total temperature to standard sea level temperature of $518.6 {}^\circ\text{R}$
κ	Blade metal angle measured from axial direction, degrees
ρ	Density, lb_m/ft^3
σ	Blade row solidity

ϕ	Camber angle, degrees
ψ	Angle of inclination between center line of bleed slot and tangent to suction surface, degrees
ω	Angular velocity of rotor, radians/sec
$\overline{\omega}$	Total pressure loss coefficient
$\frac{\overline{w} \cos \beta}{2 \sigma}$	Loss parameter

Subscripts

0	Guide vane inlet
1	Rotor inlet
2	Stator inlet or rotor exit
3	Stator exit
ad	Adiabatic
m	Mean or 50% streamline
ma	Mass averaged
θ	Tangential direction
z	Axial direction

Superscripts

'	Relative value, rotor property
---	--------------------------------

APPARATUS AND PROCEDURES

TEST FACILITY

A general arrangement of the test facility is shown in Figure 1. Air enters the test compressor after passing through the test facility filter house, an inlet duct, plenum, and bellmouth and is exhausted to the atmosphere through a diffuser. Provisions exist for maintaining compressor inlet pressures above or below atmospheric if necessary.

Two power units can be used simultaneously to drive the test compressor. One is a T56 power turbine with combustors which burn fuel mixed with high pressure air from test facility compressors; the other is a complete T56 power section. The two units are coupled by a primary gearbox whose output shaft drives a secondary gearbox which in turn drives the test compressor. Control of the test compressor speed is effected by throttling the turbine air supply with a hydraulically-operated valve and by independent fuel controls for each unit.

COMPRESSOR TEST RIG

The mechanical arrangement of the test compressor is shown in Figure 2. It consists of a cylindrical inlet section, a test compressor section, and an exhaust diffuser. The single-stage rotor is supported on two bearings whose housings are linked by a vertically-split compressor case. The compressor case houses the inlet guide vanes, the rotor tip abradable coating, the stator vanes, and the case and hub bleed manifolds. The abradable coating on the compressor cases over the rotor blade tip permits low running clearances between the blade tips and the case. The rotor is designed with an interference fit such that the rotor blade tip will run into the abradable coating at design speed. Radial growth due to centrifugal force and temperature expansion are considered. Nominal design clearances for this rotor are -0.0025 in. at 100% speed and -0.0045 in. at 110% speed. Nominal static clearance is 0.0075 in. The design of the rig allows the rapid exchange of design and off-design guide vanes without dismantling the remainder of the compressor and the exchange of stator vanes without disassembly of the entire test rig.

Airflow rate and pressure ratio are varied by throttle plates located in the exhaust diffuser. The throttles are linked by a ring and operated by a common actuator.

Provision is made in the rig for bleeding the wall boundary layers at stator tip and hub. This is accomplished by fabricating the stator flow passage walls from perforated sheet metal. Manifolds behind the perforated metal surfaces are connected by multiple tubes to separate vacuum headers for tip and hub wall bleeds. The vane suction surface bleed flow, drawn into the core through the bleed slots, is discharged through oversize hollow tip trunnions on the stator vanes which are connected to a separate collector by equal length hoses.

BLADING

The design of the stator vanes, rotor blades, and design inlet guide vanes is described in detail in Reference 6. Selected airfoil sections are: (1) 63-006-series for the inlet guide vanes, (2) double circular arc for the rotor blades, and (3) 65-series thickness distribution with circular arc meanline for the stator vanes. For convenience, however, the principal

geometric details of these components are repeated in Table I. Basic details of the slot configuration of the triple-slotted 0.75 hub diffusion factor stators are shown in Figure 3.

INSTRUMENTATION

Instrumentation was provided to obtain blade element performance for the rotor and stator row and to measure overall performance. The locations of instrumentation planes are shown in Figure 4; Figure 5 shows schematically the circumferential location of the instruments installed at each plane. The radial element locations at each plane were selected along streamlines passing through the 10, 30, 50, 70, and 90% annulus height stations from the tip at the stator inlet measurement plane. The streamline locations are shown schematically in Figure 6. Dimensioned sketches of the probes used are shown in Figure 7. Instrumentation was distributed so as to minimize area blockages and prevent immersion in upstream instrument wakes. Except at the inlet guide vane exit station duplicate instrumentation was distributed to average out any inlet guide vane effects.

Compressor Inlet Conditions

Weight flow was measured with an ASME thin plate orifice located in each branch of the triple-inlet header. Six total pressure probes and two 6-element temperature rakes were located in the cylindrical section approximately three feet upstream of the test compressor inlet for measurement of inlet total pressure and temperature. See Figure 5a. Inlet static pressure was measured at the same axial station by two static taps in the inlet wall.

Rotor Inlet—Station 1

Four approximately equally-spaced static pressure taps were located on both the inner and outer walls as shown in Figure 5b. An 8-degree wedge traverse probe was also installed to measure the radial static pressure distribution. Three radial traverse combination total pressure and yaw angle probes were used to measure the distribution of these parameters across the annulus. Total temperature was obtained from plenum thermocouples.

Stator Inlet or Rotor Exit—Station 2

Four approximately equally-spaced static pressure taps were located on both the inner and outer walls, and the radial distribution of static pressure was measured by two 8-degree wedge traverse probes as shown in Figure 5c. Three radial traverse combination probes were installed at this station to measure the radial distribution of total pressure, total temperature, and flow angle.

Stator Exit—Station 3

Four approximately equally-spaced static pressure taps were located on both inner and outer walls; two 8-degree wedge traverse probes were installed for measurement of the radial static pressure distribution as shown in Figure 5d. One traverse combination probe was installed primarily to measure flow angle. A 16-element total pressure circumferential rake, shown in Figure 7d, was installed at this station to measure discharge total pressure and stator vane wake. This rake spanned 1.08 vane spaces at the 10% streamline and 1.43 vane spaces at the 90% streamline. Total temperature was measured by four 5-element radial rakes. Inner and outer wall boundary layers were surveyed by fixed 5-element total pressure probes. All taps, probes, and radial rakes were located on extensions of mid-channel streamlines.

Special Instrumentation

In addition to the instrumentation already enumerated for blade element and overall performance, the following special instrumentation was installed. At the rotor exit, two fixed and one traverse hot-wire anemometers were installed to signal the onset of compressor stall and to provide rotating stall data. Shaft whip was monitored by means of a whip pickup, mounted in the plane of the rotor blades. Strain gages were mounted on eight rotor blades to monitor blade stresses. The 10, 50, and 90% streamline sections of the slotted vanes were each provided with 12 suction-surface and 7 pressure-surface static pressure taps as indicated in Figure 8. One core static pressure tap is provided at each section to measure bleed flow rate. The 20 static pressure taps for each streamline section are distributed between four vanes.

DETERMINATION OF ANNULUS WALL BLEED FLOW FOR STATOR VANE TESTS

With the compressor operating at design speed and pressure ratio, the circumferential total pressure rake at the stator exit was set at the streamline station 10% from the tip. Hub and tip wall bleeds were set at a nominal flow of less than 1% of compressor flow. The stator wake pattern at this bleed flow was noted, and the tip wall bleed was then increased until no further improvement in wake pattern was visually observed on a manometer bank. This bleed flow rate was defined as the "optimum" bleed rate. One limiting consideration set as a reasonable upper value, however, was to extract no more than 2.5% of compressor inlet flow per wall at design conditions.

The circumferential rake was then set at the streamline station 90% from the tip. The tip wall bleed flow rate was reset at its original low value, and the procedure described was repeated for the hub bleed. After

hub and outer wall bleed flows had been optimized, the circumferential rake was moved to the mean position. Hub and outer wall bleeds were varied simultaneously in increments from the original nominal flow rate to optimum flow. The effects on the stator wake at mean depth were studied to check that optimum hub and tip wall bleeds coincided with an optimum wake at mid-span. The valve settings for these optimum bleed flow rates were left unchanged for all subsequent speed and flow conditions.

HYSERESIS TEST WITH TRIPLE-SLOTTED 0.75 HUB DIFFUSION FACTOR STATOR

The following method was employed to determine the characteristics of this stage at entry to and when recovering from stall. One hysteresis test was made at a corrected speed of 60% with optimum vane bleed. The throttle was closed until stall cells were indicated by the hot-wire anemometers (two of which were at the 10% and one at the 90% station from the tip), thus signaling the onset of stall. At this first hysteresis data point setting, a partial data recording, which consists of data required for airflow and pressure ratio calculation, was obtained. The throttle was then closed further in steps and to the point where the stage pressure ratio leveled off at a lower pressure ratio. Three partial data recordings were obtained during this throttling. While still in stall the throttle was gradually opened in steps and three more short data recordings were made at each step until indications of stall (as signalled by the hot wire anemometers) just disappeared. At this point an eighth short data recording was made.

Rotor blade stresses were monitored continuously during the hysteresis test to ensure that excessive vibratory stresses were not encountered.

OVERALL AND BLADE ELEMENT PERFORMANCE DATA

Overall and blade element performance data were obtained at a sufficient number of points per speed line to define rotor and stage performance between choke and stall. The near-stall test point was taken as close to the rotating stall condition as could be set without actually being in rotating stall. This type of near-stall setting permitted a full data point recording. The stage stall point is defined as the onset of a steady stall cell indication on the hot-wire anemometers. At each full data point recording, fixed and traverse pressure and temperature data were recorded at five radial locations corresponding to streamlines passing through the 10, 30, 50, 70, and 90% span stations at the stator inlet measurement plane.

DATA REDUCTION

Overall performance and blade element data reduction are accomplished in one program. A second program is used to calculate pressure coefficients and slot bleed flow rates for the stator vanes.

In the first program, raw data from the test stand are read in and printed. The program converts wedge probe static pressure transducer readings to inches of mercury absolute and applies a Mach number correction. All yaw units are converted to degrees. Data recording system, wire calibration, and Mach number corrections are applied to all temperatures. Pressures recorded on the data recording system are corrected to standard inlet total pressures. The corrected data are then printed.

Circumferential arithmetic averages of total pressures, static pressures, total temperatures, and yaw angles are calculated and printed. Individual data readings are compared with the averages to validate the data. Any individual reading which differs from its respective average value by more than the prescribed deviation (0.5 in. Hg for all pressures, three degrees for the yaw angles, 1.5, 2, and 3°R, respectively, for the reference, inlet, and all the other temperatures), is not used in the final calculations. Mass-averaged values required for performance calculations are determined.

The program provides a choice of two radial distributions of static pressure: (1) distributions measured by the wedge probes and (2) linear distribution across the flow annulus calculated from the arithmetically-averaged hub and case wall static pressure taps. Overall and blade element performance are calculated and printed using the two static pressure distributions mentioned. If a continuity check at any data measurement station is not satisfied within 5%, a simple radial equilibrium solution is provided to give an indication of the problem.

Overall performance values are calculated for the inlet guide vanes and rotor and for the complete stage. The following operations were performed to determine these values.

At the inlet plenum station, the two total temperatures are arithmetically-averaged at each radial station. Mass flow is integrated radially, assuming that averaged wall static pressure exists over the entire cross section. Total pressure and temperature are then mass-averaged. Behind the rotor wall static pressures are arithmetically averaged circumferentially and all total pressures and total temperature are arithmetically averaged circumferentially at each radial station. Mass flow is radially integrated and total pressures and temperatures are radially mass-averaged.

At the stator exit, four total temperatures are arithmetically-averaged circumferentially at each radial station. Incremental mass flow is computed using an arithmetic-average of the circumferential rake total pressure readings spanning a stator vane passage at each radial station. A radial integration is made for weight flow. For performance calculations, the total pressures at each radial station are mass averaged circumferentially and the total pressures and temperatures are mass averaged radially. The overall stage pressure ratio and adiabatic efficiency are obtained using the radially mass-averaged values of pressure and temperature.

The calculations of performance variables as programmed in the data reduction programs are delineated in the Appendix.

PRESENTATION OF RESULTS

Experimental results obtained in the test program are summarized in detail for: (1) the flow generation rotor with the design inlet guide vane set and (2) the triple-slotted 0.75 hub diffusion factor stator vane. The reduced data presented were based on a linear static pressure distribution across the annulus at each axial survey station rather than on the static wedge survey values. Comparison of results using both linear and wedge static data (Reference 1) showed that, when the wedge data were considered reliable, differences in reduced data were small; there was a tendency, however, for the wedge static data to be erratic for some test points. Use of the linear static data gives a consistent basis for comparison over the test range and with the data from other tests.

OVERALL PERFORMANCE OF FLOW GENERATION ROTOR AND STAGE

Overall pressure ratio and adiabatic efficiency are each plotted versus corrected inlet flow with corrected speed as a parameter at all three vane bleed rates. These are presented in Figures 9 through 14 for the flow generation rotor performance of this stage test, and Figures 15 through 20 for the overall stage performance of this test. To indicate whether the rotor or the triple-slotted stator caused the stage to choke or stall, rotor incidence range is summarized in Table II for the flow generation rotor test of Reference 1 and the flow generation rotor test of this report. Stage rotating stall characteristics at the triple-slotted stator stall points and hysteresis points are summarized in Table III.

BLADE ELEMENT PERFORMANCE

Rotor blade and stator vane blade element characteristics were computed for the five streamline positions previously defined. The blade element parameters chosen to present the detailed performance of each blade row are as follows:

- Incidence angle, i' or i
- Total pressure loss coefficient, $\overline{\omega}'$ or $\overline{\omega}$
- Diffusion factor, D_f
- Deviation angle, δ°
- Inlet flow angle, α' or β
- Flow turning angle, $\Delta\beta'$ or $\Delta\beta$
- Inlet axial velocity, V_z
- Inlet Mach number, M' or M

Rotor blade element data are plotted as a function of incidence angle with corrected speed as a parameter for each of the streamline stations. The blade element data obtained during the stage test with all three vane bleed flow rates are shown in Figures 21 through 23. For comparison and to aid the analysis of the rotor blade performance, blade element data for the rotor are plotted versus percent annulus height in Figures 24 through 26 for the flows which gave the best approximation of design incidence angle at design speed at all three vane bleed flow rates. Design values are also plotted for comparison. Mass flux distributions out of the rotor corresponding to the design flow rate for the various vane bleed flow rates are plotted and compared with the design flow distribution in Figures 27 through 29. Rotor blade element performances are evaluated, Figures 30 through 32, by comparing the loss parameter versus diffusion factor at the 10, 50, and 90% streamline stations from the tip with the NACA correlation curve from Reference 2.

Stator vane blade element data are also plotted as a function of incidence with corrected speed as a parameter for each streamline station for all three vane bleed rates in Figures 33 through 35. Also presented are the annulus wall bleed rates in Figures 36 through 38 and the triple-slotted vane bleed flow rates in Figures 39 and 40 obtained during tests where the various vane bleed rates were employed. Blade element data of the slotted stator vane for conditions nearest to the design incidence angle are plotted against the percent annulus height, Figures 41 through 43, to aid stator vane performance analysis and for comparison for the various vane bleed flow rates. Stator vane blade element performance is also presented in Figures 44 through 46 where the loss parameter versus diffusion factor for the 10, 50, and 90% streamline stations from tip, is compared with the NACA correlation curve from Reference 2.

The pressure and suction surface static pressure distributions, along the 10, 50, and 90% streamlines from the tip, of the triple-slotted stator are presented in Figures 47 through 55 for all the speed lines and vane bleed rates tested.

Stator wakes obtained with the optimum, mean, and zero vane bleed rates are plotted in Figures 56 through 58.

The variations in the stator wake at the 10, 50, and 90% streamlines from the tip, during wall bleed optimization, are presented in Figure 59.

To enable compressor designers to evaluate and apply the results of this test, a detailed summary of vector diagrams, blade element characteristics and loss data at each streamline station is also provided for all three vane bleed flow rates employed. These summaries are presented in Tables IV through VI for the optimum, mean, and zero vane bleed flow rates, respectively.

DISCUSSION OF RESULTS

The method of presentation using the overall and blade element parameters for evaluating the performance has been described in detail. Since the figures and tables are self-explanatory, only general observations are made.

OVERALL PERFORMANCE

Flow Generation Rotor

Flow generation rotor pressure ratio and adiabatic efficiency measured during the test with the triple-slotted stator are given in Figures 9 through 14. At the design point pressure ratio of 1.37:1 and with optimum vane bleed the measured airflow was 94.1 lb/sec with an adiabatic efficiency of 96.7%. The pressure ratio-flow results are in good agreement with the rotor test results without stator vanes (Reference 1). When the maximum value of adiabatic efficiencies are examined for 100% corrected speed, however, a value of 97.7% is shown for this test as compared with 92.5% for the flow generation rotor test at the same measured flow rate. This apparent discrepancy is attributed to the method of calculation which uses stator exit temperature to compute rotor efficiency (Equation (A2) in the Appendix). For tests with stators, bleed was used at the stator end walls. Because the rotor exit temperature is high in the end regions this wall bleed leads to a reduction in mass-averaged temperature in the case of "rotor only" tests where no wall bleed was used. This reduction of temperature is reflected in a higher rotor efficiency for the test of the rotor with stators.

At the design pressure ratio with mean and zero vane bleed flow rates the efficiency was 94.0% and 94.3%, respectively, with corresponding airflow rates of 95.2 lb/sec and 94.6 lb/sec.

A prime concern during the design phase of the flow generation rotor, discussed in the design report, Reference 6, was that sufficient flow range would be available to avoid excessive limitations on the stator operating range by the rotor or facility. In this report, Table 2 gives a summary of rotor incidence angles (near stall and choke) at hub, mean, and tip streamlines. The stall incidence angles correspond to the minimum flow rate due to either rotor or stator stall. The choke incidence angles correspond to the maximum flow rate due either to rotor choke, stator choke, or facility pressure loss limitations.

Rotor incidence angle differences at stall observed between slotted stator test and flow generation rotor test are small, and stage stall may be caused by rotor stall rather than stator stall. The comparisons of incidence angles also indicate that the stator limited the maximum flow at 60% and 80% corrected speed. At 100% corrected speed the rotor incidence angles indicate that either the rotor is choking or the facility pressure loss is controlling. It is believed that the facility exit duct pressure loss is controlling

at these relatively low pressure with high flow conditions. These observations are, in general, true for all the bleed rates employed.

Triple-Slotted Stator Stage

The overall stage pressure ratio and adiabatic efficiencies are shown in Figures 15 through 20, for all three vane bleed flow rates. During these tests only the design inlet guide vanes were employed.

Stage design pressure ratio and adiabatic efficiency are 1.35 and 85.5%, respectively, at a design flow rate of 88.2 lb/sec as reported in Reference 6. At the design equivalent rotor speed with the optimum vane bleed flow rate a maximum stage adiabatic efficiency of 87.0% was obtained with a flow rate of 94.0 lb/sec and a pressure ratio of 1.353. The maximum stage adiabatic efficiency obtained with the mean vane bleed flow rate was 87.8% at a flow rate of 93.4 lb/sec and a pressure ratio of 1.365. The maximum stage efficiency with zero vane bleed flow was 86.3% at a flow rate of 93.1 lb/sec and a pressure ratio of 1.365. At the flow generation rotor condition of 94.1 lb/sec corrected flow rate, the stage pressure ratio was equivalent to its design pressure ratio of 1.350 and the measured adiabatic efficiency was 86.2% for optimum vane bleed. At this flow rate, with the vane bleeds set at the mean and zero flow rates, the values obtained for the pressure ratio were 1.355 and 1.344, respectively; the adiabatic efficiencies were 87.0% and 85.2%, respectively. For simplicity, the stage adiabatic efficiency, presented herein, is not penalized by the case and hub wall bleed flows. Inasmuch as the rotor loading is not compatible with the stator loading, the stage efficiency is seen to be inordinately low and of secondary interest.

The overall stage performance of the triple slotted stator with optimum and mean vane bleed flows are comparable, but the performance with zero vane bleed is inferior. This can be shown in the following comparisons. The total pressure recovery of the triple-slotted stator at a flow of 94.1 lb/sec with optimum vane bleed is 0.986 (1.35/1.37), which agrees with the design total pressure recovery of 0.986 (1.35/1.37). The design average total pressure recovery of the triple-slotted stator with mean vane bleed shows an improvement to 0.988 (1.355/1.37). The design average total pressure recovery of the triple-slotted stator with zero vane bleed was lower than the recovery obtained for the optimum and mean vane bleed flows, at a value of 0.981 (1.344/1.37).

Annulus Wall Bleed for Stator Test

Annulus wall bleed over the stator row at tip and hub surfaces was defined at 100% corrected speed and rotor pressure ratio of 1.37 by monitoring visually the circumferential rake and boundary layer total pressure rakes at tip and hub. The boundary layer rakes showed separation on the wall at wall bleed flow rates below about 0.5%. Increase in wall bleed flow rates above 0.5% gave improvements in stator wakes as indicated by the rakes at

10 and 90% of passage height. Optimum wall bleed flow at design speed and pressure ratio, with maximum vane bleed, was selected as 1.95 and 1.84% for the hub and tip, respectively. Wall bleed flow rates greater than the selected rates gave negligible improvements in the wake configurations. The tip and hub bleed valves were held fixed throughout all remaining test points.

The tip and hub wall bleed rates experienced throughout this test with the fixed bleed line valve settings are summarized in Figures 36 through 38 for the optimum, mean, and zero vane bleed flow rates, respectively.

Hysteresis and Rotating Stall Results—Triple-Slotted Stator Stage

This test was made to determine whether the stall of this stage is gradual or abrupt, and whether the stall would disappear and the stage recover smoothly. Flow values at the onset of rotating stall and during the hysteresis tests are shown in Figure 15. Rotating stall data during the hysteresis test are summarized in Table III.

The onset of rotating stall at each corrected speed is indicated by the hot-wire anemometer located at the 90% streamline station. Rotor stall was abrupt at all speeds as indicated by stall zone progression to the tip of the rotor with only a slight increase in back pressure.

At 60% corrected speed, an 8-point hysteresis loop test was conducted. The pressure ratio and flow rates are shown in Figure 15. A hysteresis effect, in terms of pressure ratio and flow rate, was indicated from measurements defining the path from point H₁ to H₈. The initial throttling from H₁ to H₂ resulted in the stage dropping into deep stall as indicated by the sharp reduction in pressure ratio and flow. The pressure ratio remained essentially constant at this level for all throttle settings from H₂ through H₇. The flow pressure ratio path from H₇ to H₈ was not defined. However, at H₈ the indications of rotating stall had just disappeared and the stage was again operating on the unstalled leg of its characteristic. The maximum vibratory blade stresses encountered during the hysteresis test were 17,800 psi. The stresses recorded during the stall tests showed maximum values of 20,600 psi. There were indications, from the frequent recurrence of vibratory stress peaks that these high stresses prevailed for significant periods when the stage was in stall. The vibratory blade stresses which were experienced were also considered to be at a potentially damaging level, since the prescribed vibratory stress limit was exceeded in some cases.

Rotative speed, frequency, and number of stall zones for rotating stall tests are summarized in Table III. Just after the onset of stall, a stall zone was recorded in the tip region and in the hub region. The rotative speeds of the cells in both regions ranged from 27 to 45% rotor speed in the direction of rotation. Their frequencies varied from 31 to 200 cps depending on the corrected speeds run and the number of stall cells observed. Multiple stall cells at the tip and hub were recorded during rotating stall tests at 100% design speed and zero vane bleed. In stall, during the hysteresis test, cell rotative speed was approximately 28% of rotor speed in the direction of rotation and the frequency was 43 cps.

High rotor blade transient vibratory stresses prevented radial traversing of the hot-wire probe. It appears, however, that the stall zone extended across the blade span.

BLADE ELEMENT PERFORMANCE

An extensive study of the inlet guide vanes, both at design and off-design conditions, was made as reported in Reference 1. Investigation into the possible persistence of the inlet guide vane wakes through the rotor, at the design flow rate condition, indicated the attenuation of these wakes before entering the stator rows. In view of these results, repeated study of inlet guide vane flow for each test was found unnecessary.

Rotor

Diffusion factor, deviation angle, and loss coefficient data throughout the rotor operating range for the triple-slotted stator stage test are summarized in Figures 21 through 23. In general, the measured loss coefficients at all vane bleed rates were equal to or less than the design values at design speed and incidence angle at the 10, 30, 50, 70, and 90% streamline stations. The measured loss coefficients at the mean and zero vane bleed rates were slightly lower than those with optimum bleed. The data also indicates the loss coefficient at the 50% streamline is not affected by vane bleed. The loss coefficient does not reflect a difference in efficiency as a result of wall bleed since the loss coefficient was obtained by using both the pressure and temperature measured at the rotor discharge, whereas the rotor efficiency was based on the stator discharge temperature.

Primary rotor blade element performance for the double circular arc blade during the stator test is shown in Figures 24 through 26. Rotor blade data measured for both the flow generation rotor and the triple-slotted stator stage tests, operating near the design incidence angle at design corrected speed, are compared with the design values. The selection of measured data was based on the best agreement with the design incidence angle values since the rotor exceeded its design pressure ratio.

The diffusion factors were higher than the design values for tests with all three vane bleed rates. The values of deviation angles were significantly less than the design values. These results were similar to those observed in References 1 and 7. The lower than design deviation angles result in an effective overcambering of the rotor blade, producing an excessive amount of work. The combination of higher work input and lower axial exit velocity results in higher than design values of diffusion factors.

The radial distribution of mass flux at the rotor outlet for the triple-slotted stator stage test are compared with the design and flow generation rotor mass flow distributions in Figures 27 through 29. A flow shift to the

tip occurred experimentally with respect to the design distribution due to the low deviation angles in the tip region of the rotor. An additional mass flow shift with zero and mean bleed, but not with optimum bleed, was observed between the measured test values of the flow generation rotor test, Reference 1, and the 0.75 hub diffusion factor triple-slotted stator stage test reported herein. This additional mass flow shift at the rotor outlet could be due to the stator loss effect upon radial equilibrium. It could also be due to an effective blockage in the hub region caused by the separation of the boundary layer at the stator suction surface inducing a secondary flow and end wall effects. The stator exit hub wall boundary layer rake, however, did not indicate any wall boundary layer separation.

Rotor loss parameter data at the 10, 50, and 90% streamline stations are shown in Figures 30 through 32. Minimum loss coefficient values are indicated as filled symbols when they could be defined. Minimum loss data for the tip region or 10% streamline station are found to lie generally on the lower band of the data scatter at all vane bleed flow rates. Loss data for the mid-span and hub region are found to agree very well with the NACA correlation curves in the test diffusion factor range, at all vane bleed rates.

Stator

Figures 33 through 35 present the stator blade element performance along the blade annulus height in terms of loss coefficient, deviation angle, and diffusion factor as a function of incidence angle. Measurements were taken with optimum, mean, and zero vane bleed rates. Losses at design speed and incidence were higher than design at all streamline measuring stations and at all vane bleed rates tested. In the inner half of the blade the losses tended to increase with decreased bleed while the losses in the outer half of the blade were essentially independent of the bleed rate. The deviation angle was lower than design at all test conditions, the largest difference from design being at the 10% and 90% streamline positions. The result of the lower deviation angle at design speed and incidence produces an effective over-cambering and higher than design turning.

The diffusion factor at design incidence is equal to or greater than design at optimum vane bleed but shows a decreasing trend with reduced bleed flows.

The radial variation of blade element data for the triple-slotted stator near the corrected inlet flow rate of 94.1 lb/sec is compared with the design values in Figures 41 through 43. The inlet axial velocity and incidence angle plots of these figures indicate a mass flow shift with respect to the measured values for the flow generation rotor, Reference 1, as well as the design, Reference 6. This flow shift is due to the rotor performance as previously discussed in the rotor section of this report and in Reference 1. Other results shown in Figures 41 through 43 are that the deviation angles are less and flow turning greater than the respective design values. Measured losses at the hub and tip regions

were found to be greater than the design values for all vane bleed rates. As bleed flow rates were reduced, losses at the 50% streamline station gradually increased while the hub and tip losses decreased. This produced a nearly flat loss curve of higher than design value at zero bleed.

Minimum loss coefficient points obtained from Figures 33 through 35 are compared with the NACA loss parameter versus diffusion factor correlation (Reference 2) in Figures 44 through 46 for the 10, 50, and 90% streamline stations from the tip. At all the vane bleed flow rates, the tip data of the triple-slotted stator generally lie above an extension of the NACA correlation at the higher speeds. The mean and hub data, however, generally fall below the extension of the NACA curves of Reference 2. The results are similar for all the bleed flow rates used.

The results of this test presented in Figures 41 through 43, indicate that varying the bleed flow rate has little or no effect upon the flow turning angle or deviation angle at the 30, 50, 70, and 90% from the tip streamline stations. At the 10% from the tip streamline location the flow did exhibit a reduction in turning and increase in positive deviation angle as bleed flow was reduced. This behavior of the turning and deviation angles with reduced bleed was in direct contrast with the results of the single-slotted bleed 0.65 hub diffusion factor test reported in Reference 7 wherein the flow near the hub showed a decrease in turning and increase in positive deviation angle with reduced bleed. In view of the losses, turning angles and diffusion factors, the use of the mean vane bleed rate appeared to be as effective as the optimum vane bleed rate. Additional experimental data, however, would be needed to reach a definite conclusion.

Typical triple-slotted stator wake distributions are shown in Figures 56 through 58. Selected cases nearest the design incidence angle, which show the increasing wake trough pressure depressions as inlet Mach number increases, are given in Figures 56a through 56c, 56e, and 56i for the optimum vane bleed flow rate; 57a, 57b, and 57d for the mean; and 58b, for the vane bleed reduced to zero.

Figures 56d through 56h illustrate the effects of increasing incidence angle at the 100% corrected speed with the vane bleed set at the optimum rate. The mean streamline data are particularly revealing. At 100% speed and at approximately the same Mach number this streamline position is relatively insensitive over a broad range of incidence angles. For the vane bleeds reduced to the mean and zero values the effect of increasing incidence angle is presented in Figures 57c through 57f and 58a through 58d, respectively. The wake surveys at high positive incidence angles, displayed in Figures 56h, 57f, and 58d, show a marked resemblance to each other.

Wake survey data were recorded during the wall bleed optimization runs at the design stage pressure ratio of 1.35 and 100% corrected speed in Figure 59.

Integrating the tip values indicated that the total pressure at stator exit was approximately 35.8 in. Hg before and 35.3 in. Hg after optimization. The total pressure difference between rotor and stator was 2.4 in. Hg before optimization and 2.6 in. Hg after optimization. Thus, a slight increase in pressure loss was observed although optimization decreased the difference between maximum and minimum pressure values in the wake distribution. An integration at the hub gave stator exit total pressure values of 34.0 in. Hg before optimization and 34.9 in. Hg after optimization. The total pressure difference between rotor and stator exit stations was 3.2 in. Hg before optimization and 2.6 in. Hg after optimization of the wall bleed flow. Thus, in this case the magnitude of the hub pressure loss as well as the difference between maximum and minimum pressure values in the distribution were decreased as shown in Figure 59. It is also evident that increased wall bleed reduced the end wall region flow disturbances and stator losses at the hub but increased the losses at the tip and mean sections. Higher wall bleed rates, obtained by increasing the orifice pressure differential above 30 in. H_2O at the tip, and 29 in. H_2O at the hub, have little effect on increasing wake total pressure at these depth locations.

Stator Static Pressure Distributions

Suction surface static pressure distributions shown in Figures 47 through 55 give inconclusive evidence in determining the existence of boundary layer separation. The static pressure distributions indicate that boundary layer separation was possibly attenuated at high speeds by the influence of the suction slots. There are also indications in the data of separation when vane bleed was not employed. It would be difficult to establish the existence of boundary layer separation from the static pressure distribution plots in general, though individual cases may be singled out where the existence of this phenomenon may be detected. The static pressure obtained at lower speeds also provides insufficient information to establish separation with certainty.

The absence of flow separation or a reattached boundary layer flow may also be evidenced from the loss coefficients which show low values. Based upon the available data, it would be difficult to attribute the higher than the design values at the hub and tip regions to a secondary flow phenomenon rather than a possible flow separation.

Stator Slot Bleed Flow

Stator slot bleed flow rates were calculated and presented as a percentage of the total mass flow in Figures 39 and 40. The data indicated that the optimum bleed rate of 1.4% of the total flow was higher than the design value at design flow conditions. The mean vane bleed was 0.66% of the total flow at design conditions, and was less than the amount designed to prevent separation. The losses obtained with this reduced vane bleed were not as high as to indicate severe separation. This bleed rate could, therefore, be sufficient to provide effective boundary layer control and prevent separation.

CONCLUDING REMARKS

Discussion of experimental results has been based on work completed to date. Analysis of the data compiled on bleed techniques as applied to stator vanes indicates the following points:

1. A hysteresis effect was indicated in terms of pressure ratio and mass flow rate at 60% design speed. The onset of stall was abrupt with stall cells first appearing at the hub.
2. Total pressure loss coefficients at design speed and incidence were higher than the design value at all streamline measuring stations and at all vane bleed rates tested. In the inner half of the blade the losses tended to increase with decreased vane bleed whereas they were essentially independent of vane bleed in the outer half of the blade.
3. The triple-slotted bleed, 0.75 hub diffusion factor stator turning angle was greater than the design value.
4. Suction surface static pressure distributions give inconclusive evidence as to the effectiveness of this bleed technique for controlling separation.
5. The use of wall bleeds are seen to aid the control of the boundary layer flow. Wall bleeds have a greater influence on flow at the stator hub than at the tip.

REFERENCES

1. Miller, M. L. and Beck, T. E. Single-Stage Experimental Evaluation of Boundary Layer Blowing Techniques for High Lift Stator Blades, II—Data and Performance of Flow Generation Rotor and Single Slotted 0.75 Hub Diffusion Factor Stator. NASA CR-54565 (Allison EDR 5691). February 1968.

2. Aerodynamics Design of Axial Flow Compressors. NASA SP-36. 1965.
3. Miller, M. L. and Seren, G. Single-Stage Experimental Evaluation of Boundary Layer Blowing Techniques for High Lift Stator Blades, III—Data and Performance of Single-Slotted 0.65 Hub Diffusion Factor Stator. NASA CR-54566 (Allison EDR 5759). June 1968.
4. Carmody, R. H. and Seren, G. Single-Stage Experimental Evaluation of Boundary Layer Blowing Techniques for High Lift Stator Blades, IV—Data and Performance of Single-Slotted 0.75 Hub Diffusion Factor Stator. NASA CR-54567 (Allison EDR 5861). August 1968.
5. Rockenbach, R. W. Single-Stage Experimental Evaluation of Slotted Rotor and Stator Blading. Part IX—Final Report NASA CR-54553, Pratt and Whitney Aircraft Division of United Aircraft Corporation, Florida Research and Development Center.
6. Miller, M. L. and Chapman, D. C. Single-Stage Experimental Evaluation of Boundary Layer Bleed Techniques for High Lift Stator Blade, I—Compressor Design. NASA CR-54569 (Allison EDR 5658). February 1968.
7. Carmody, R. H. and Seren, G. Single-Stage Experimental Evaluation of Boundary Layer Bleed Techniques for High Lift Stator Blades, II—Data and Performance of Single-Slotted 0.65 Hub Diffusion Factor Stator. NASA CR-54570 (Allison EDR 5862). August 1968.

APPENDIX

PERFORMANCE EQUATIONS

The following overall and blade element performance parameters were calculated for the analysis of test data and the evaluation of the slotted stator performance.

WEIGHT FLOW

Overall performance is presented as a function of corrected weight flow, defined as

$$\frac{W_a \sqrt{\theta}}{\delta} \quad (A1)$$

ADIABATIC EFFICIENCY

Adiabatic efficiency for the inlet guide vane and rotor combination is

$$\eta_{ad2} = \frac{\left(\frac{P_{t2, ma}}{P_{t0}} \right)^{(\gamma-1)/\gamma} - 1}{\frac{T_{t3, ma}}{T_{t0}} - 1} \quad (A2)$$

and for the guide vane, rotor, and stator is

$$\eta_{ad3} = \frac{\left(\frac{P_{t3, ma}}{P_{t0}} \right)^{(\gamma-1)/\gamma} - 1}{\frac{T_{t3, ma}}{T_{t0}} - 1} \quad (A3)$$

DIFFUSION FACTOR

For the rotor, diffusion factor is defined as

$$D_{f2} = 1 - \frac{V'_2}{V'_1} + \frac{V'_{\theta 2} - V'_{\theta 1}}{2 \sigma V'_1} \quad (A4)$$

and for the stator as

$$D_{f_3} = 1 - \frac{V_3}{V_2} + \frac{V_{\theta_2} - V_{\theta_3}}{2 \sigma V_2} \quad (A5)$$

These quantities are calculated using the appropriate velocity triangle values previously computed by the program.

DEVIATION ANGLE

Rotor blade deviation is defined as

$$\delta_2^\circ = \beta_2' - \kappa_2' \quad (A6)$$

and stator deviation as

$$\delta_3^\circ = \beta_3' - \kappa_3 \quad (A7)$$

where κ_2' is the rotor blade exit metal angle based on the mean camber line for a double-circular arc airfoil and κ_3 is the stator vane exit metal angle based on the circular arc camber line used for the 65-series airfoil.

INCIDENCE ANGLE

Rotor blade incidence is defined as

$$i_1' = \beta_1' - \kappa_1' \quad (A8)$$

and stator incidence as

$$i_2 = \beta_2 - \kappa_2 \quad (A9)$$

where κ_1' is the rotor blade inlet metal angle based on the mean camber line for a double-circular arc airfoil and κ_2 is the stator vane inlet metal angle based on the circular arc camber line.

TOTAL PRESSURE LOSS COEFFICIENT

Total pressure loss coefficient for the rotor is defined as

$$\frac{-l}{\omega} = \frac{\left[1 + \frac{\gamma-1}{2} \frac{(\omega R_2)^2}{\gamma g \rho T_{t1}} \left(1 - \frac{R_1^2}{R_2^2} \right) \right]^{\gamma/(\gamma-1)} \left[1 - \frac{P_{t2}/P_{t1}}{(T_{t2}/T_{t1})^{\gamma/(\gamma-1)}} \right]}{1 - \left[1 + \frac{\gamma-1}{2} (M_1')^2 \right]^{-\gamma/(\gamma-1)}} \quad (A10)$$

and for the inlet guide vanes as

$$\bar{\omega} = \frac{1 - \frac{P_{t1}}{P_{t0}}}{1 - \left[1 + \frac{\gamma - 1}{2} (M_0)^2 \right] - \gamma / (\gamma - 1)} \quad (A11)$$

and stator as

$$\bar{\omega} = \frac{1 - \frac{P_{t3}}{P_{t2}}}{1 - \left[1 + \frac{\gamma - 1}{2} (M_2)^2 \right] - \gamma / (\gamma - 1)} \quad (A12)$$

PRESSURE COEFFICIENT

Pressure coefficient (S) is defined by

$$S = \frac{P_{t2} - p}{q_2} \quad (A13)$$

where:

P_{t2} = total pressure at stator inlet

p = static pressure at a given point on the vane surface

$q_2 = \frac{\gamma p_2 M_2^2}{2}$ = dynamic pressure at stator inlet

VANE BLEED FLOW

The flow rate through the bleed slot was calculated using the formula given in Reference 6.

$$\dot{m} = K_T K_A \frac{P_{t2} A}{\sqrt{T_{t2}}} \quad (A14)$$

where; A is the bleed slot area in square inches given as

$$A = h \times L,$$

K_A is the aspect ratio coefficient, correcting for the slot end wall effects. In the slot sizing calculations used for this configuration K_A was taken as 0.95.

K_T is the experimental flow coefficient defined by the formula,

$$K_T = 2.06 \left[\left(\frac{P_{t_{core}}}{P_{t_2}} \right)^{1.43} - \left(\frac{P_{t_{core}}}{P_{t_2}} \right)^{1.71} \right]^{0.5}$$

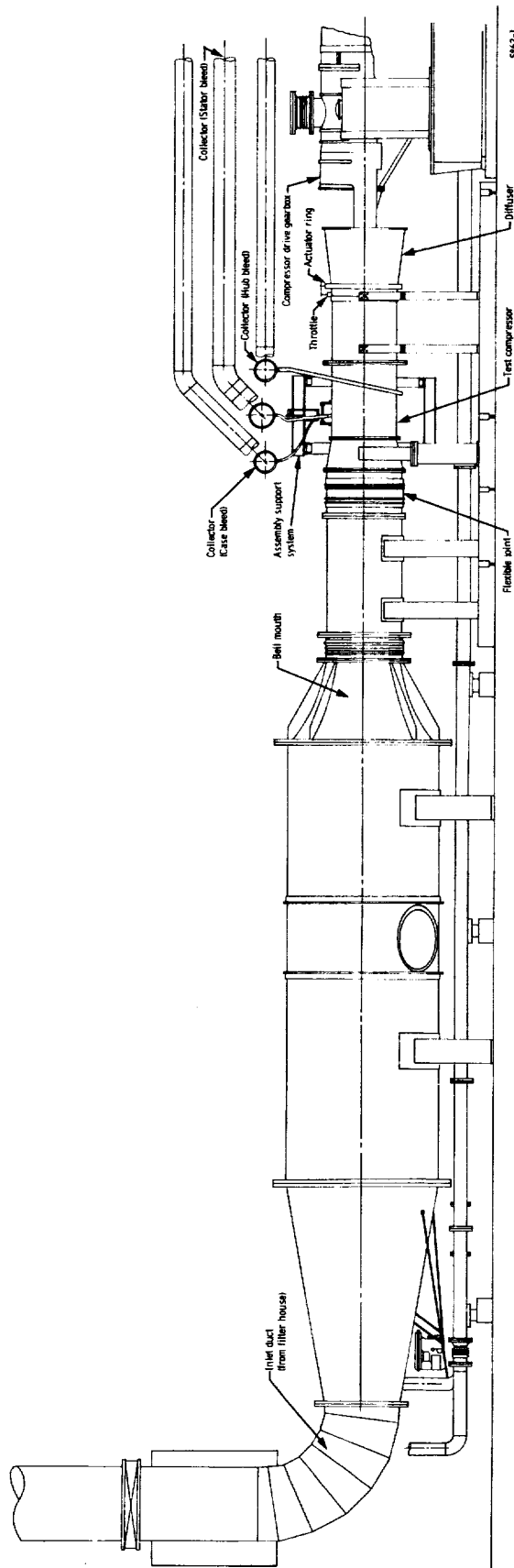


Figure 1. Compressor test facility.

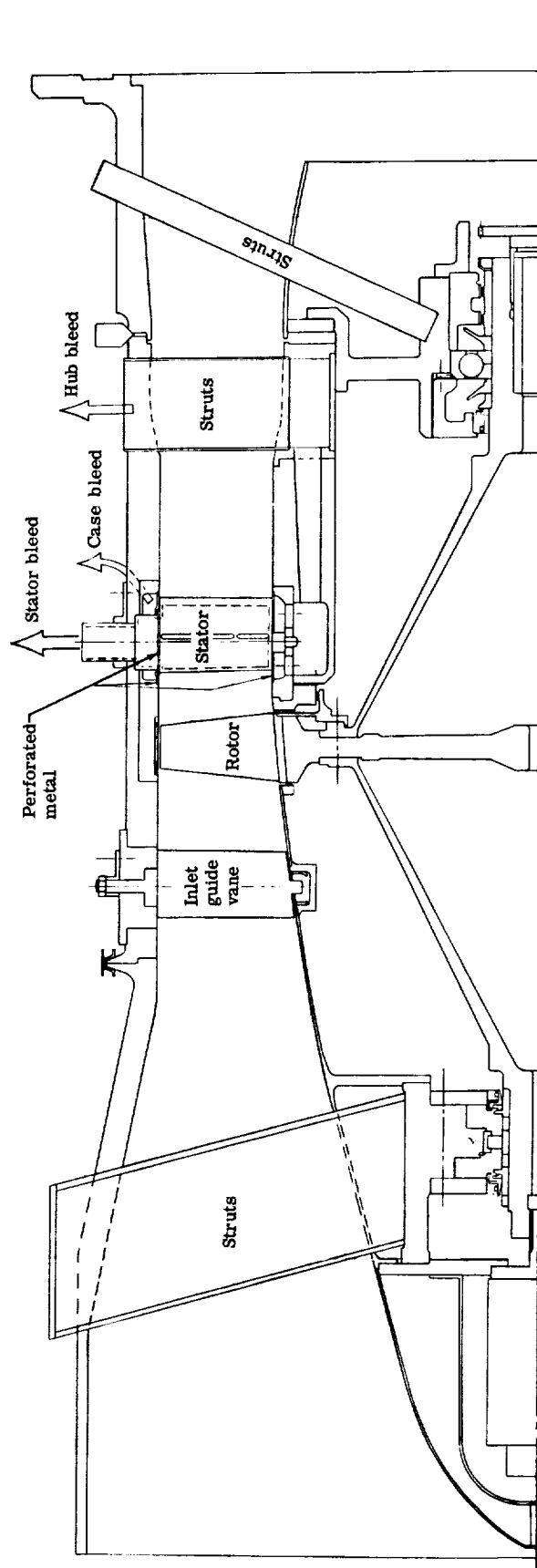
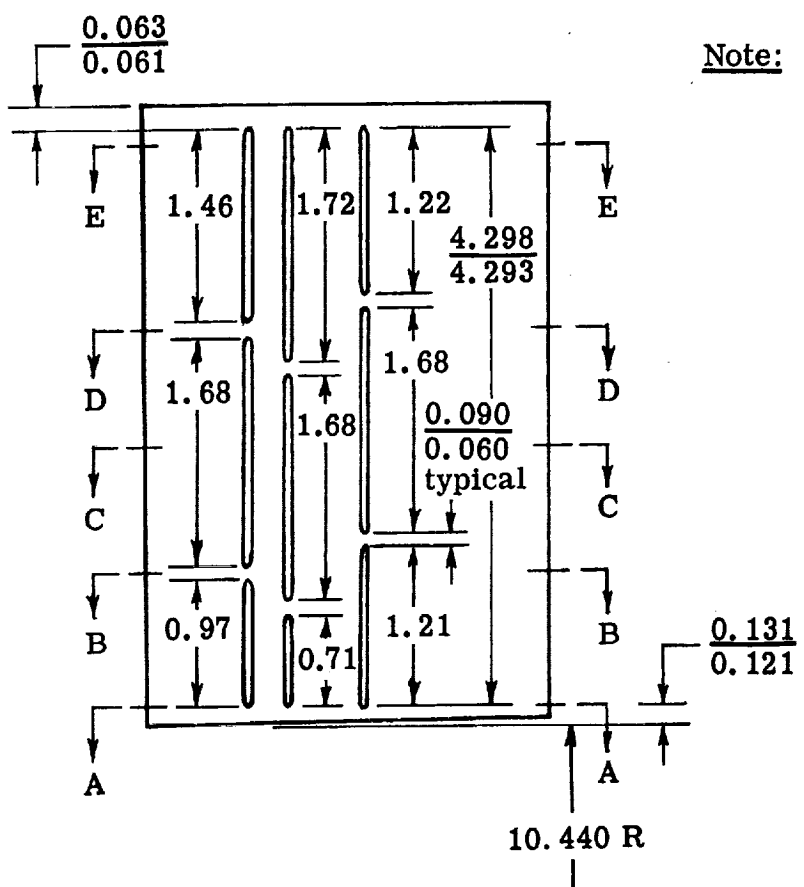
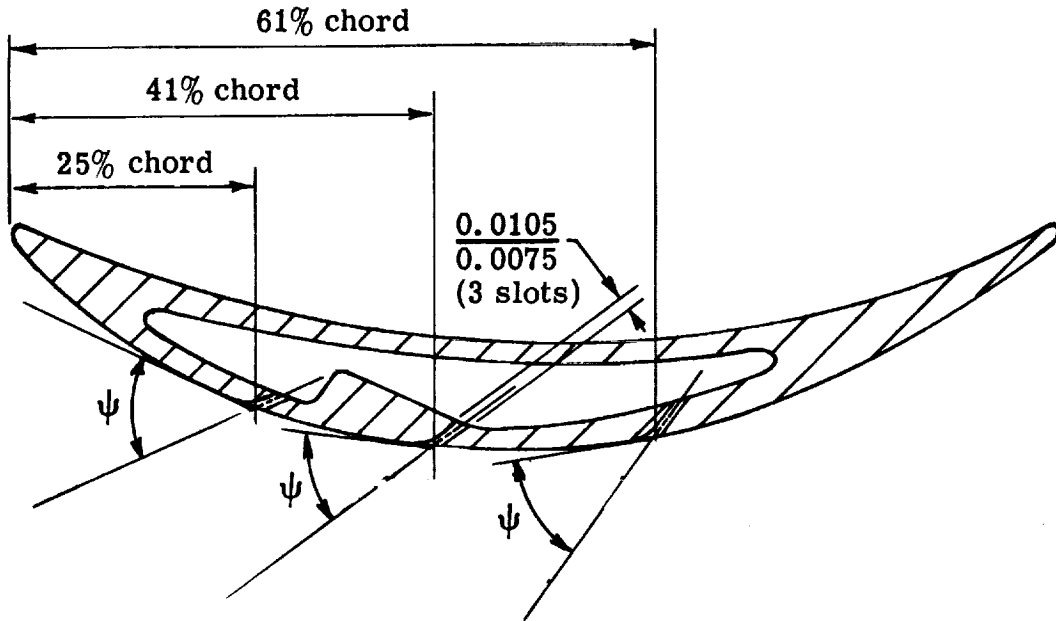


Figure 2. Layout of compressor test rig.



5944-3

Figure 3. Triple slotted 0.75 hub diffusion factor stator slot configuration.

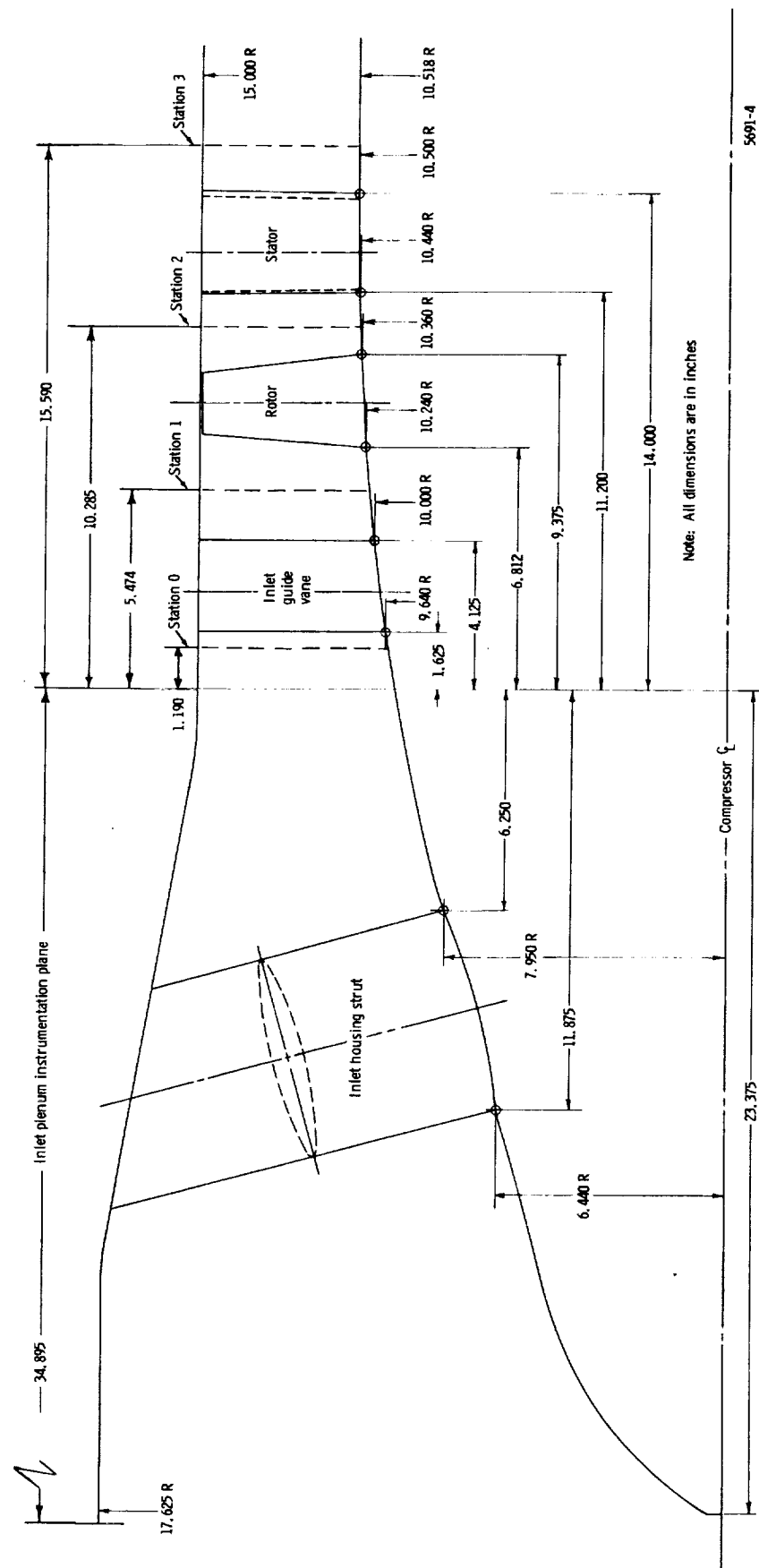


Figure 4. Test rig compressor flow path.

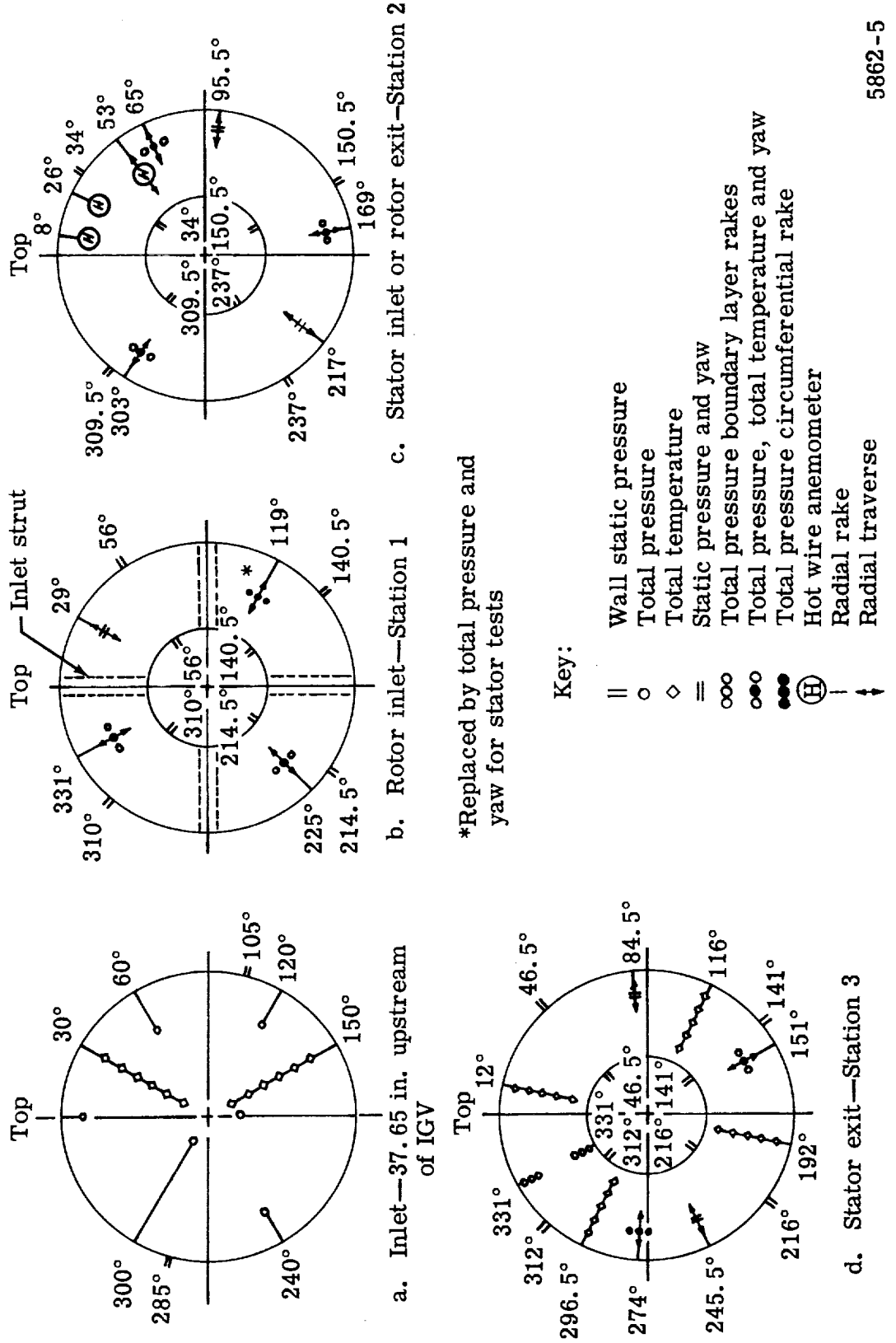


Figure 5. Circumferential location of instrumentation viewed downstream.

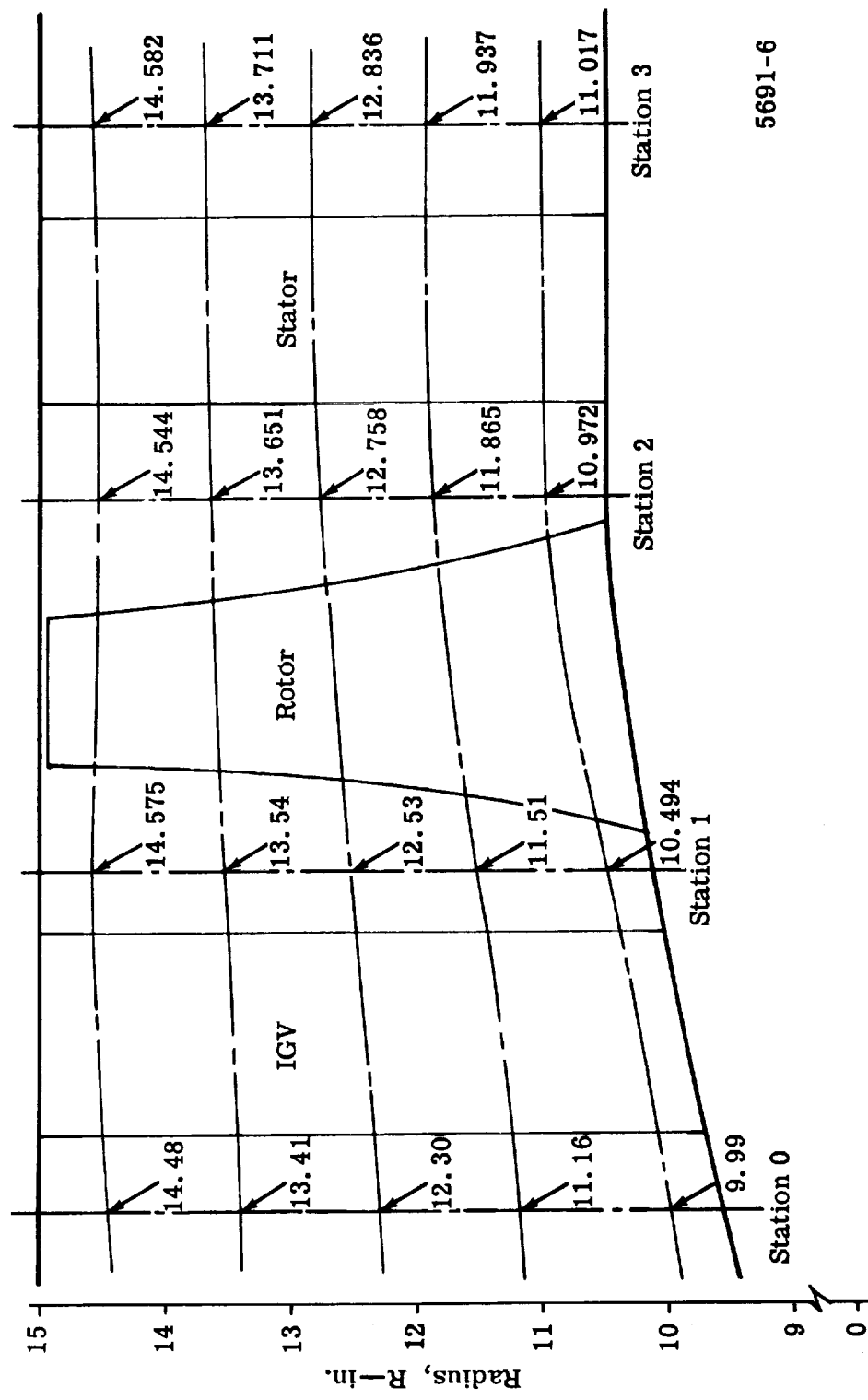


Figure 6. Radial location of streamlines for instrumentation positions.

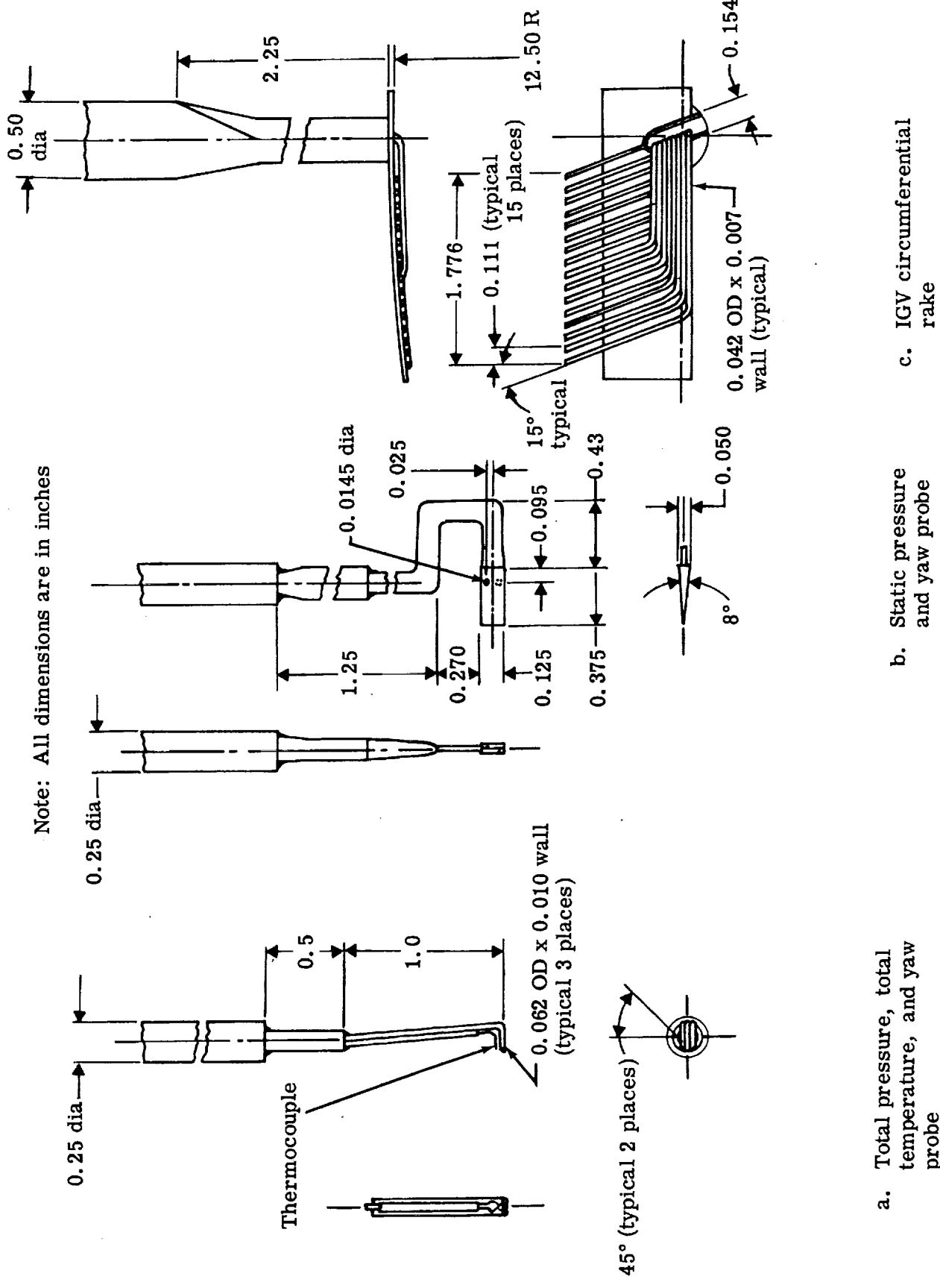
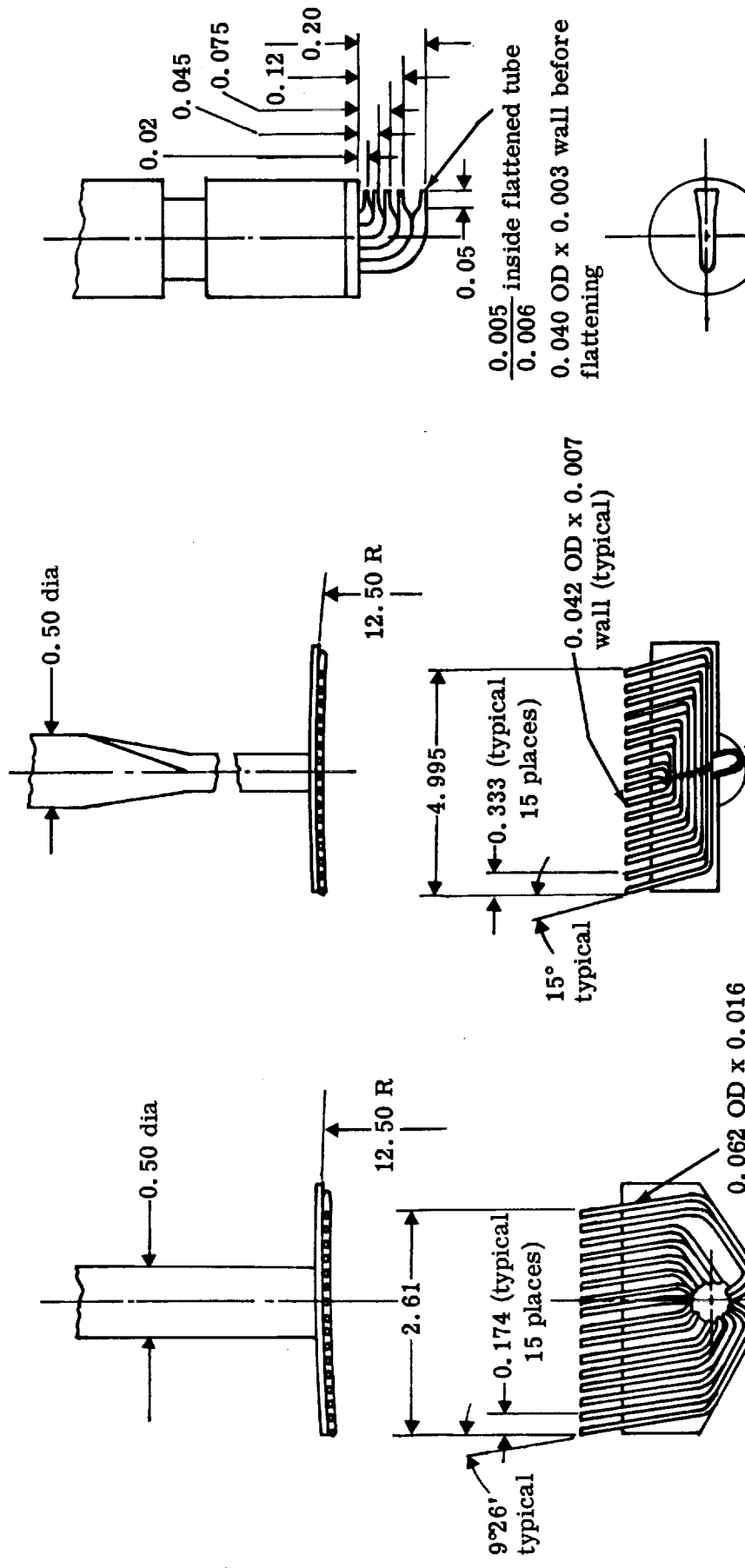


Figure 7. Schematics of survey instrumentation.

Note: All dimensions are in inches



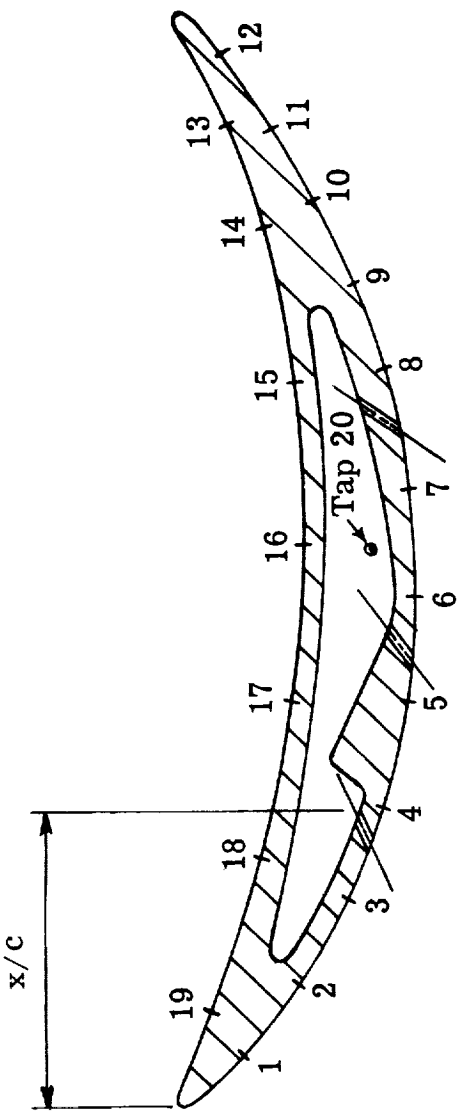
d. Stator circumferential rake

e. IGV wake persistence circumferential rake

f. Boundary layer probe for tip and hub

5691-8

Figure 7. Schematics of survey instrumentation.



Tap	1	2	3	4	5	6	7	8	9	10	11	12
$x/c - \%$	4.32	11.29	19.26	27.22	36.52	46.48	56.44	67.40	75.03	82.67	89.31	95.65
Vane No.	1	2	3	4	1	2	3	4	1	2	3	4

Tap	13	14	15	16	17	18	19	20
$x/c - \%$	91.40	80.35	66.07	51.46	36.85	22.58	8.63	—
Vane No.	1	2	3	4	1	2	3	4

5944-9

Figure 8. Triple-slotted stator vane static pressure tap locations at 10, 50, and 90% streamlines.

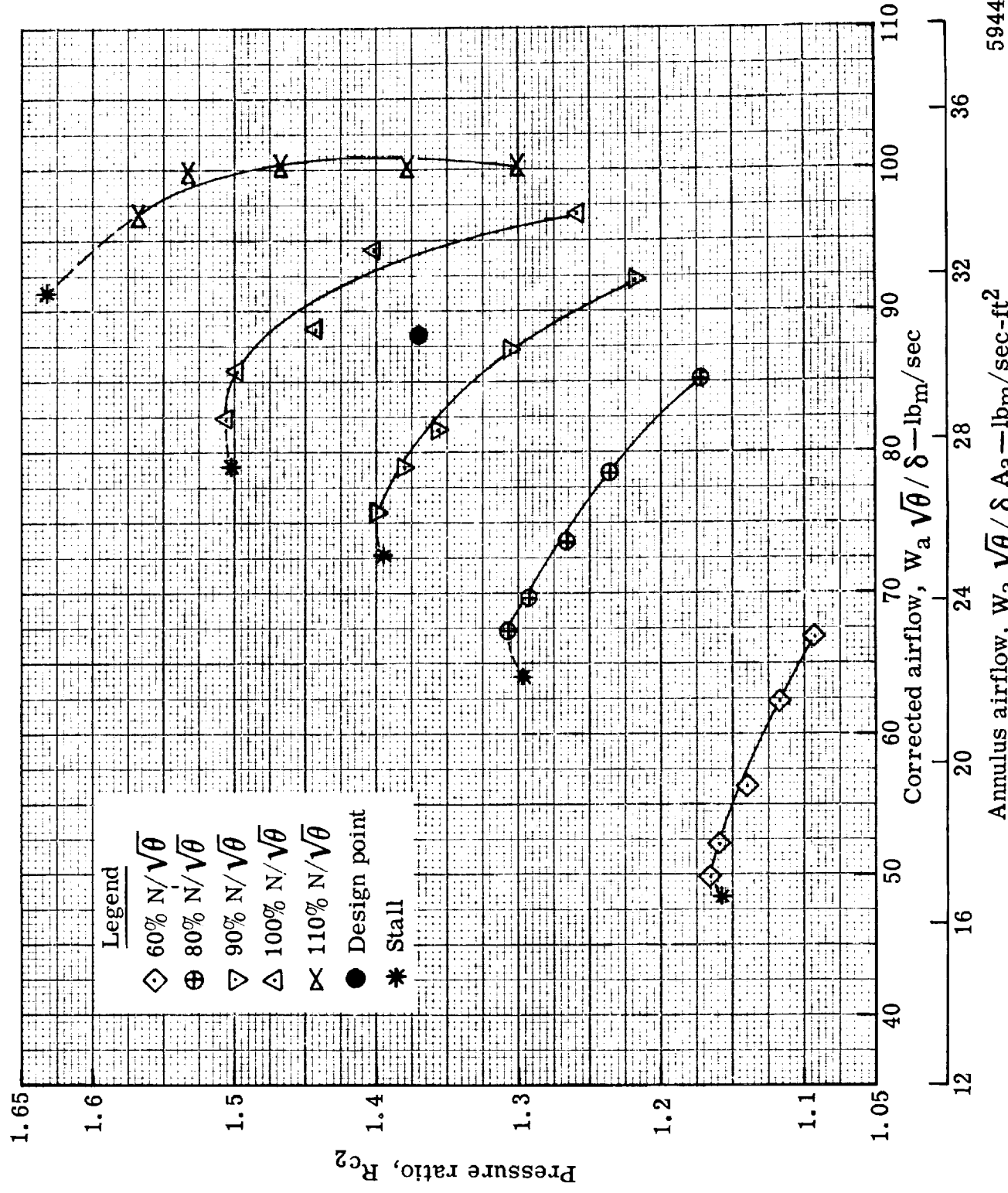


Figure 9. Flow generation rotor overall performance in stage test with the vane bleed flow at the optimum rate—pressure ratio.

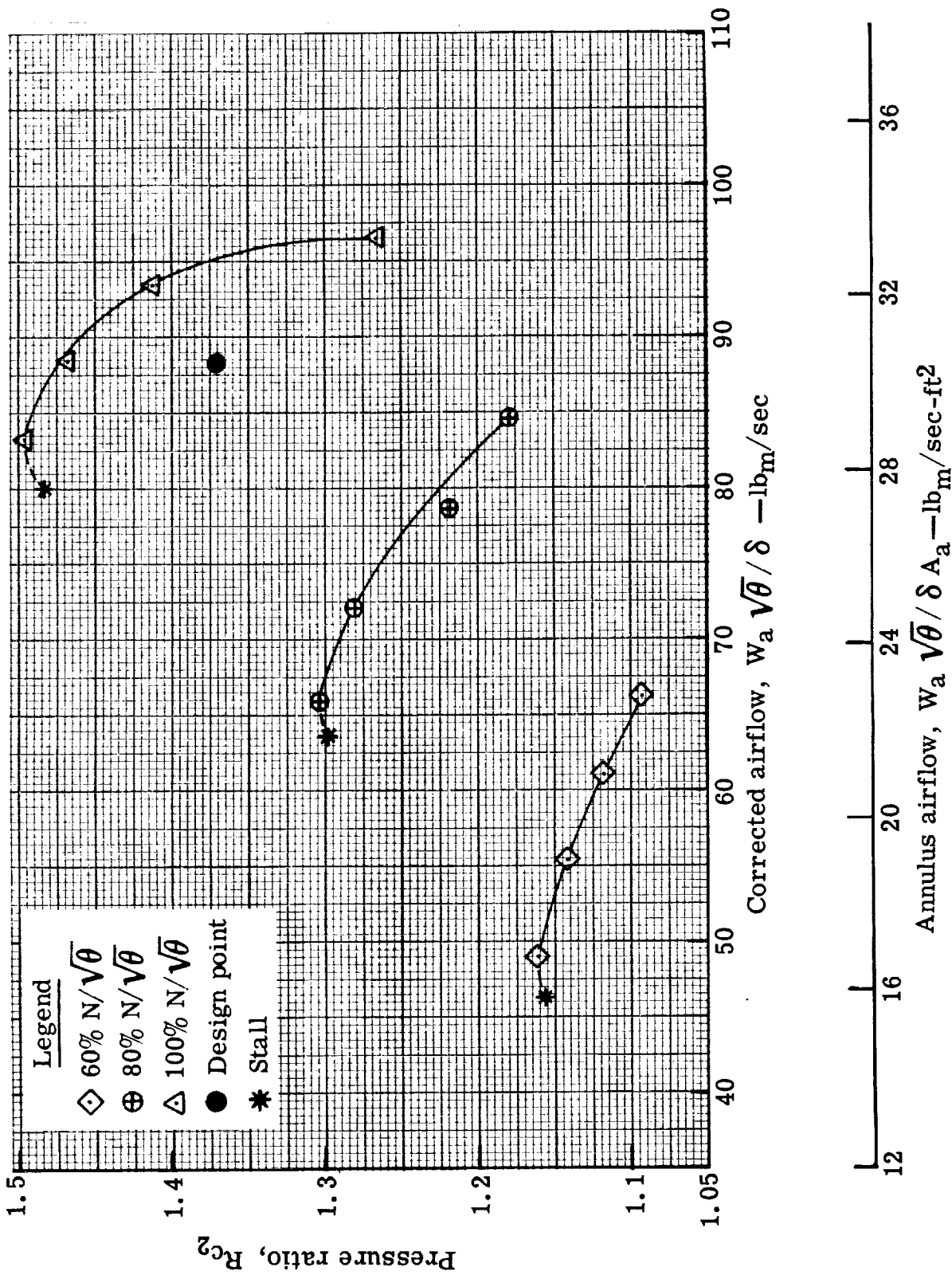


Figure 10. Flow generation rotor overall performance in stage test with the mean vane bleed flow rate—pressure ratio.

5944-11

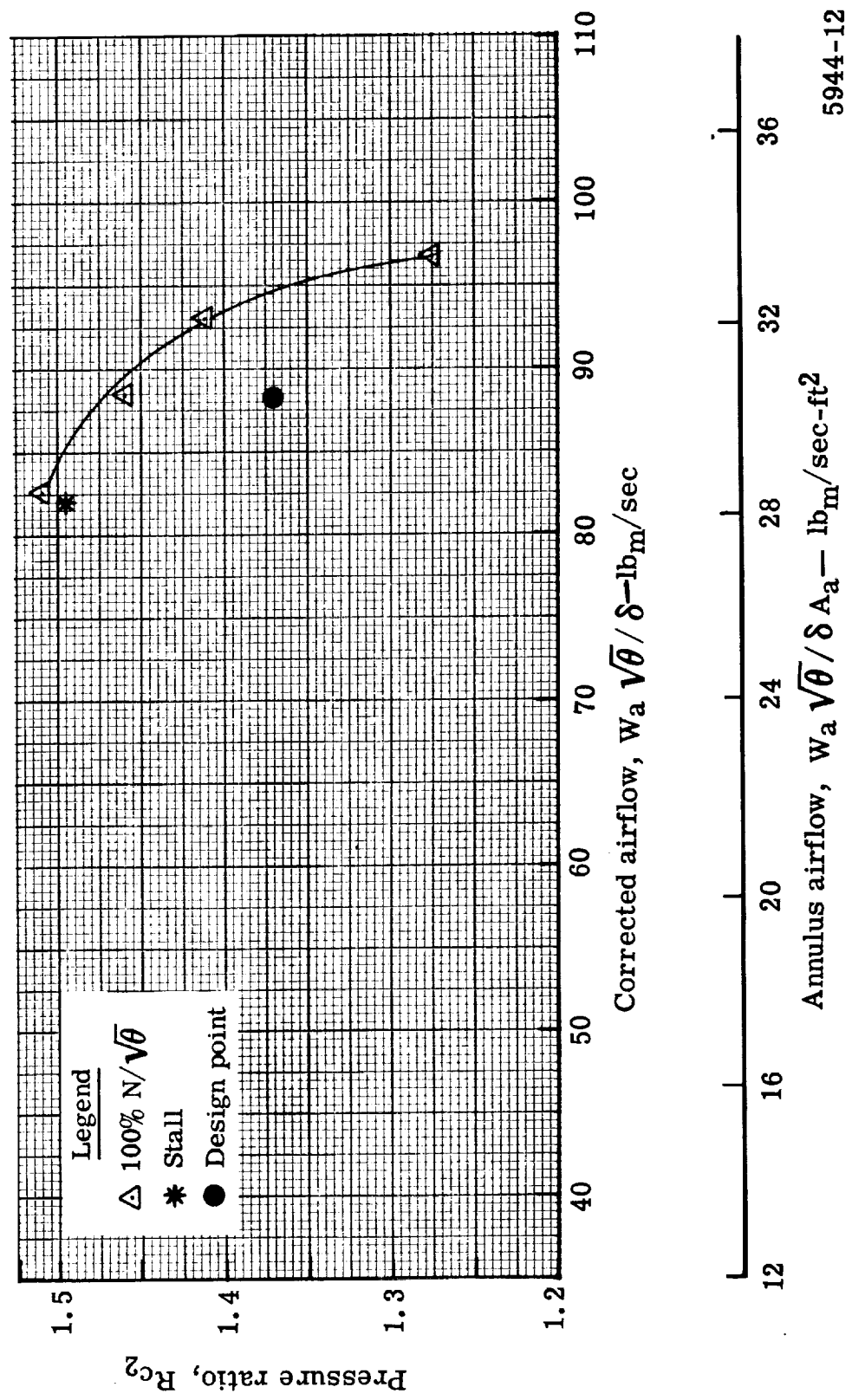


Figure 11. Flow generation rotor overall performance in stage test with zero vane bleed flow rate—pressure ratio.

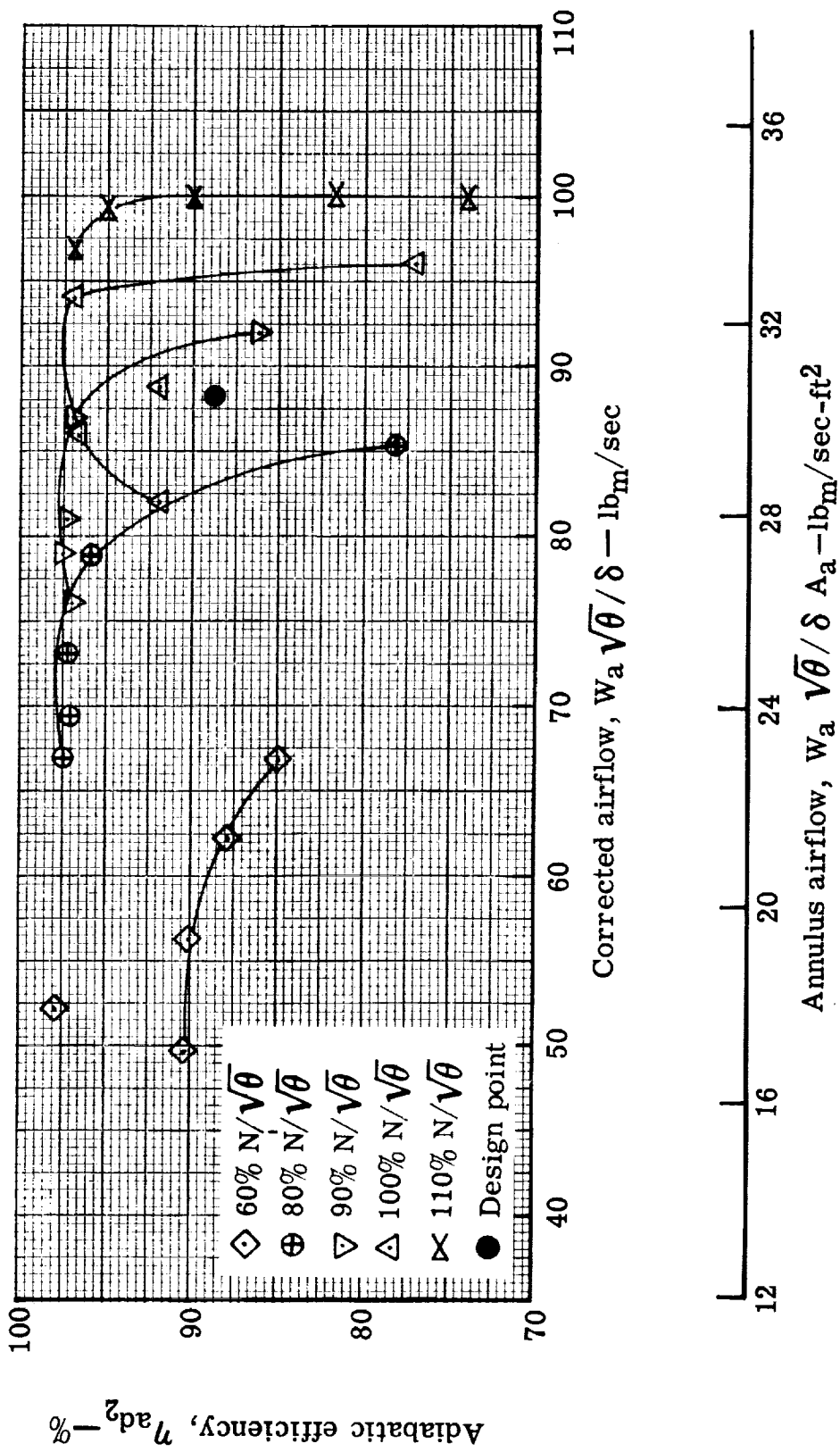


Figure 12. Flow generation rotor overall performance in stage test with the vane bleed flow at the optimum rate—adiabatic efficiency.

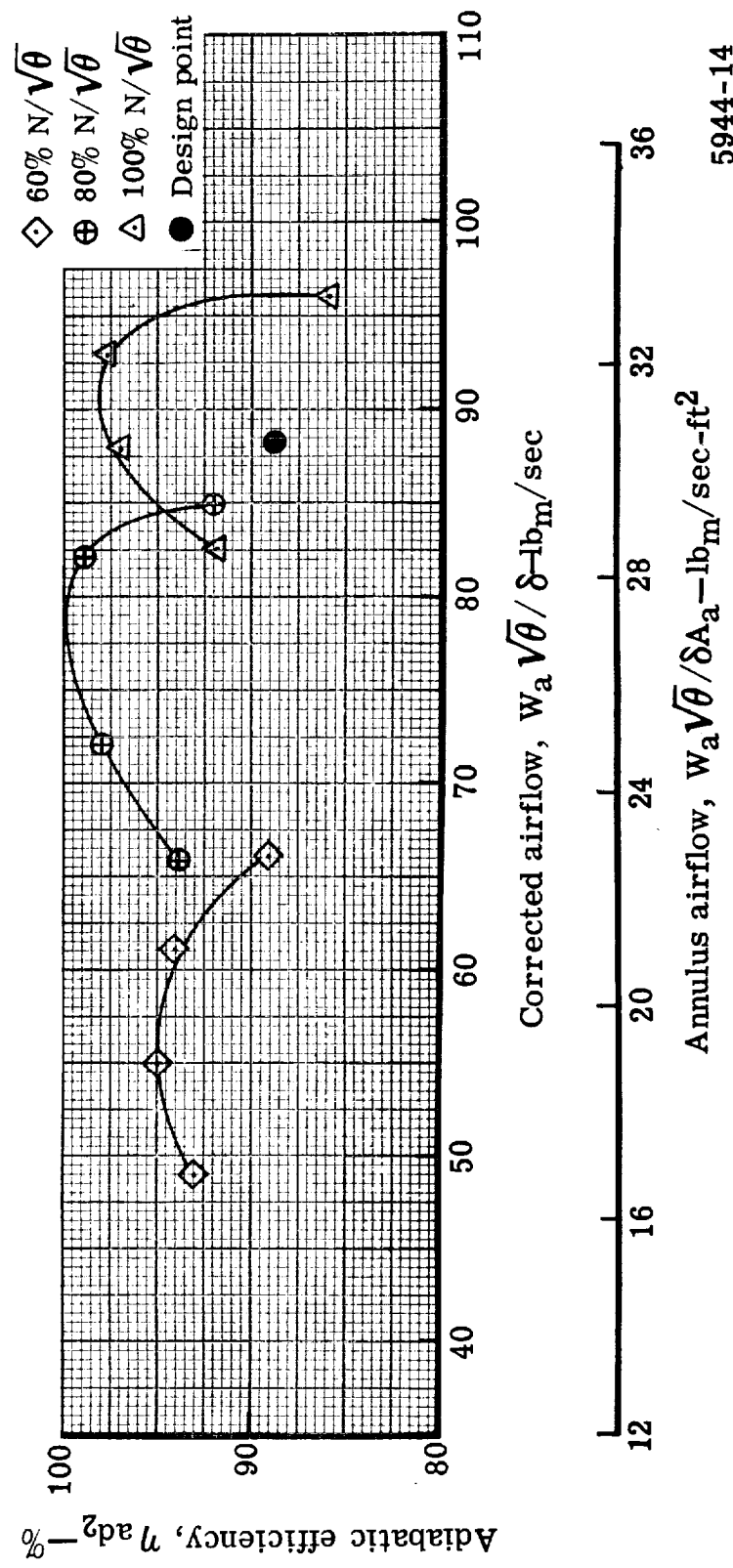


Figure 13. Flow generation rotor overall performance in stage test with the mean vane bleed flow rate—adiabatic efficiency.

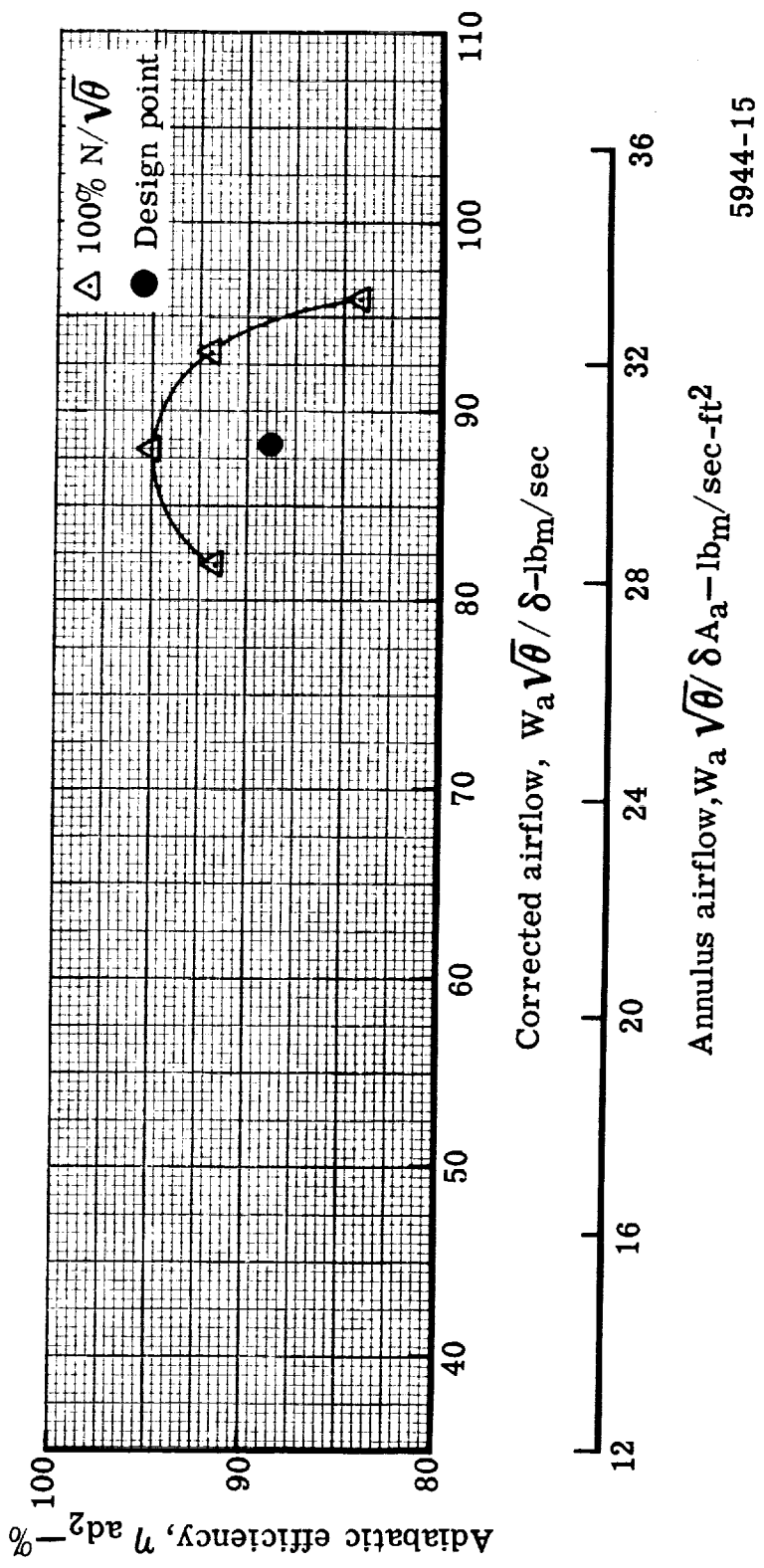


Figure 14. Flow generation rotor overall performance in stage test with zero vane bleed flow rate—adiabatic efficiency.

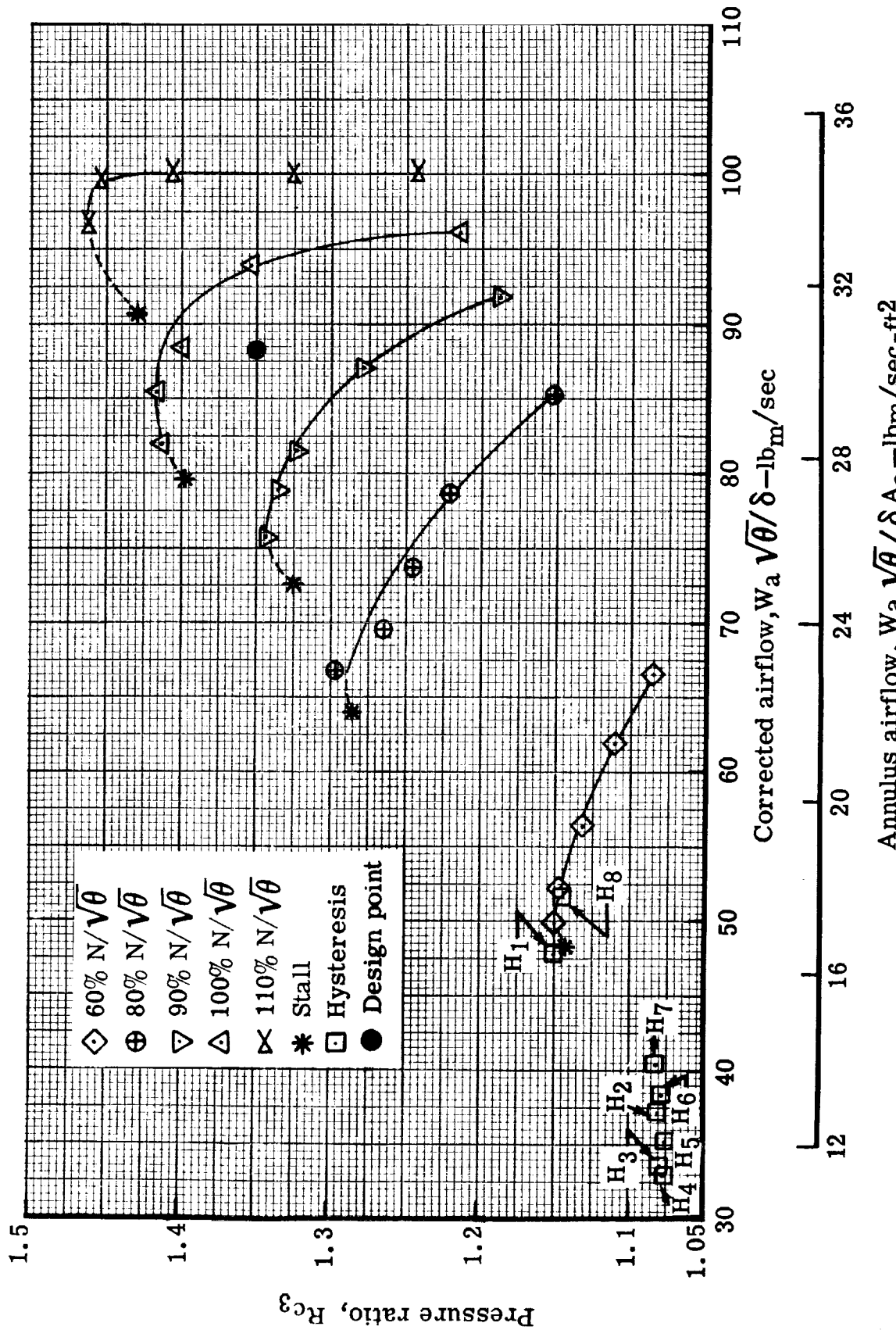


Figure 15. Overall stage performance of triple-slotted stator with the vane bleed flow at the optimum rate—pressure ratio.
5944-16

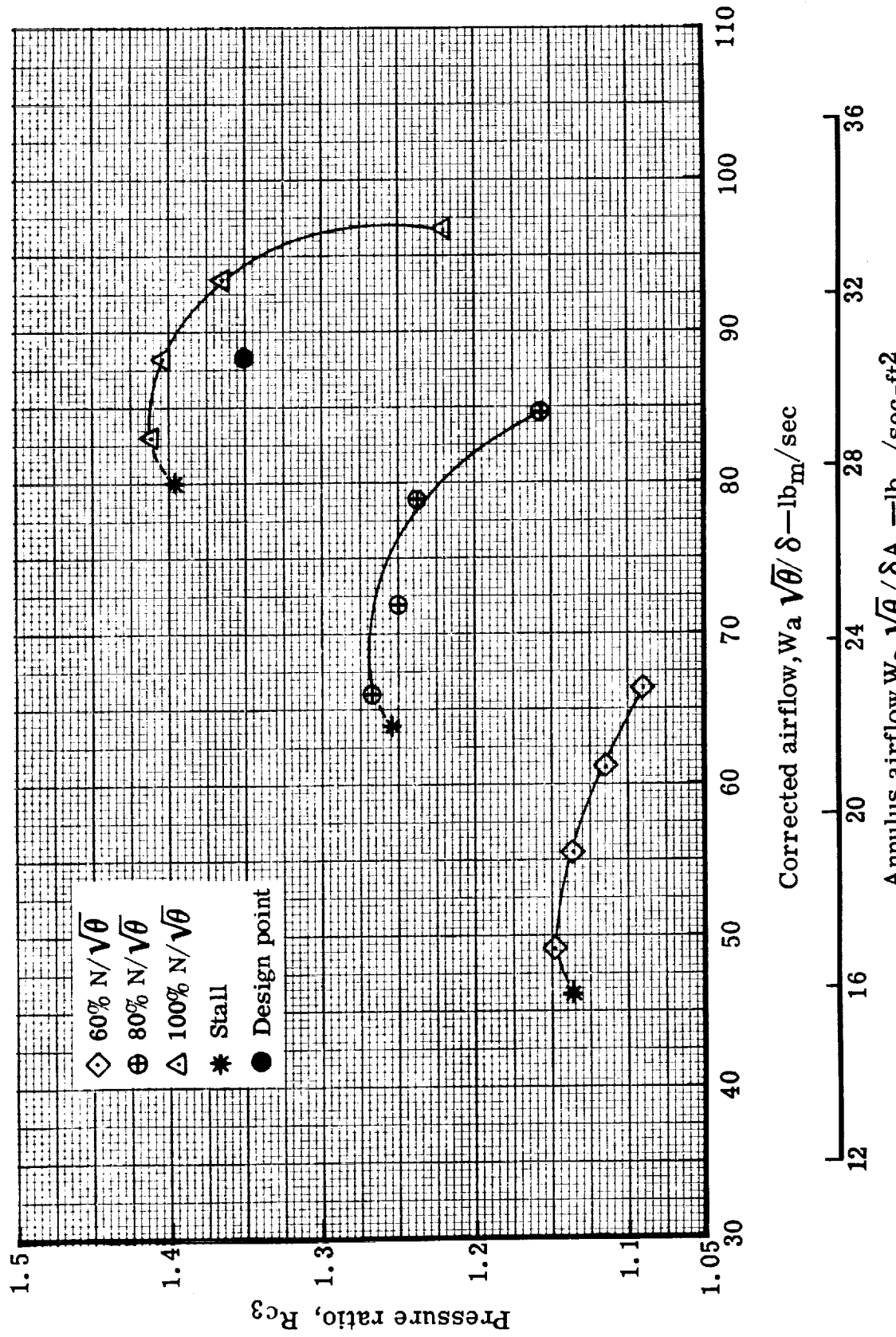


Figure 16. Overall stage performance of triple-slotted stator with the mean vane bleed flow rate-pressure ratio.
5944-17

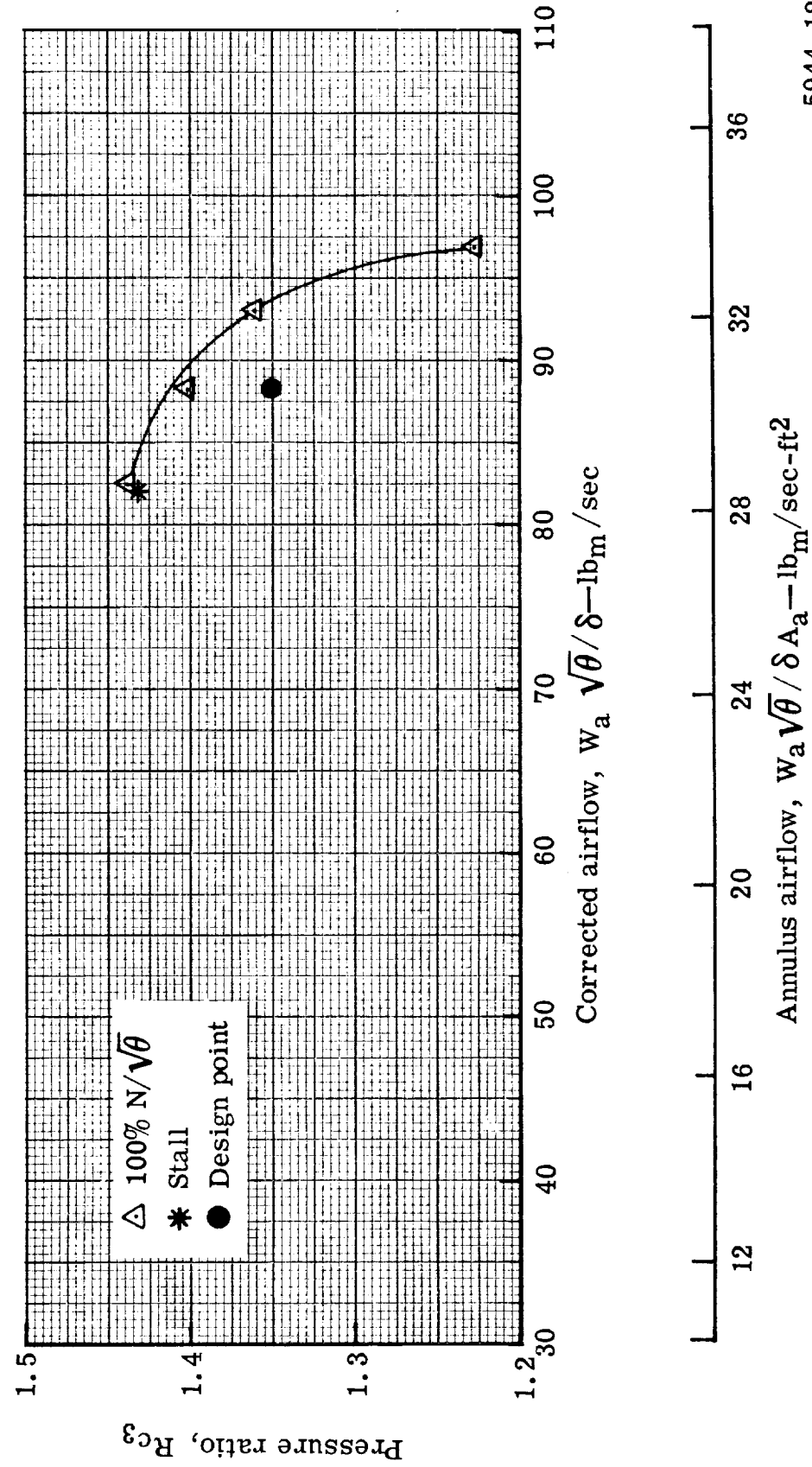


Figure 17. Overall stage performance of triple-slotted stator with zero vane bleed flow rate—pressure ratio.

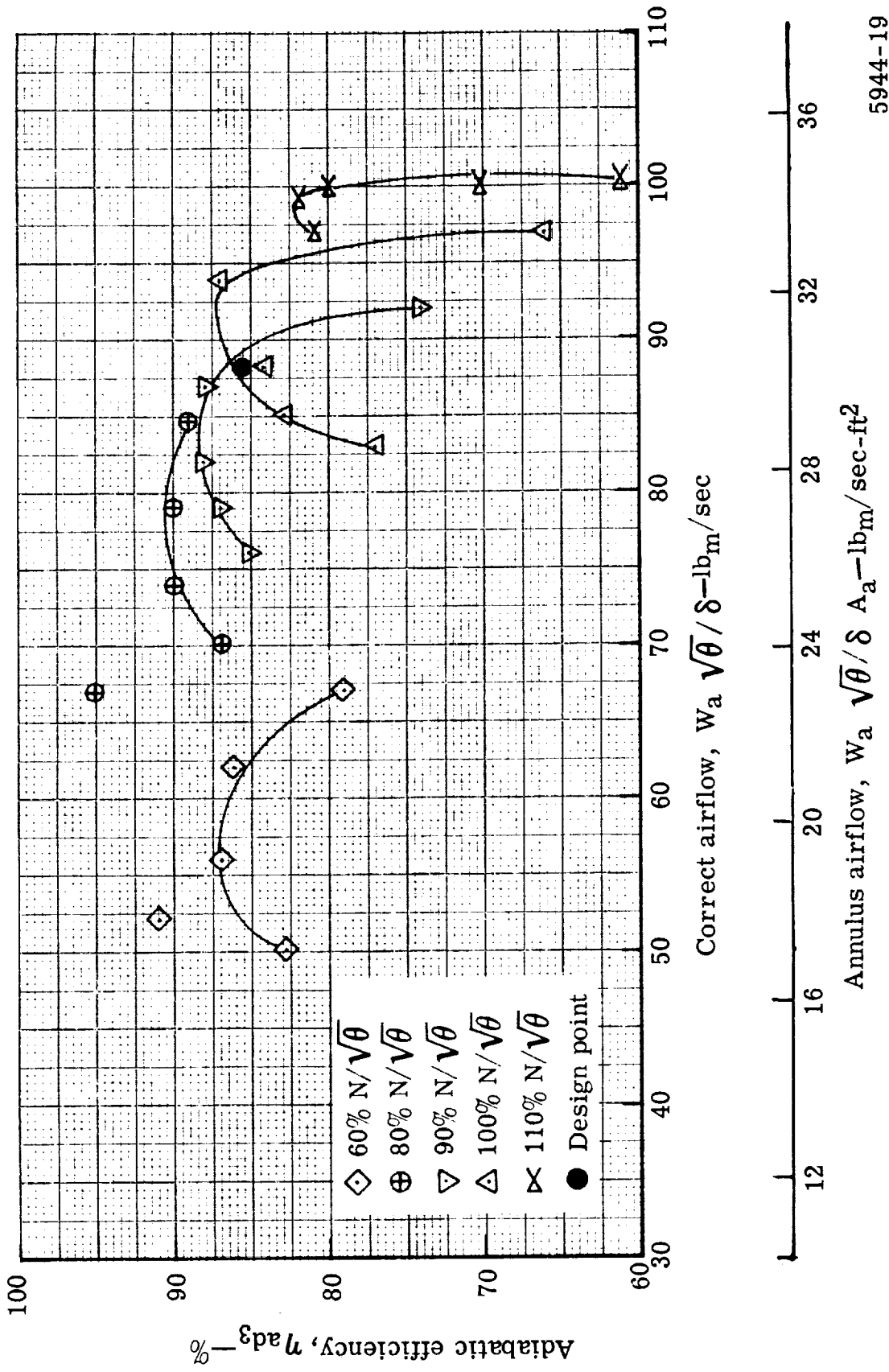


Figure 18. Overall stage performance of triple-slotted stator with the vane bleed flow at the optimum rate—adiabatic efficiency.

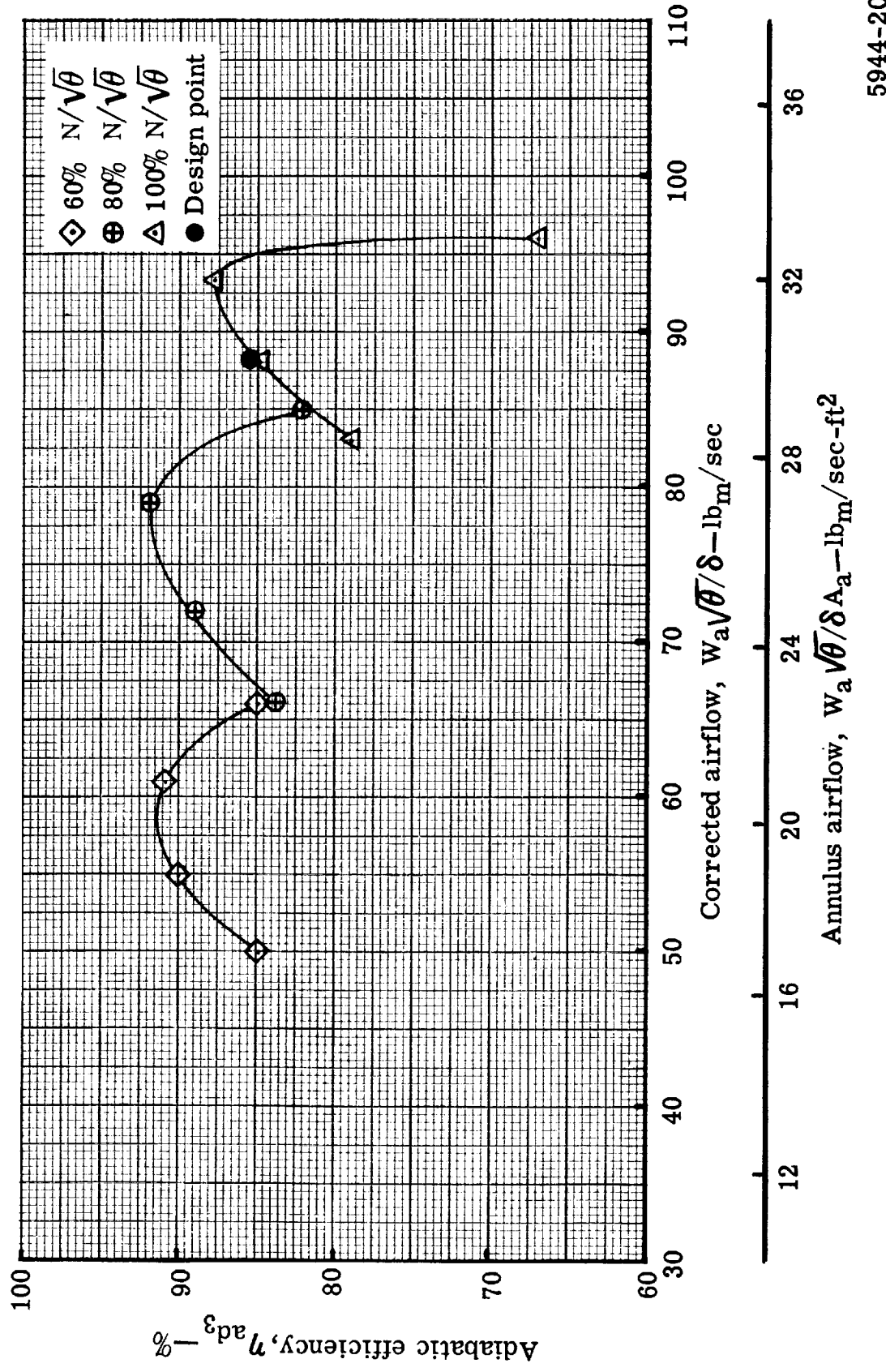


Figure 19. Overall stage performance of triple-slotted stator with the mean vane bleed flow rate—adiabatic efficiency.

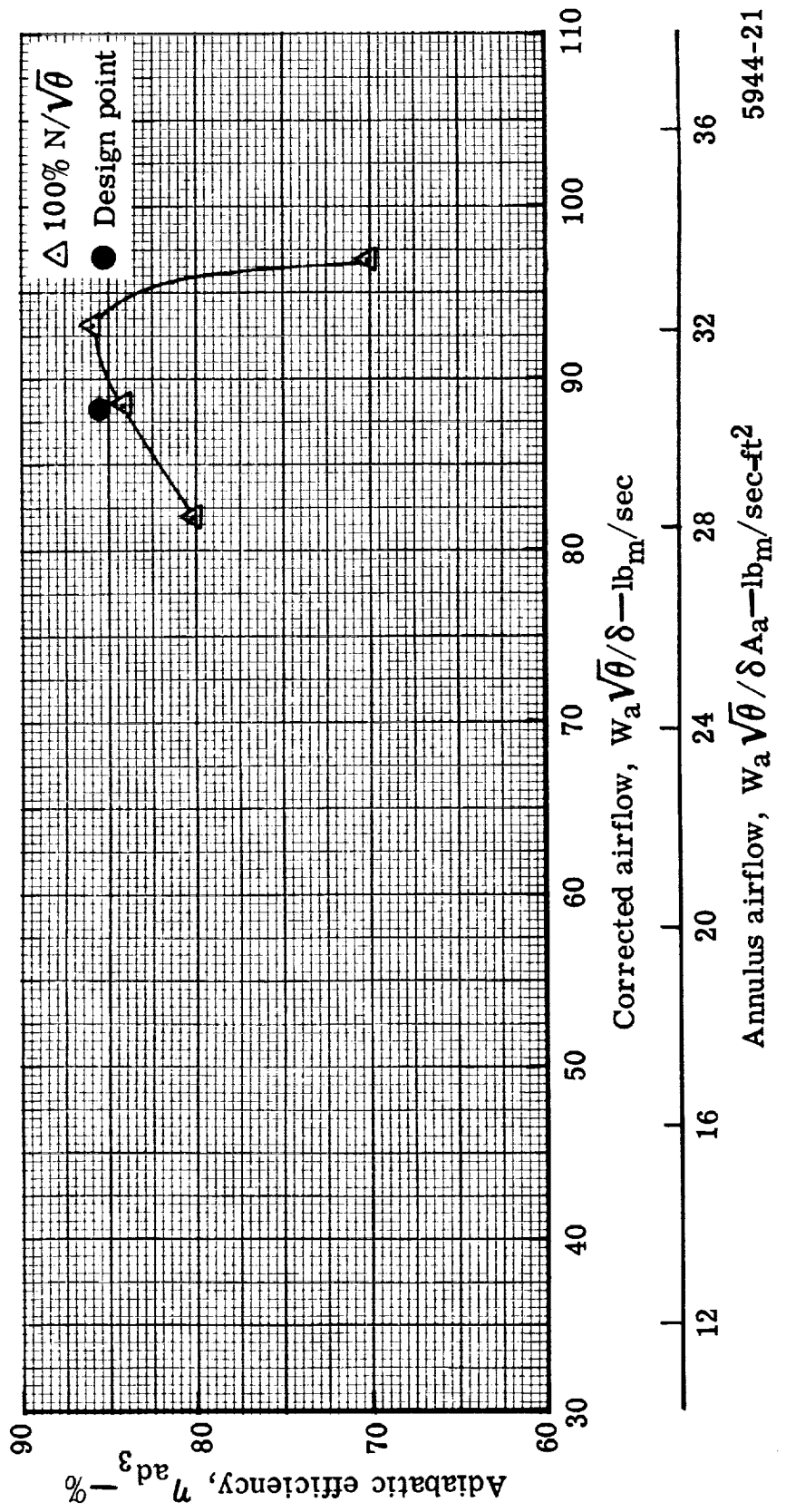


Figure 20. Overall stage performance of triple-slotted stator with zero vane bleed flow rate—adiabatic efficiency.

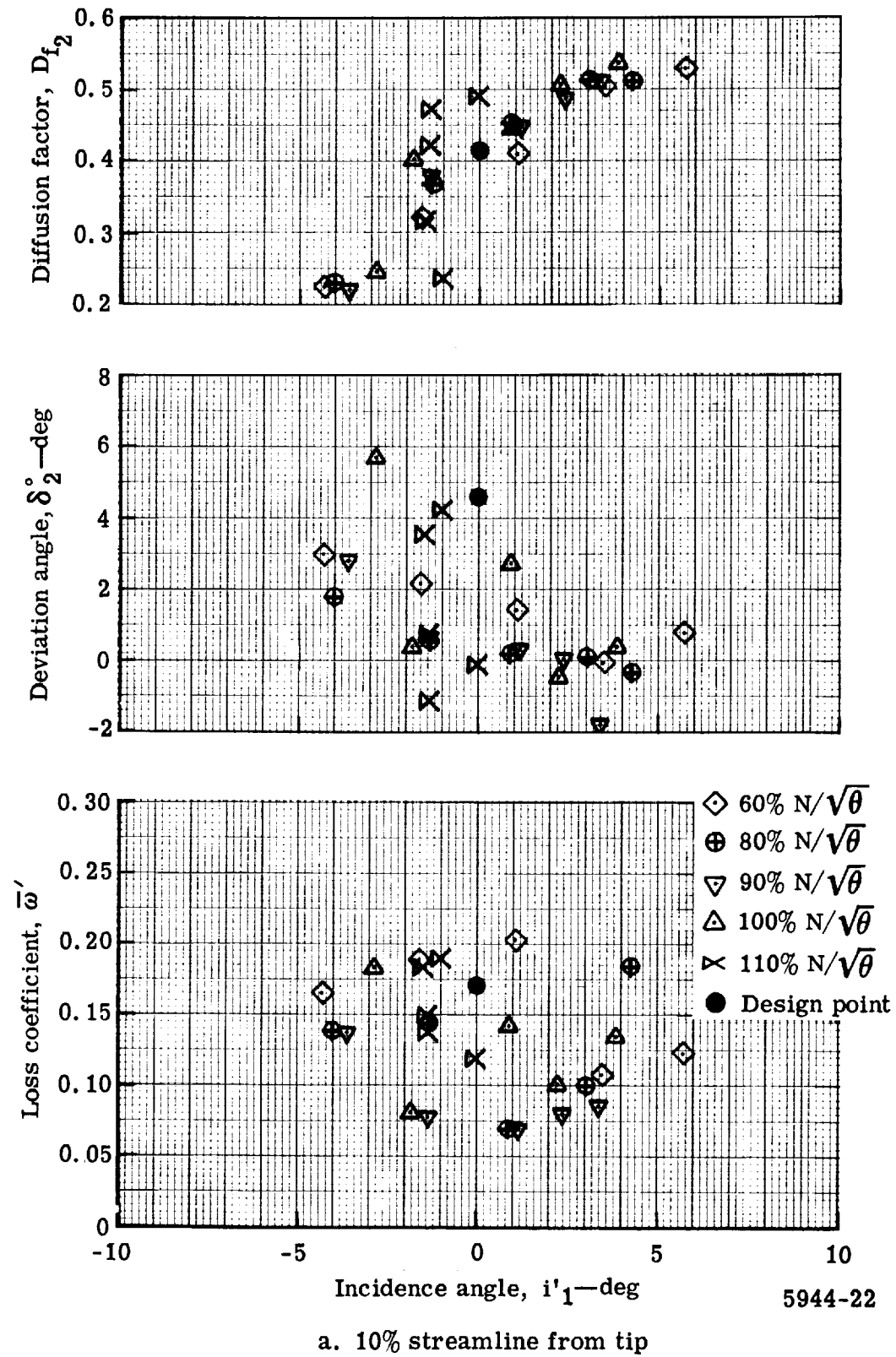


Figure 21. Rotor blade element performance for stage test with the vane bleed flow at the optimum rate.

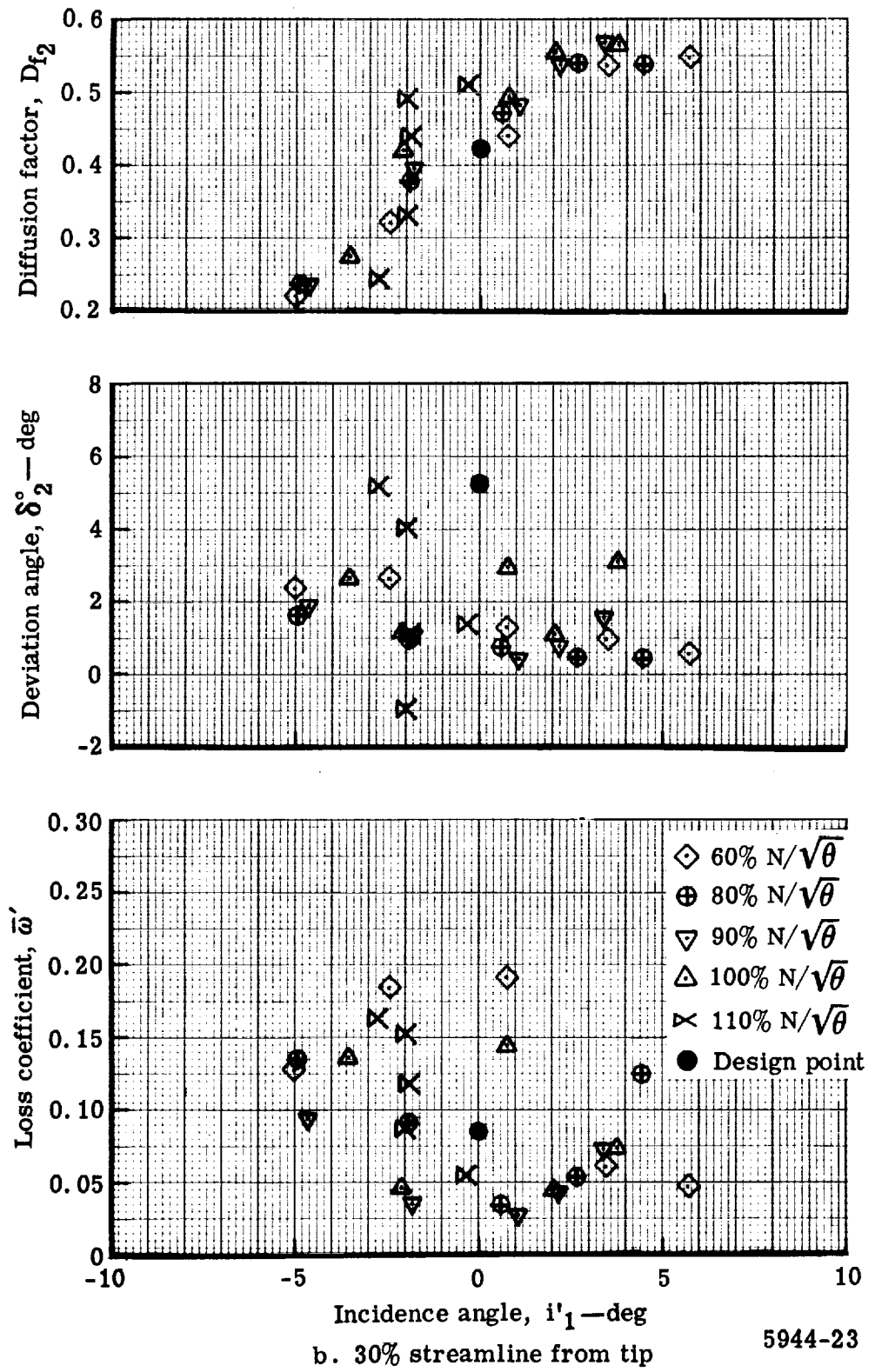
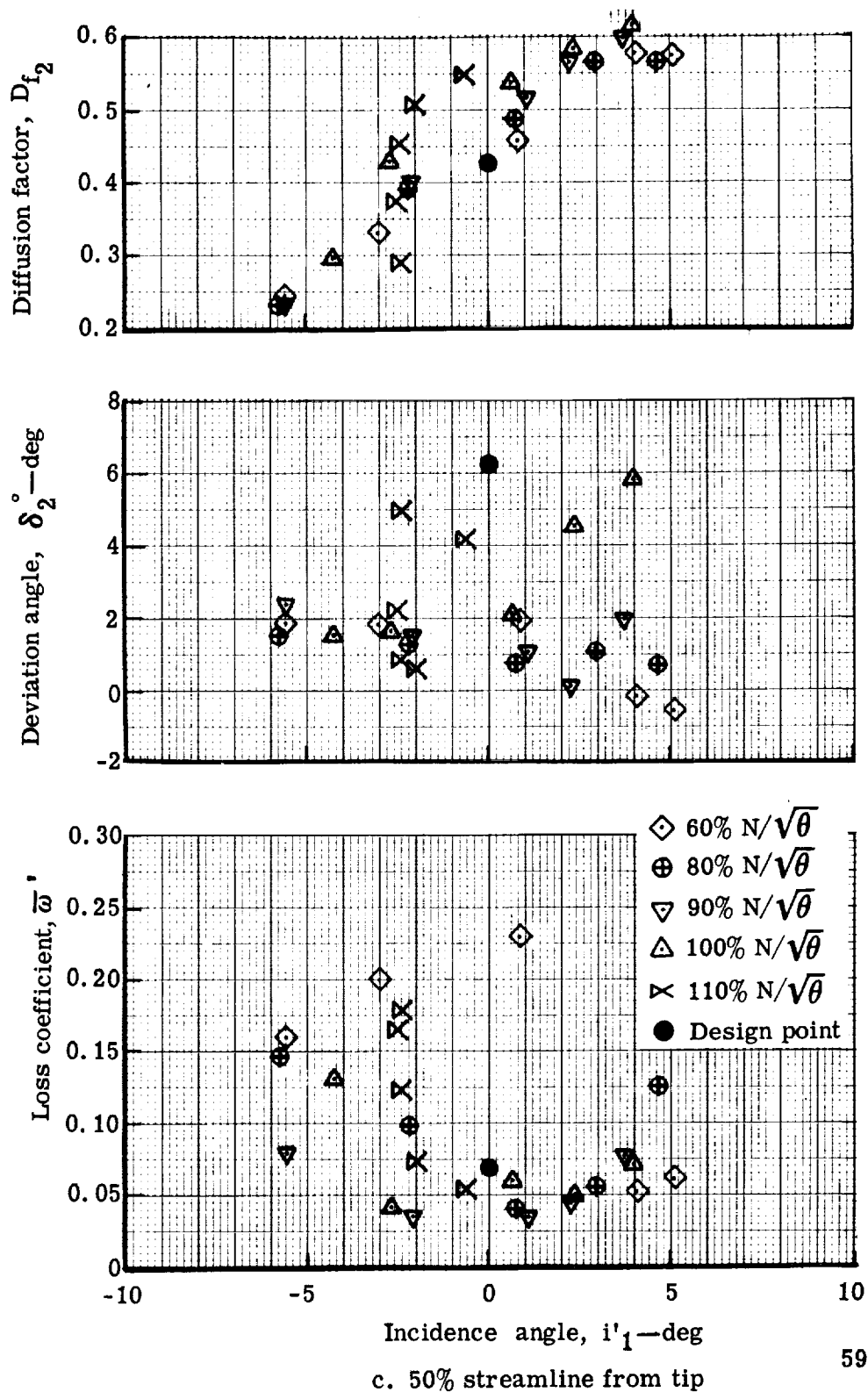
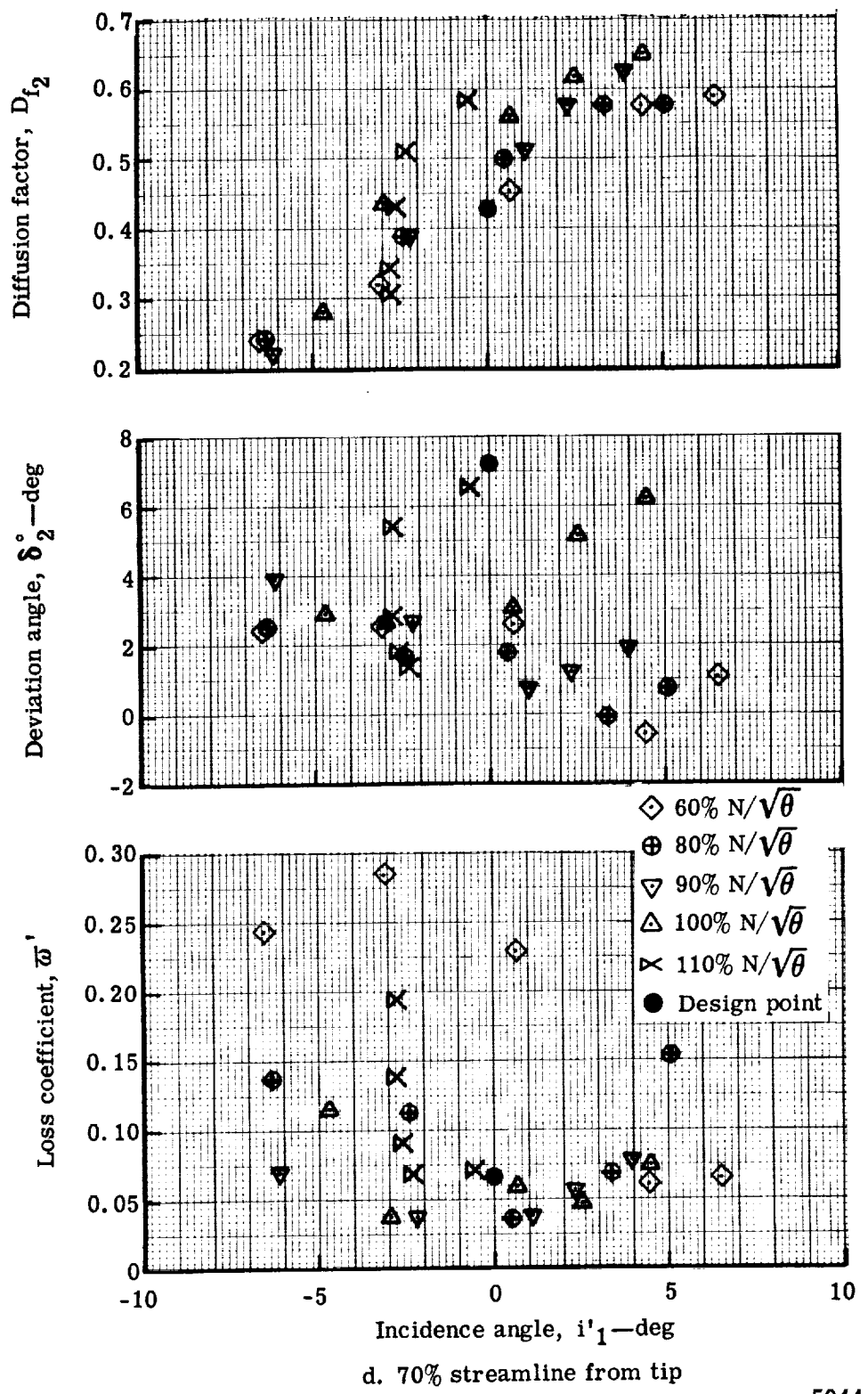


Figure 21. Rotor blade element performance for stage test with the vane bleed flow at the optimum rate.



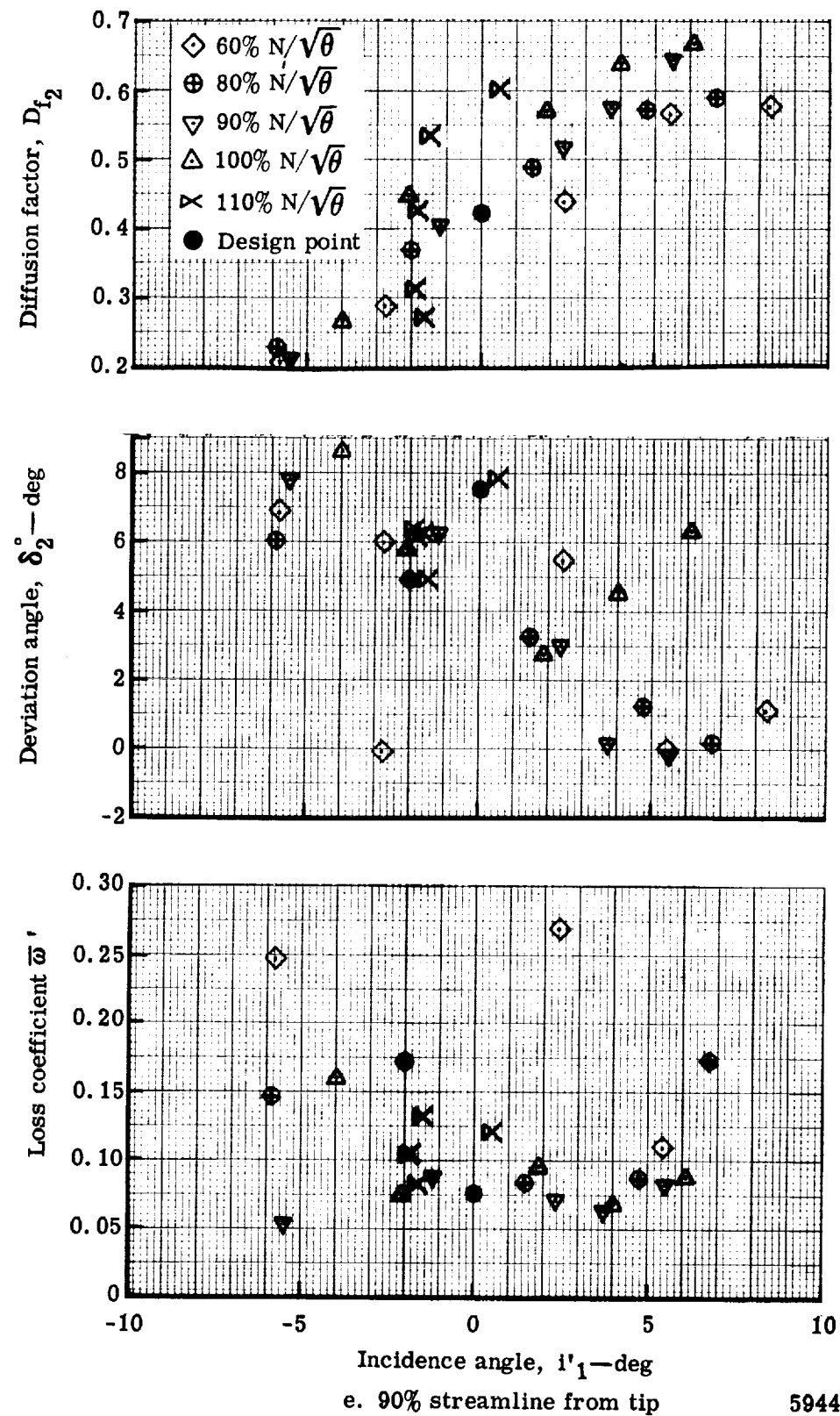
5944-24

Figure 21. Rotor blade element performance for stage test with the vane bleed flow at the optimum rate.



5944-25

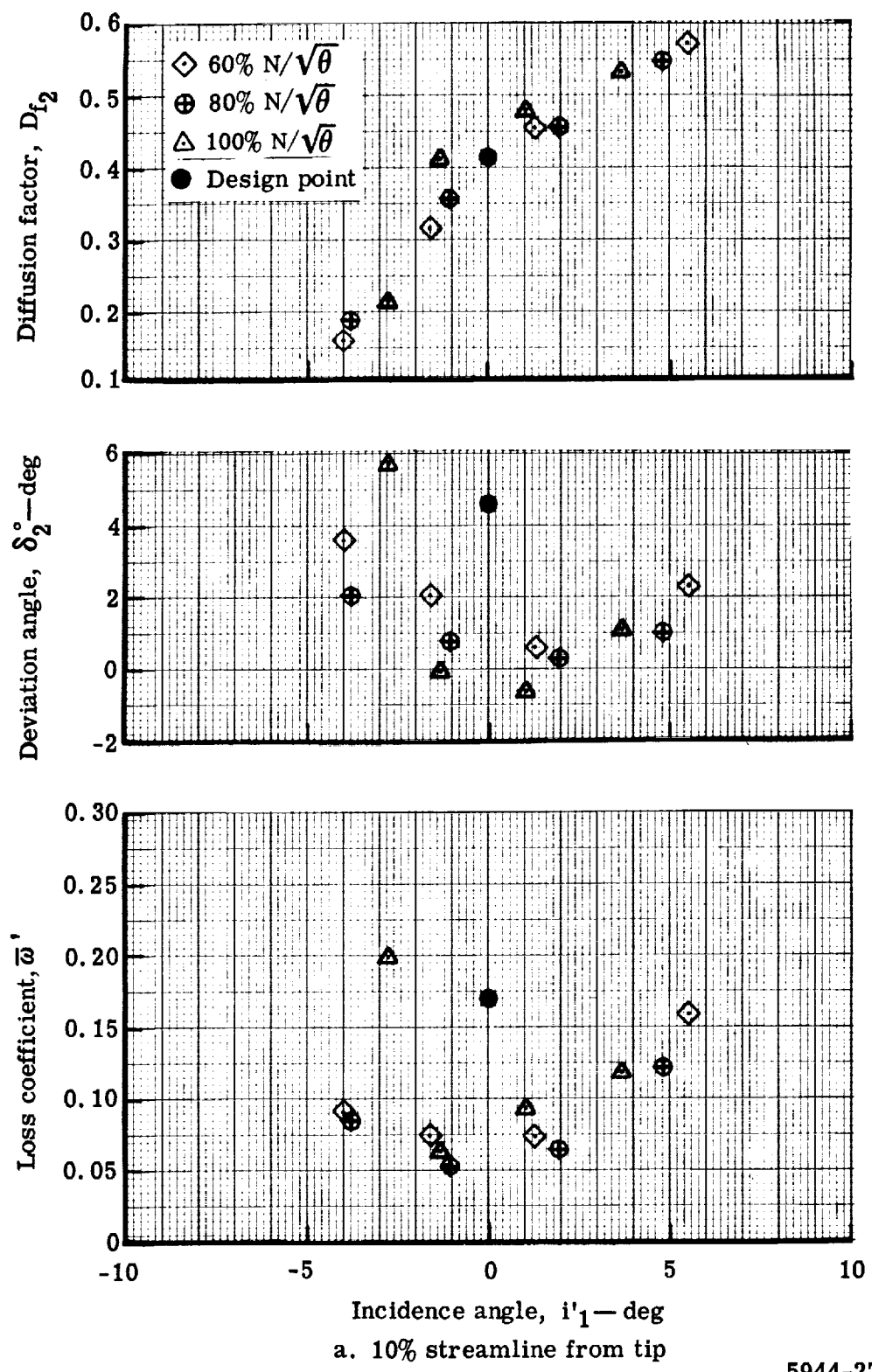
Figure 21. Rotor blade element performance for stage test with the vane bleed flow at the optimum rate.



e. 90% streamline from tip

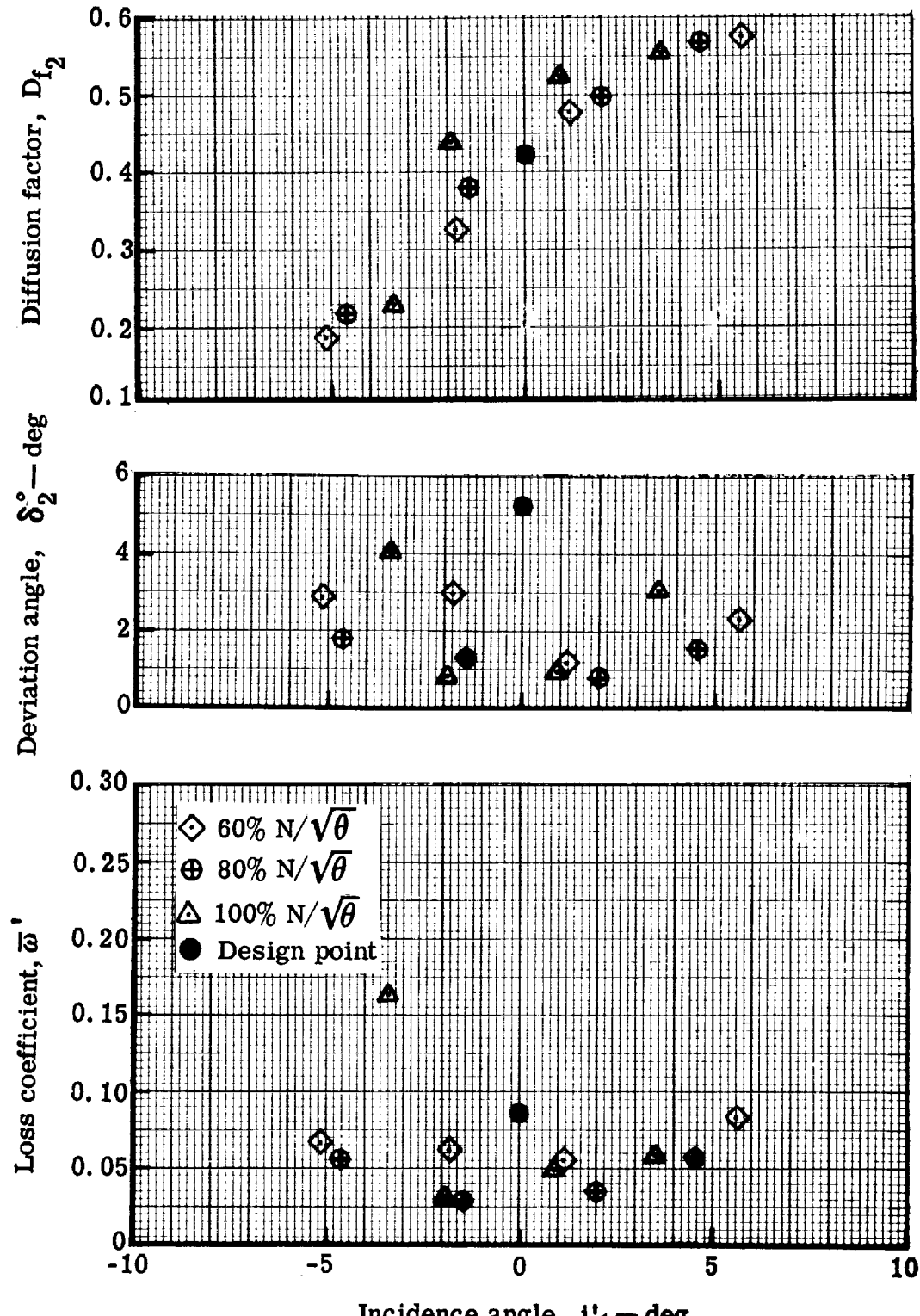
5944-26

Figure 21. Rotor blade element performance for stage test with the vane bleed flow at the optimum rate.



5944-27

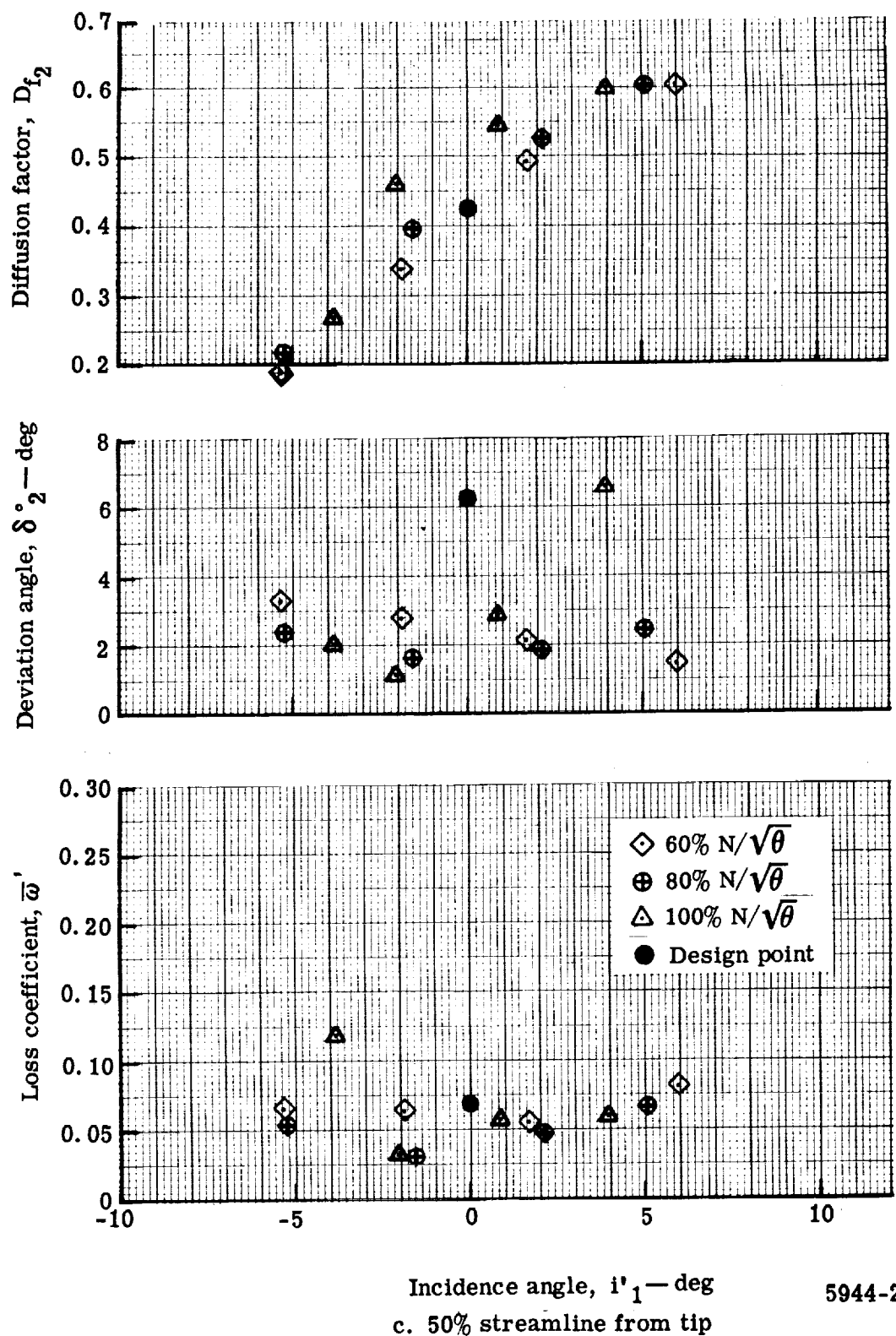
Figure 22. Rotor blade element performance for stage test with the mean vane bleed flow rate.



b. 30% streamline from tip

5944-28

Figure 22. Rotor blade element performance for stage test with the mean vane bleed flow.



Incidence angle, i'_1 — deg 5944-29
c. 50% streamline from tip

Figure 22. Rotor blade element performance for stage test with the mean vane bleed flow rate.

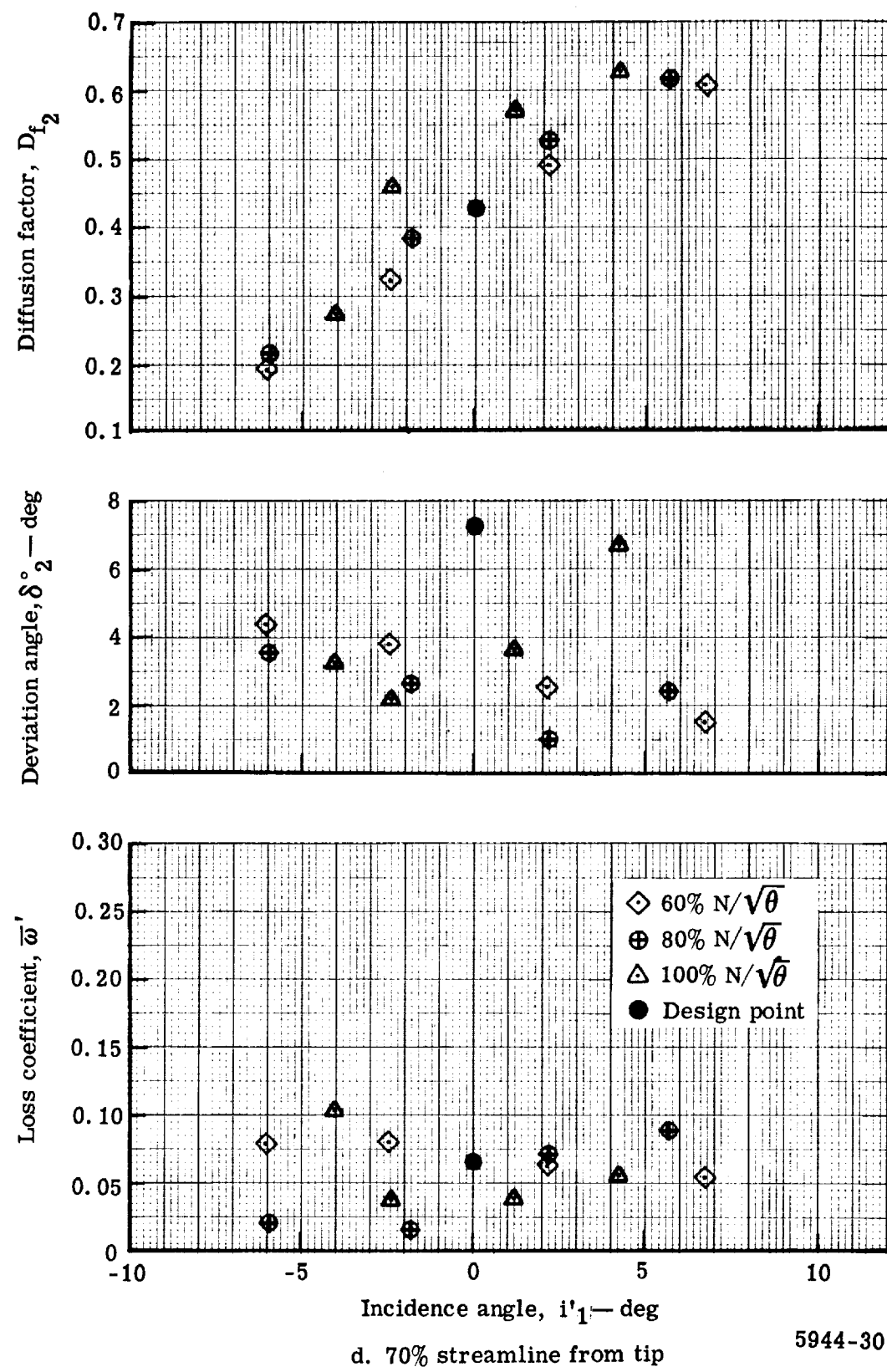


Figure 22. Rotor blade element performance for stage test with the mean vane bleed flow rate.

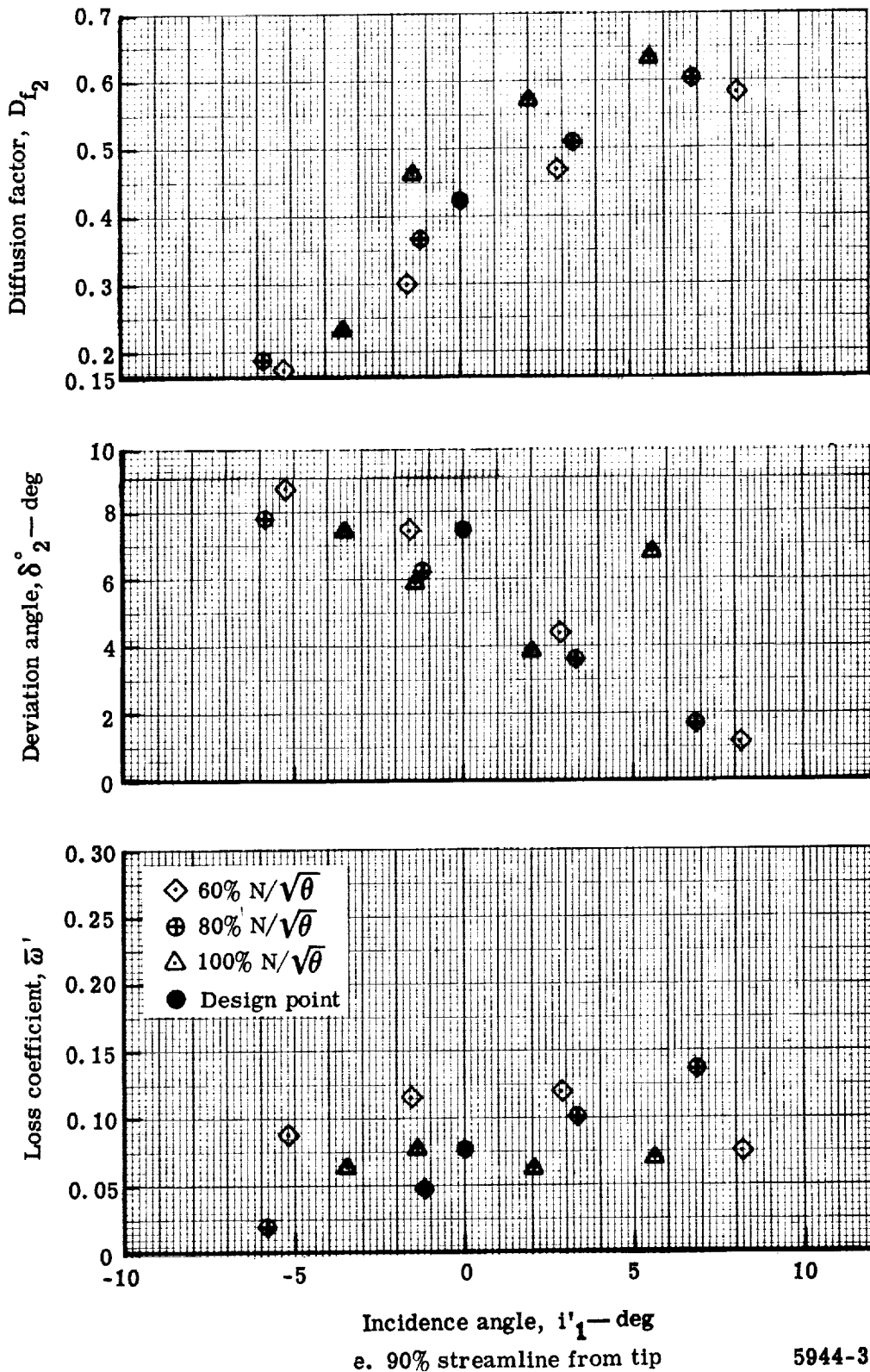


Figure 22. Rotor blade element performance for stage test with the mean vane bleed flow rate.

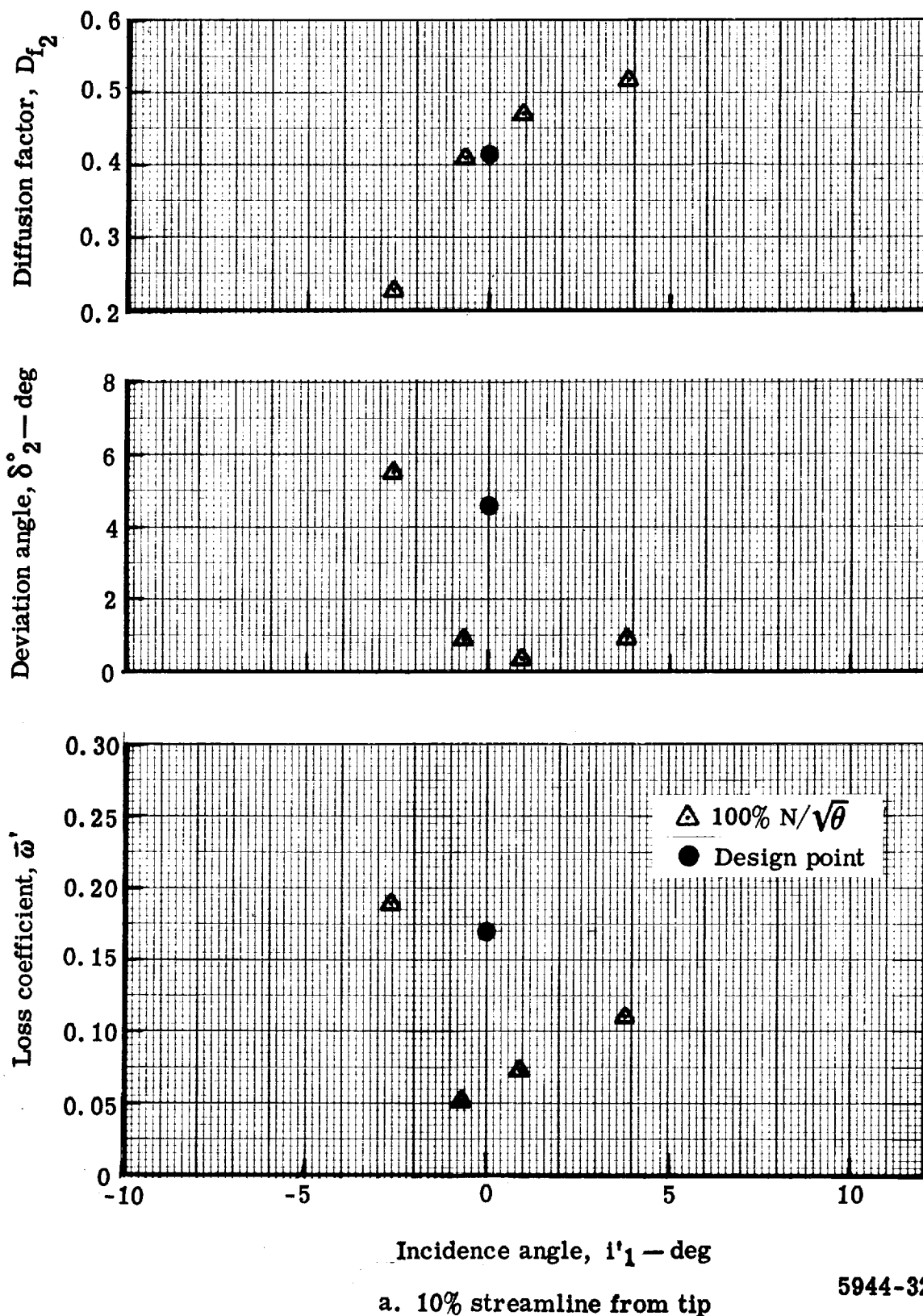


Figure 23. Rotor blade element performance for stage test with zero vane bleed flow rate.

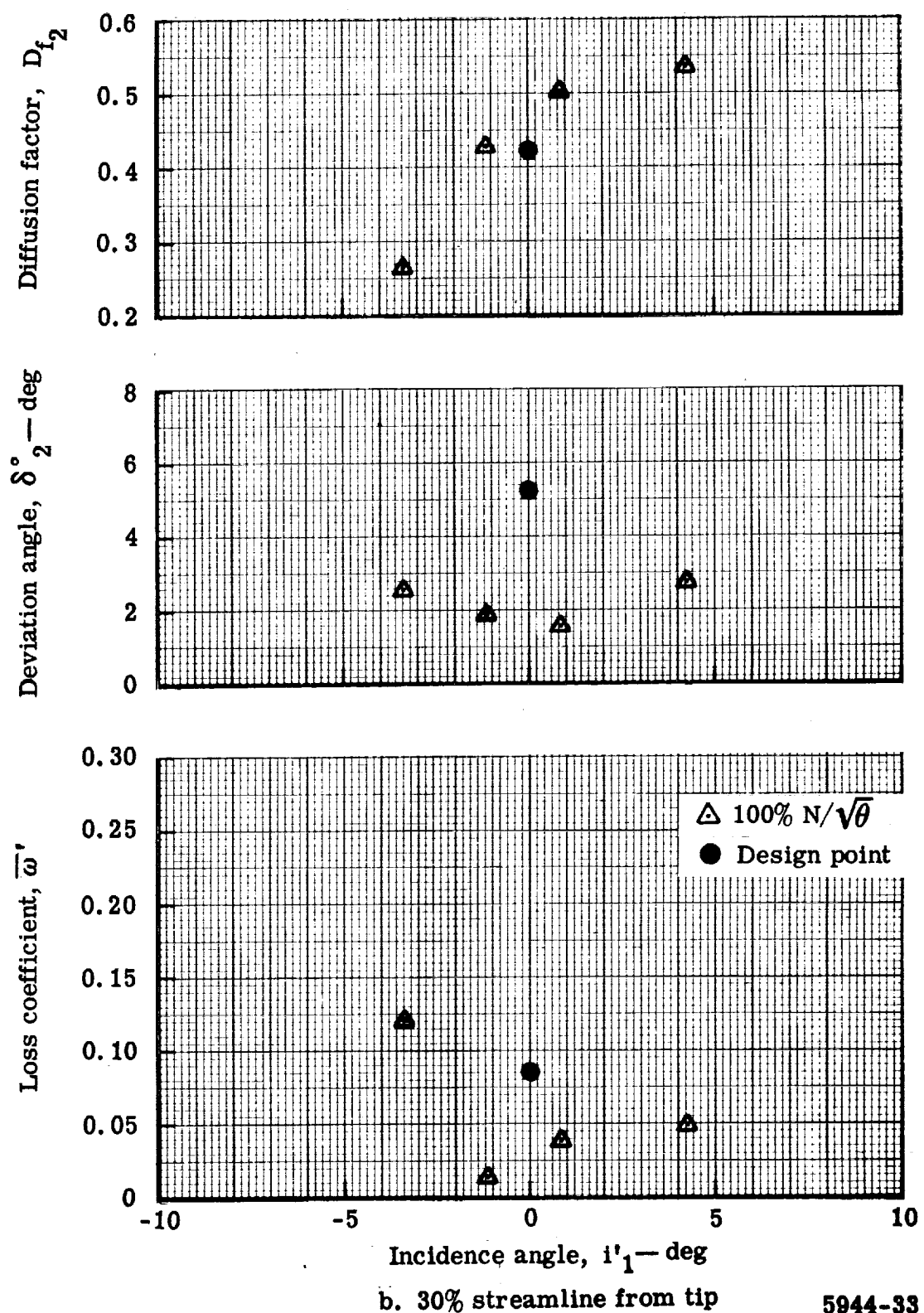


Figure 23. Rotor blade element performance for stage test with zero vane bleed flow rate.

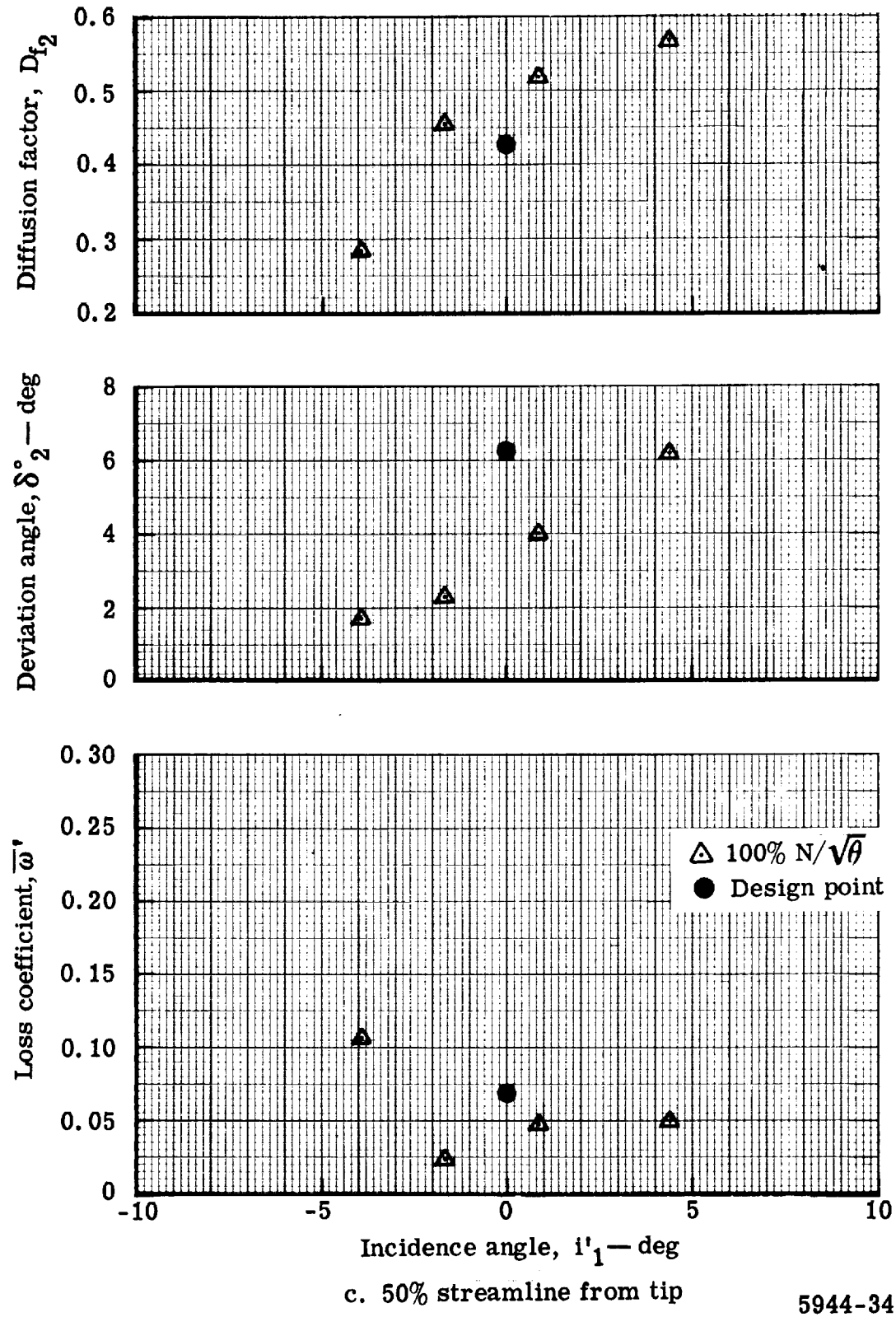


Figure 23. Rotor blade element performance for stage test with zero vane bleed flow rate.

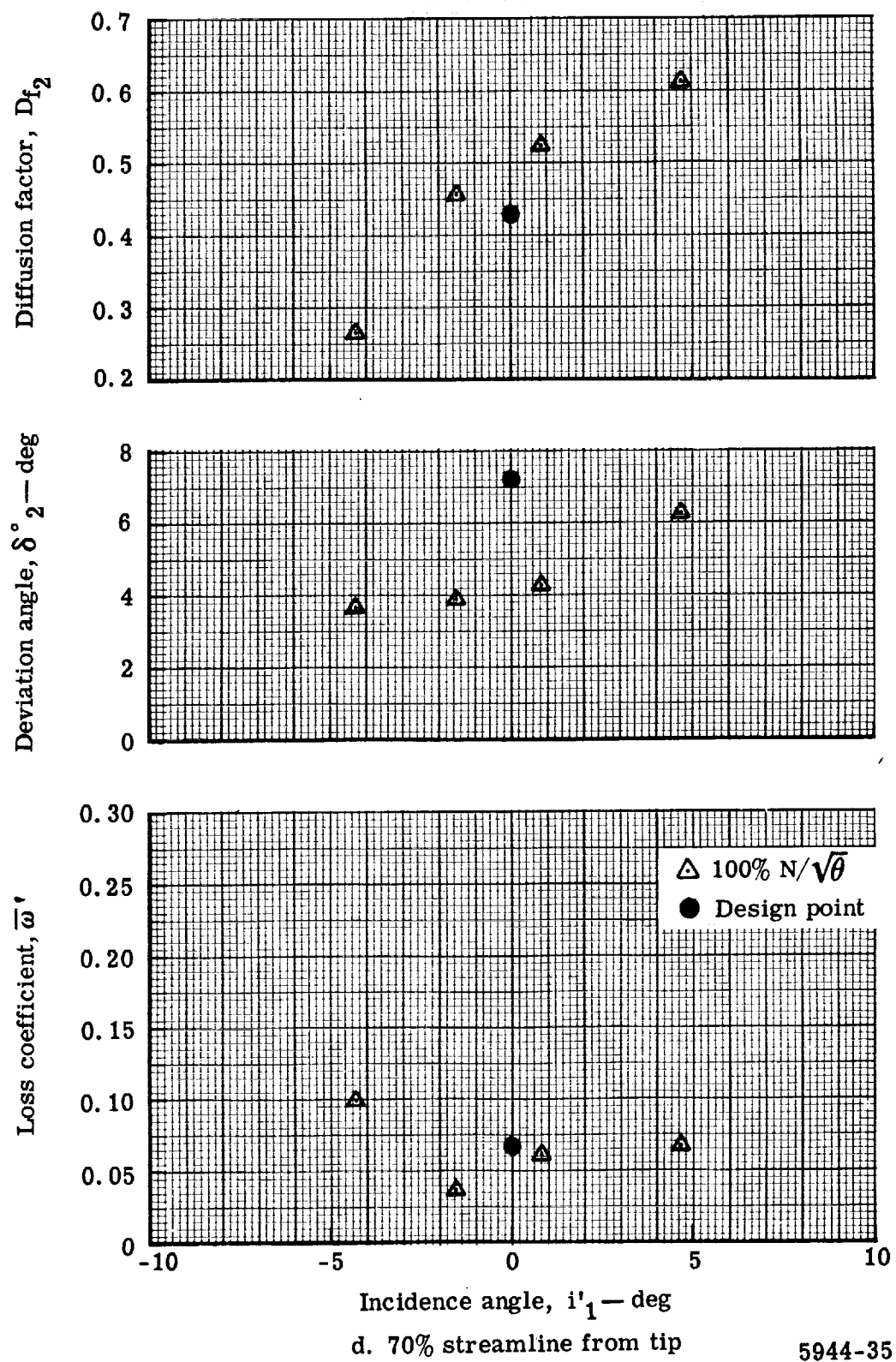


Figure 23. Rotor blade element performance for stage test with zero vane bleed flow rate.

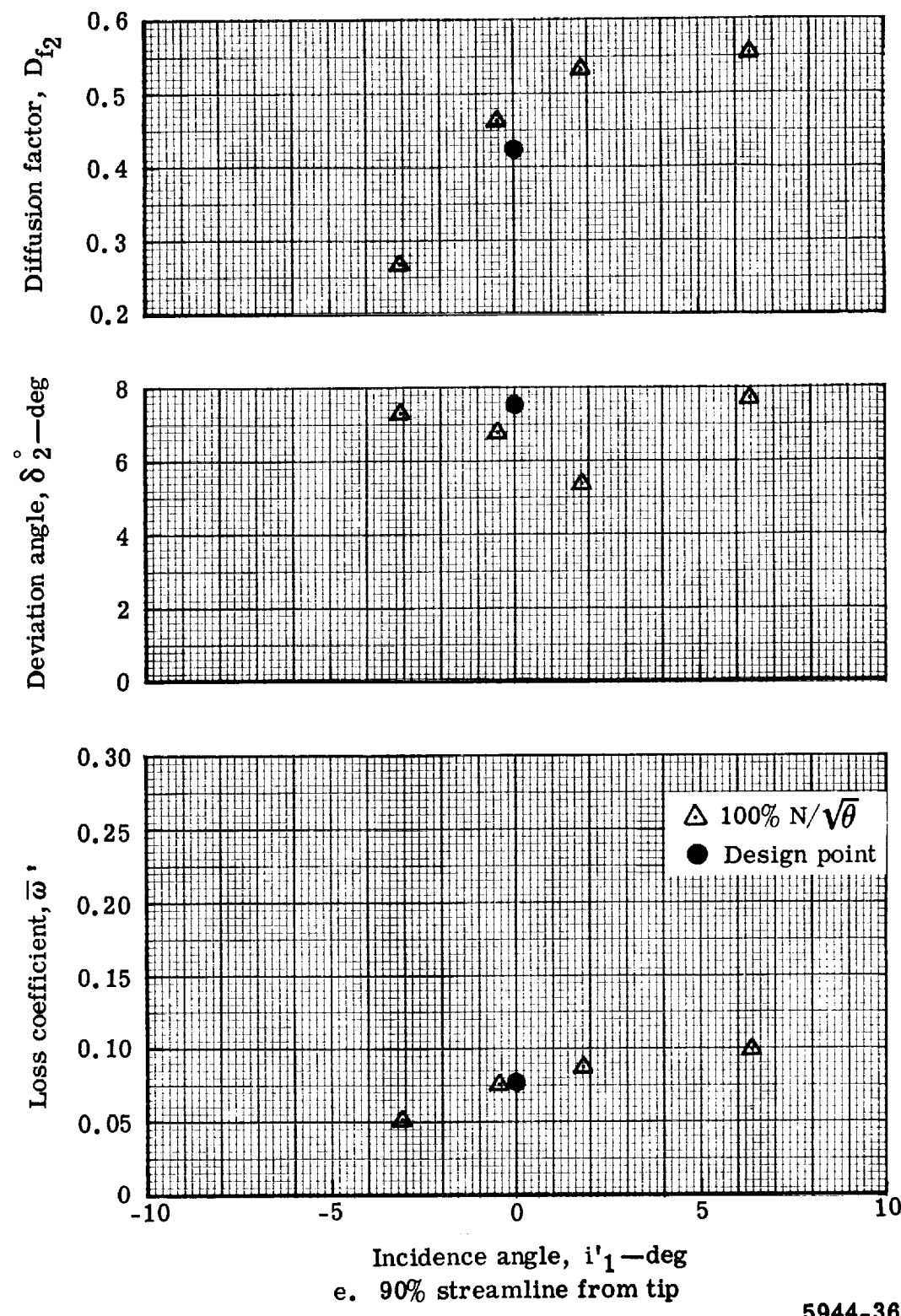


Figure 23. Rotor blade element performance for stage test with zero vane bleed flow rate.

— Design, $W_a \sqrt{\theta} / \delta = 88.2 \text{ lb}_m/\text{sec}$, $N/\sqrt{\theta} = 100\%$
 ○ Flow generation rotor test, $W_a \sqrt{\theta} / \delta = 89.3 \text{ lb}_m/\text{sec}$, $N/\sqrt{\theta} = 99.3\%$
 □ Triple-slotted stator test, $W_a \sqrt{\theta} / \delta = 88.6 \text{ lb}_m/\text{sec}$, $N/\sqrt{\theta} = 99.8\%$

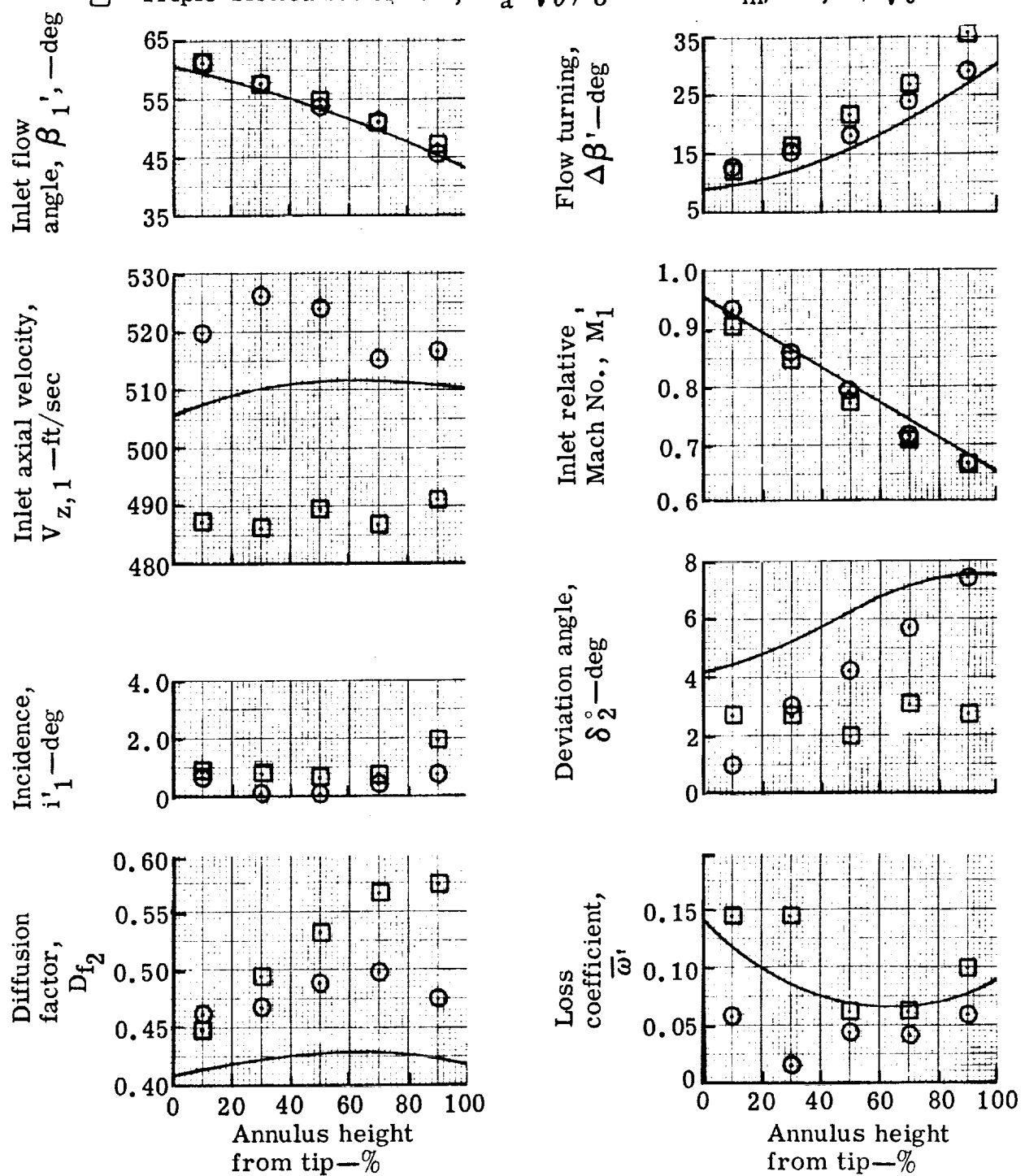


Figure 24. Radial variation of rotor blade element performance with the vane bleed flow at the optimum rate.

5944-37

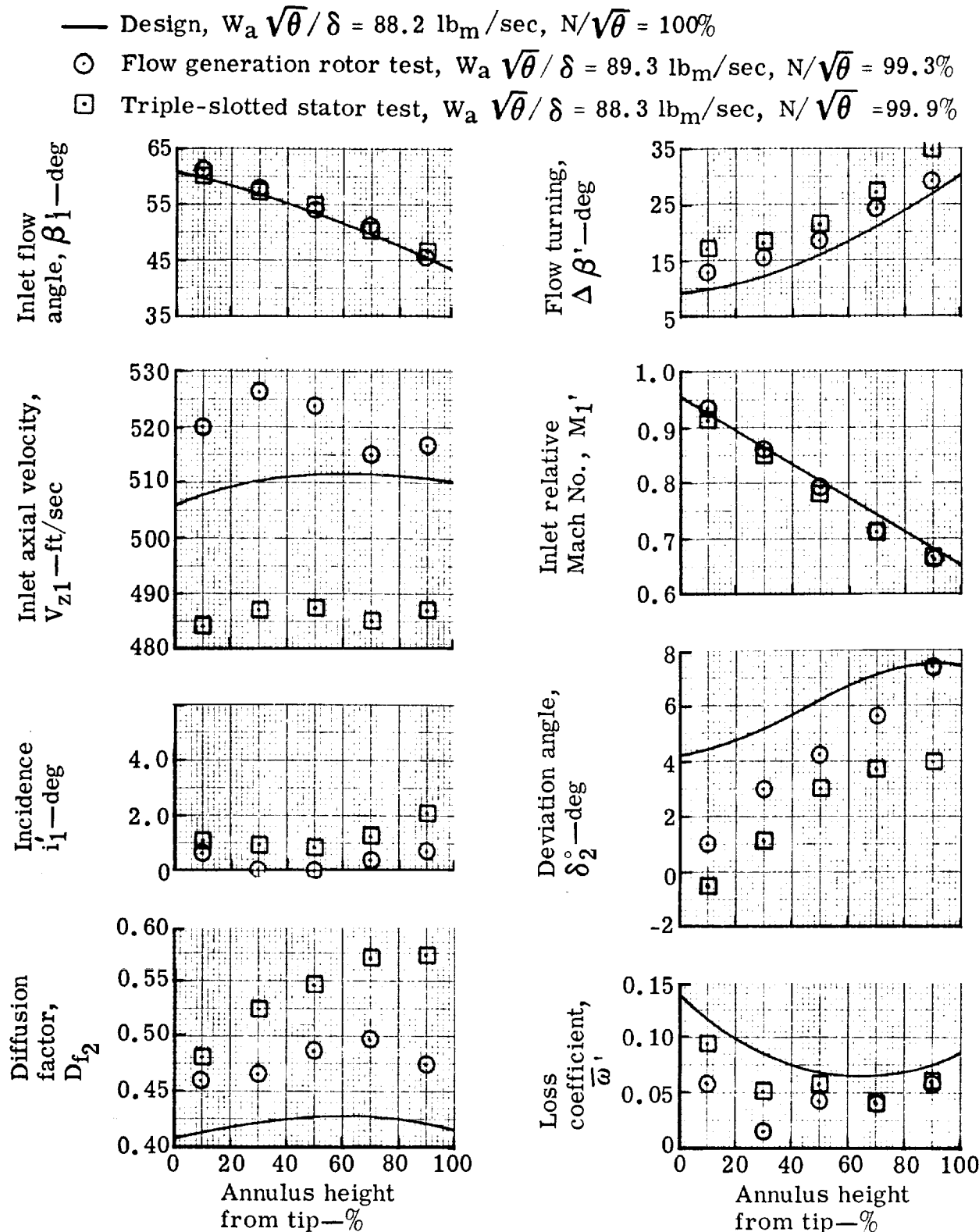


Figure 25. Radial variation of rotor blade element performance with the mean vane bleed flow rate.

5944-38

— Design, $W_a \sqrt{\theta} / \delta = 88.2 \text{ lb}_m/\text{sec}$, $N/\sqrt{\theta} = 100\%$
 ○ Flow generation rotor test, $W_a \sqrt{\theta} / \delta = 89.3 \text{ lb}_m/\text{sec}$, $N/\sqrt{\theta} = 99.3\%$
 □ Triple-slotted stator test, $W_a \sqrt{\theta} / \delta = 88.3 \text{ lb}_m/\text{sec}$, $N/\sqrt{\theta} = 99.7\%$

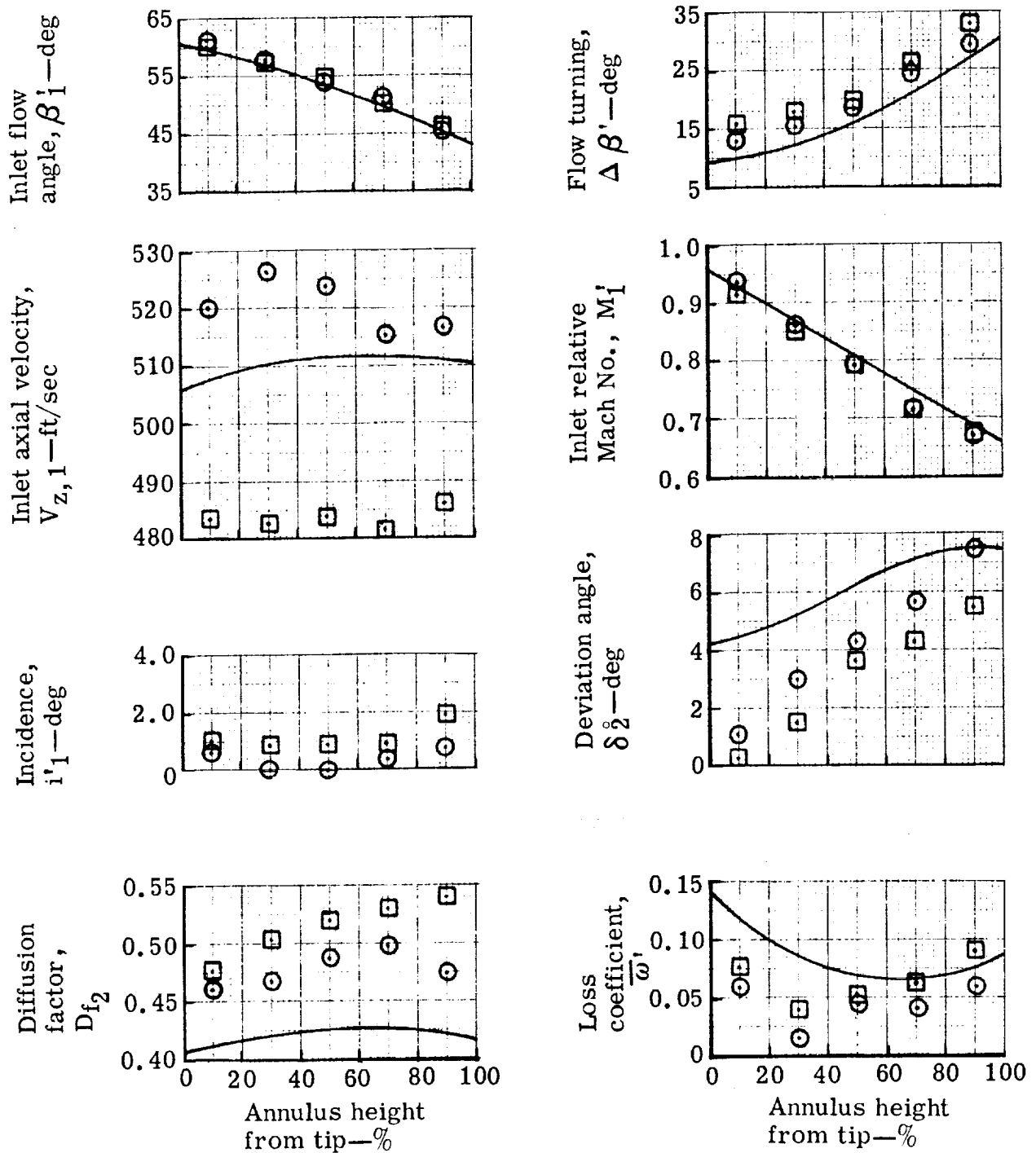


Figure 26. Radial variation of rotor blade element performance with zero vane bleed flow rate.

5944-39

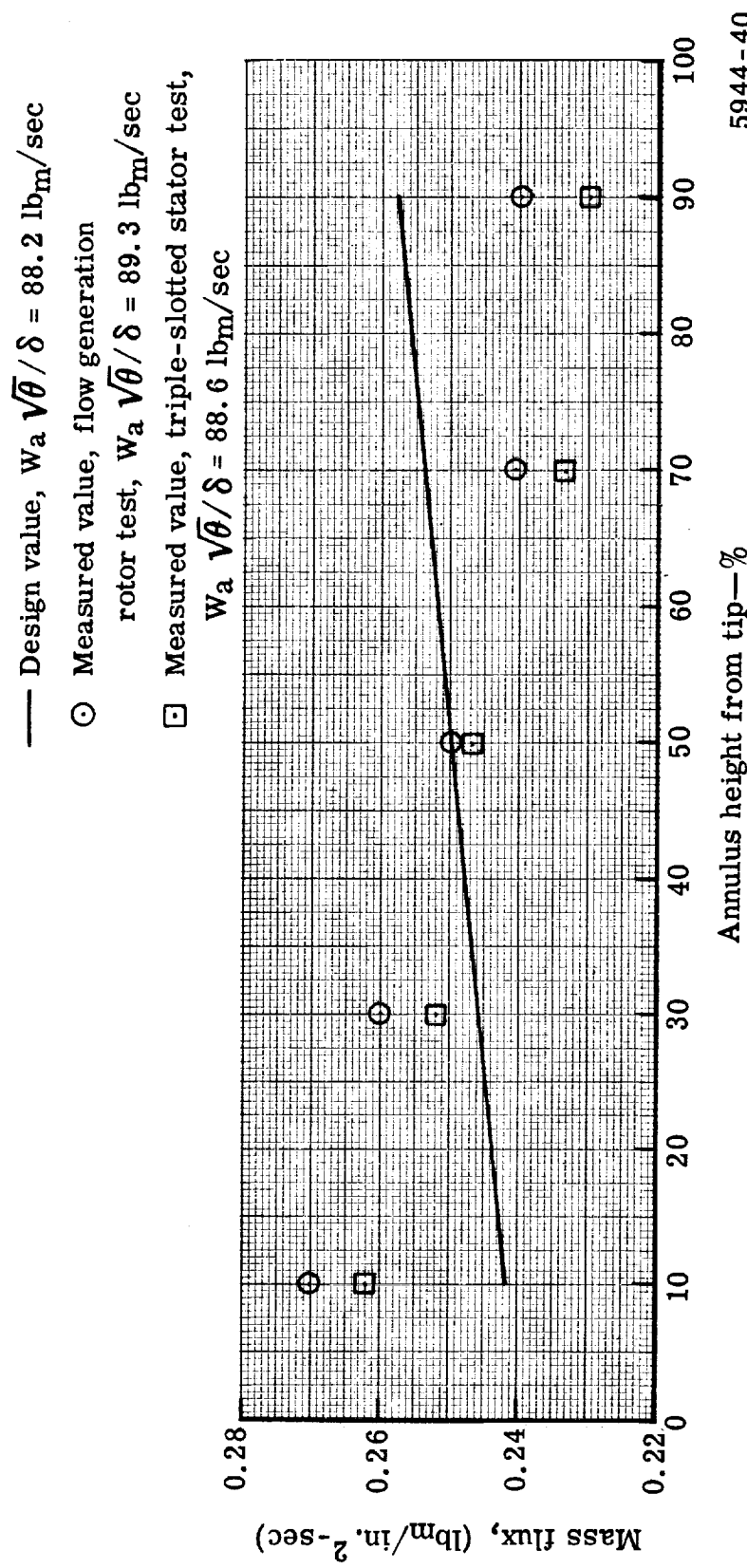


Figure 27. Rotor out radial mass flux distribution at design speed with the vane bleed flow at the optimum rate.

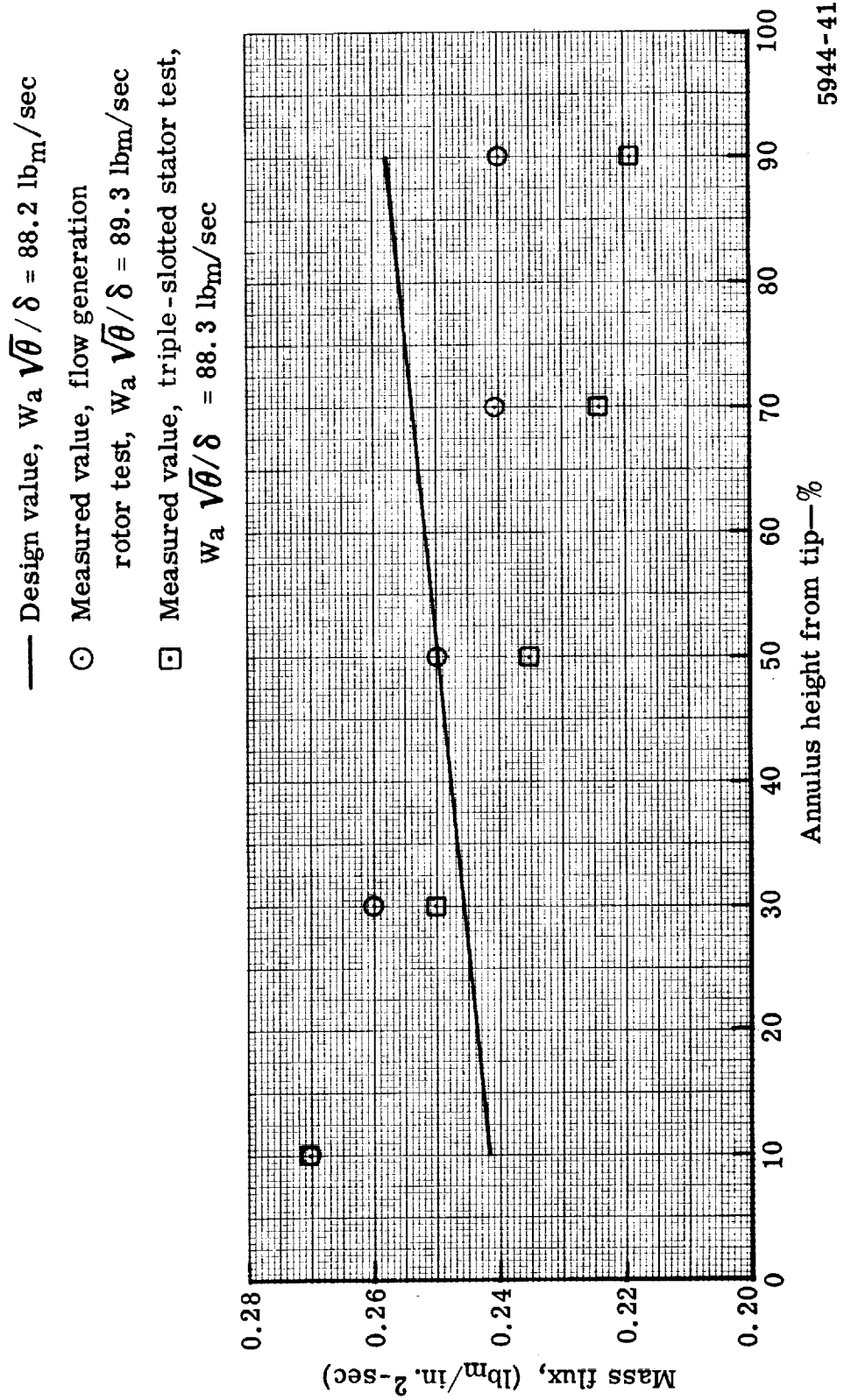


Figure 28. Rotor out radial mass flux distribution at design speed with the mean vane bleed flow rate.

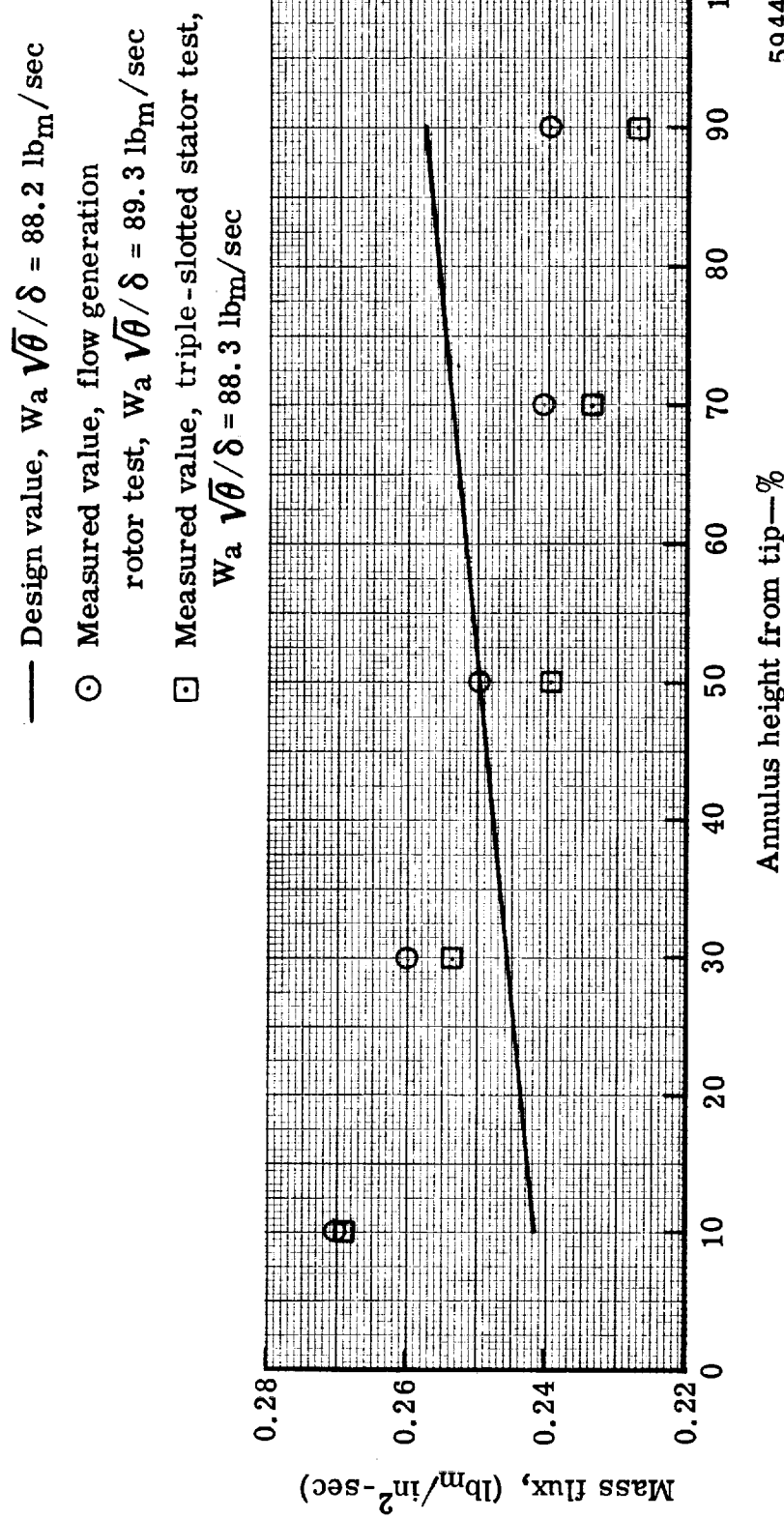


Figure 29. Rotor out radial mass flux distribution at design speed with zero vane bleed flow rate.

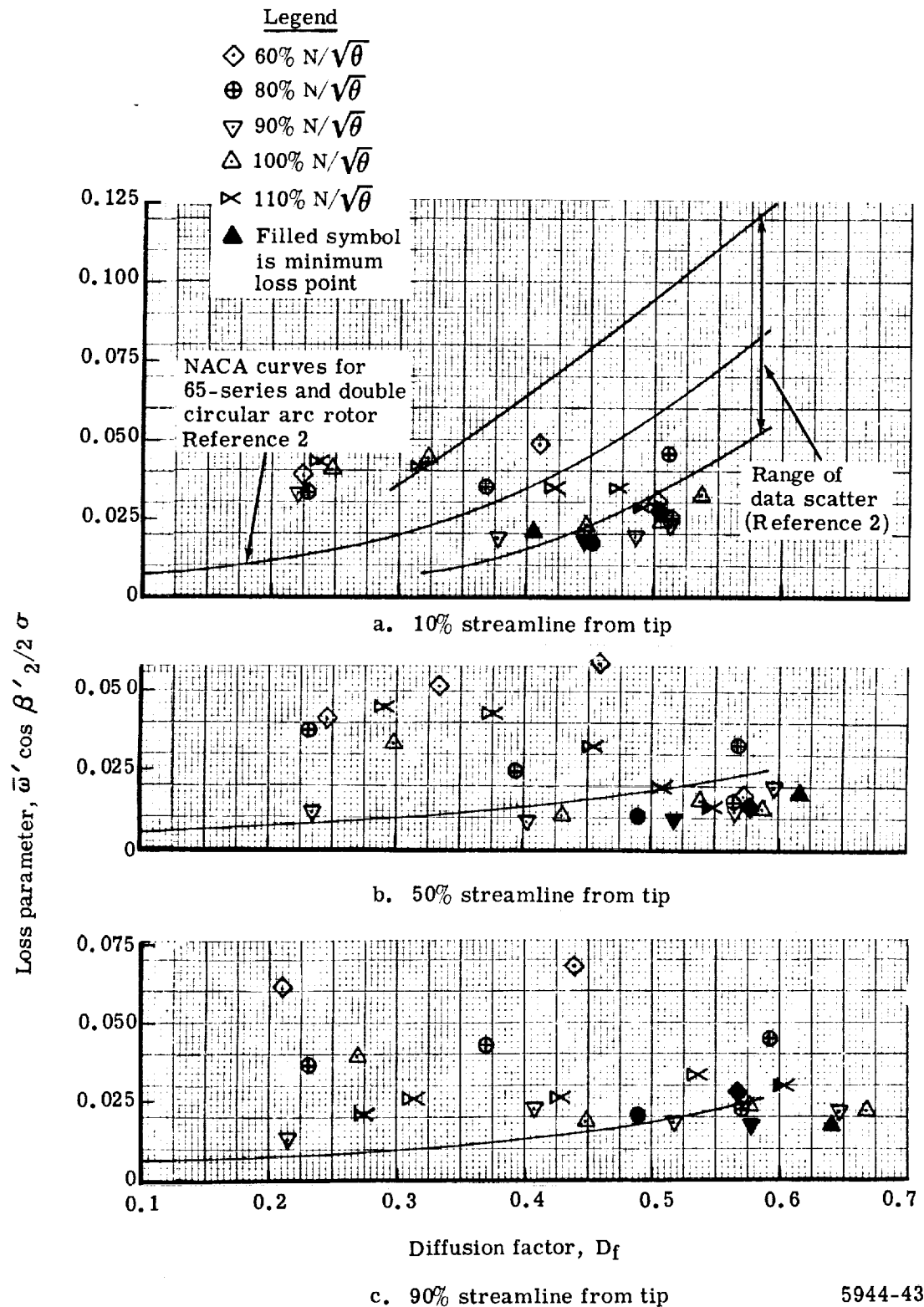


Figure 30. Rotor loss parameter versus diffusion factor with the vane bleed flow at the optimum rate.

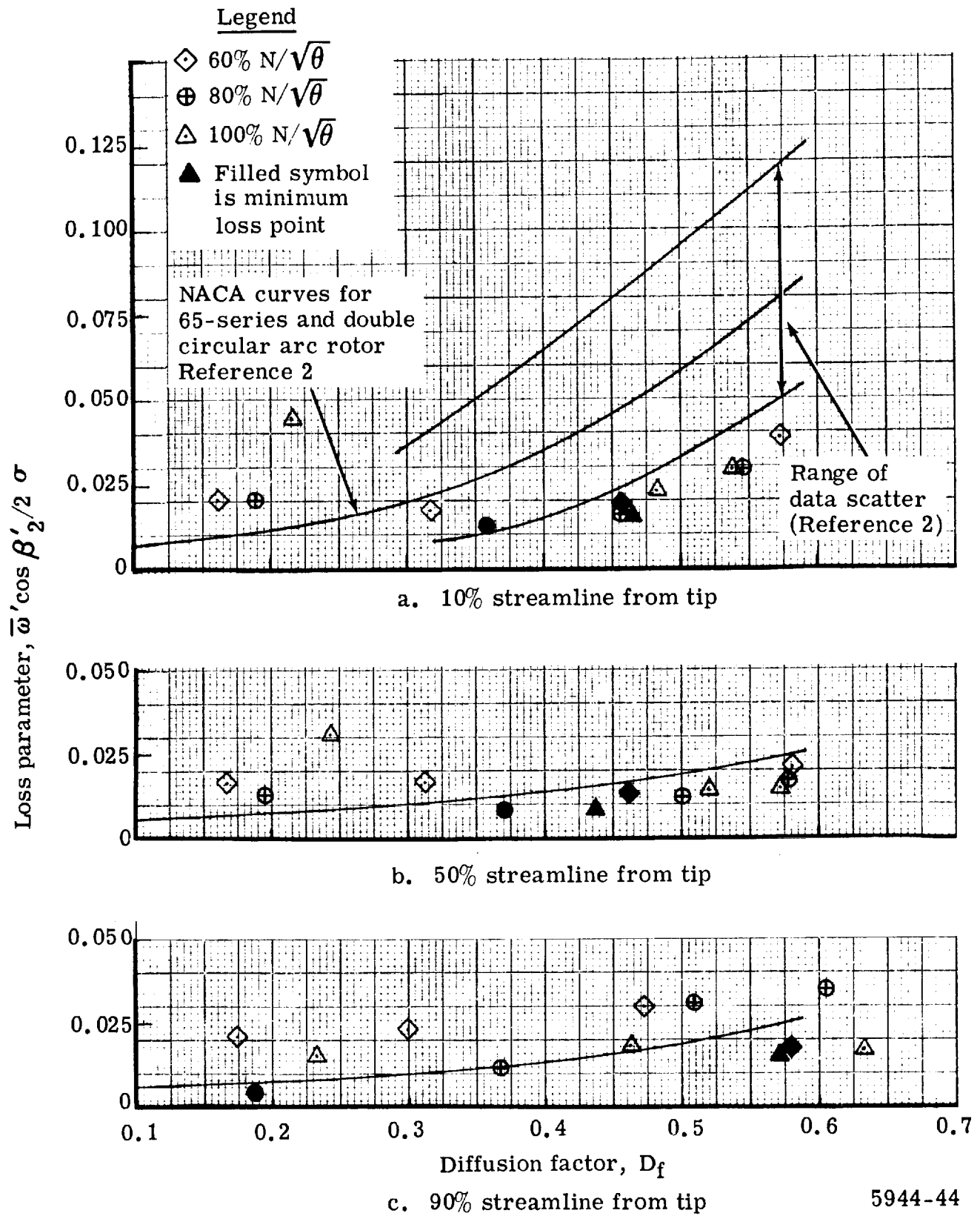


Figure 31. Rotor loss parameter versus diffusion factor with the mean vane bleed flow rate.

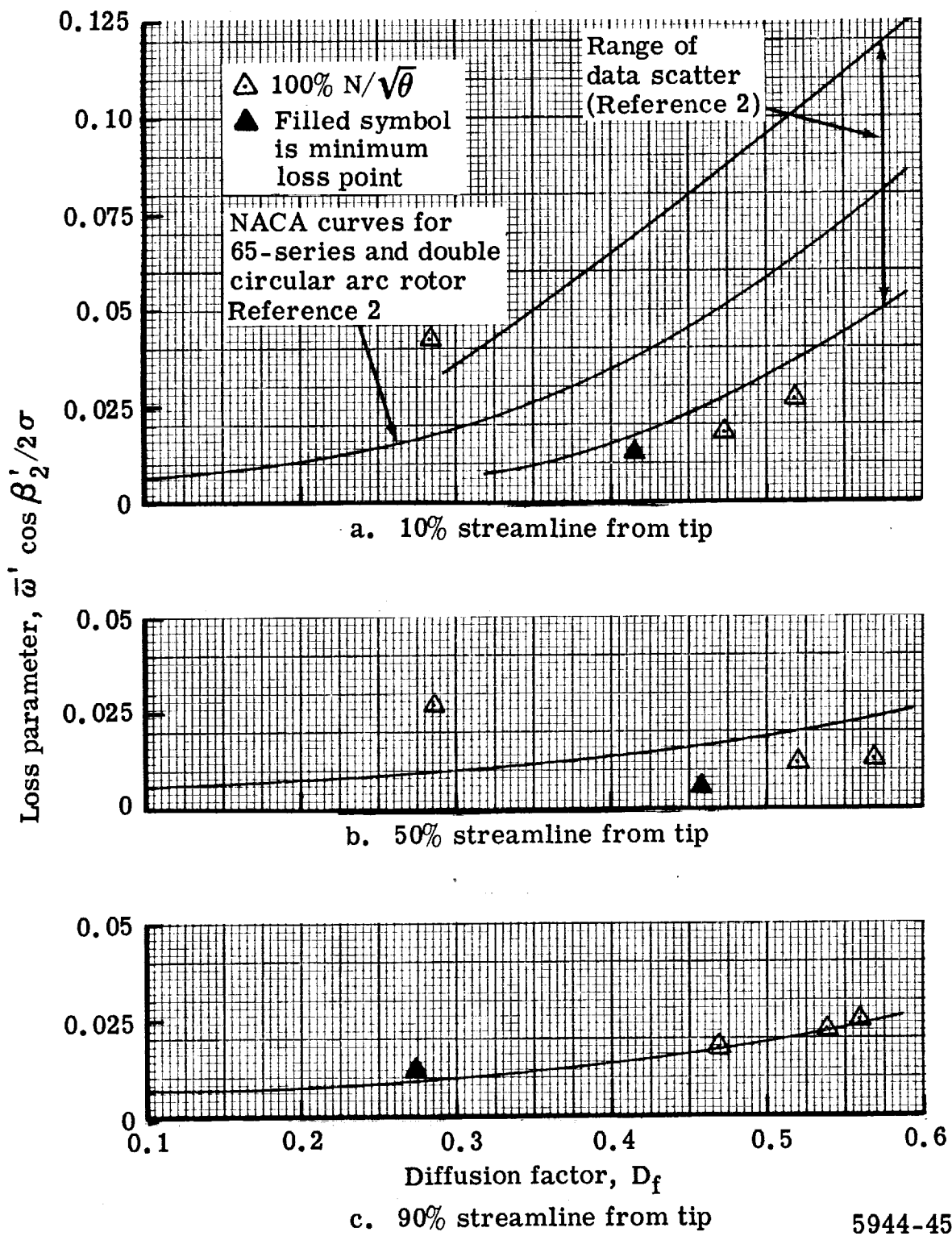
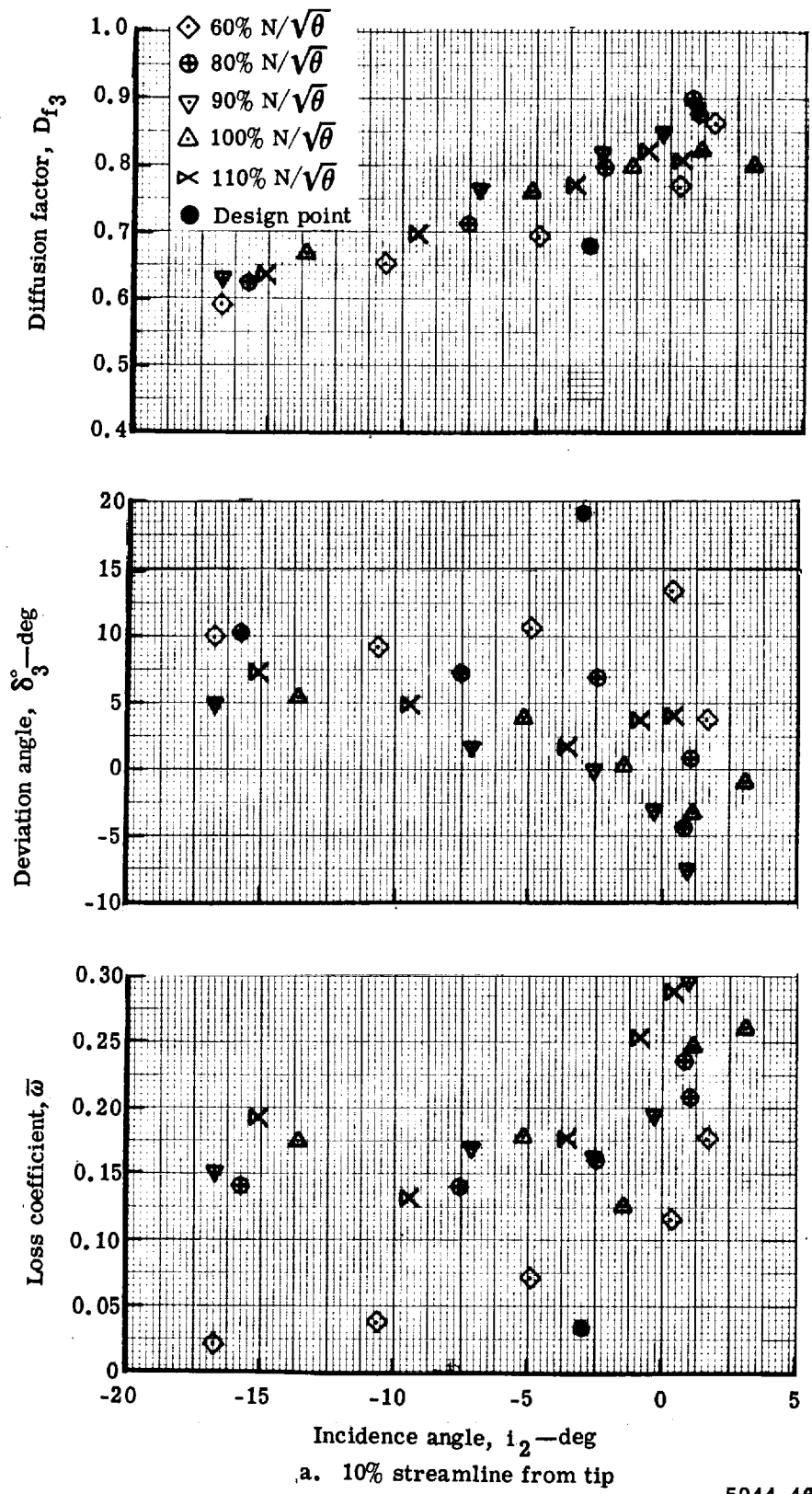
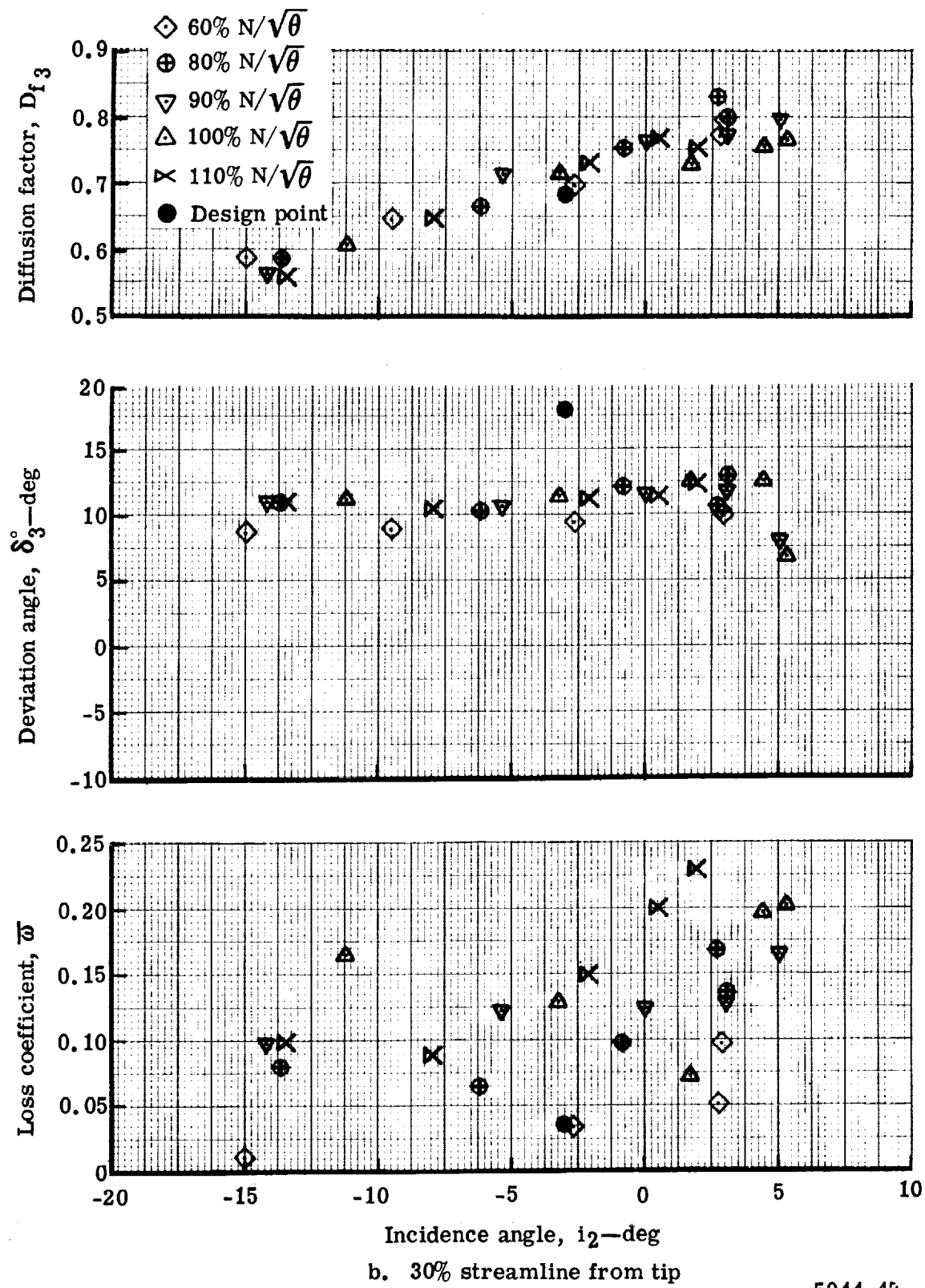


Figure 32. Rotor loss parameter versus diffusion factor with zero vane bleed flow rate.



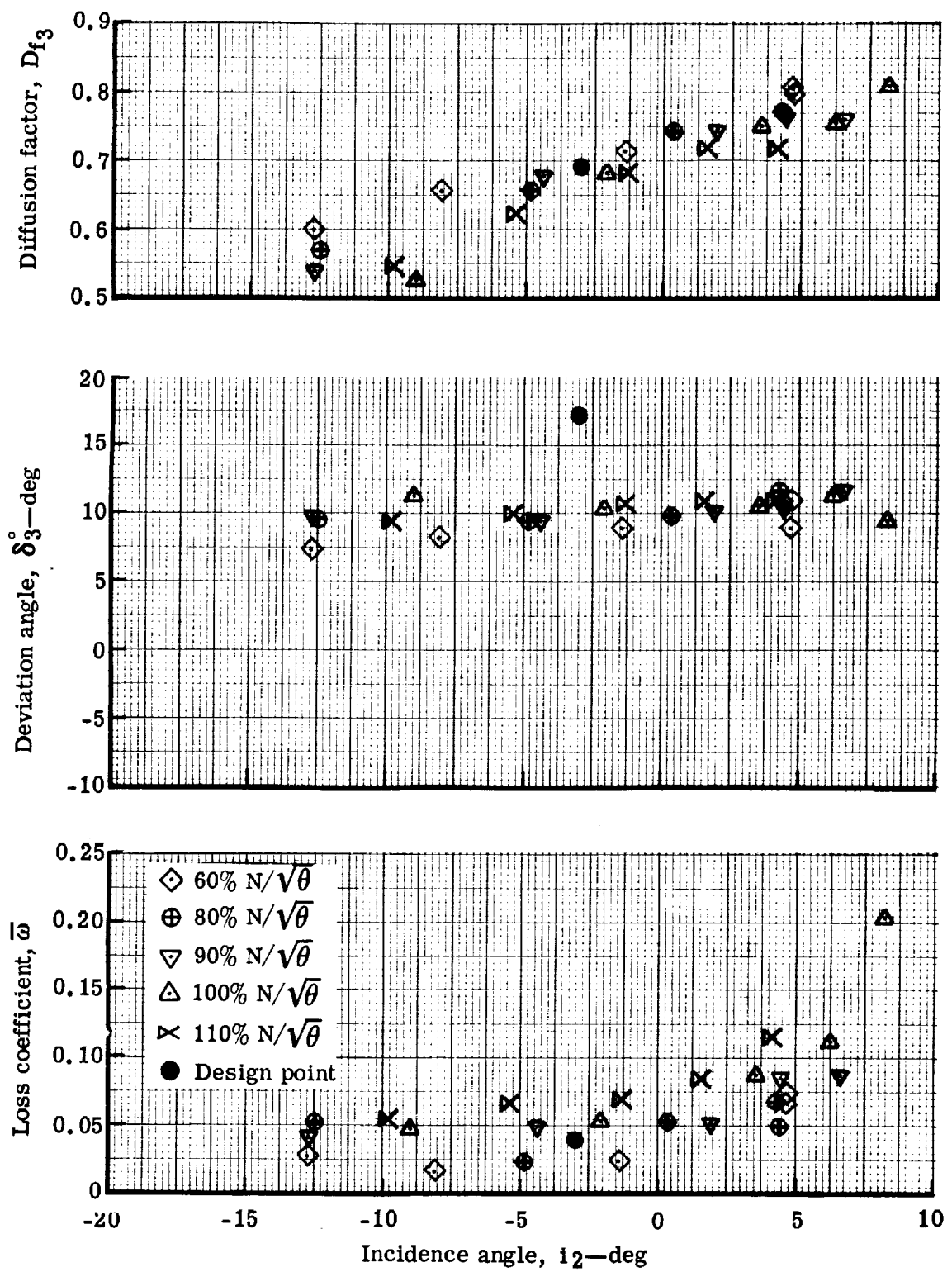
5944-46

Figure 33. Triple-slotted stator blade element performance with the vane bleed flow at the optimum rate.



5944-47

Figure 33. Triple-slotted stator blade element performance with the vane bleed flow at the optimum rate.



5944-48

Figure 33. Triple-slotted stator blade element performance with the vane bleed flow at the optimum rate.

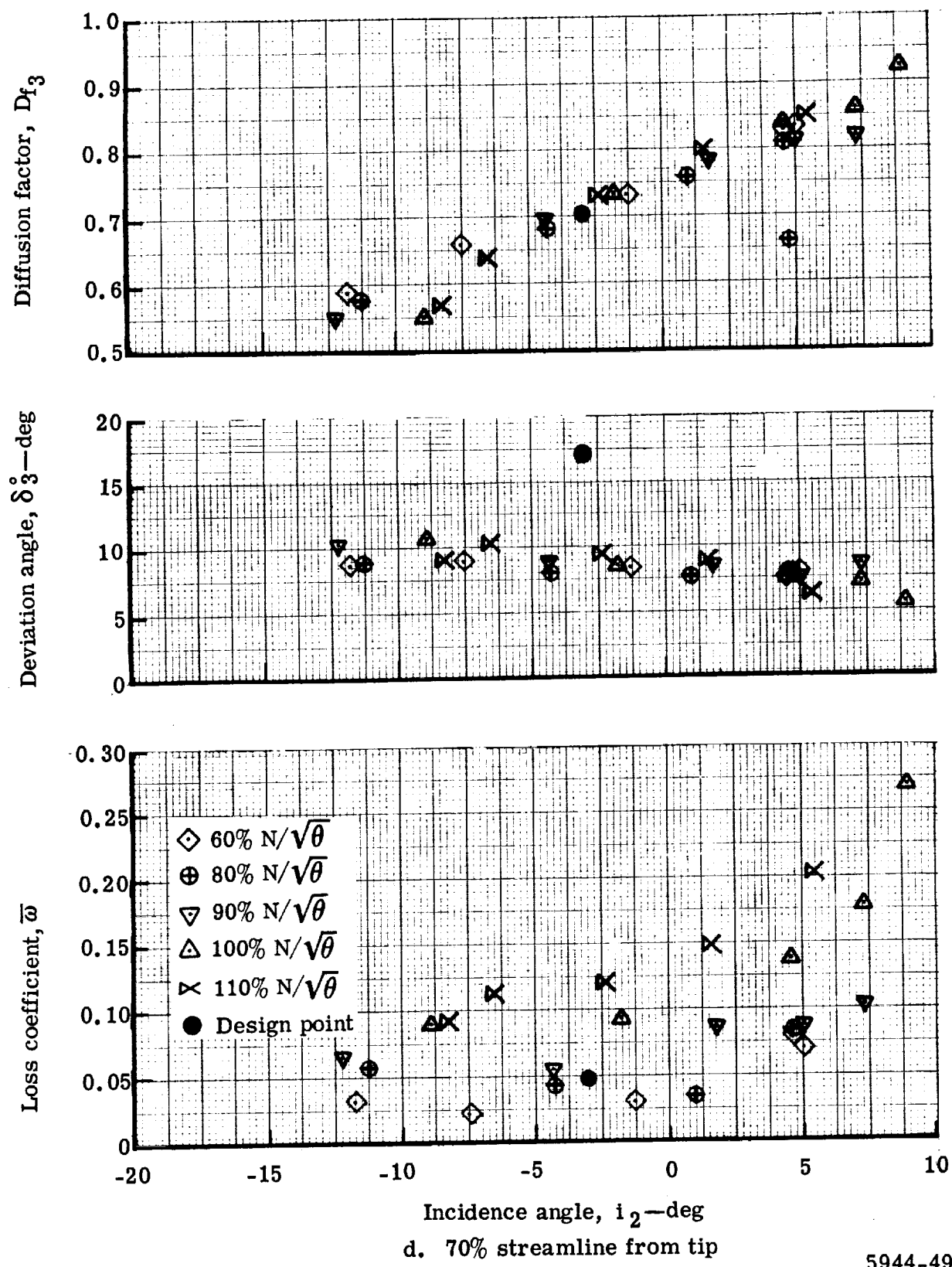


Figure 33. Triple-slotted stator blade element performance with the vane bleed flow at the optimum rate.

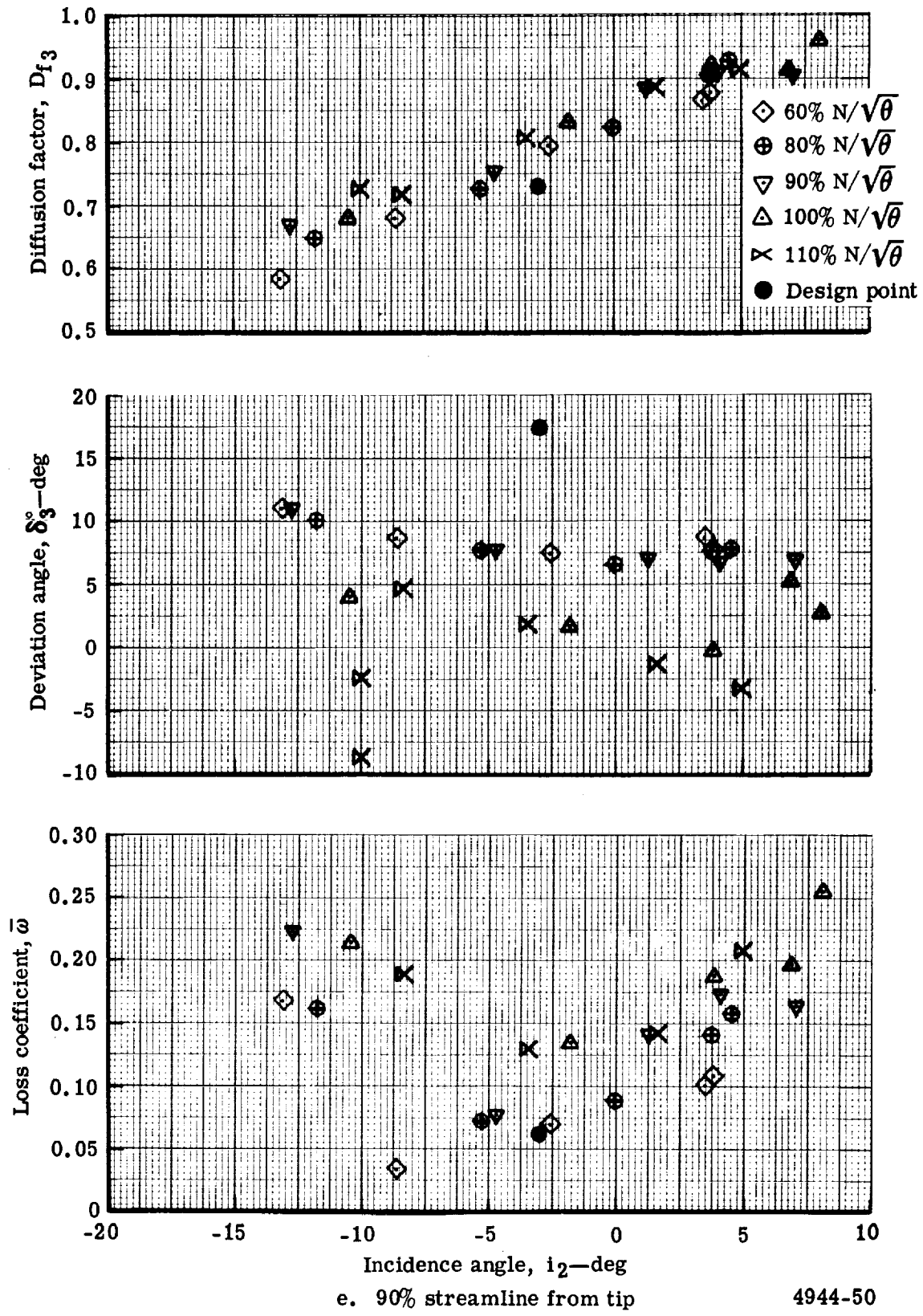


Figure 33. Triple-slotted stator blade element performance with the vane bleed flow at the optimum rate.

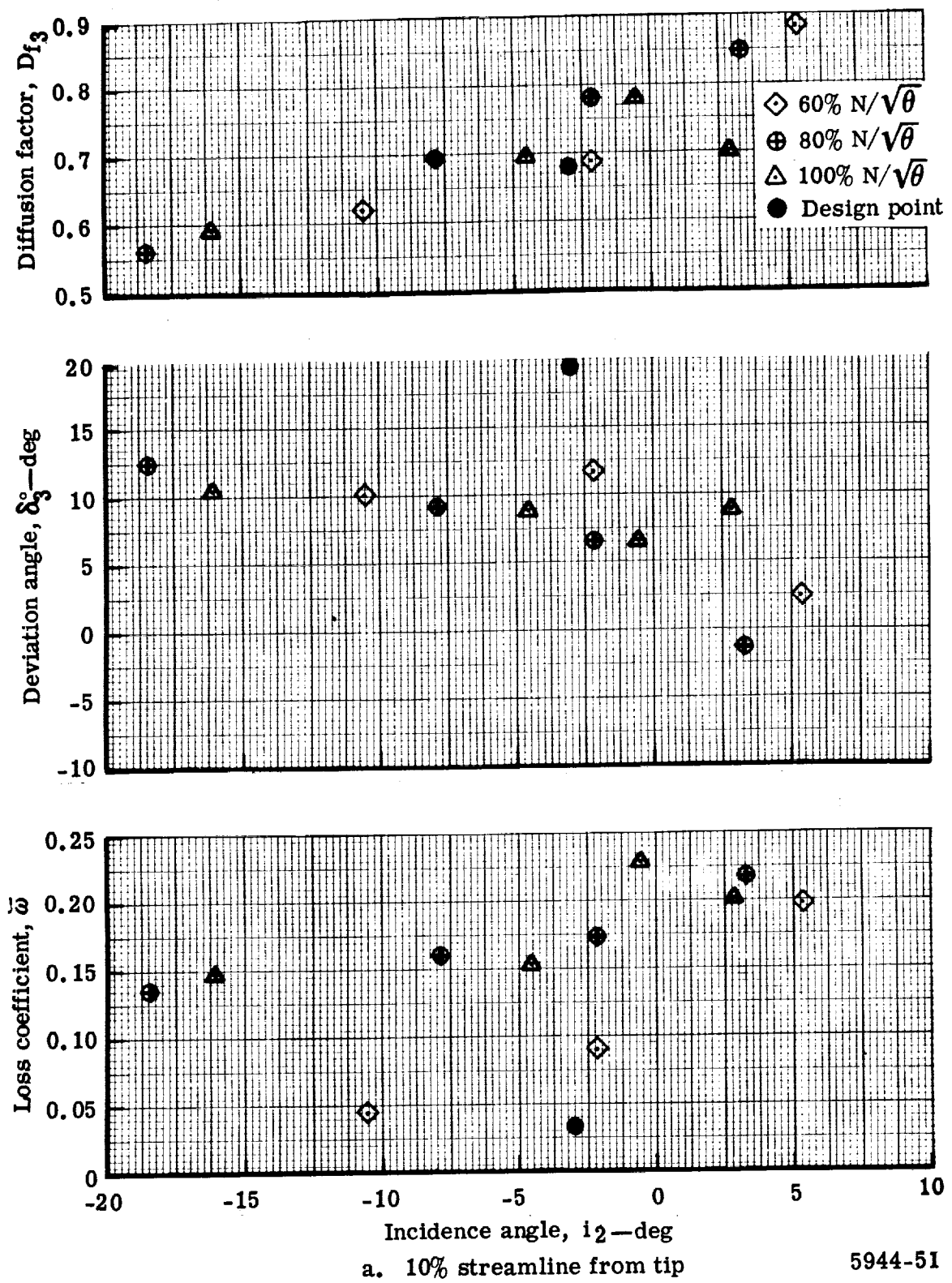


Figure 34. Triple-slotted stator blade element performance with the mean vane bleed flow rate.

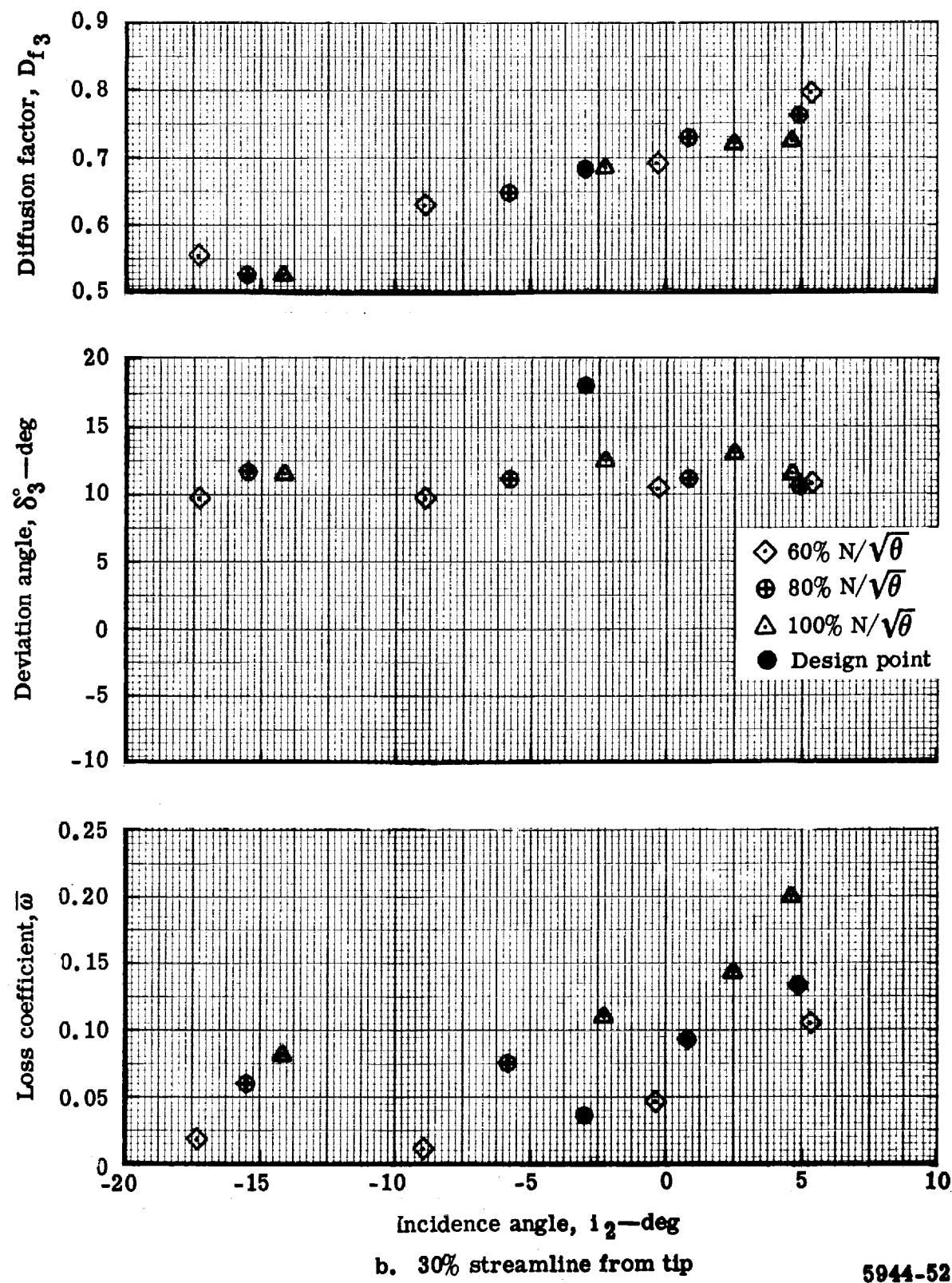


Figure 34. Triple-slotted stator blade element performance with the mean vane bleed flow rate.

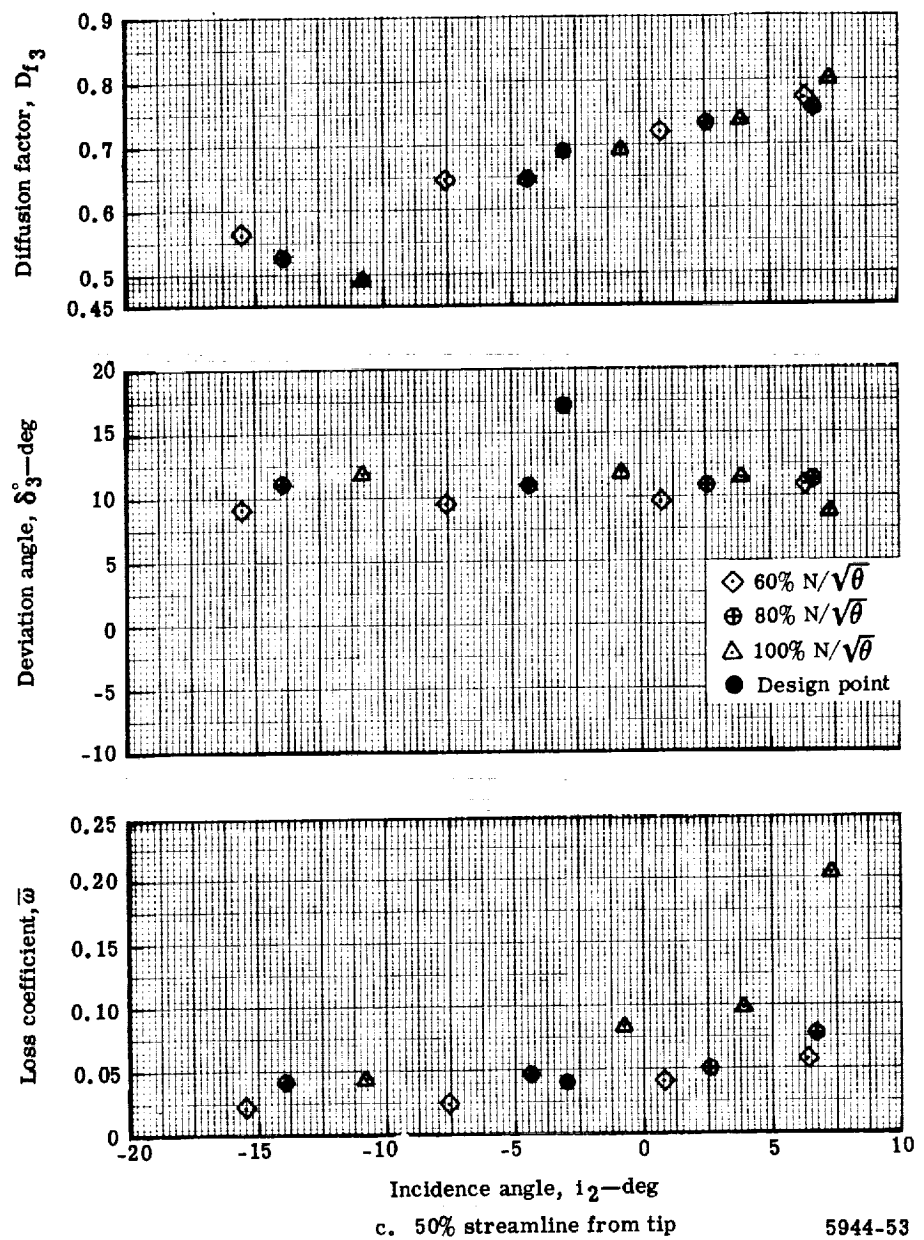
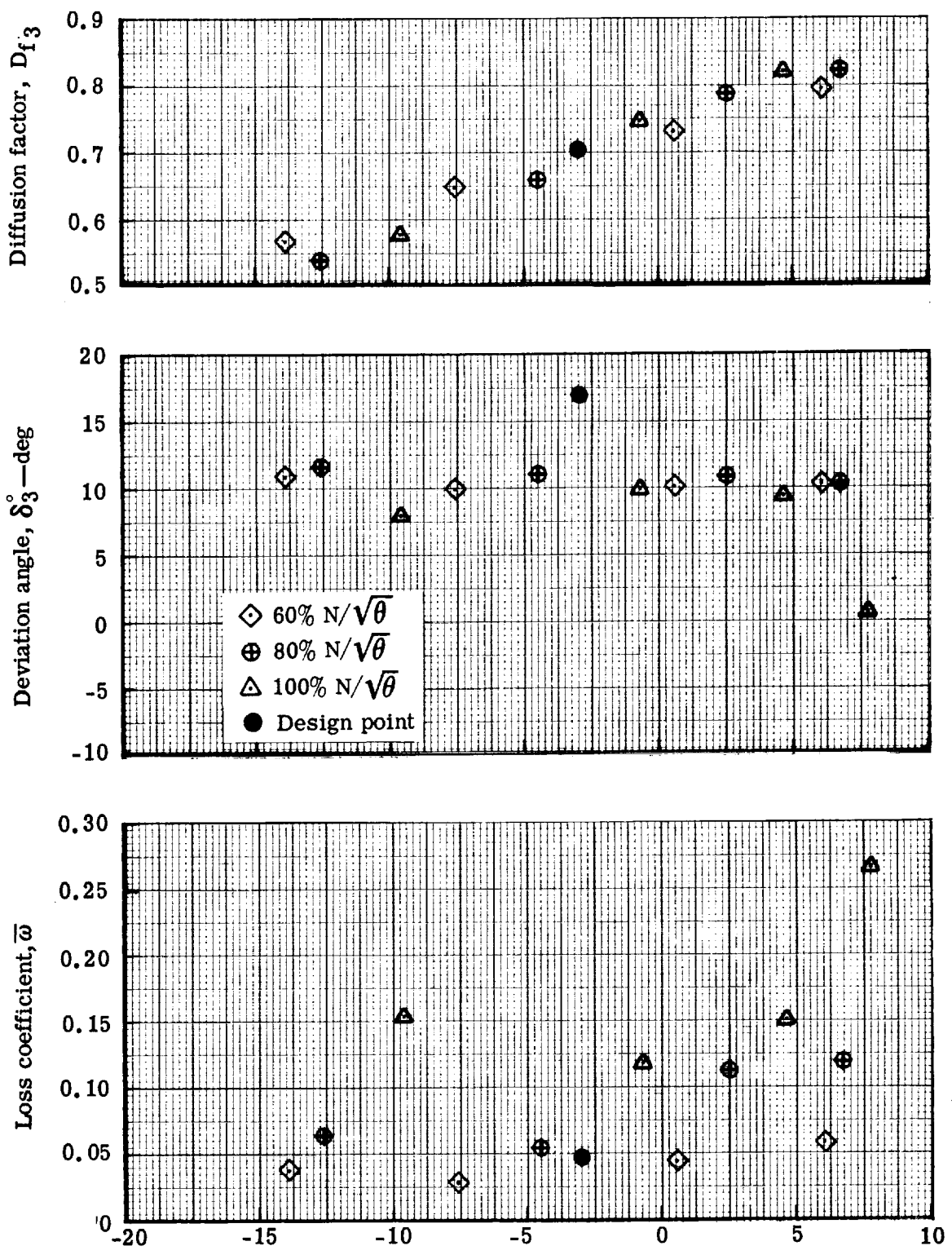


Figure 34. Triple-slotted stator blade element performance with the mean vane bleed flow rate.



d. 70% streamline from tip

5944-54

Figure 34. Triple-slotted stator blade element performance with the mean vane bleed flow rate.

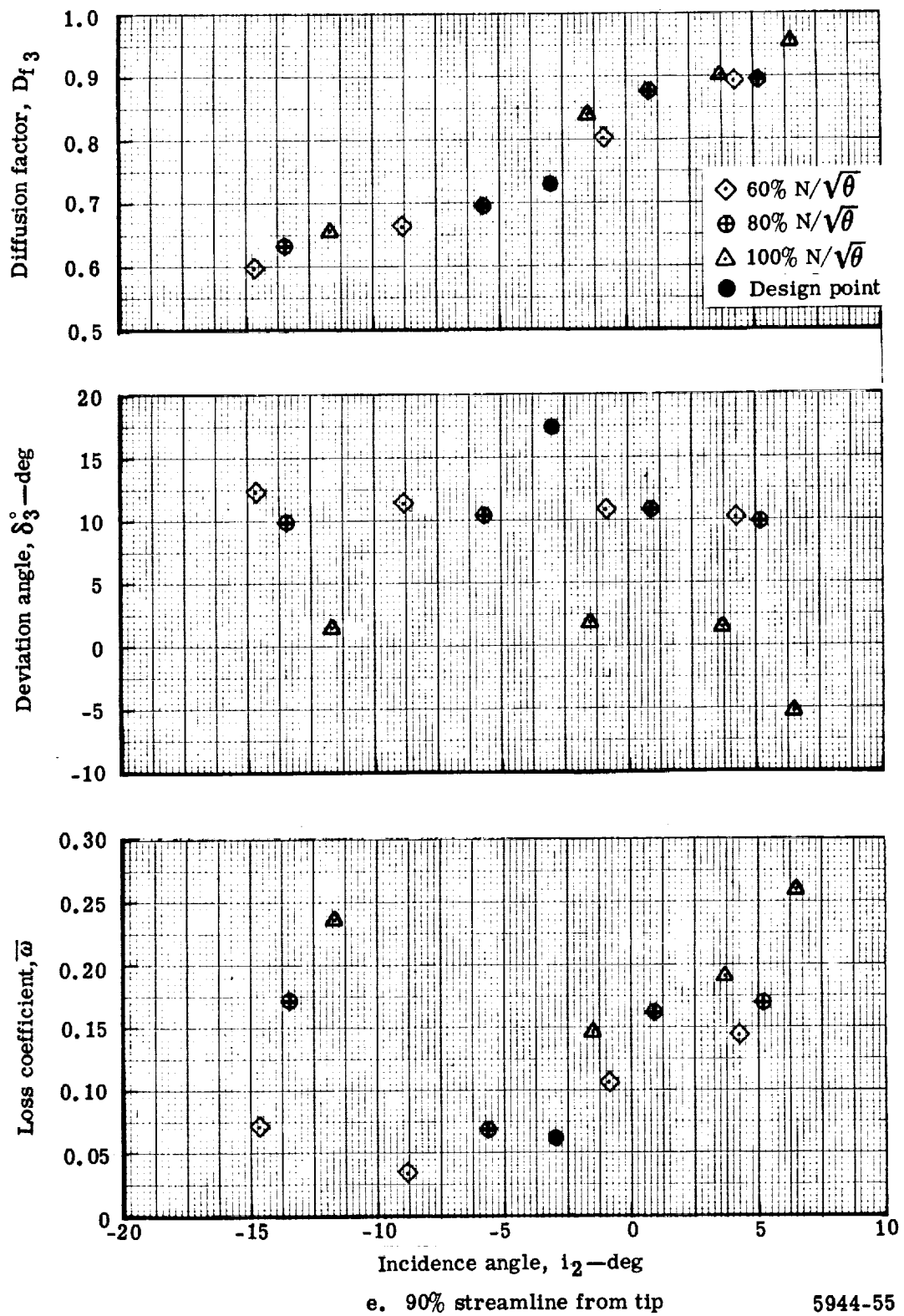


Figure 34. Triple-slotted stator blade element performance with the mean vane bleed flow rate.

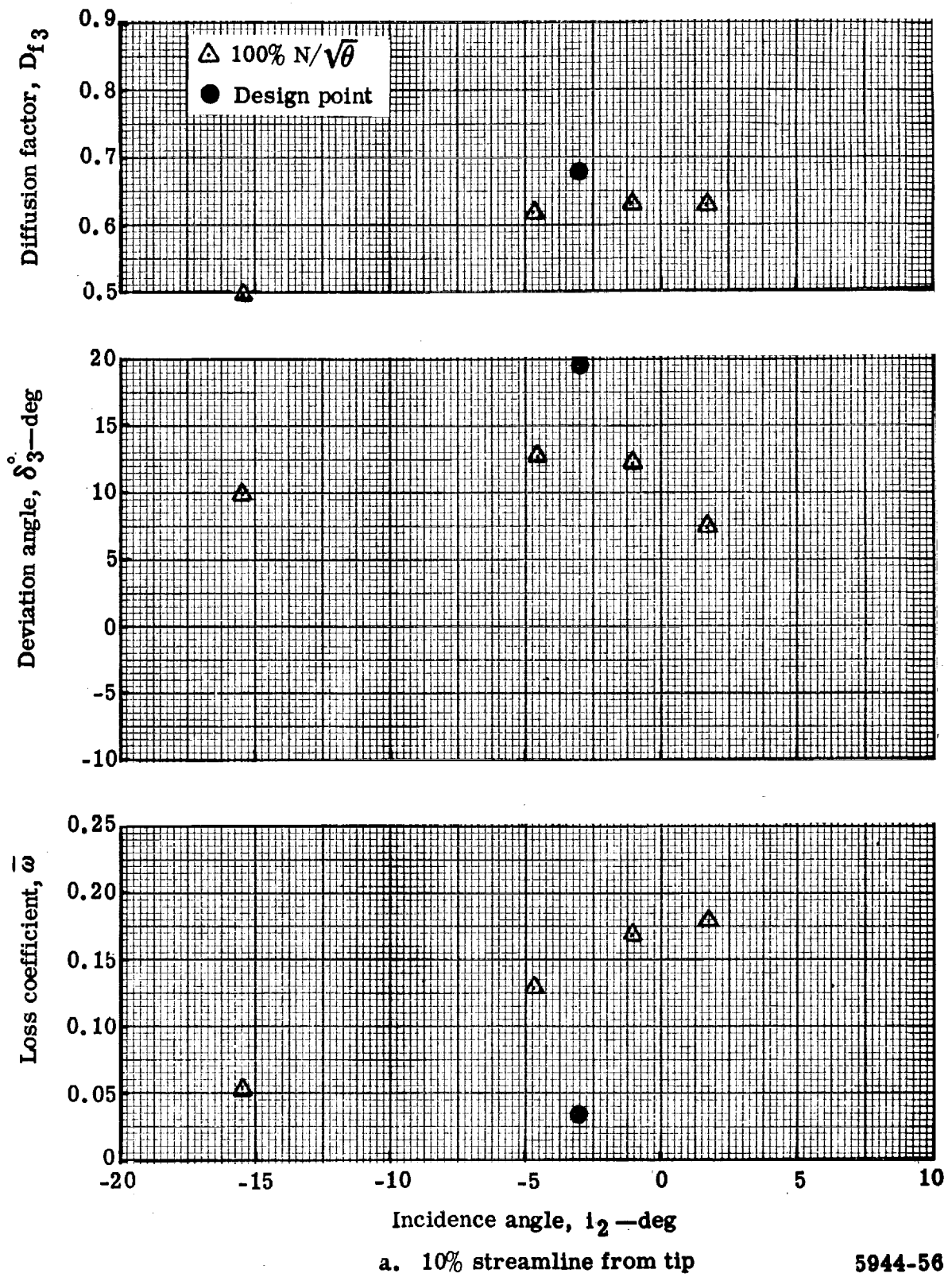


Figure 35. Triple-slotted stator blade element performance with zero vane bleed flow rate.

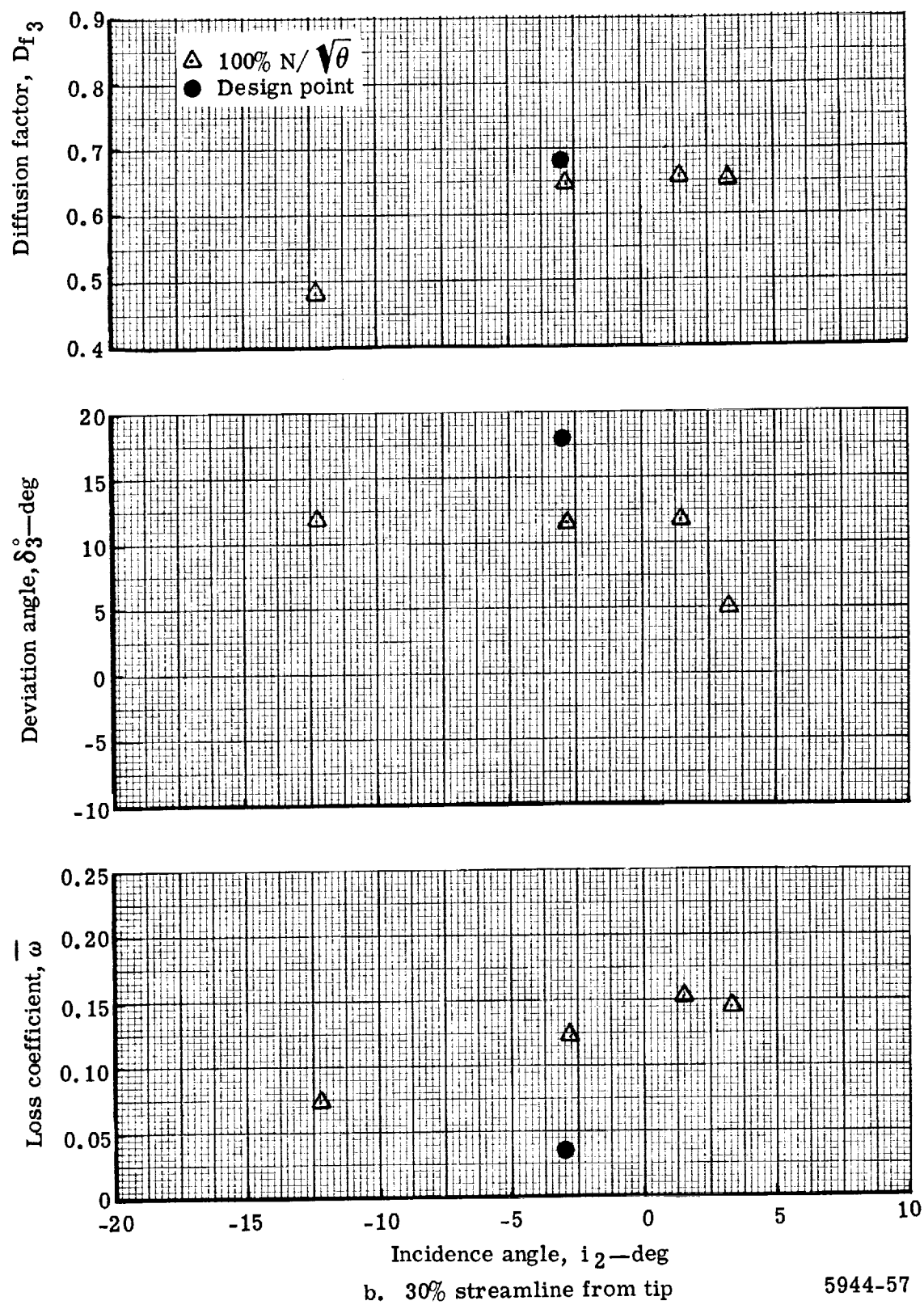


Figure 35. Triple-slotted stator blade element performance with zero vane bleed flow rate.

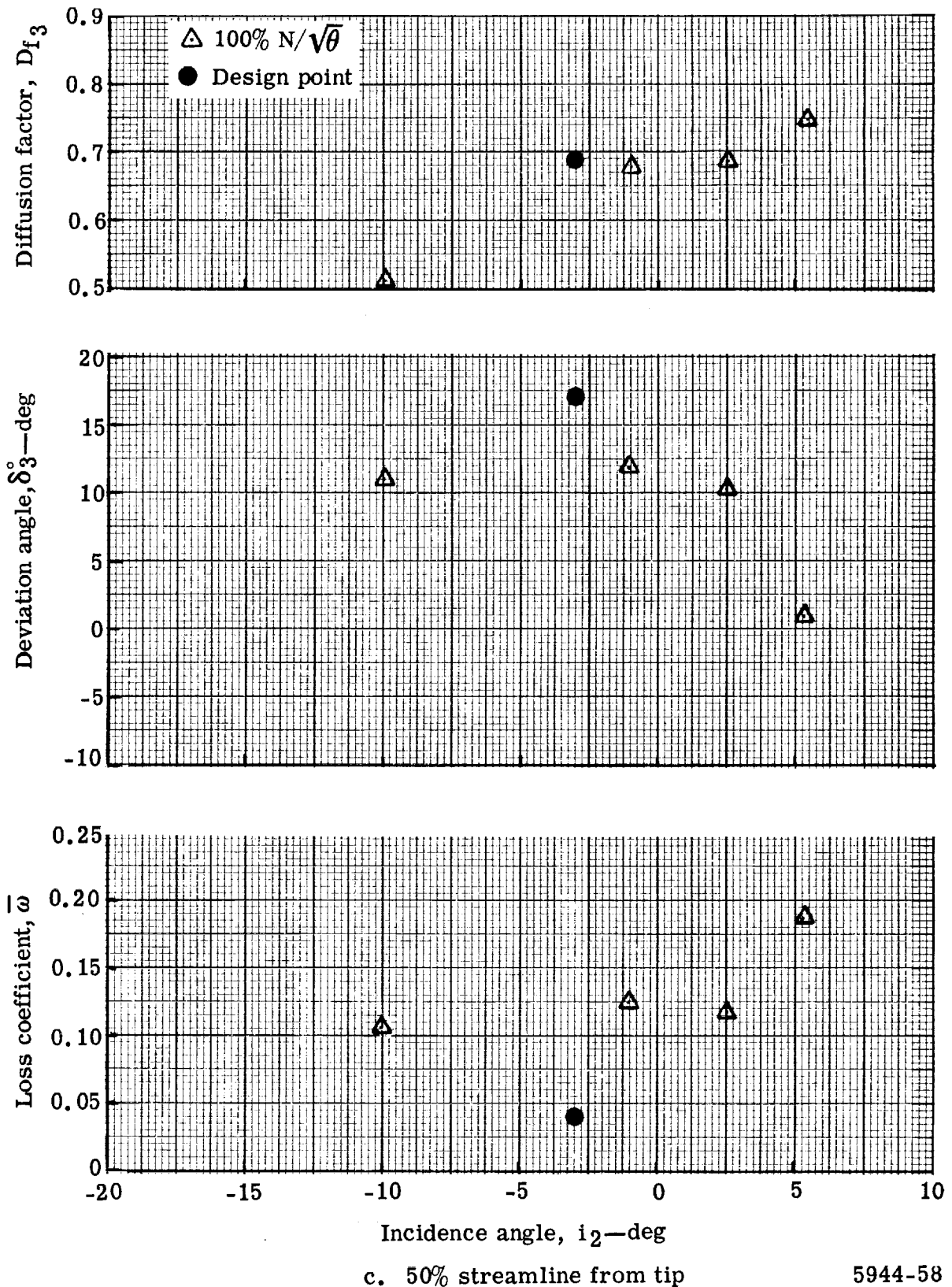


Figure 35. Triple-slotted stator blade element performance with zero vane bleed flow rate.

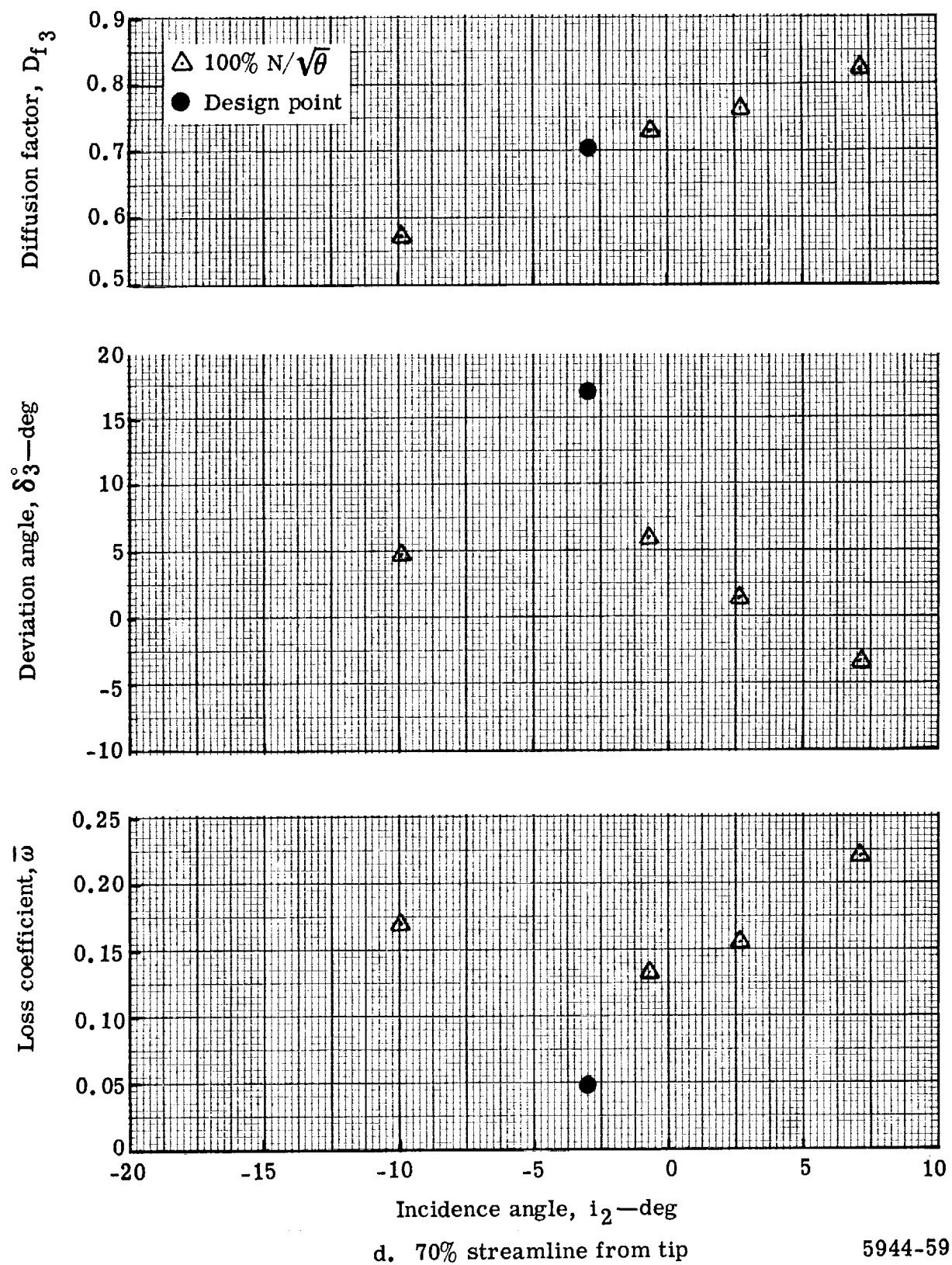


Figure 35. Triple-slotted stator blade element performance with zero vane bleed flow rate.

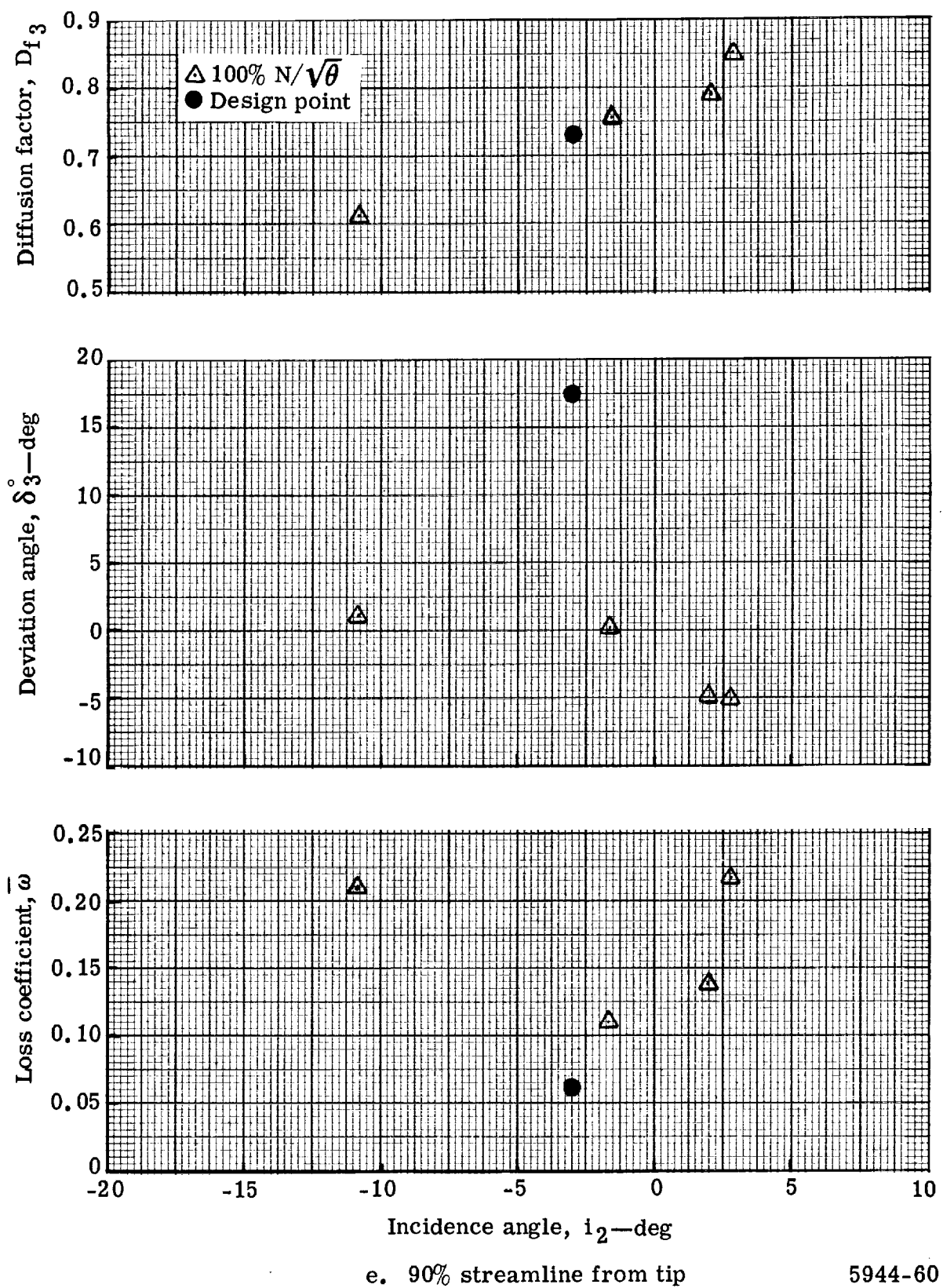
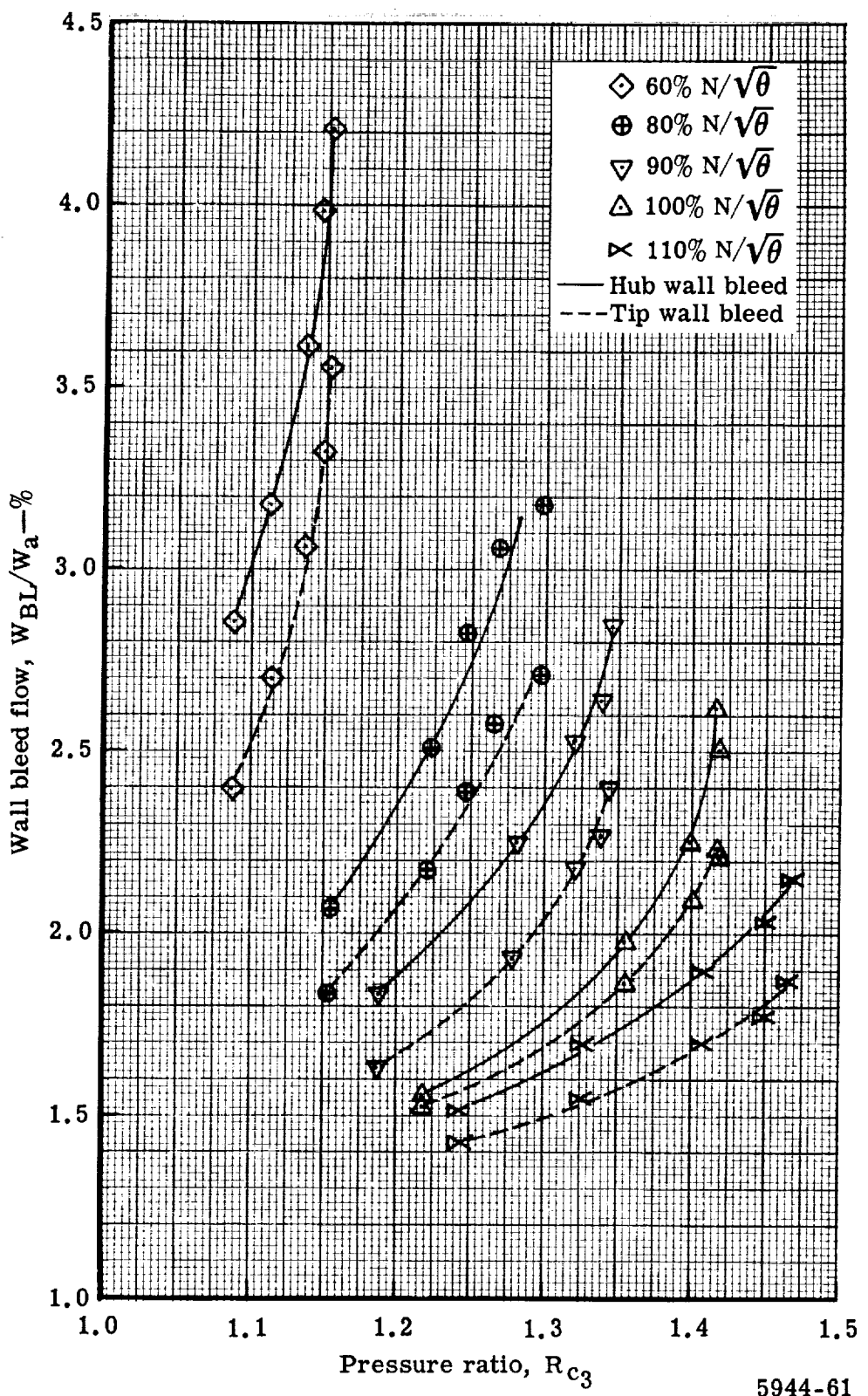


Figure 35. Triple-slotted stator blade element performance with zero vane bleed flow rate.



5944-61

Figure 36. Variation of wall bleed flow with stage pressure ratio and vane bleed flow at the optimum rate.

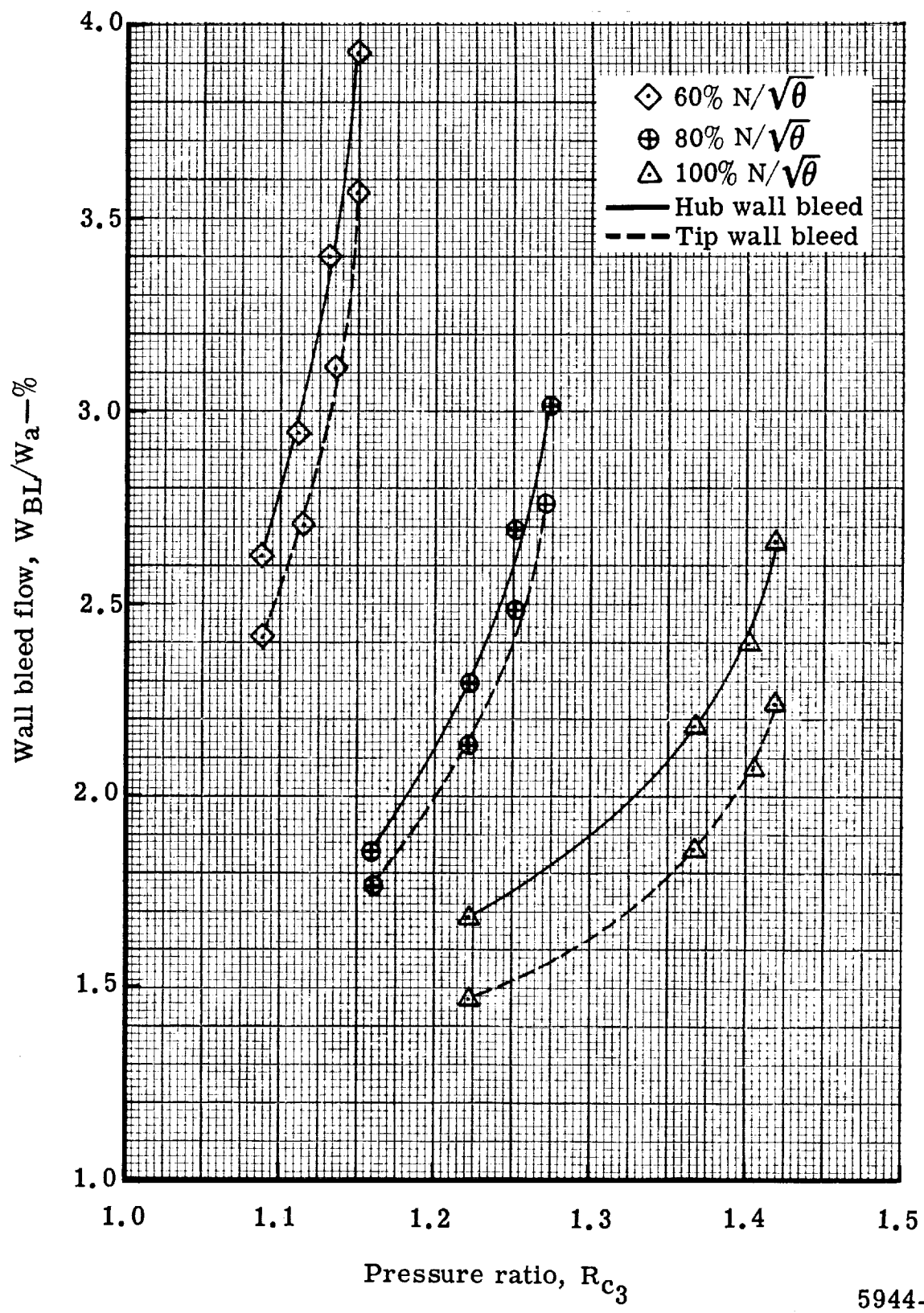


Figure 37. Variation of wall bleed flow with stage pressure ratio and mean vane bleed flow rate.

5944-62

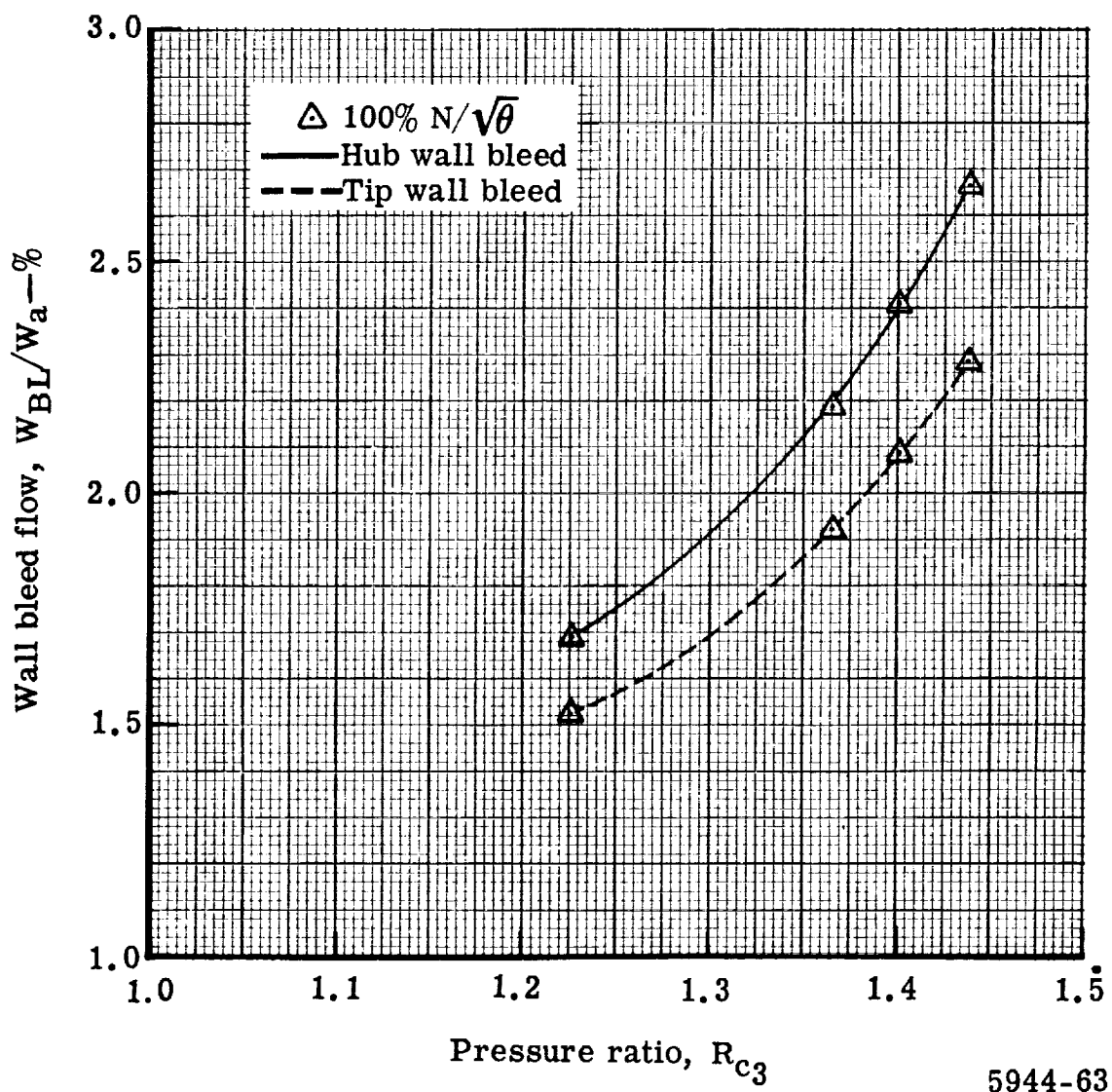


Figure 38. Variation of wall bleed flow with stage pressure ratio and zero vane bleed flow rate.

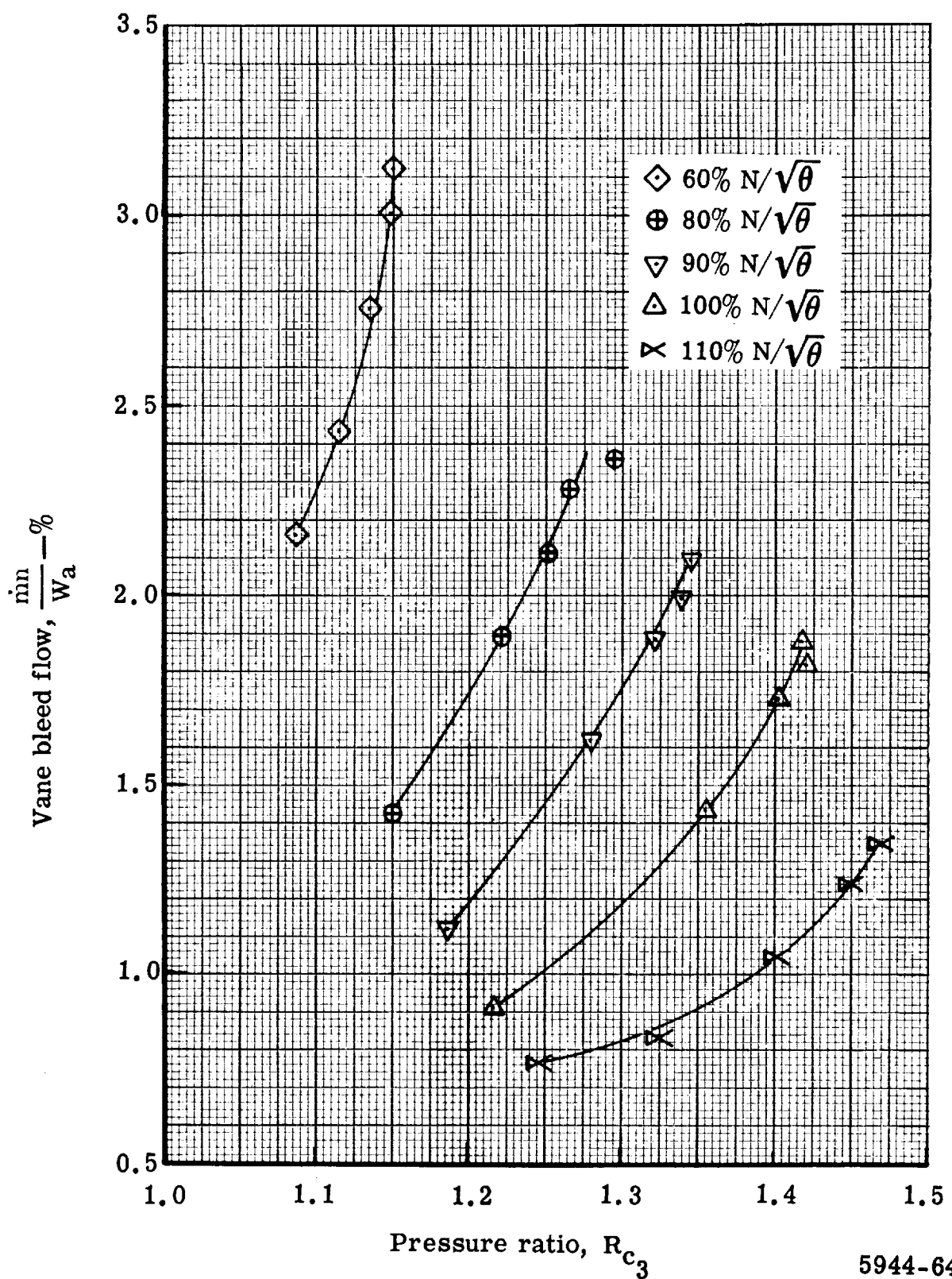


Figure 39. Variation of vane bleed flow at optimum bleed rate with stage pressure ratio.

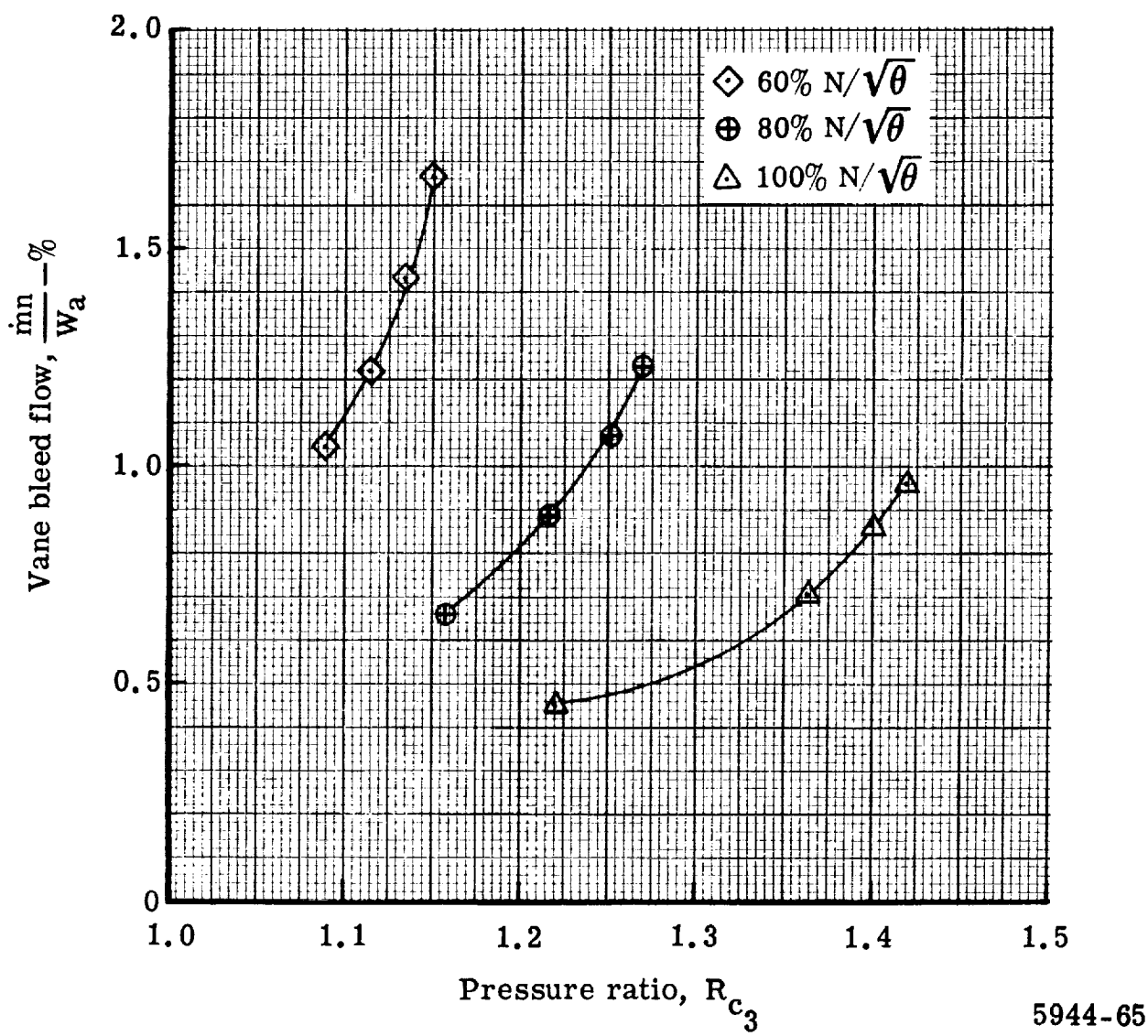
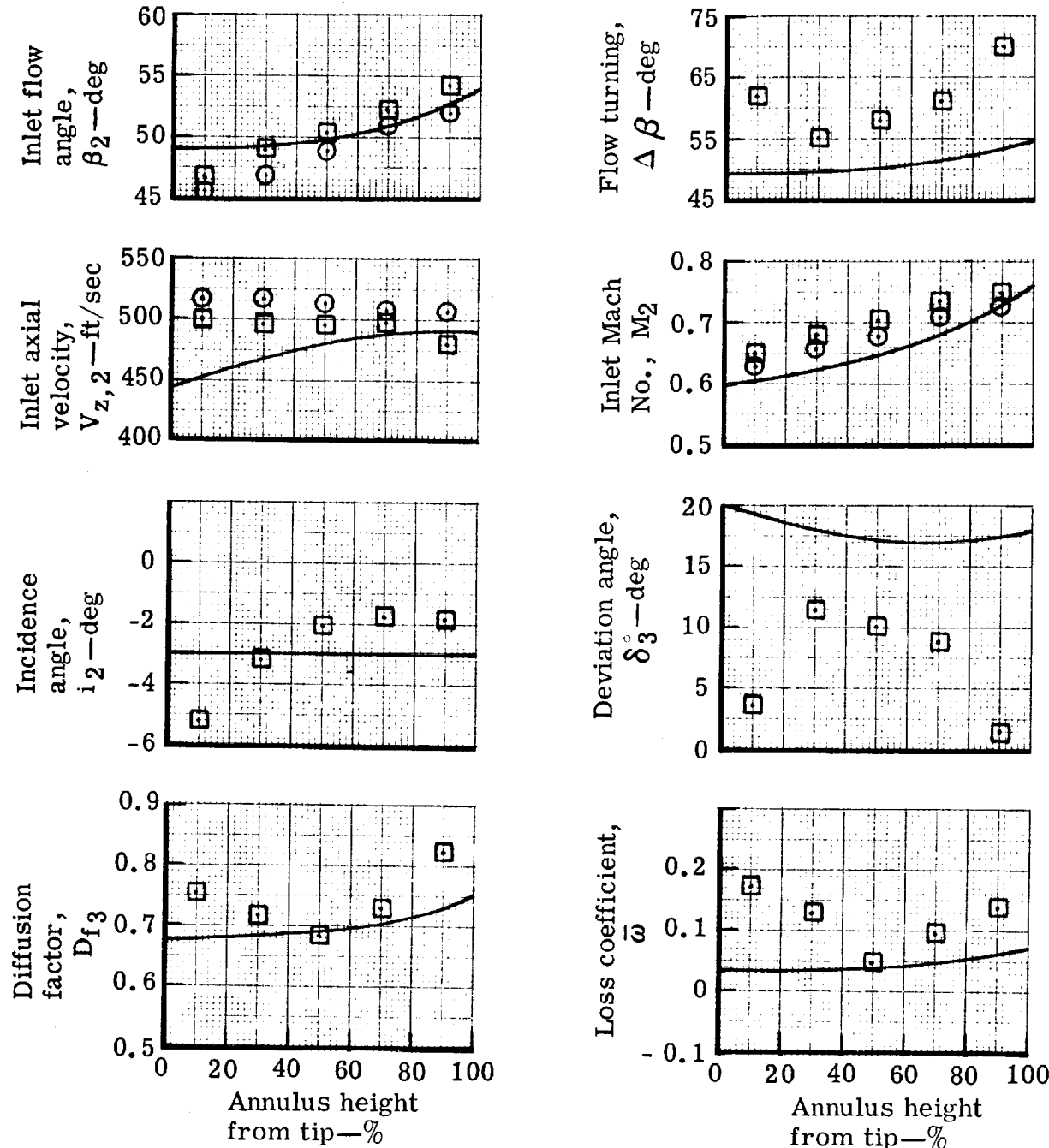


Figure 40. Variation of vane bleed flow at the mean vane bleed flow rate with stage pressure ratio.

- Design, $W_a \sqrt{\theta} / \delta = 88.2 \text{ lb}_m/\text{sec}$, $N/\sqrt{\theta} = 100\%$
 ○ Flow generation rotor test, $W_a \sqrt{\theta} / \delta = 93.4 \text{ lb}_m/\text{sec}$, $N/\sqrt{\theta} = 99.8\%$
 □ Triple-slotted stator test, $W_a \sqrt{\theta} / \delta = 94.1 \text{ lb}_m/\text{sec}$, $N/\sqrt{\theta} = 99.8\%$



5944-66

Figure 41. Radial variation of triple-slotted $0.75 D_f$ stator blade element performance with the vane bleed flow at the optimum rate.

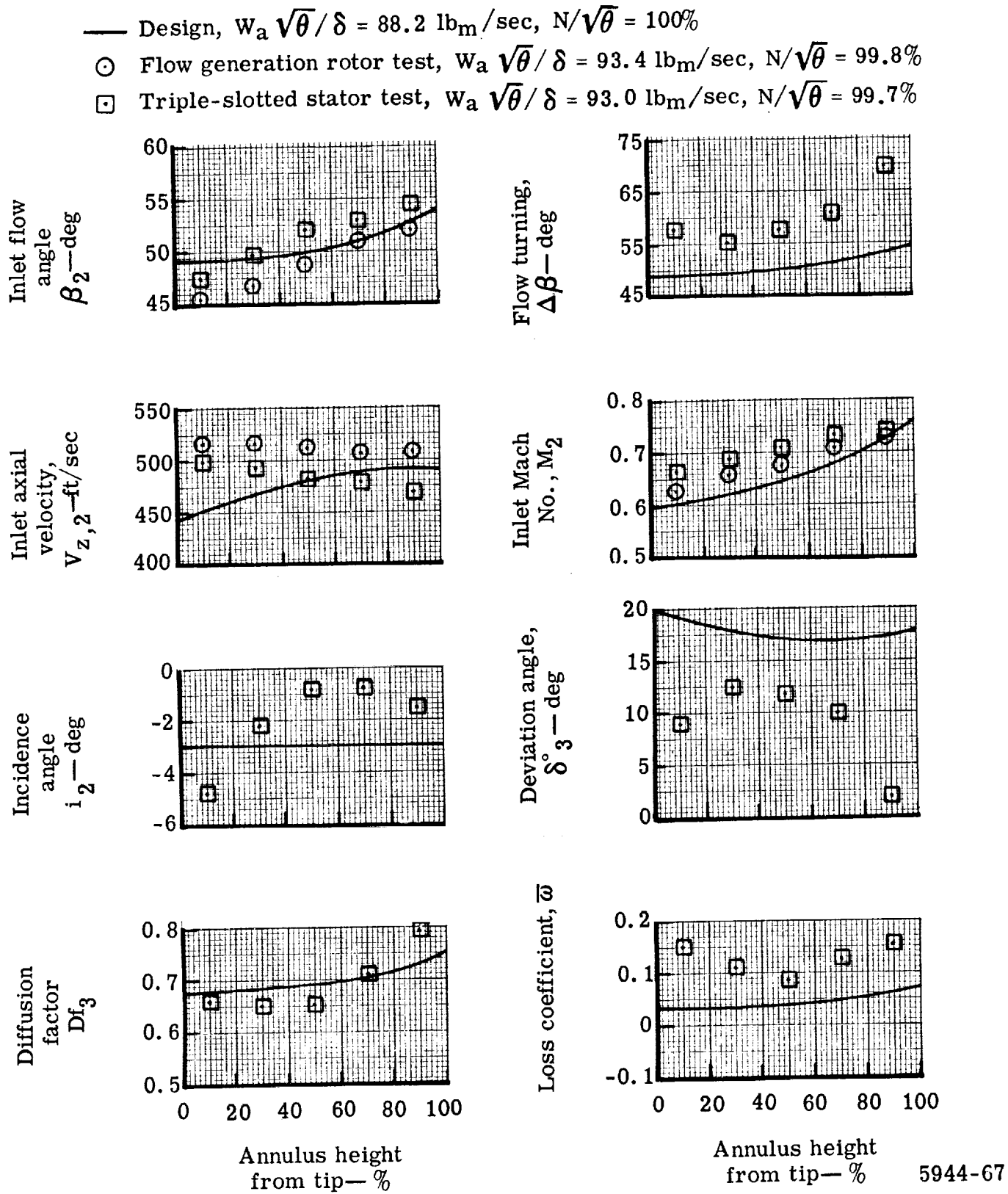
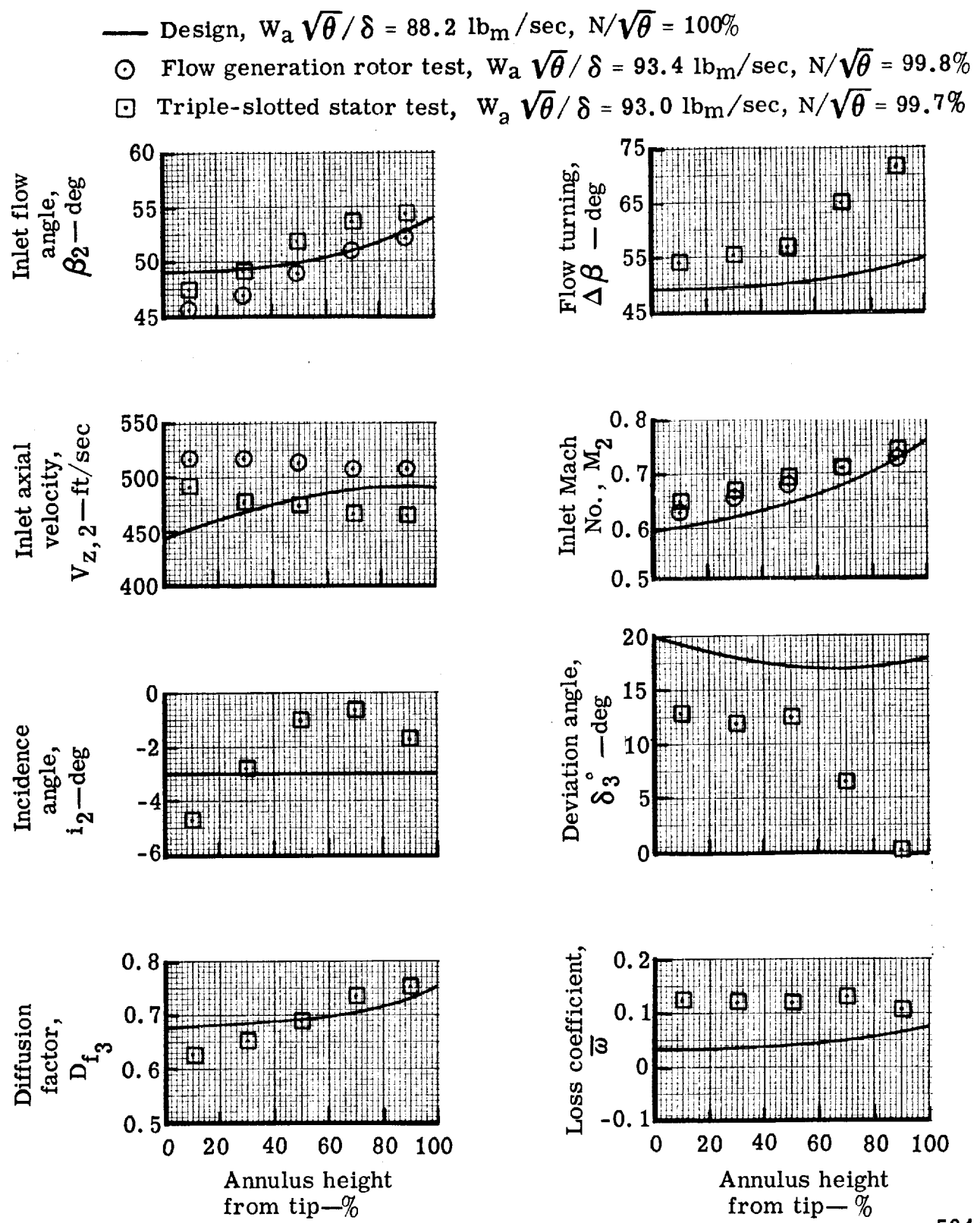
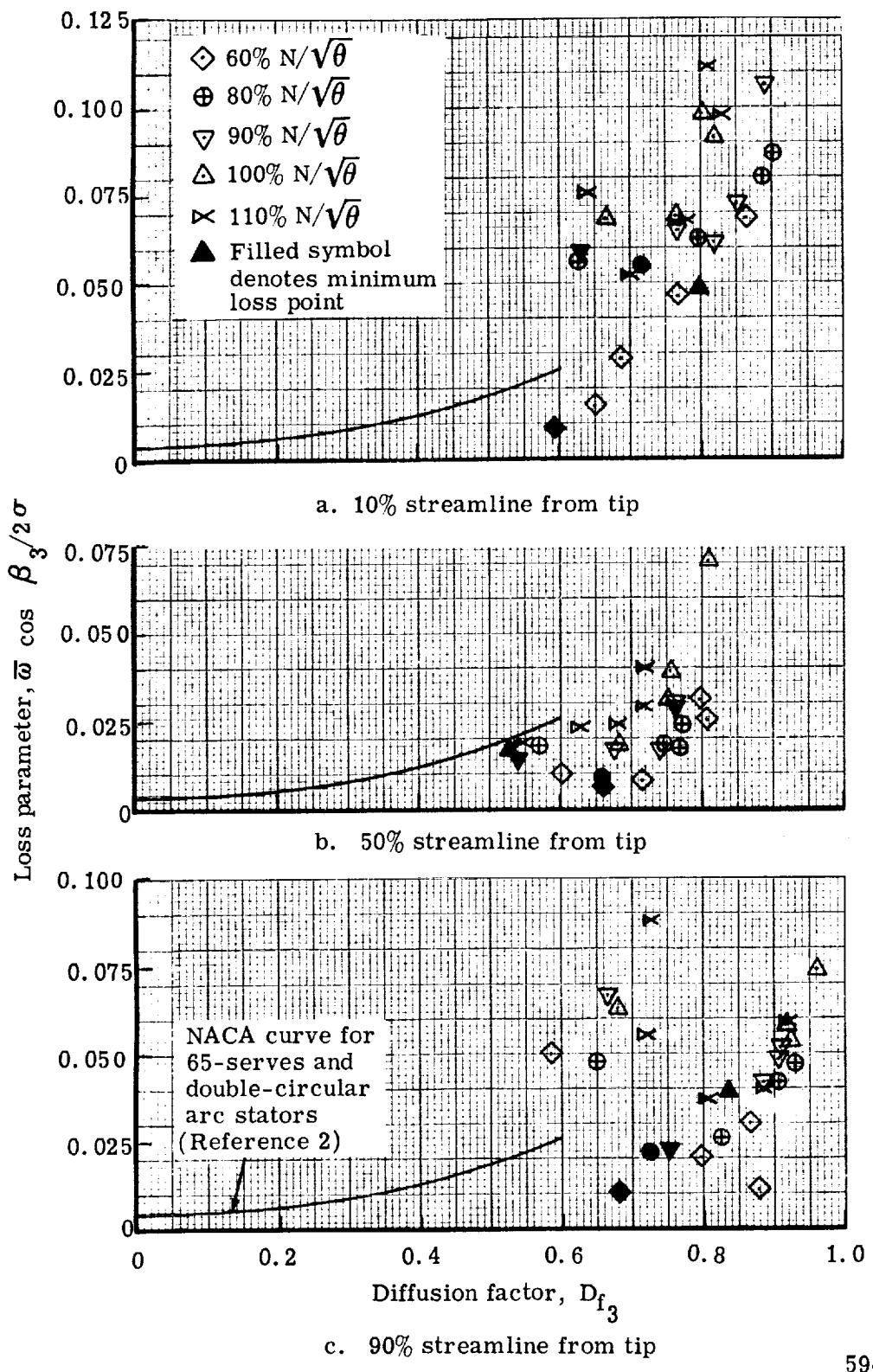


Figure 42. Radial variation of triple-slotted 0.75 D_f stator blade element performance with the mean vane bleed flow rate.



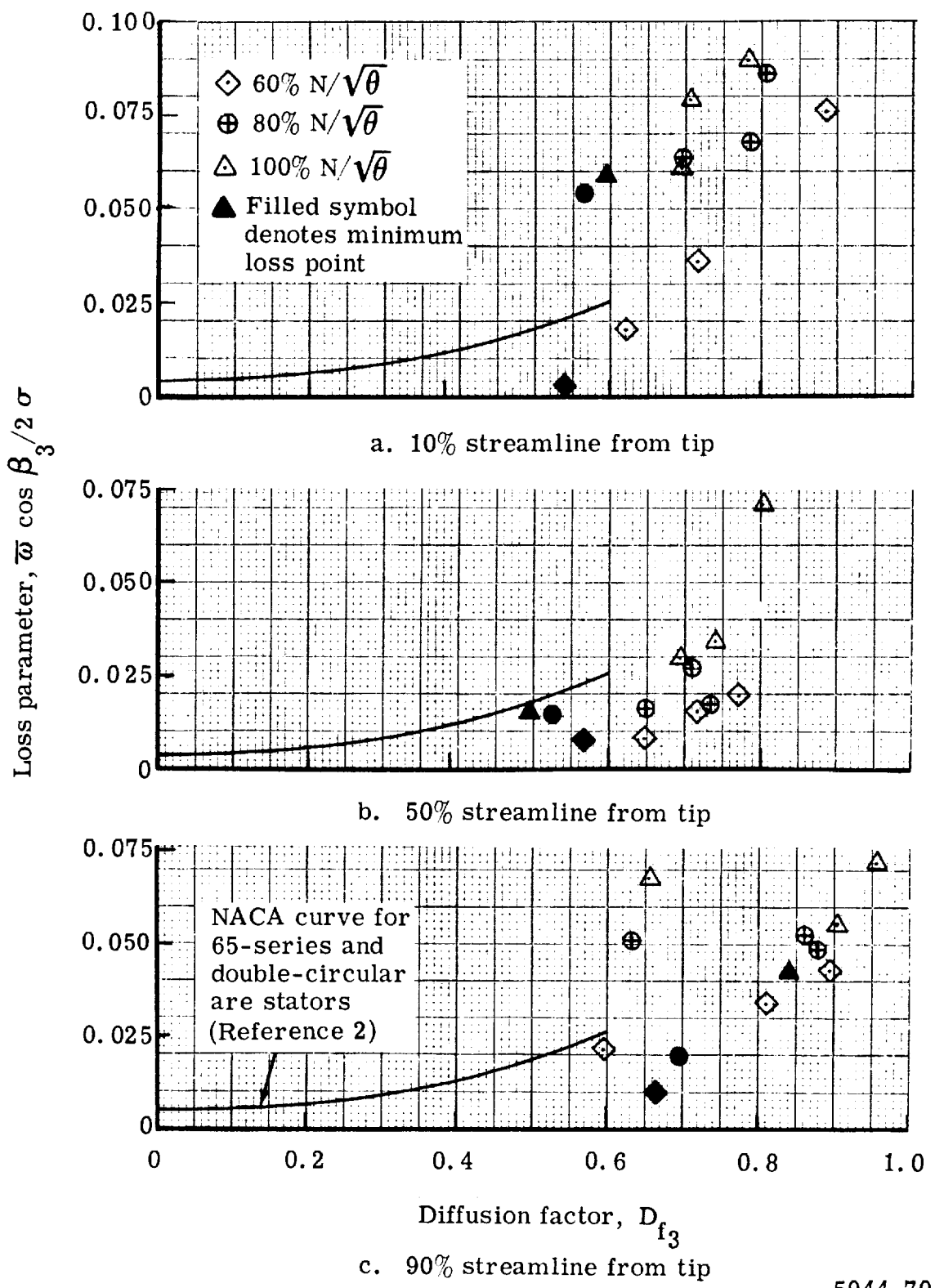
5944-68

Figure 43. Radial variation of triple-slotted 0.75 D_f stator blade element performance with zero vane bleed flow rate.



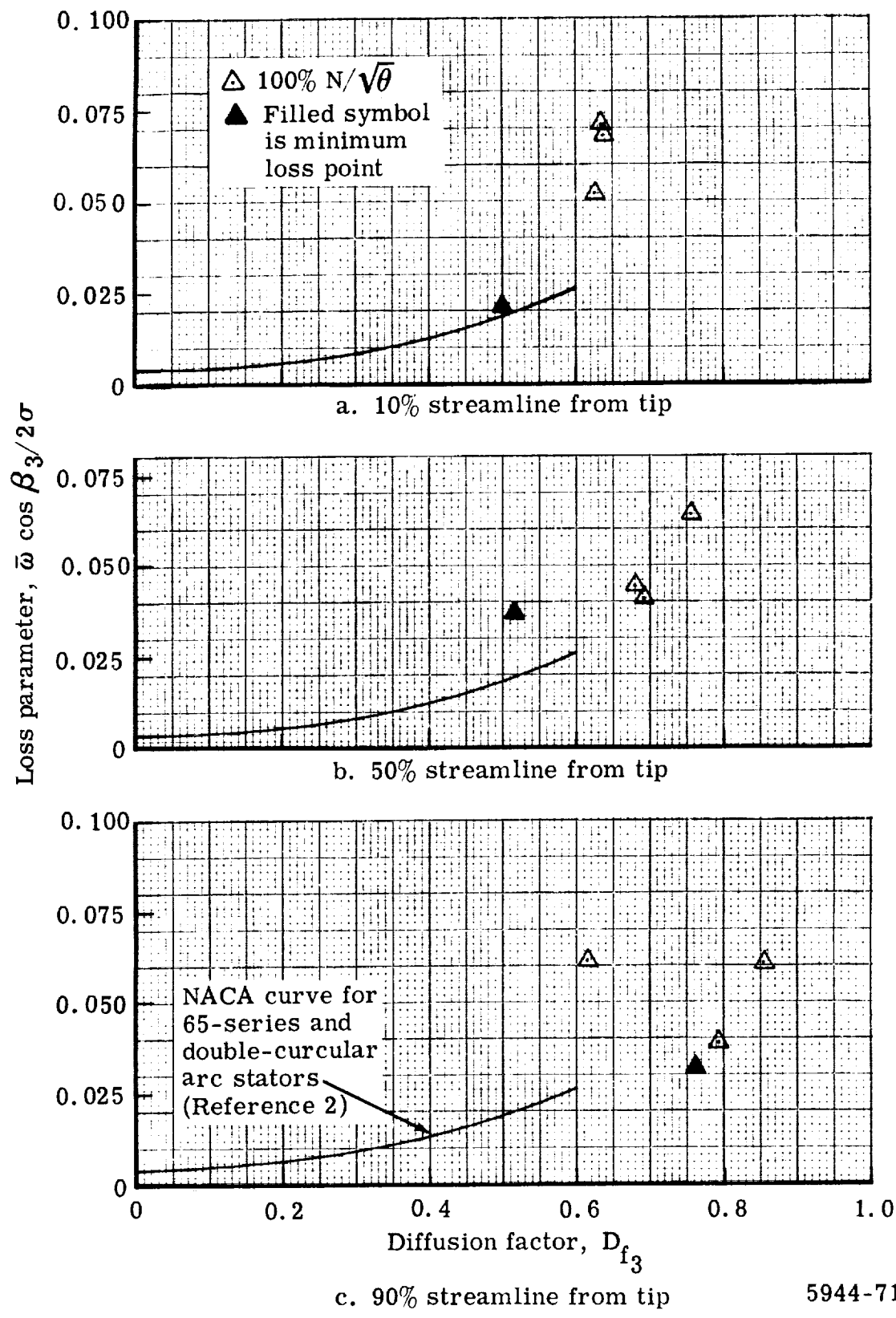
5944-69

Figure 44. Stator loss parameter versus diffusion factor with the vane bleed flow at the optimum rate.



5944-70

Figure 45. Stator loss parameter versus diffusion factor with the mean vane bleed flow rate.



5944-71

Figure 46. Stator loss parameter versus diffusion factor with zero vane bleed flow rate.

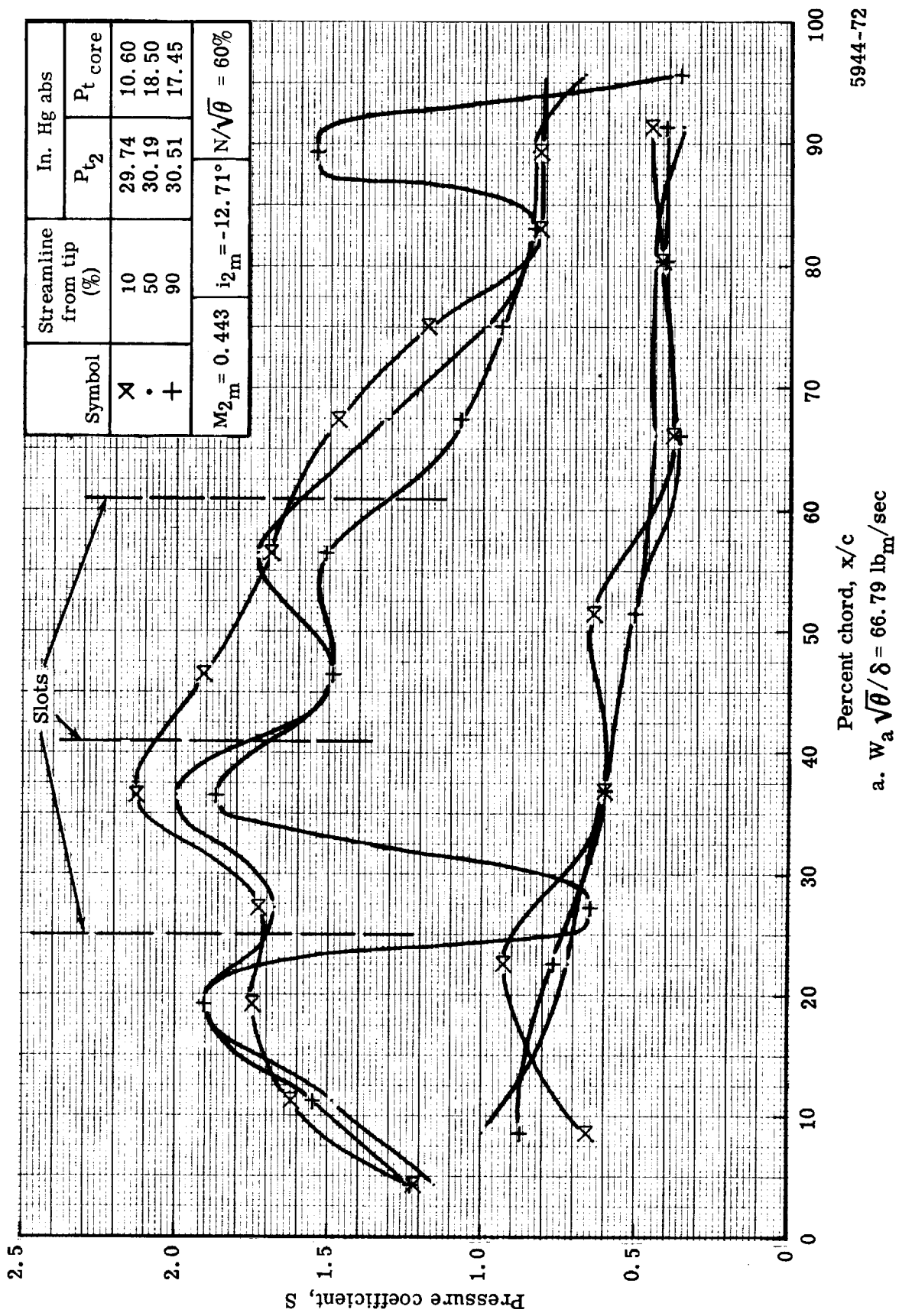


Figure 47. Triple-slotted stator static pressure distribution at 60% speed and vane bleed flow at the optimum rate.

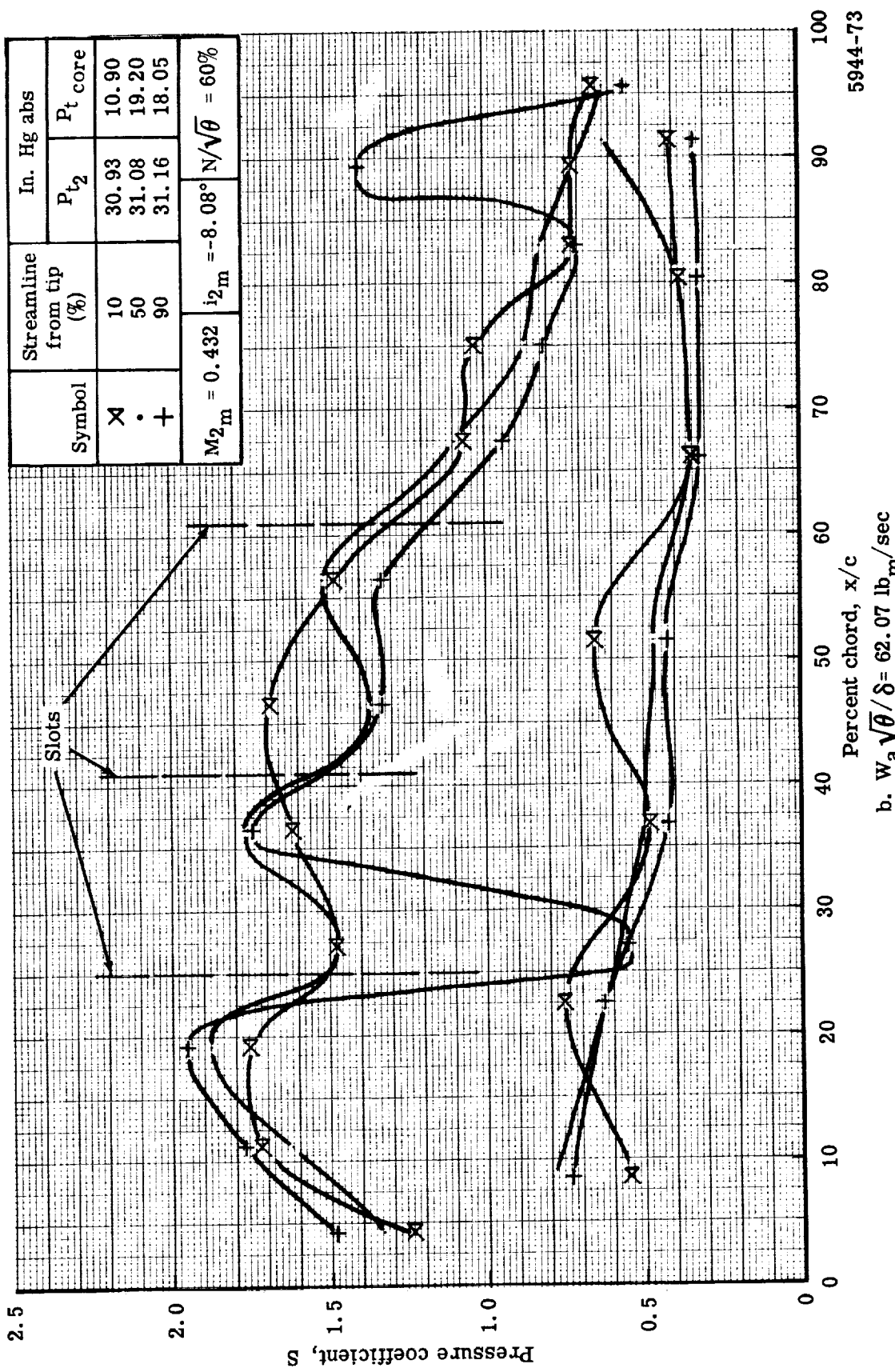


Figure 47. Triple-slotted stator static pressure distribution at 60% speed and vane bleed flow at the optimum rate.

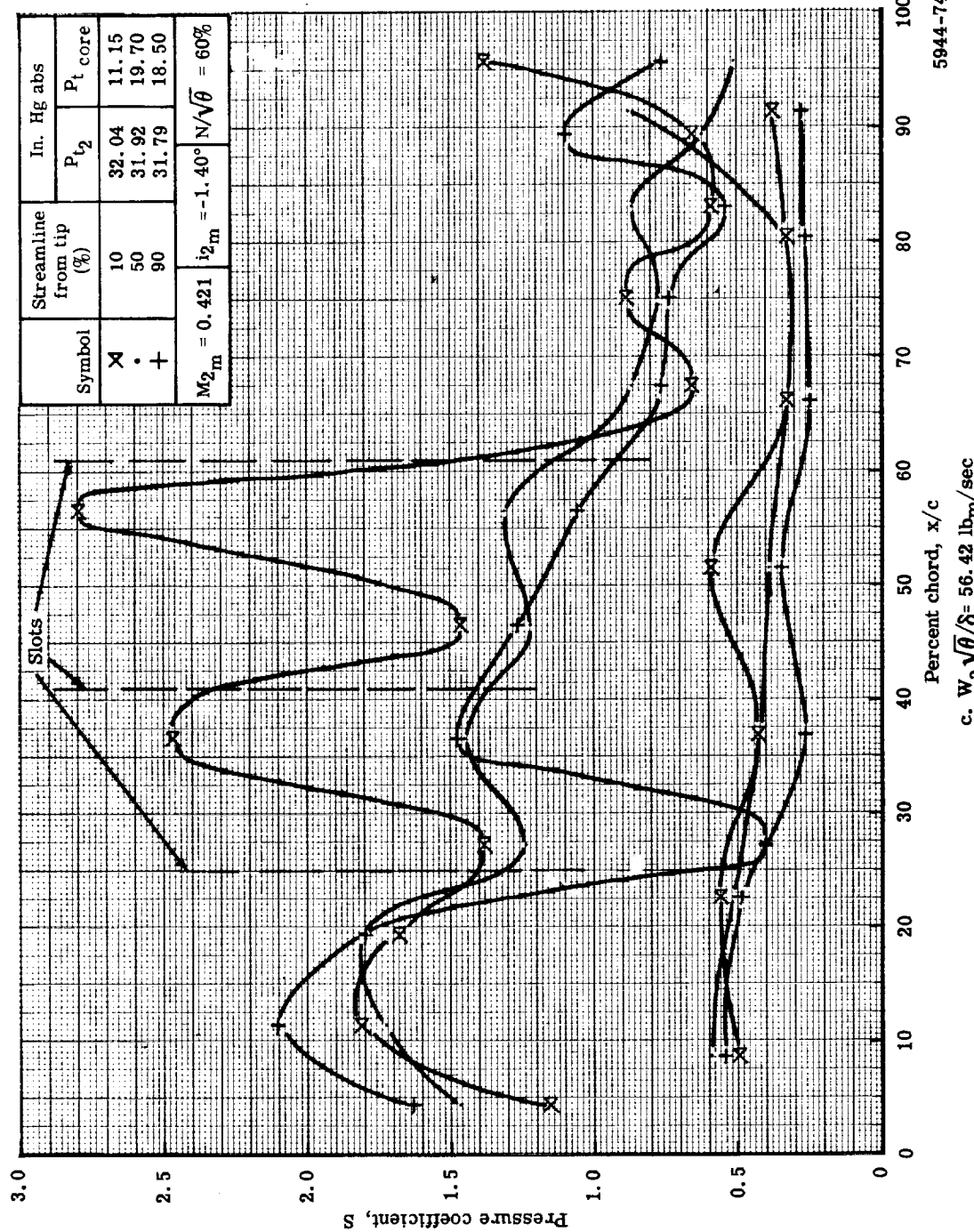


Figure 47. Triple-slotted stator static pressure distribution at 60% speed and vane bleed flow at the optimum rate.

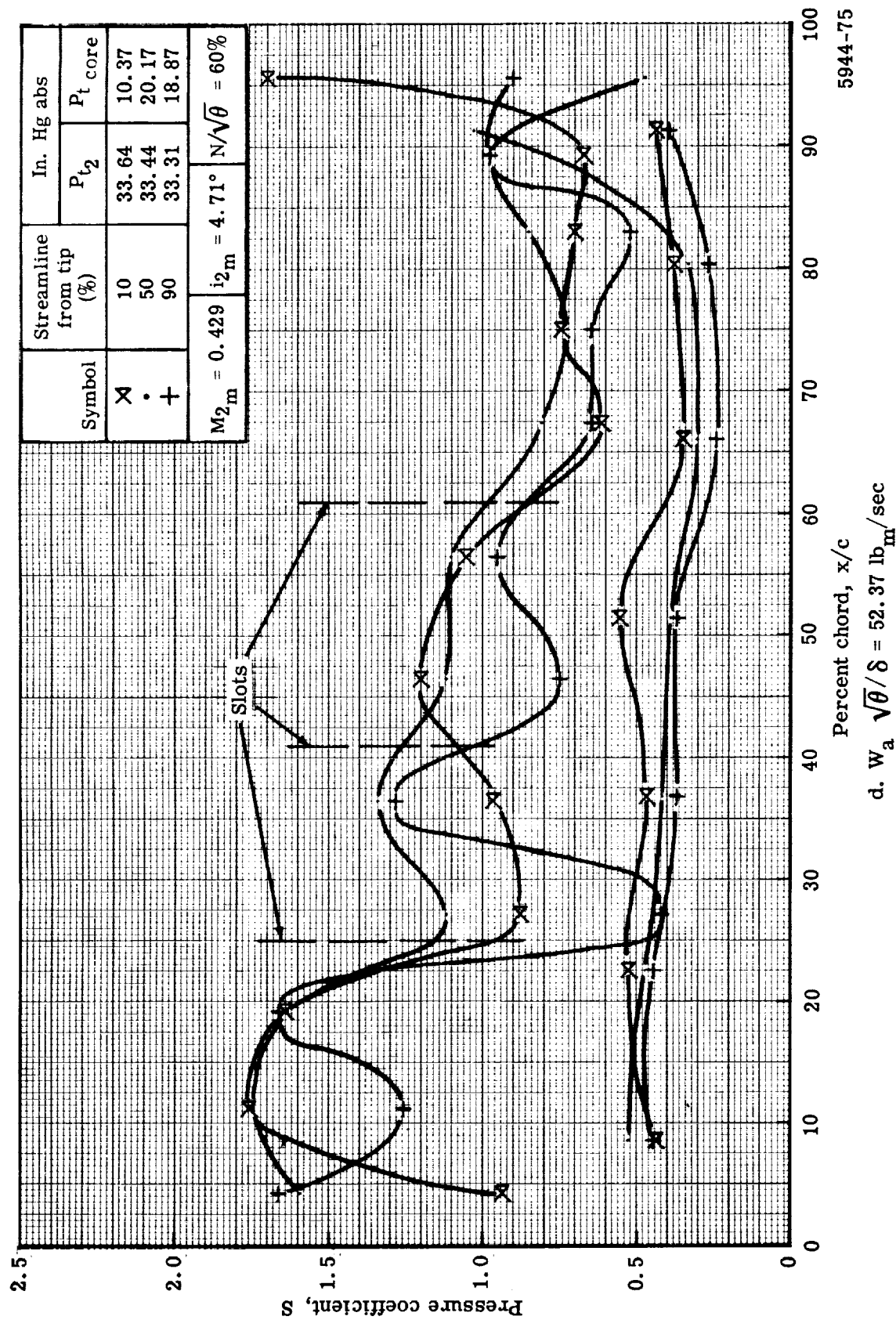


Figure 47. Triple-slotted stator static pressure distribution at 60% speed and vane bleed flow at the optimum rate.

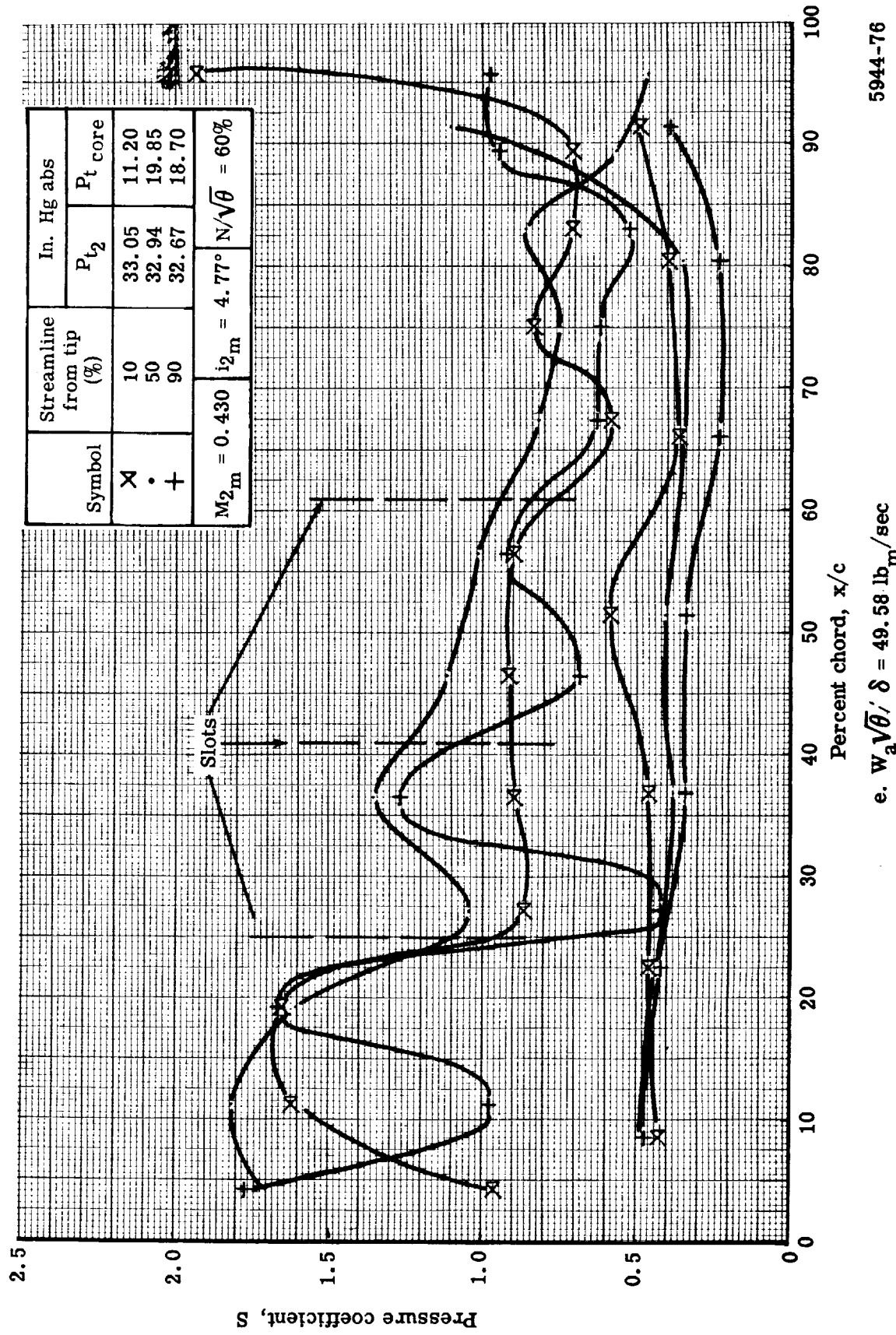
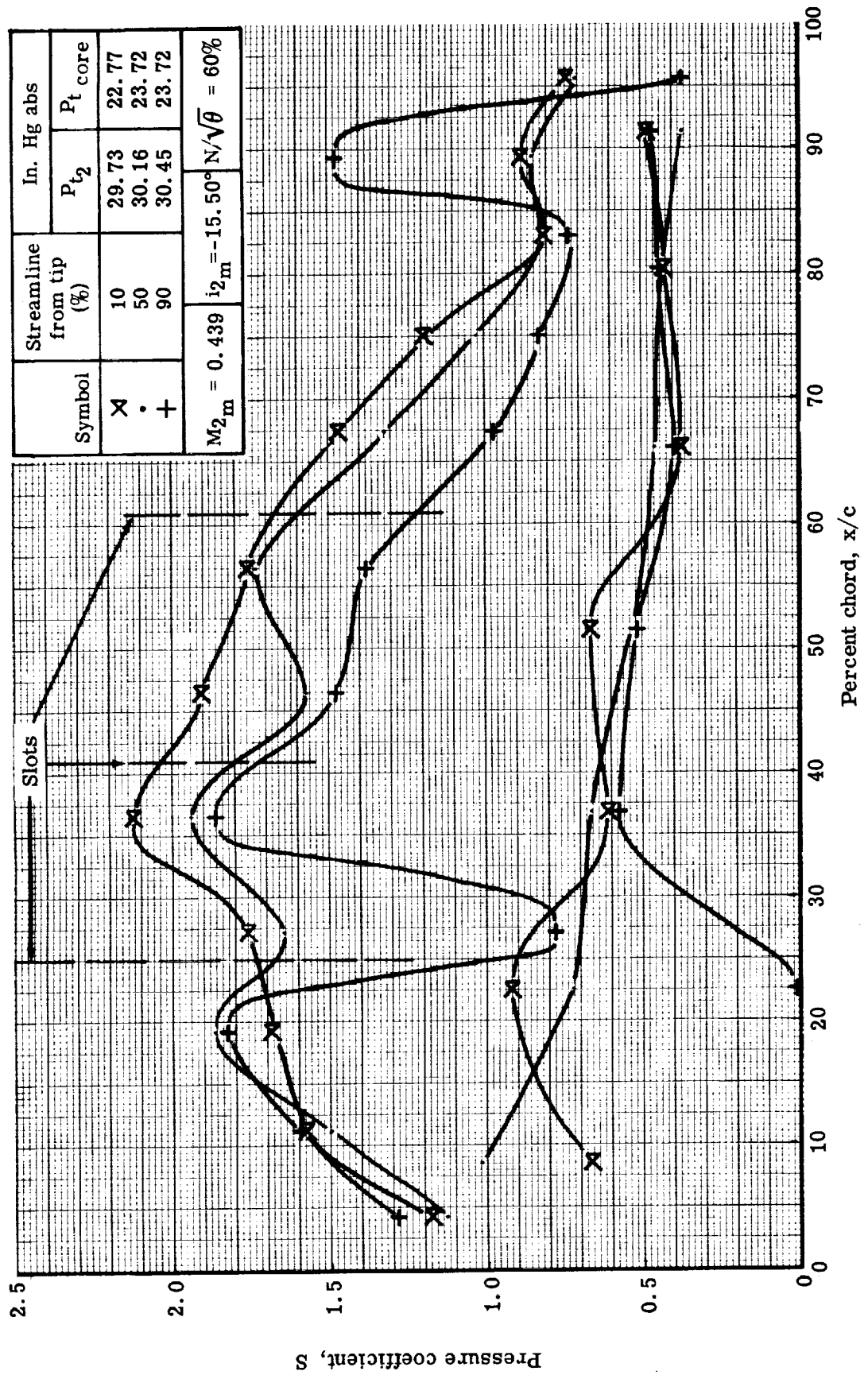


Figure 47. Triple-slotted stator static pressure distribution at 60% speed and vane bleed flow at the optimum rate.



a. $W_a \sqrt{\theta}/\delta = 66.21 \text{ lb}_M/\text{sec}$ 5944-77

Figure 48. Triple-slotted stator static pressure distribution at 60% speed and mean vane bleed flow rate.

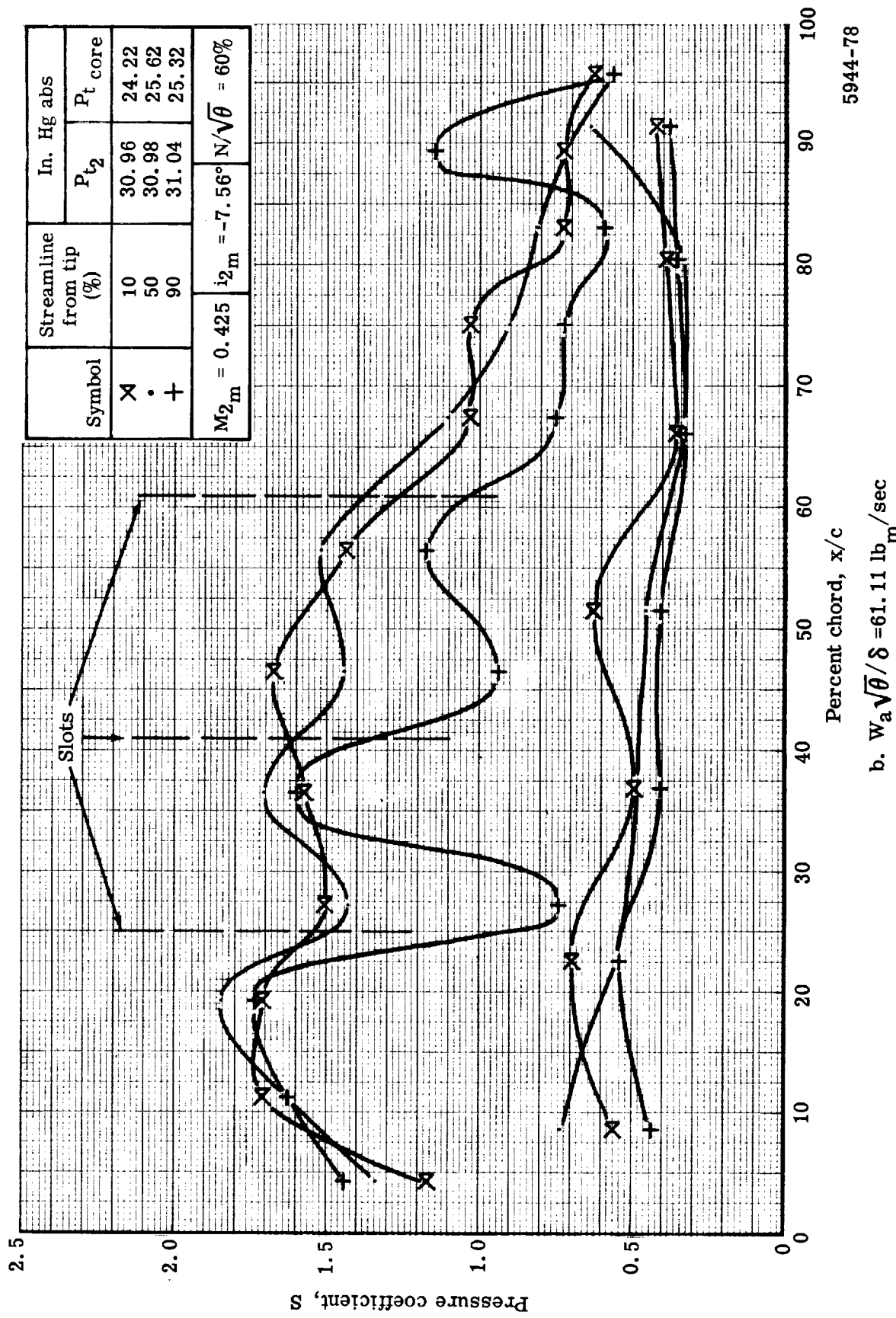


Figure 48. Triple-slotted stator static pressure distribution at 60% speed and mean vane bleed flow rate.

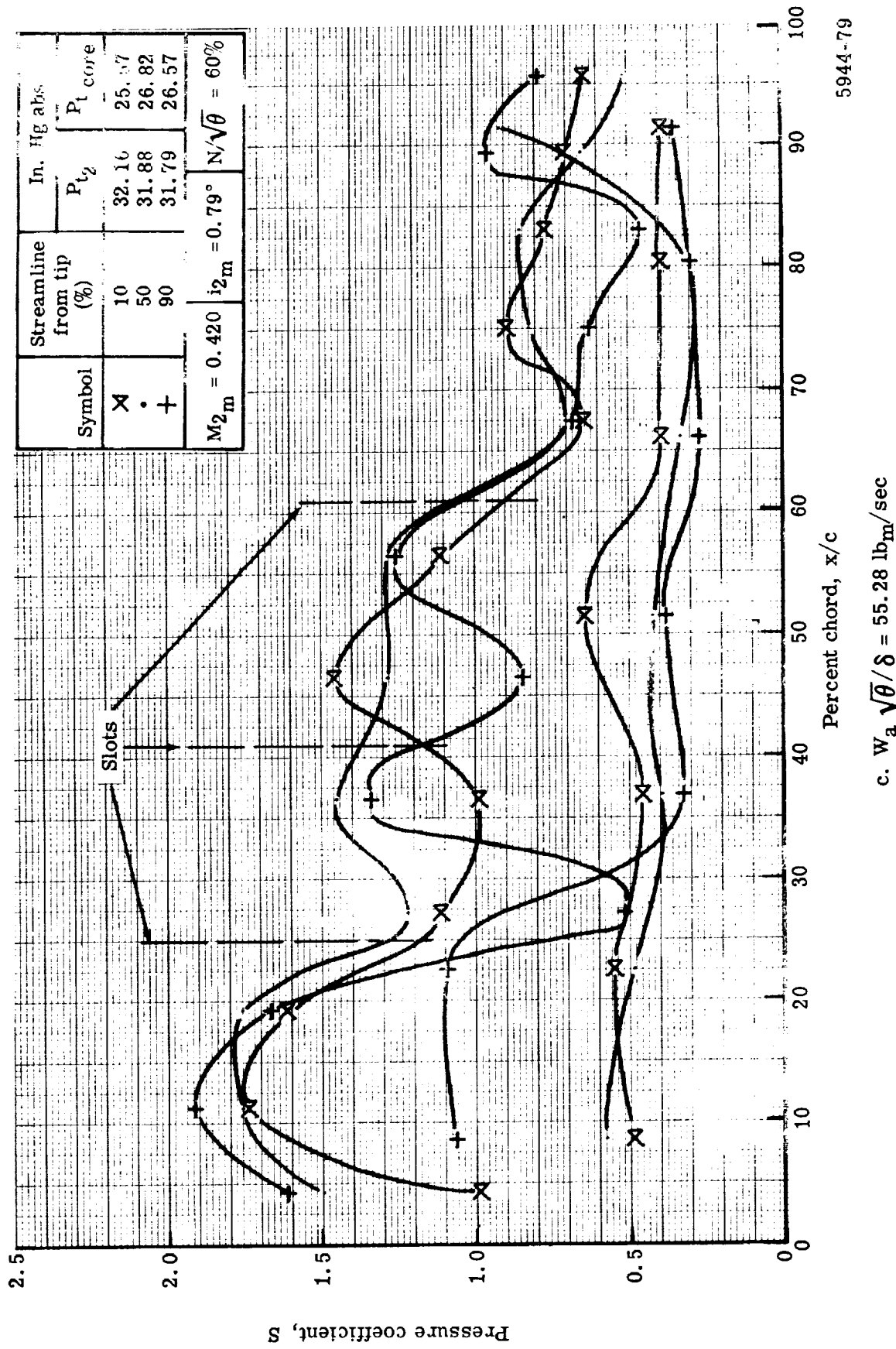


Figure 48. Triple-slotted stator static pressure distribution at 60% speed and mean vane bleed flow rate

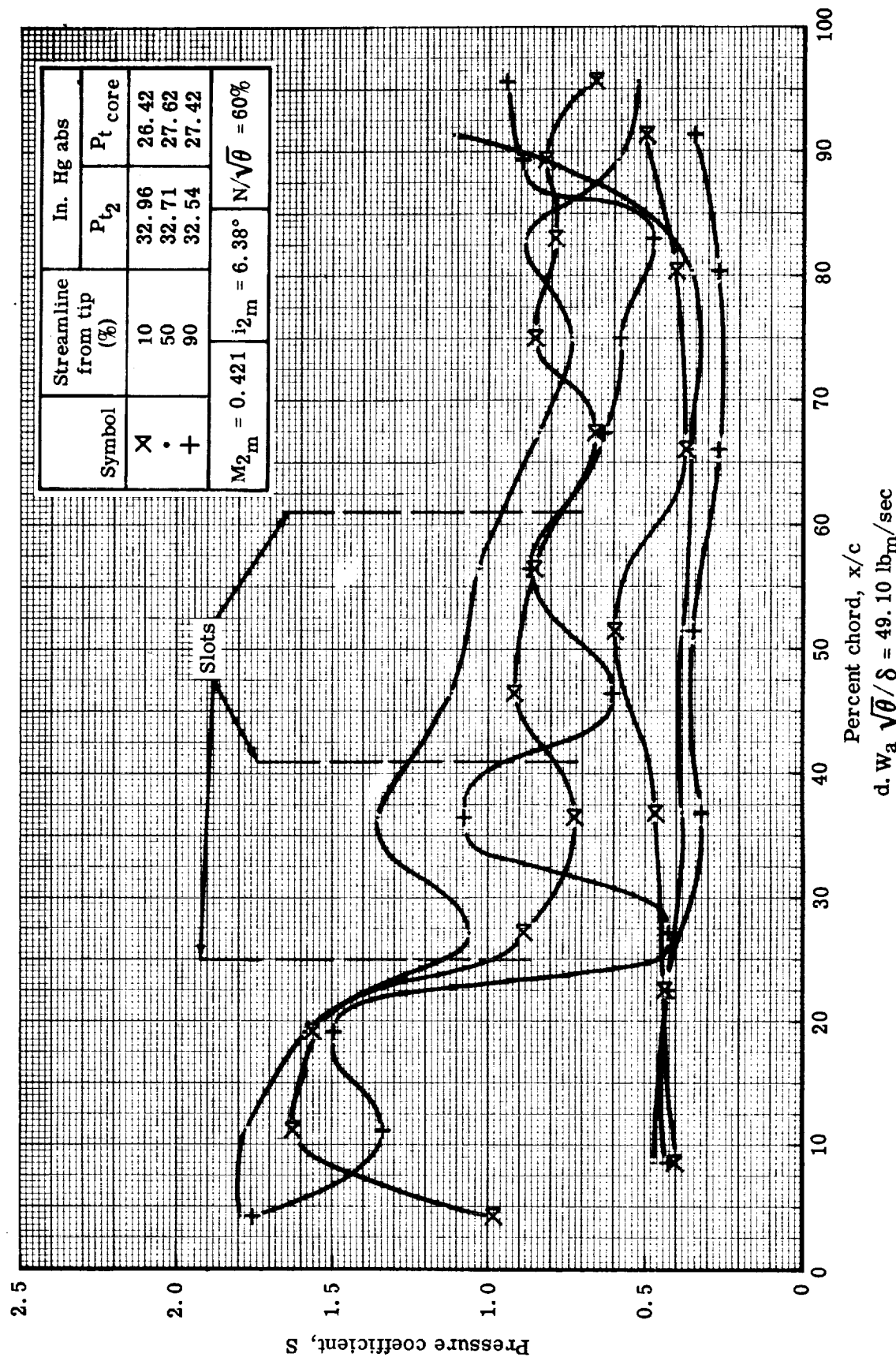
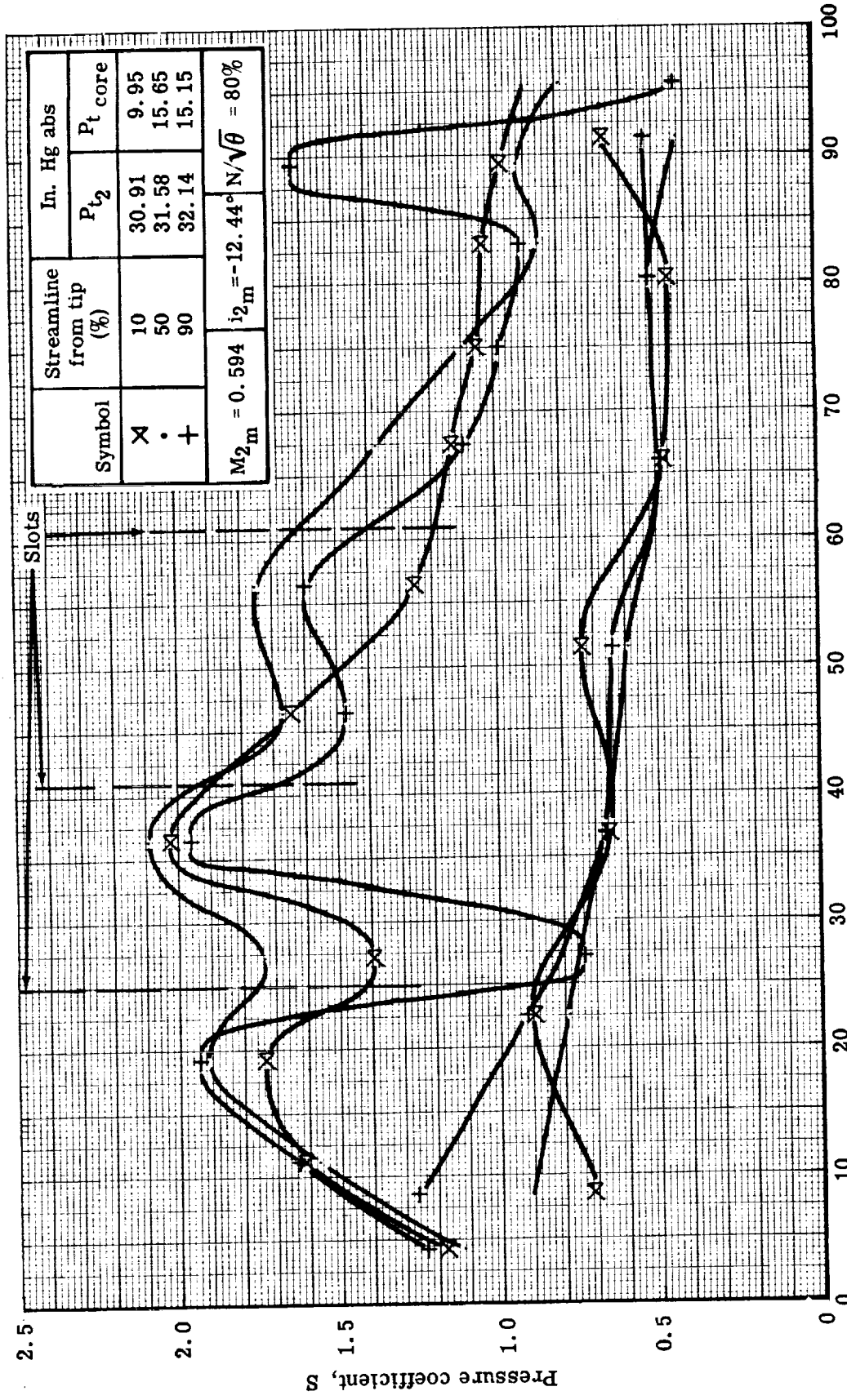


Figure 48. Triple-slotted stator static pressure distribution at 60% speed and mean vane bleed flow rate.

$$d. w_a \sqrt{\theta}/\delta = 49.10 \text{ lb}_m/\text{sec}$$

5944-80



5944-81

Figure 49. Triple-slotted stator static pressure distribution at 80% speed and vane bleed flow at the optimum rate.

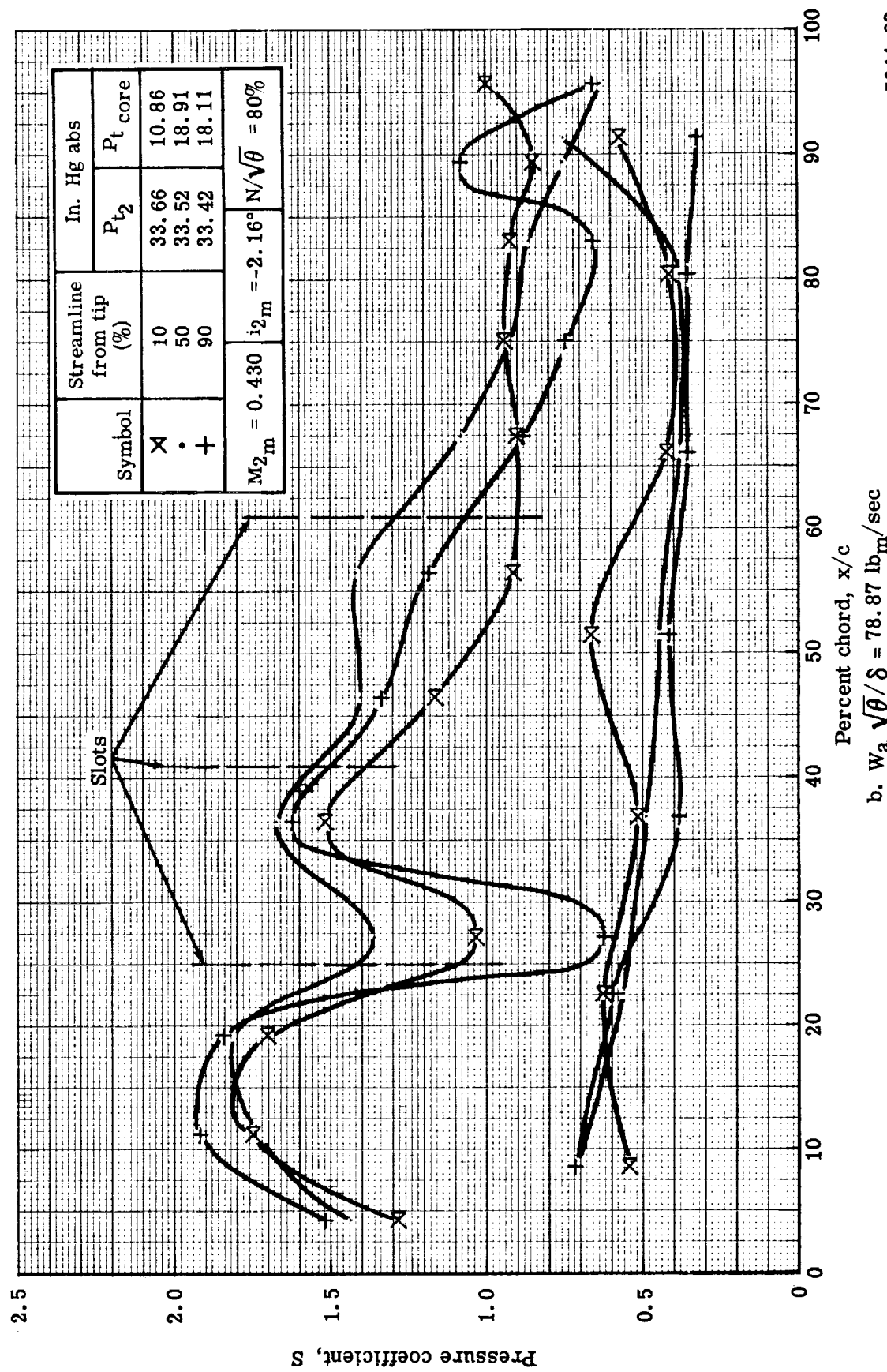


Figure 49. Triple-slotted stator static pressure distribution at 80% speed and vane bleed flow at the optimum rate.

5944-82

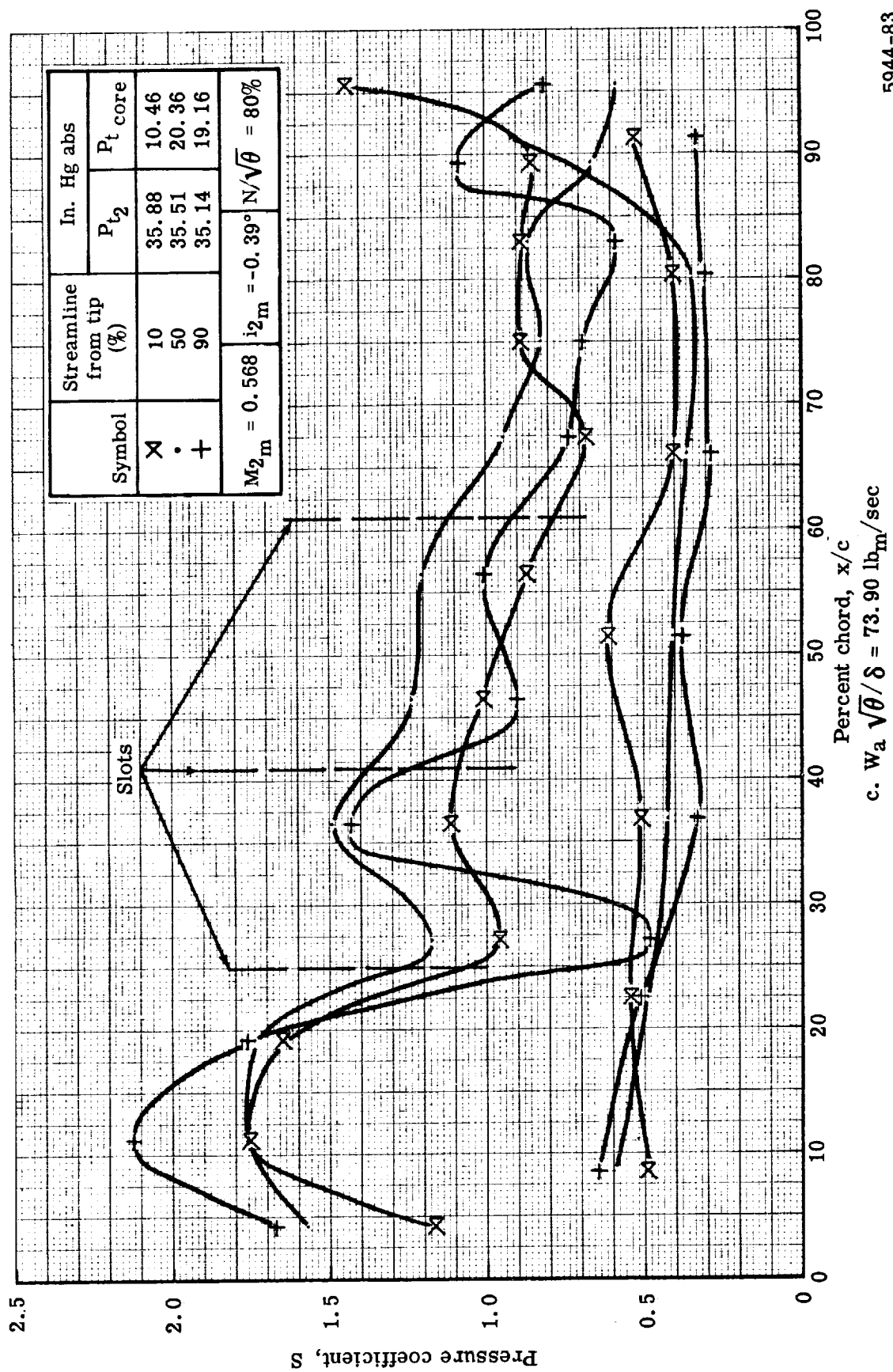


Figure 49. Triple-slotted stator static pressure distribution at 80% speed and vane bleed flow at the optimum rate.
5944-83

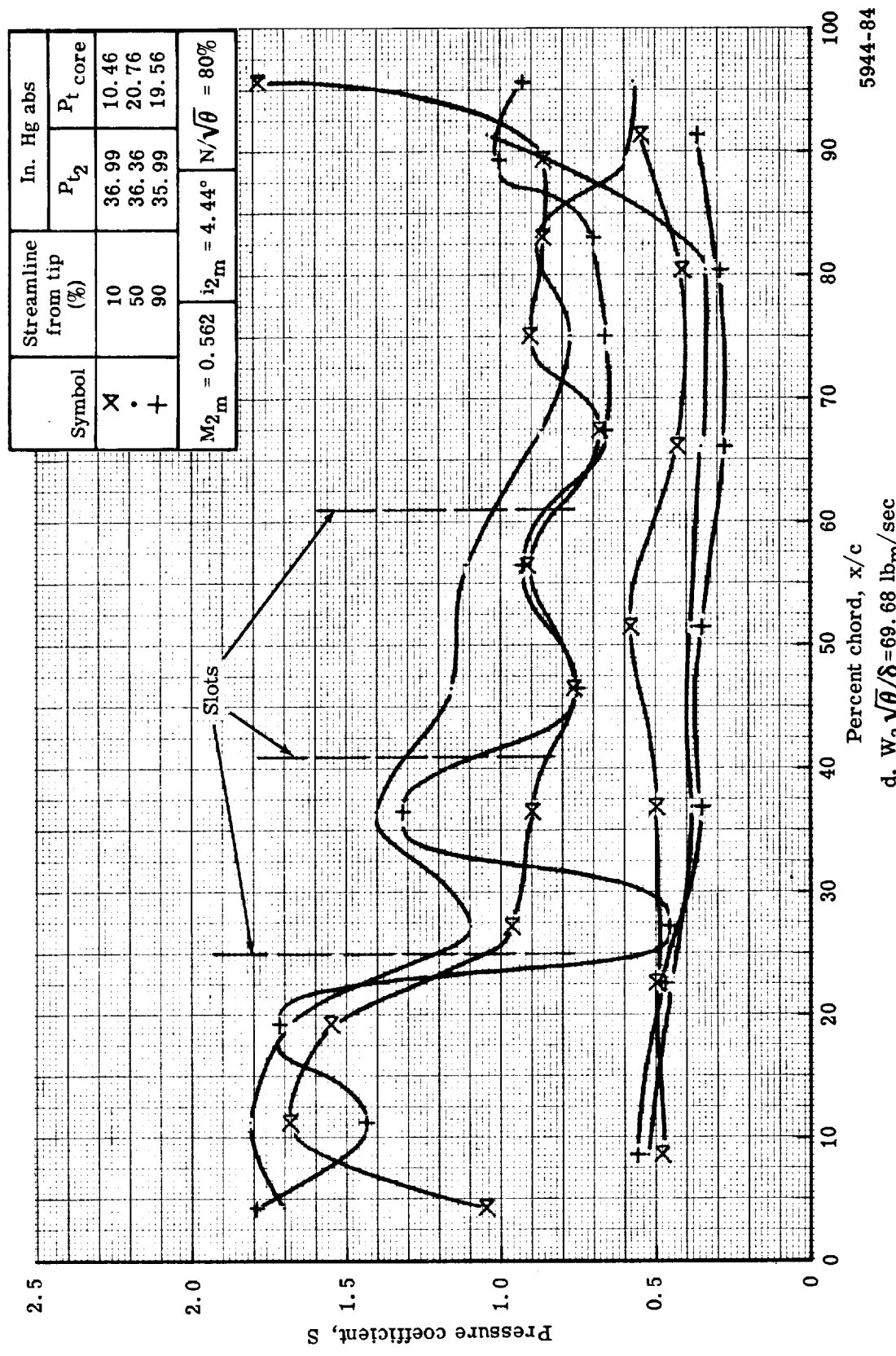


Figure 49. Triple-slotted stator static pressure distribution at 80% speed and vane bleed flow at the optimum rate.

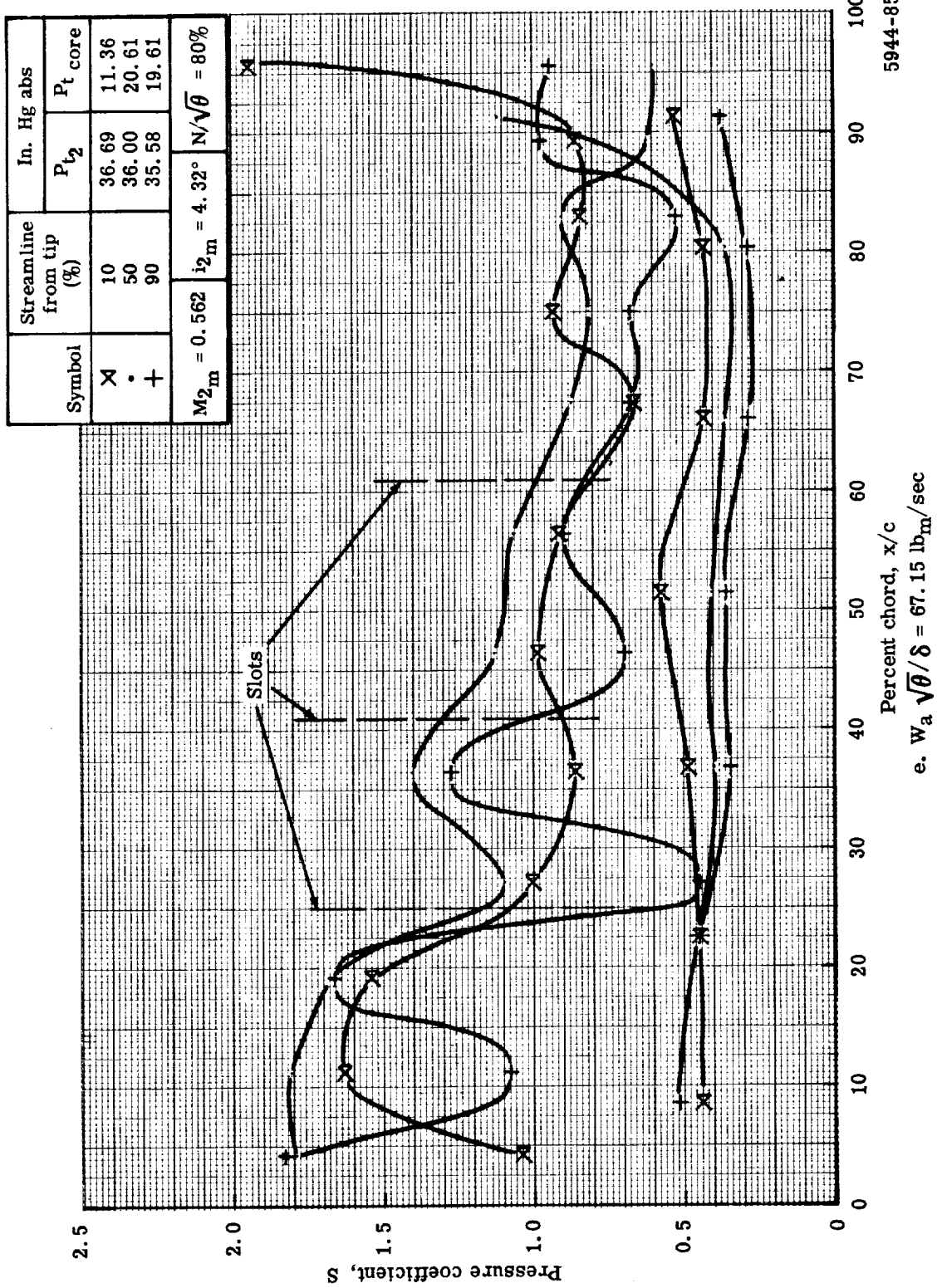


Figure 49. Triple-slotted stator static pressure distribution at 80% speed and vane bleed flow at the optimum rate.

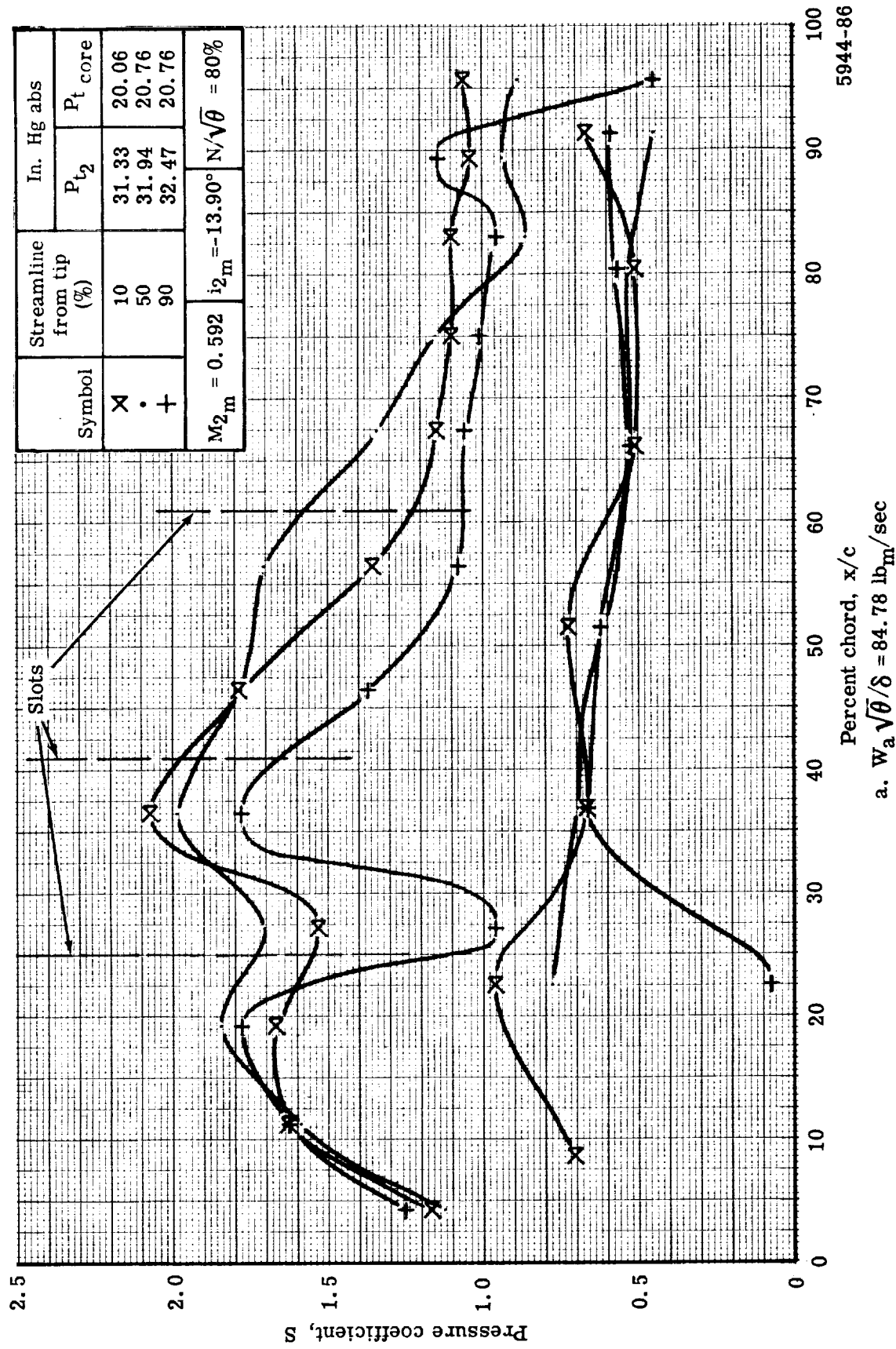


Figure 50. Triple-slotted stator static pressure distribution at 80% speed and mean vane bleed flow rate.

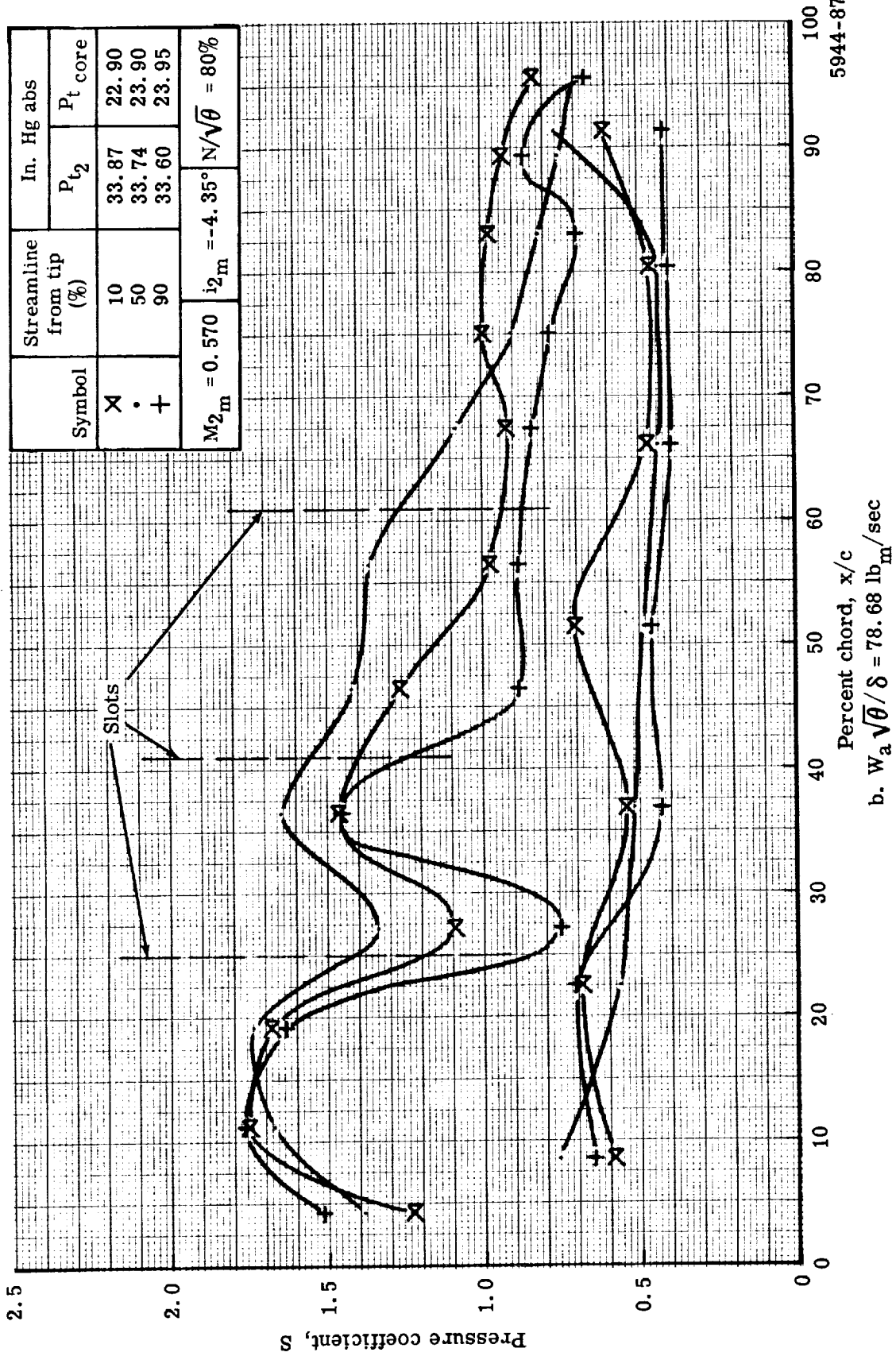


Figure 50. Triple-slotted stator static pressure distribution at 80% speed and mean vane bleed flow rate.

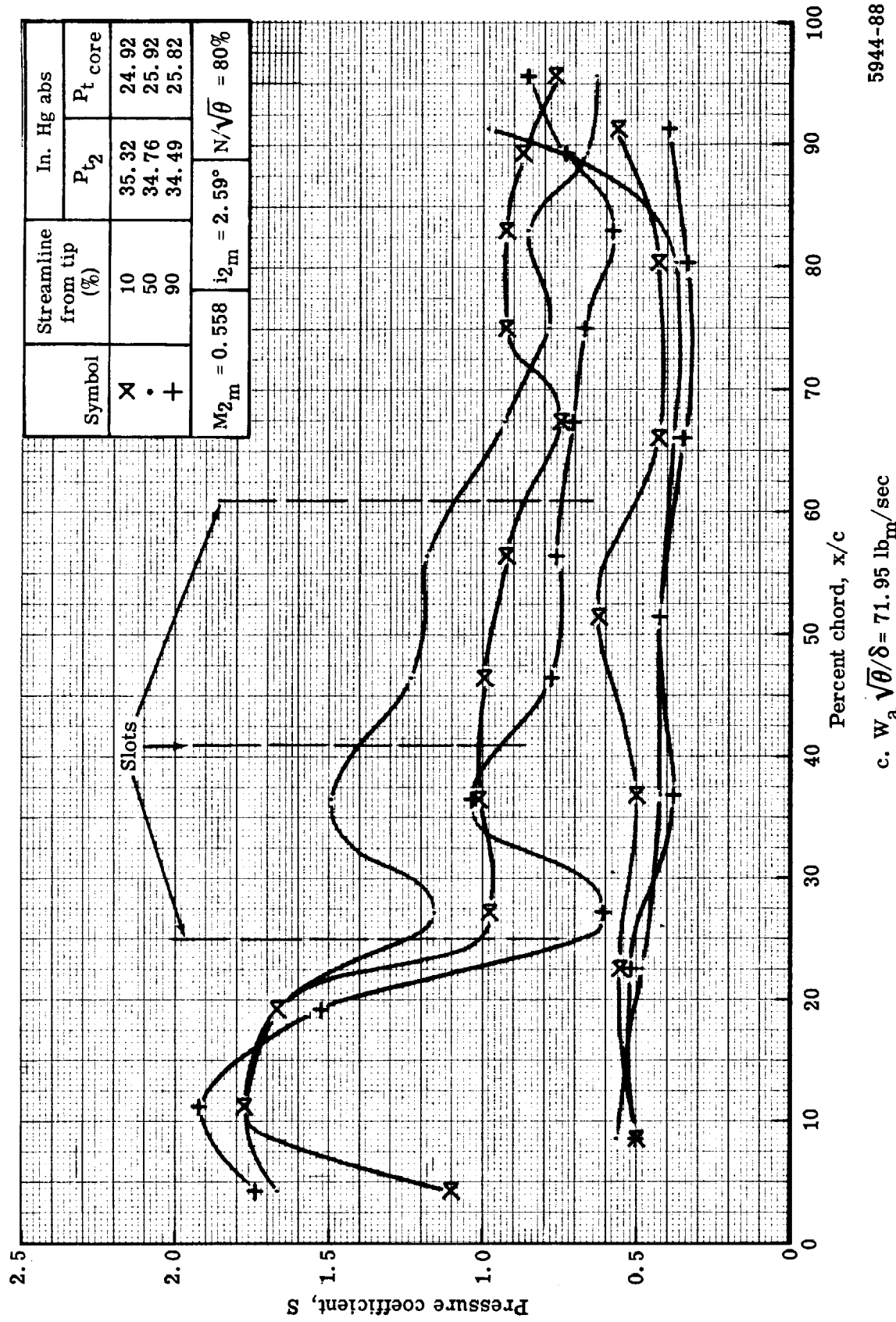


Figure 50. Triple-slotted stator static pressure distribution at 80% speed and mean vane bleed flow rate.

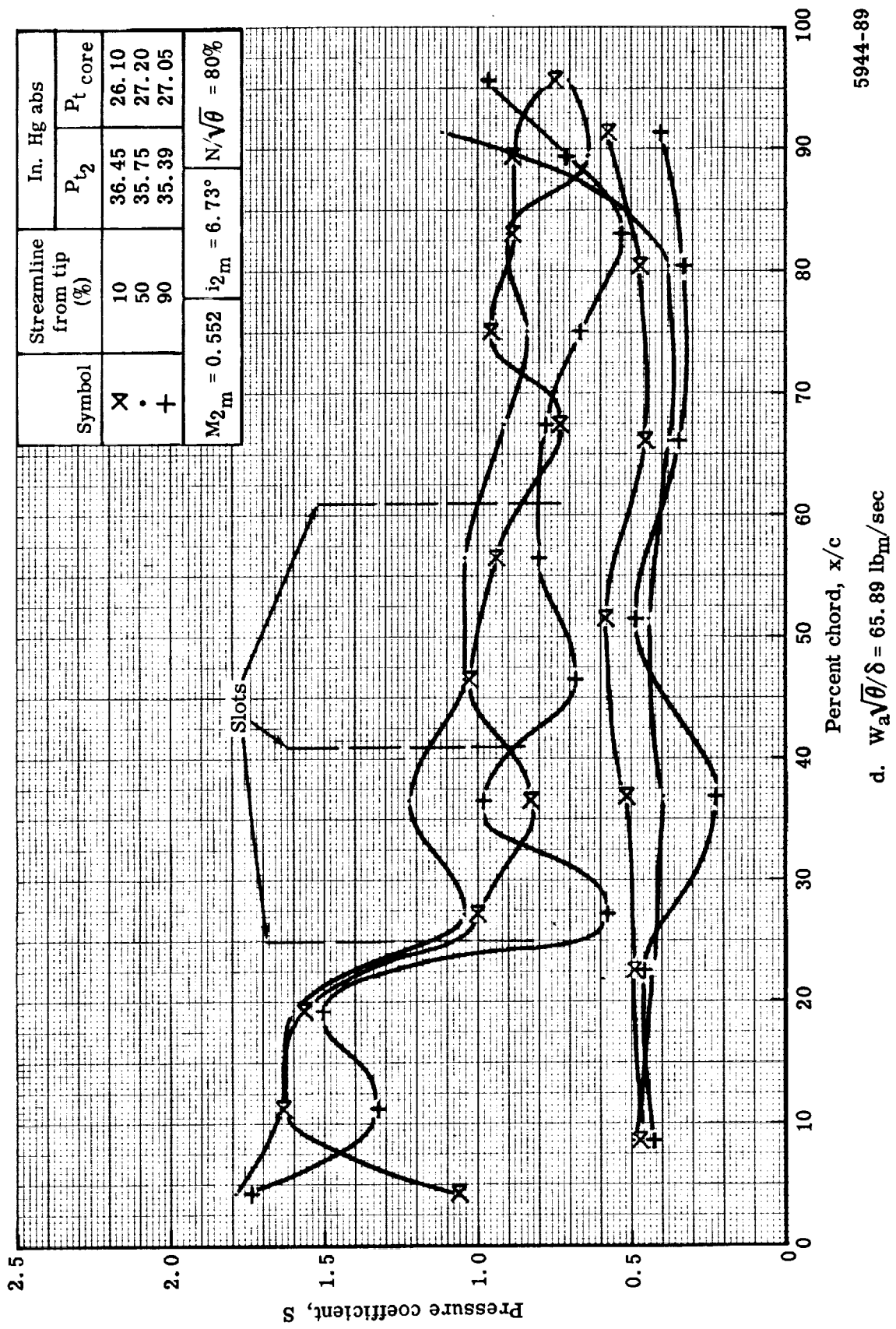


Figure 50. Triple-slotted stator static pressure distribution at 80% speed and mean vane bleed flow rate.

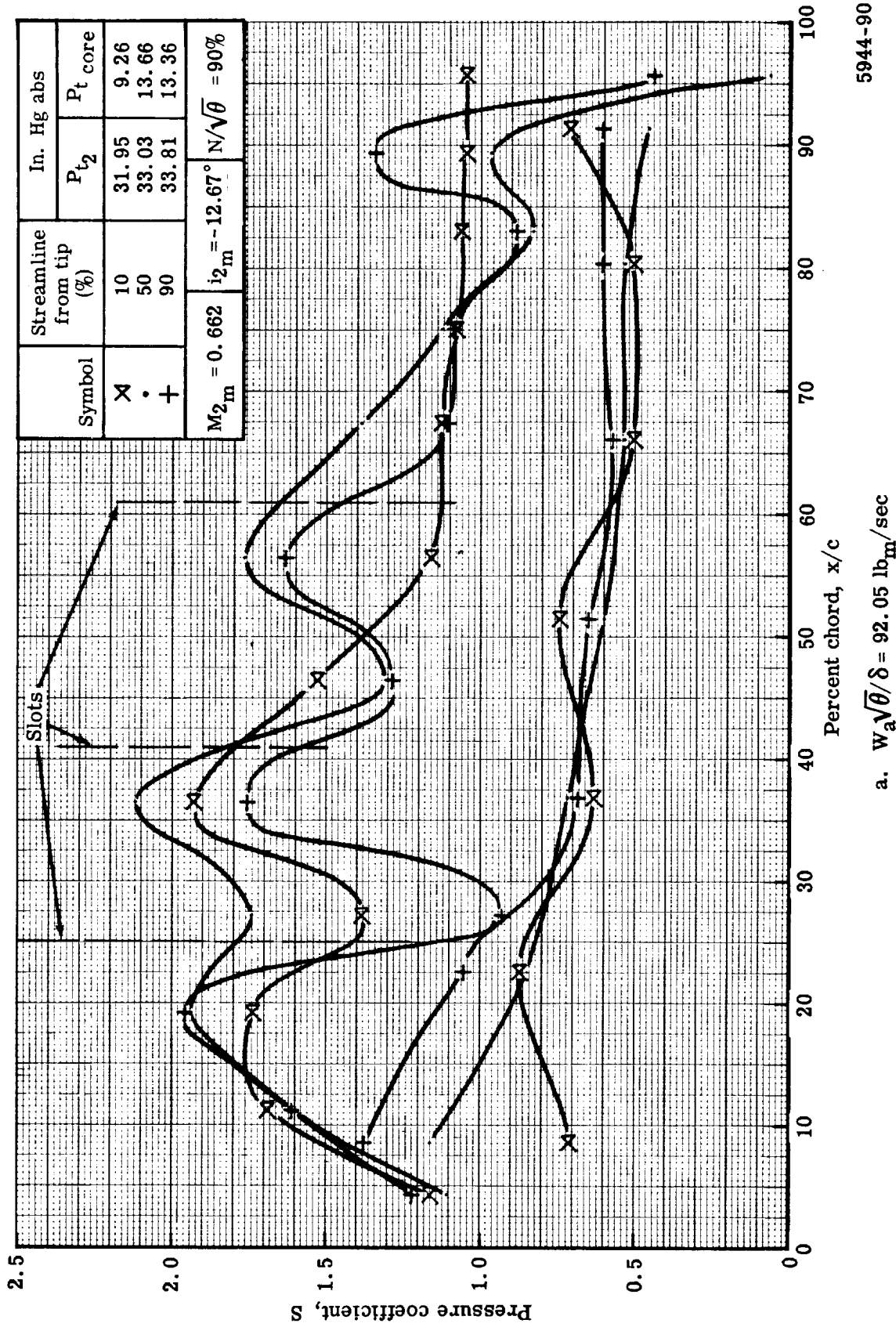


Figure 51. Triple-slotted stator static pressure distribution at 90% speed and vane bleed flow at the optimum rate.

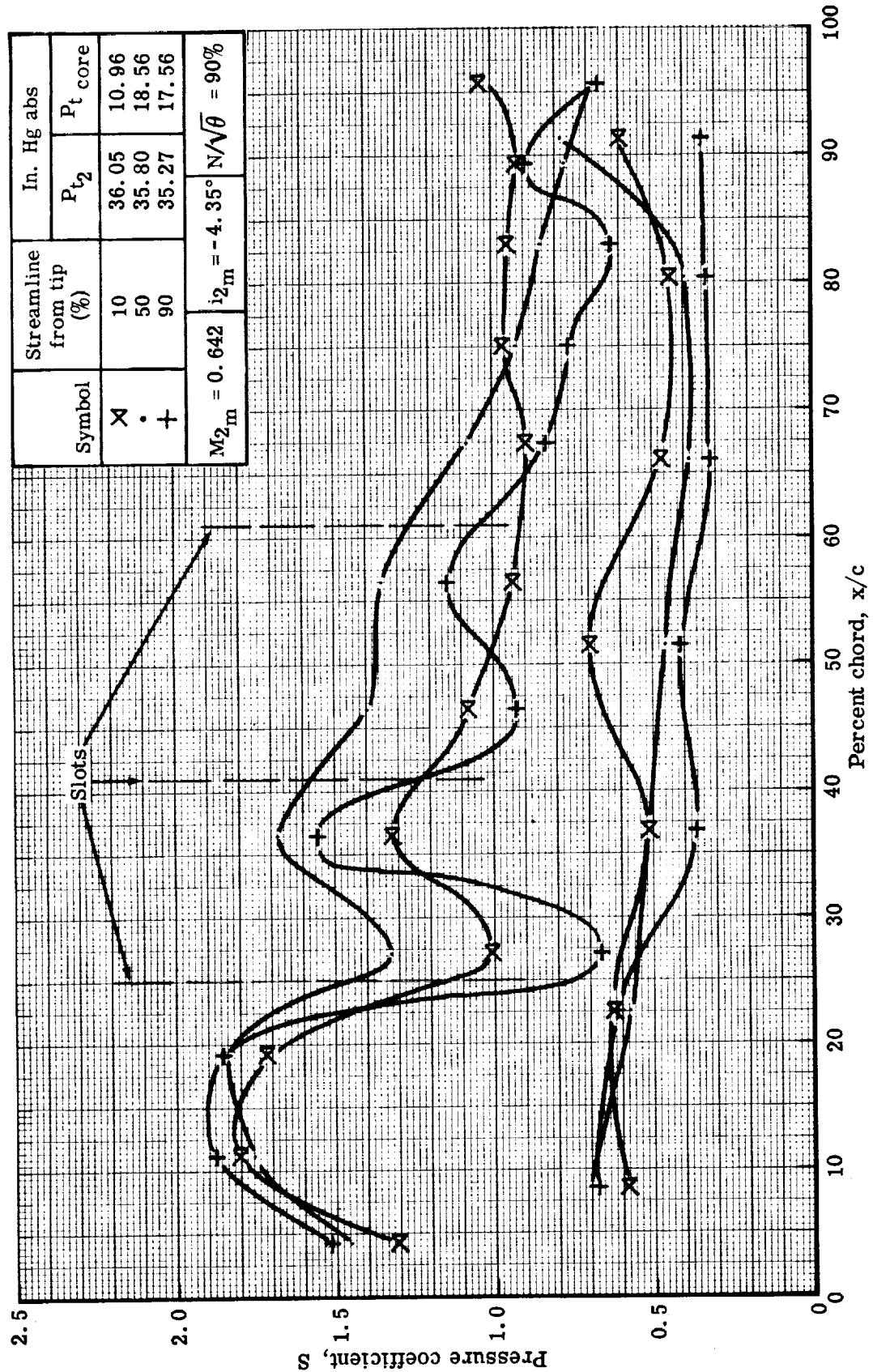


Figure 51. Triple-slotted stator static pressure distribution at 90% speed and vane bleed flow at the optimum rate.

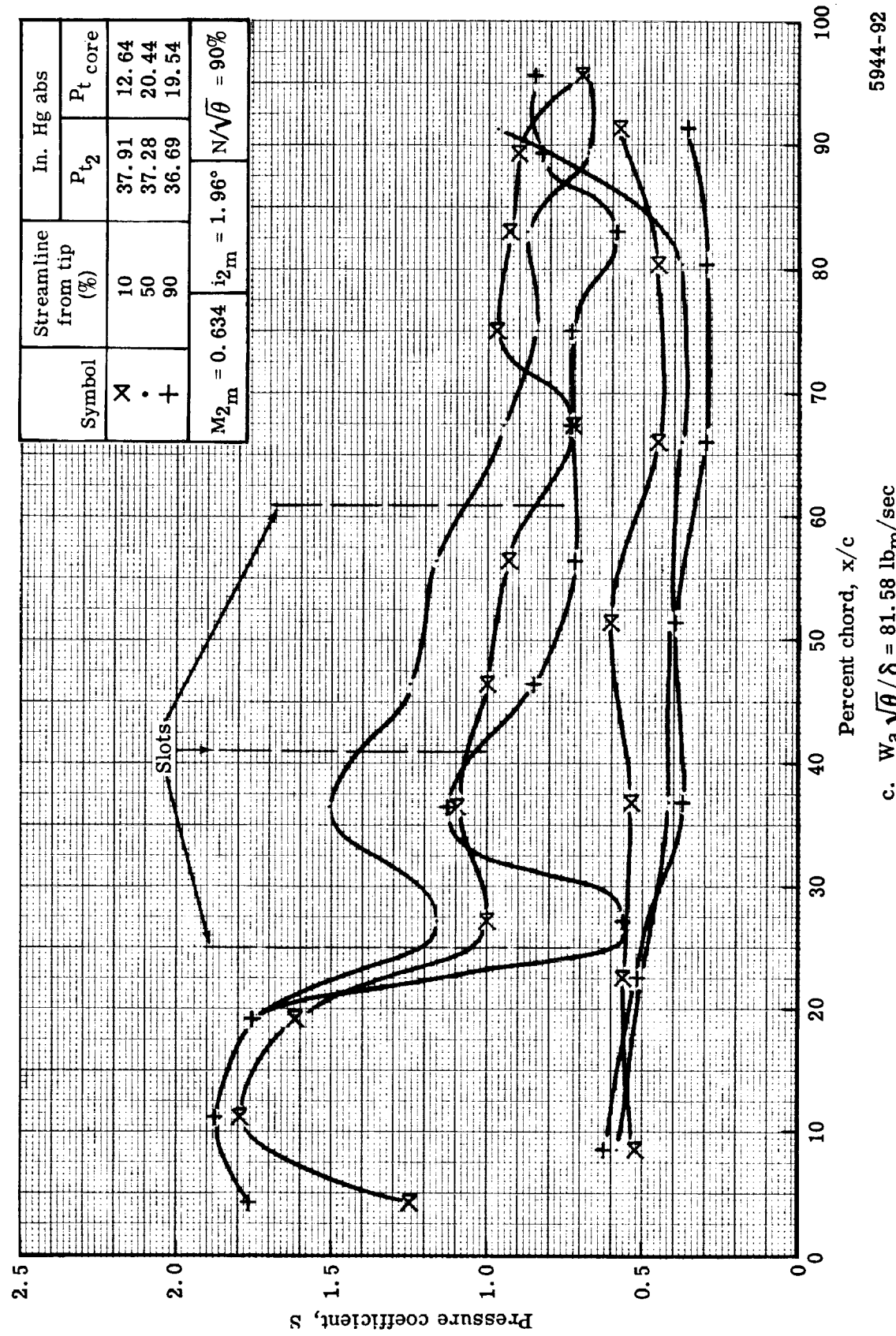


Figure 51. Triple-slotted stator static pressure distribution at 90% speed and vane bleed flow at the optimum rate.

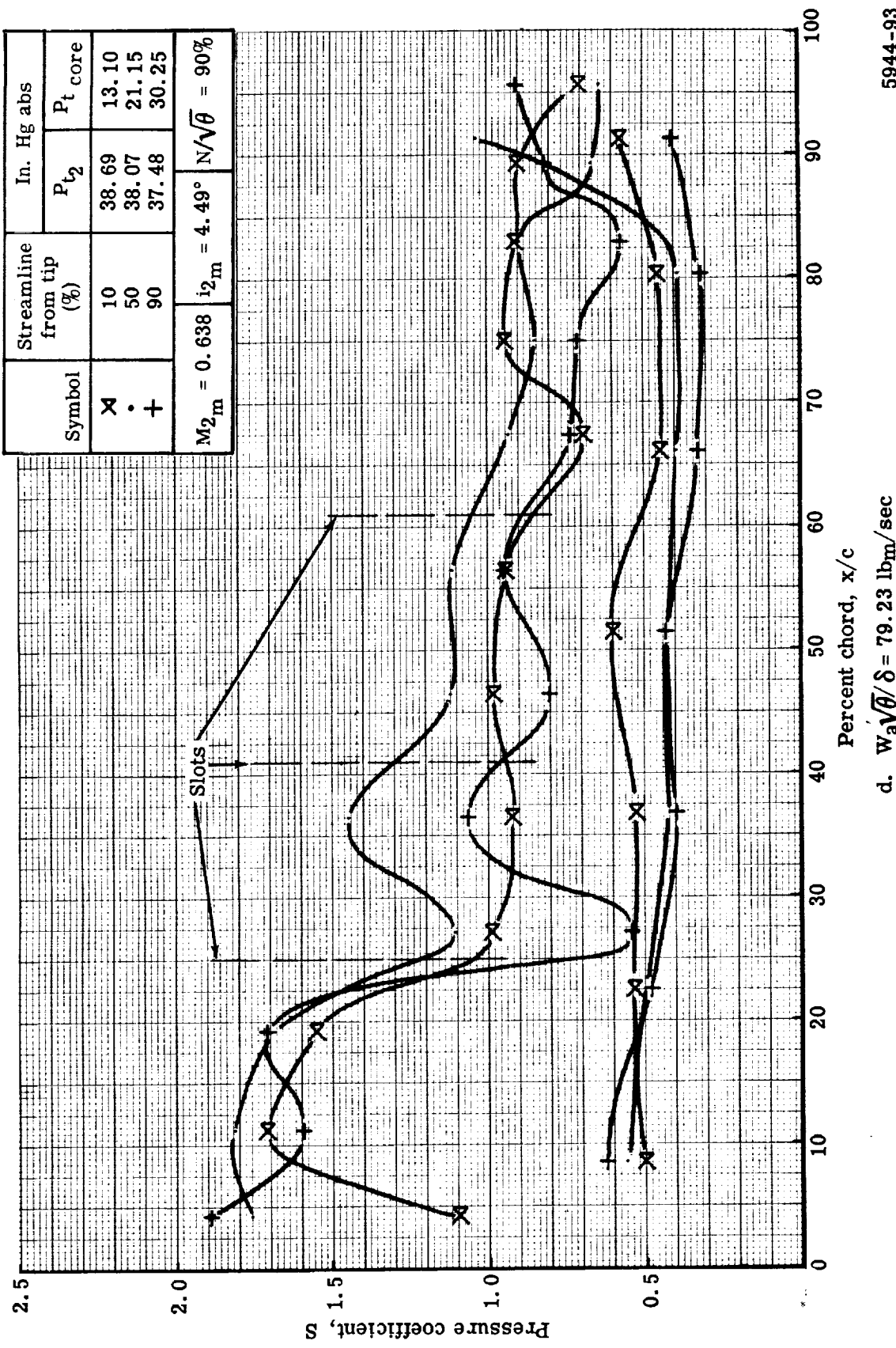


Figure 51. Triple-slotted stator static pressure distribution at 90% speed and vane bleed flow at the optimum rate.

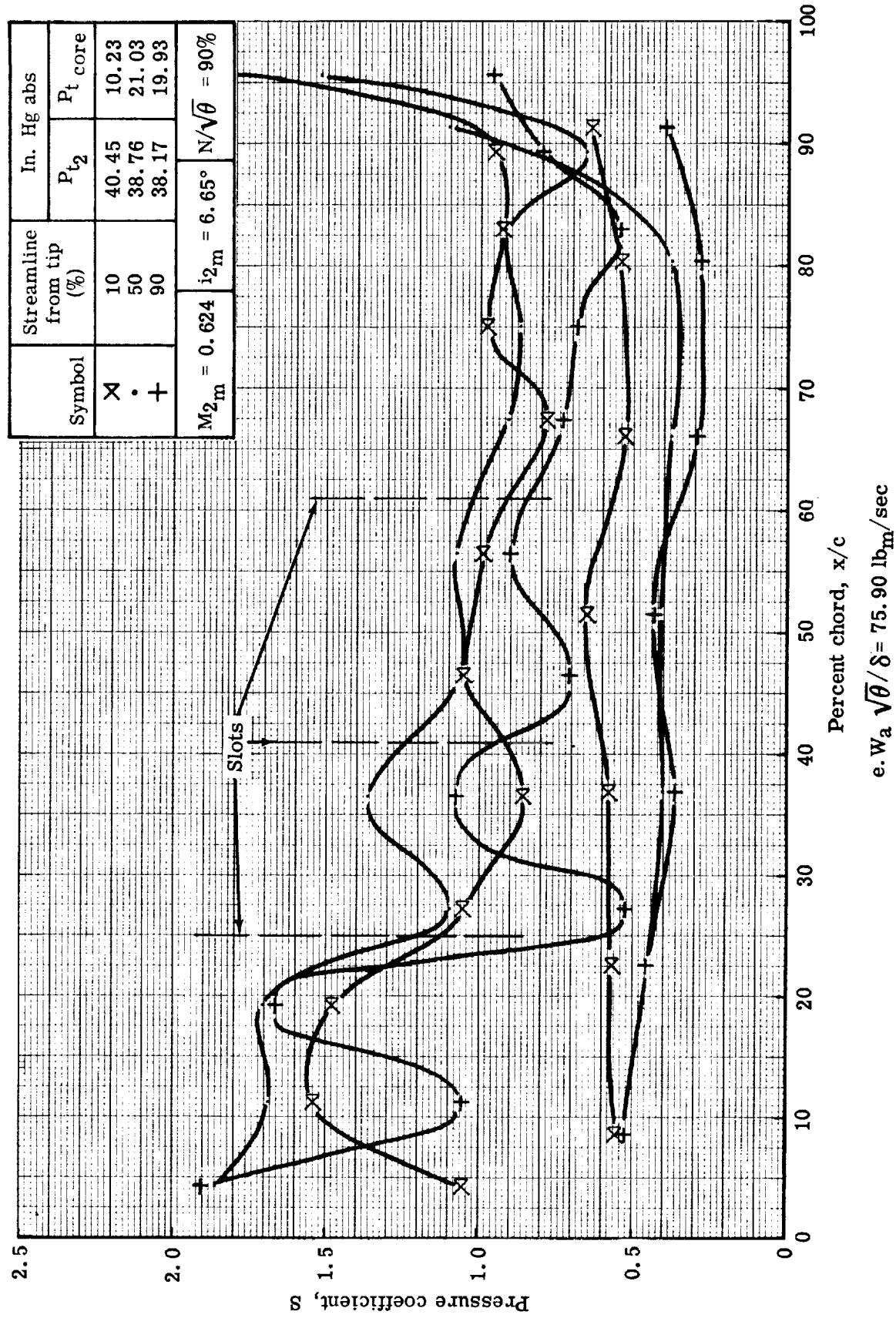


Figure 51. Triple-slotted stator static pressure distribution at 90% speed and vane bleed flow at the optimum rate.

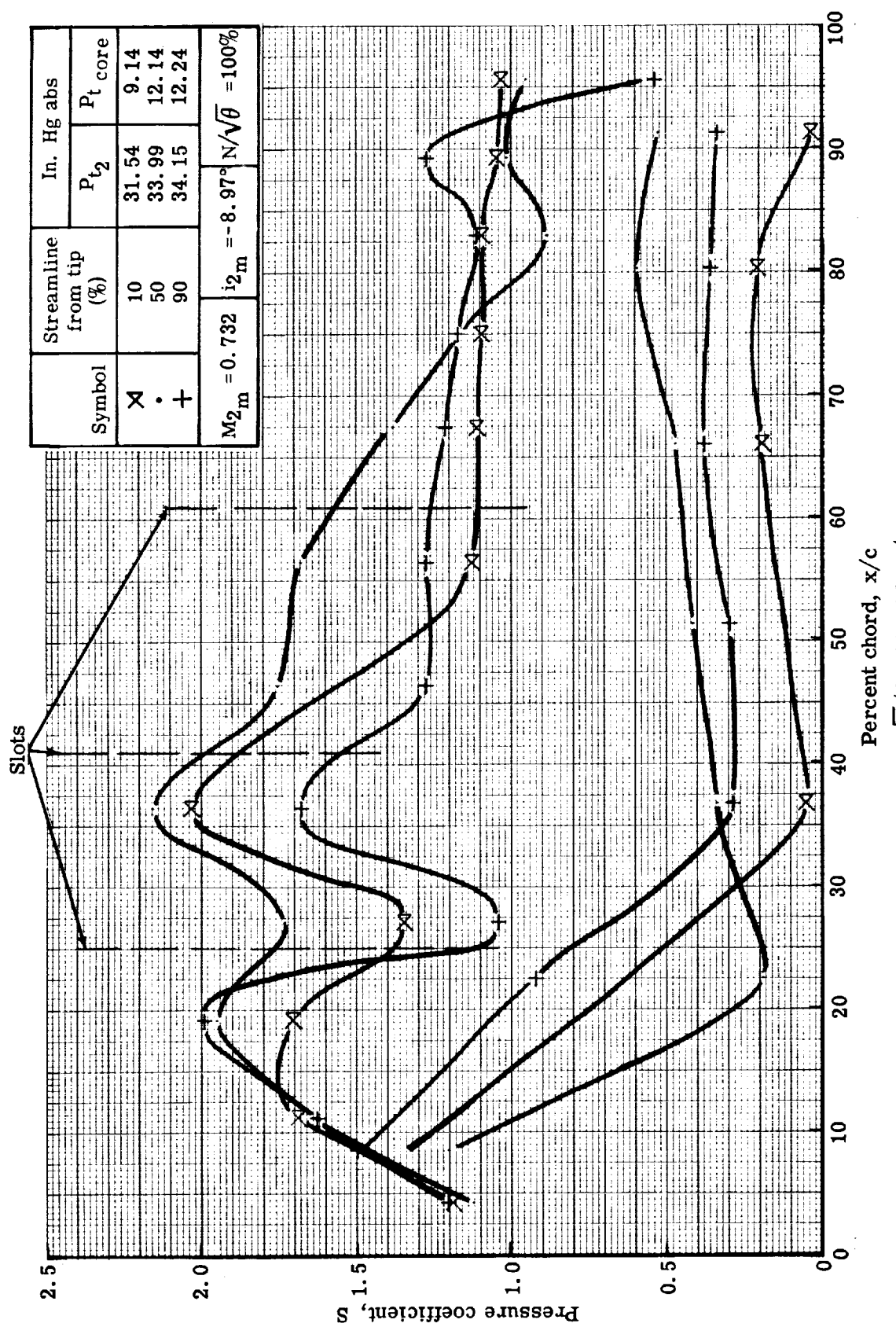


Figure 52. Triple-slotted stator static pressure distribution at 100% speed and vane bleed flow at the optimum rate.
5944-95

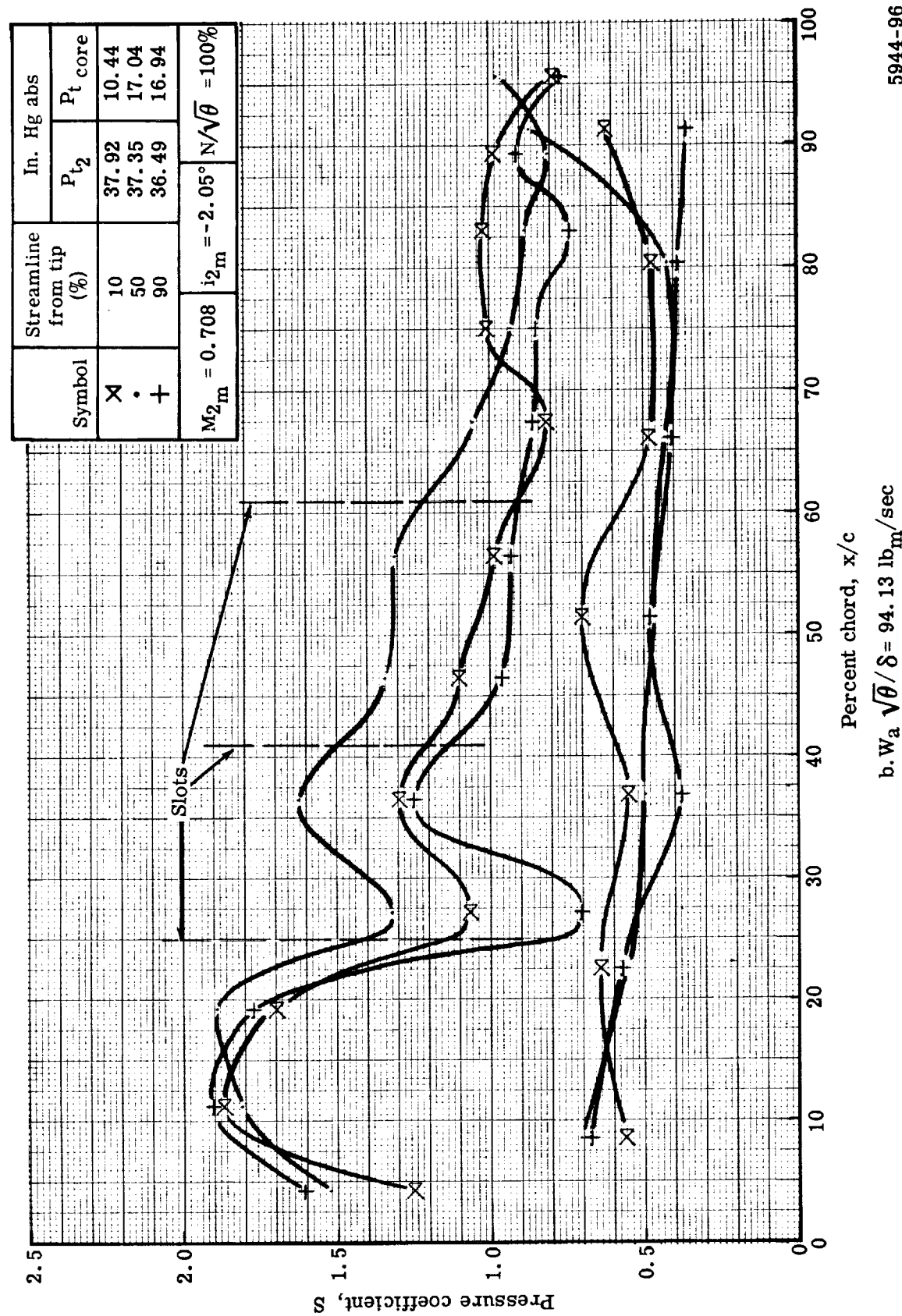
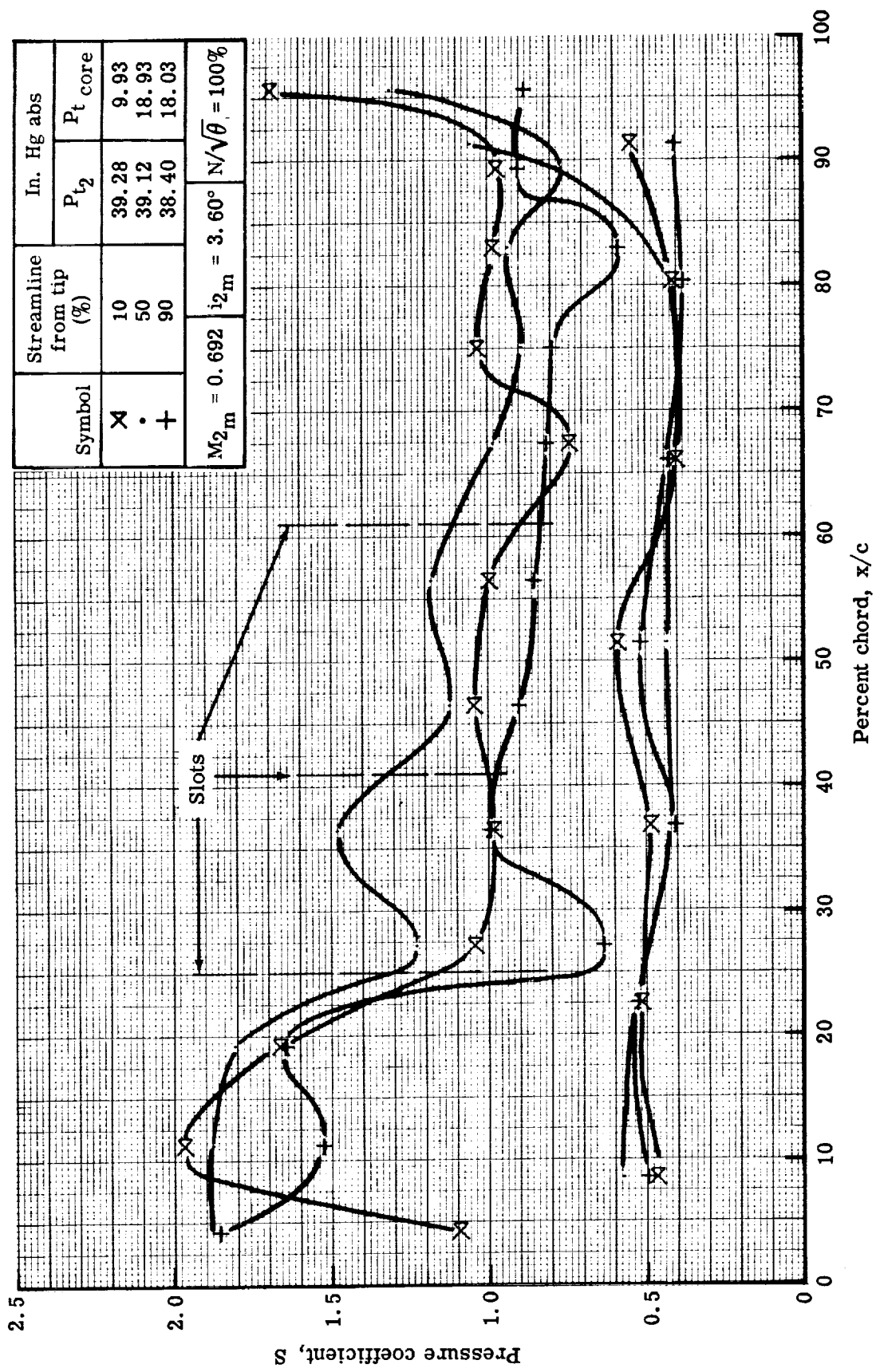


Figure 52. Triple-slotted stator static pressure distribution at 100% speed and vane bleed flow at the optimum rate.



c. $w_a \sqrt{\theta}/\delta = 88.55 \text{ lb}_m/\text{sec}$
 Figure 52. Triple-slotted stator static pressure distribution at 100% speed and vane bleed flow at the optimum rate.

5944-97

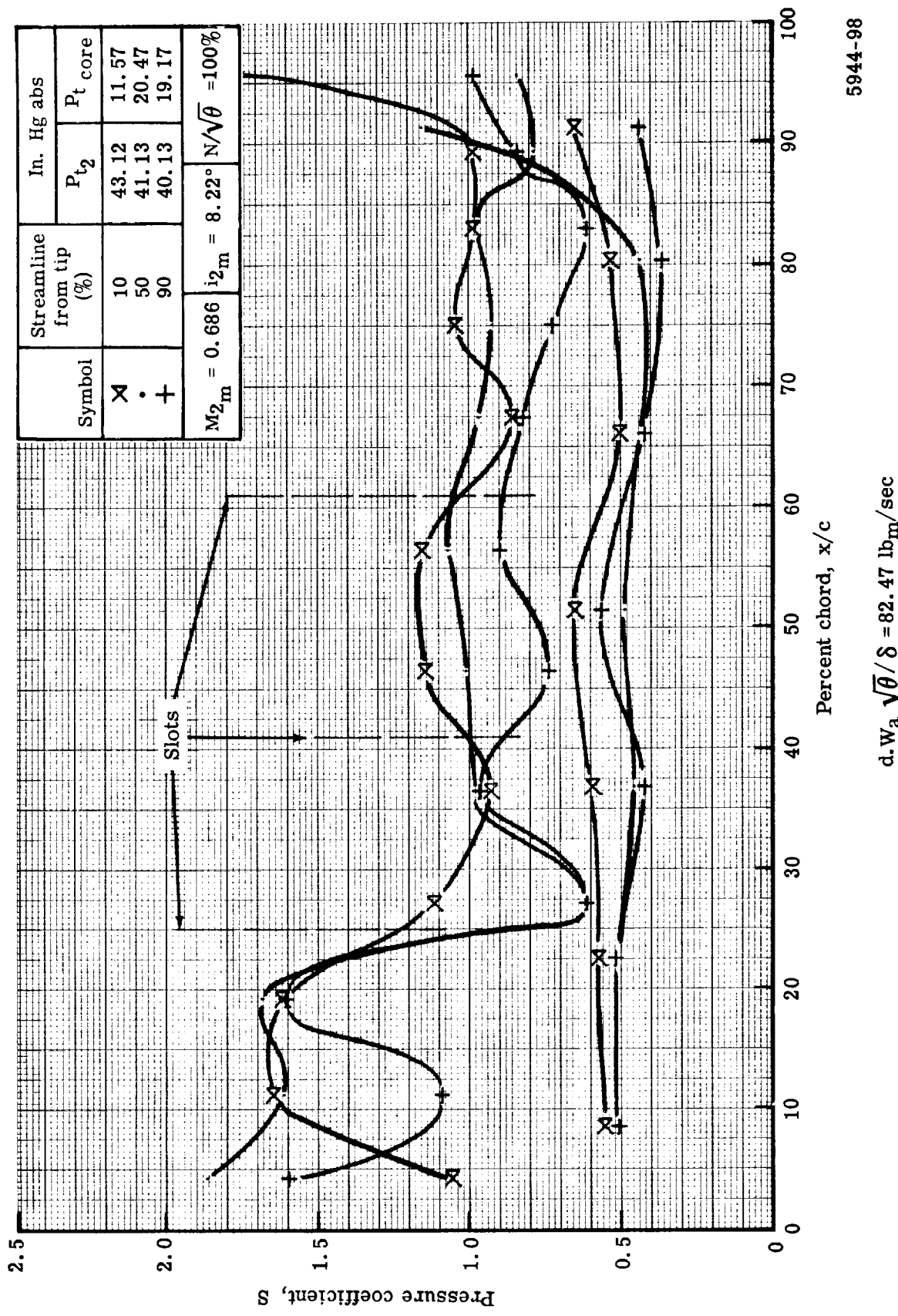


Figure 52. Triple-slotted stator static pressure distribution at 100% speed and vane bleed flow at the optimum rate.

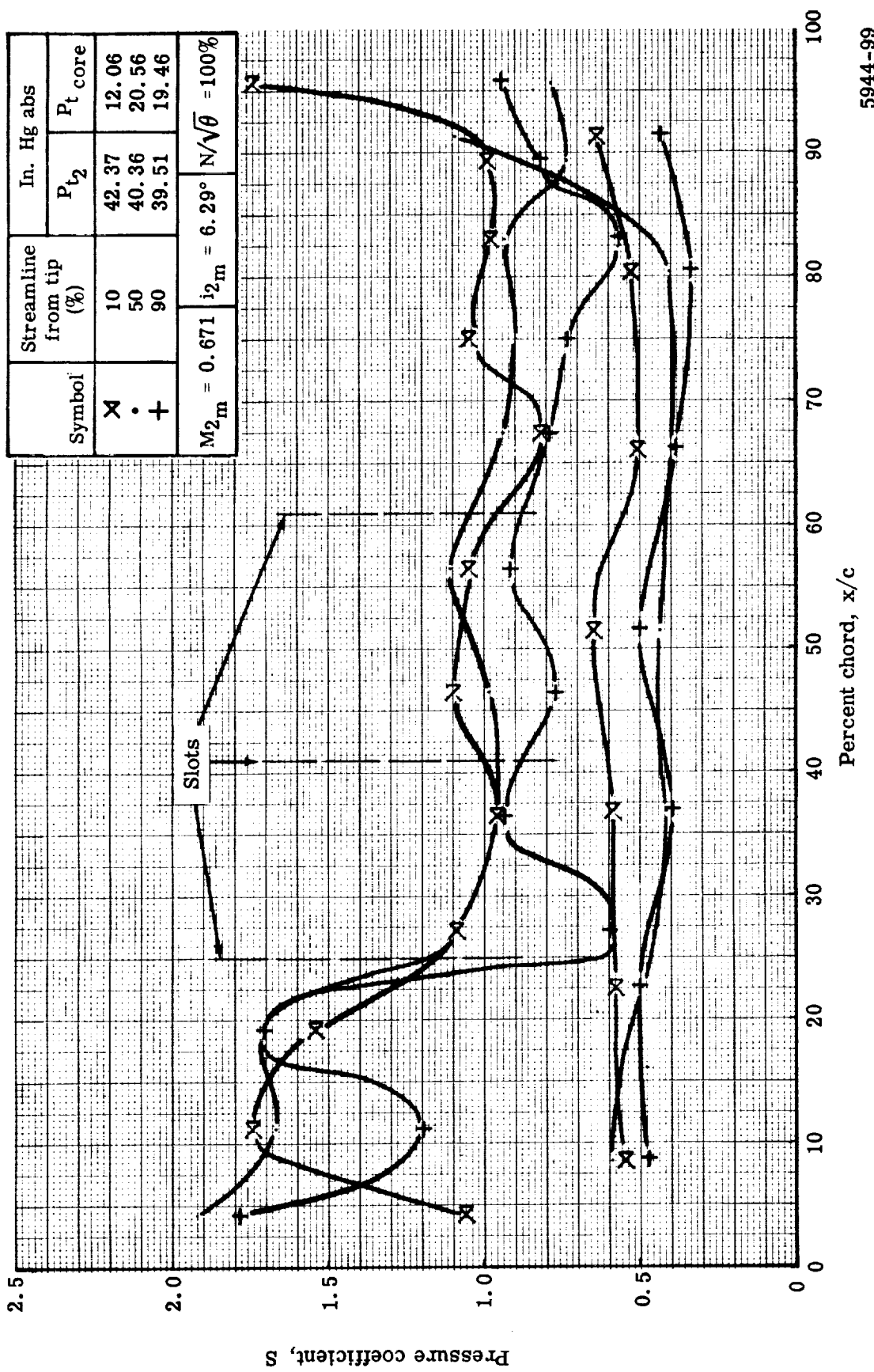


Figure 52. Triple-slotted stator static pressure distribution at 100% speed and vane bleed flow at the optimum rate.

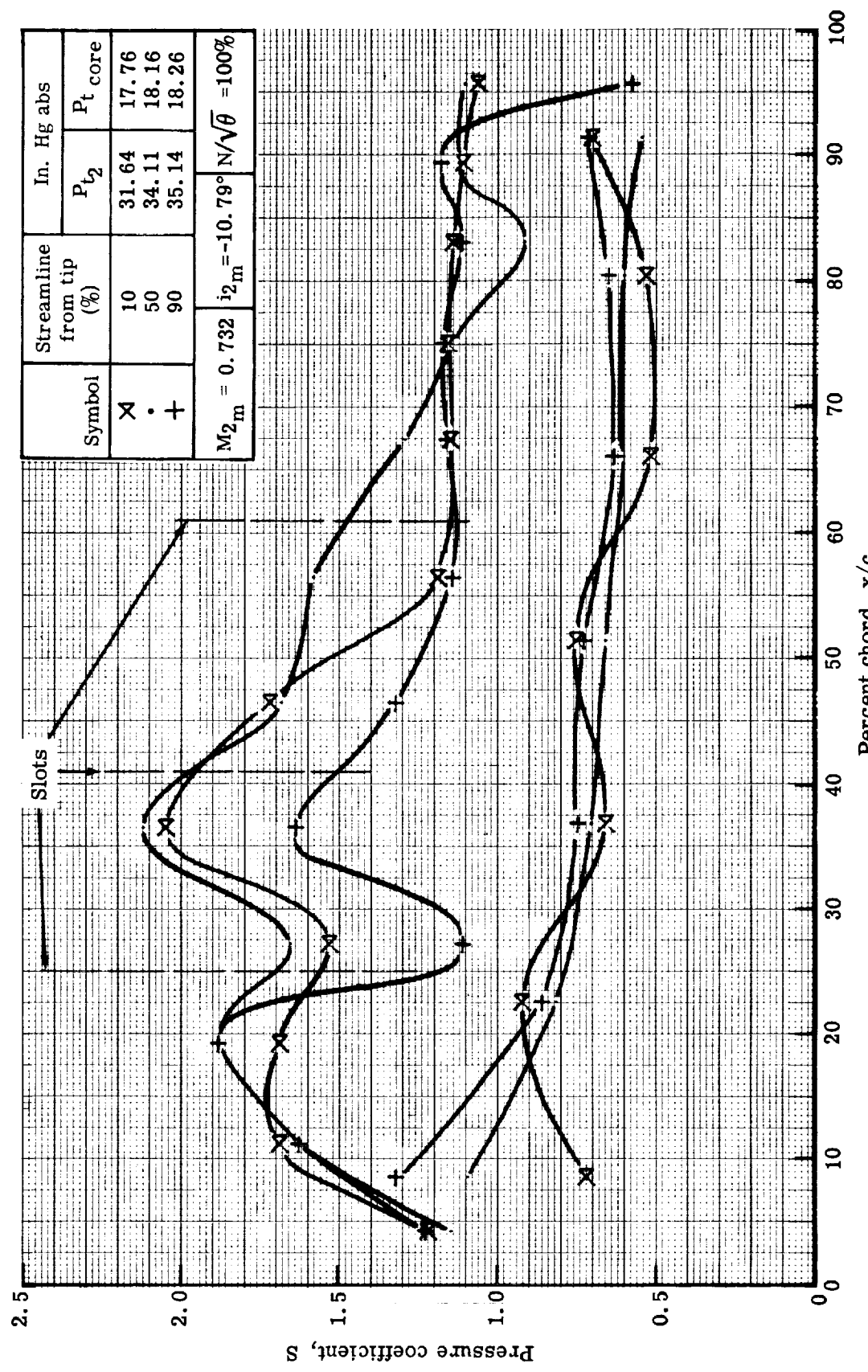


Figure 53. Triple-slotted stator static pressure distribution at 100% speed and mean vane bleed flow rate.

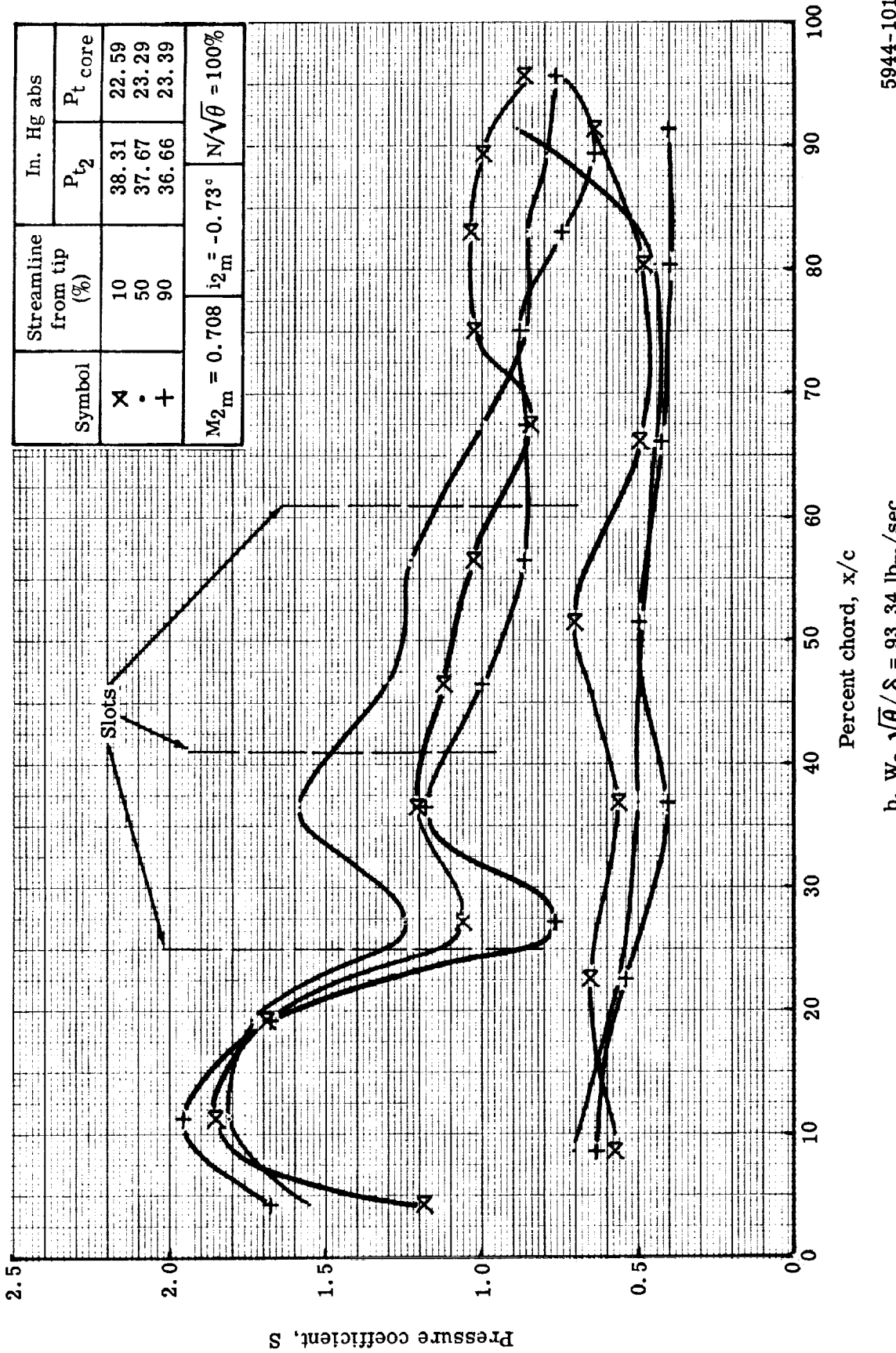


Figure 53. Triple-slotted stator static pressure distribution at 100% speed and mean vane bleed flow rate.

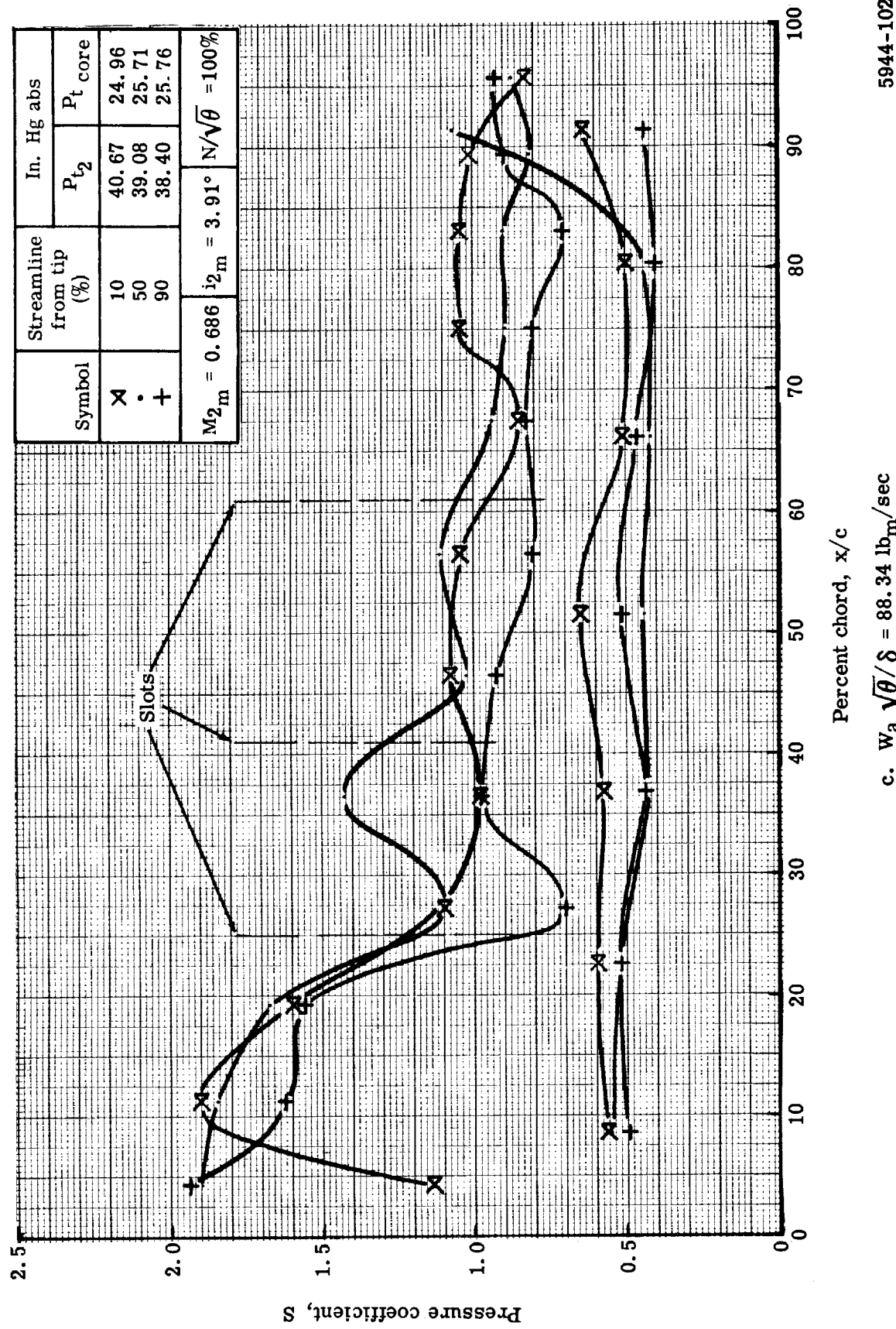


Figure 53. Triple-slotted stator static pressure distribution at 100% speed and mean vane bleed flow rate.

5944-102

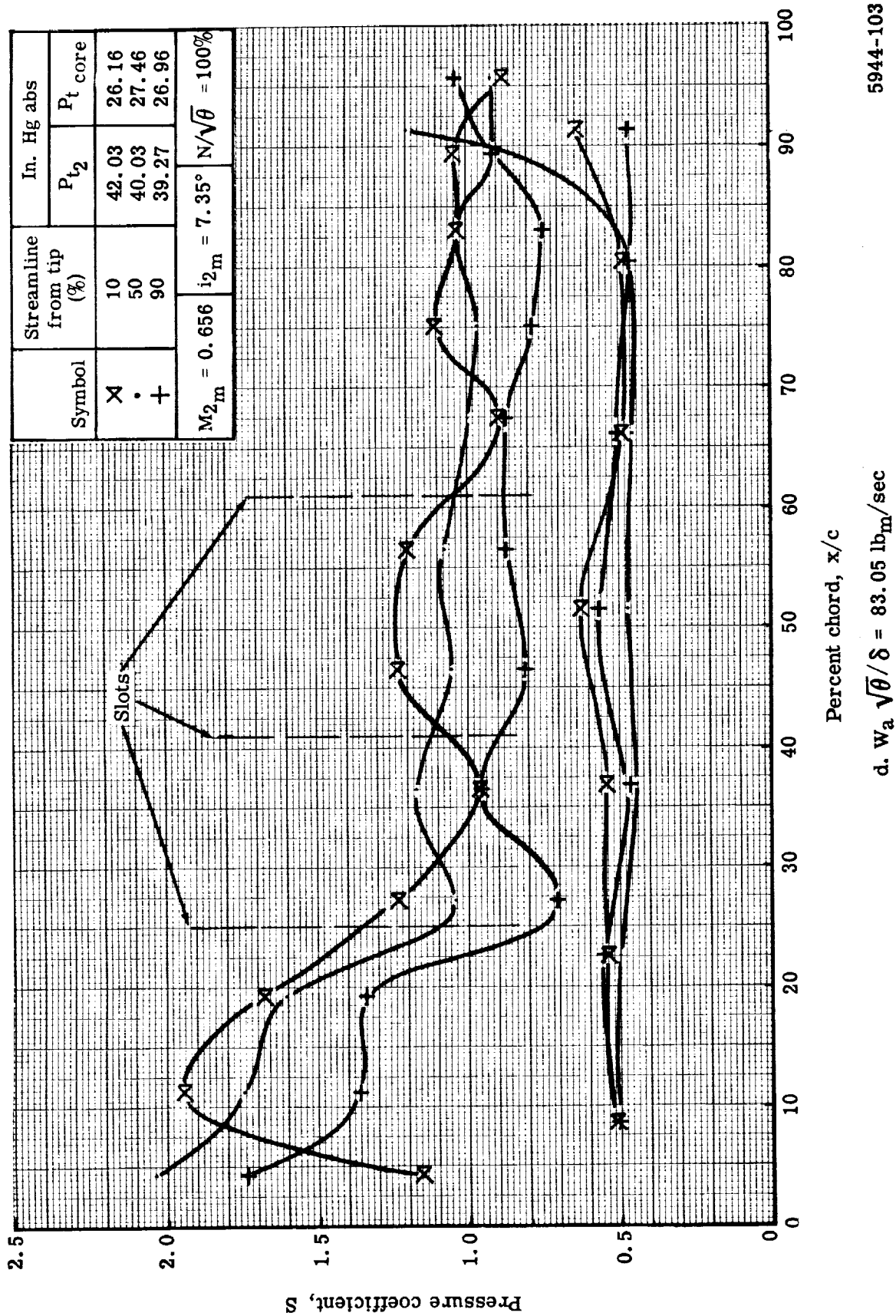


Figure 53. Triple-slotted stator static pressure distribution at 100% speed and mean vane bleed flow rate.

5944-103

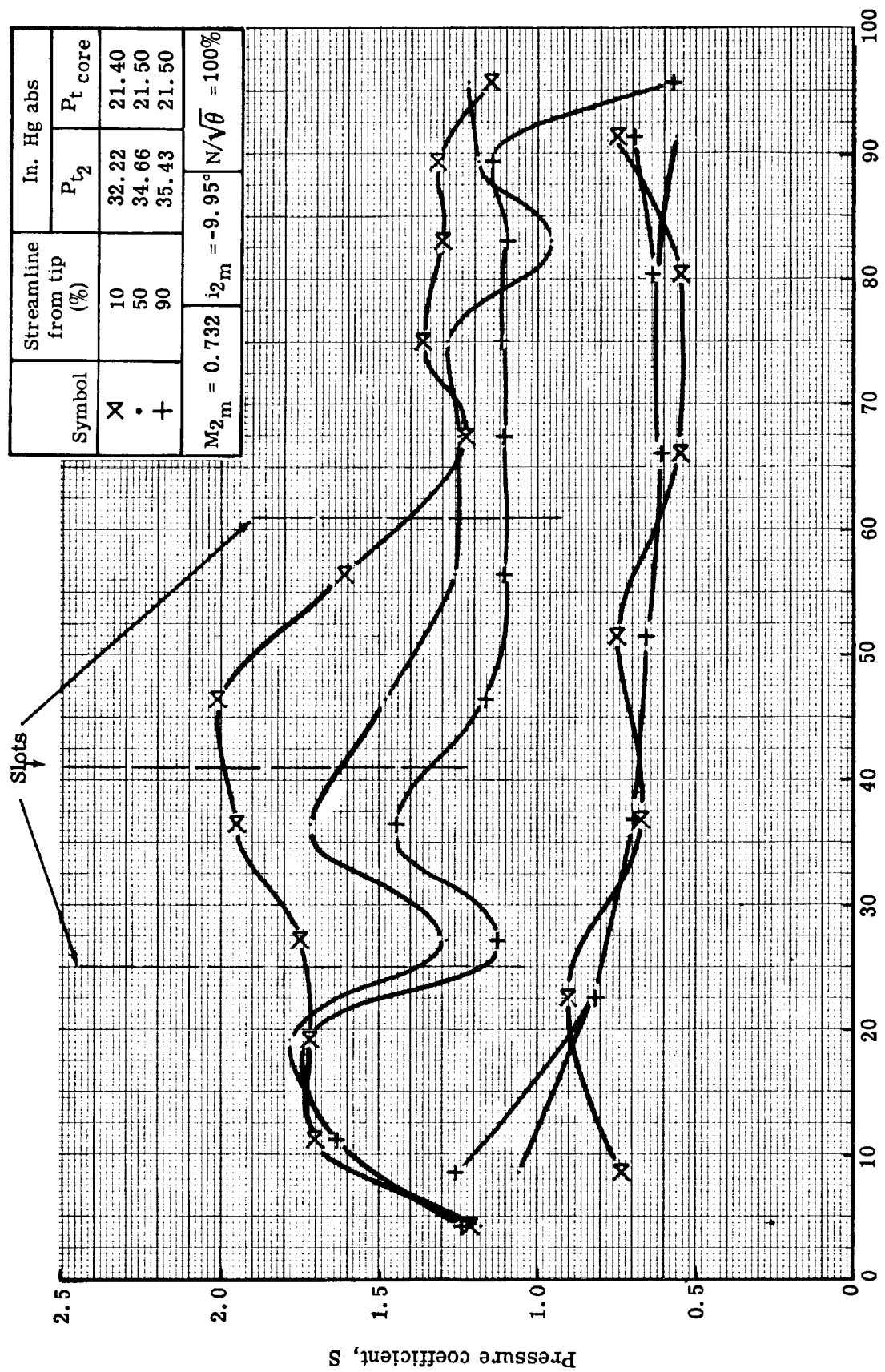


Figure 54. Triple-slotted stator static pressure distribution at 100% speed and zero vane bleed flow rate.
5944-104

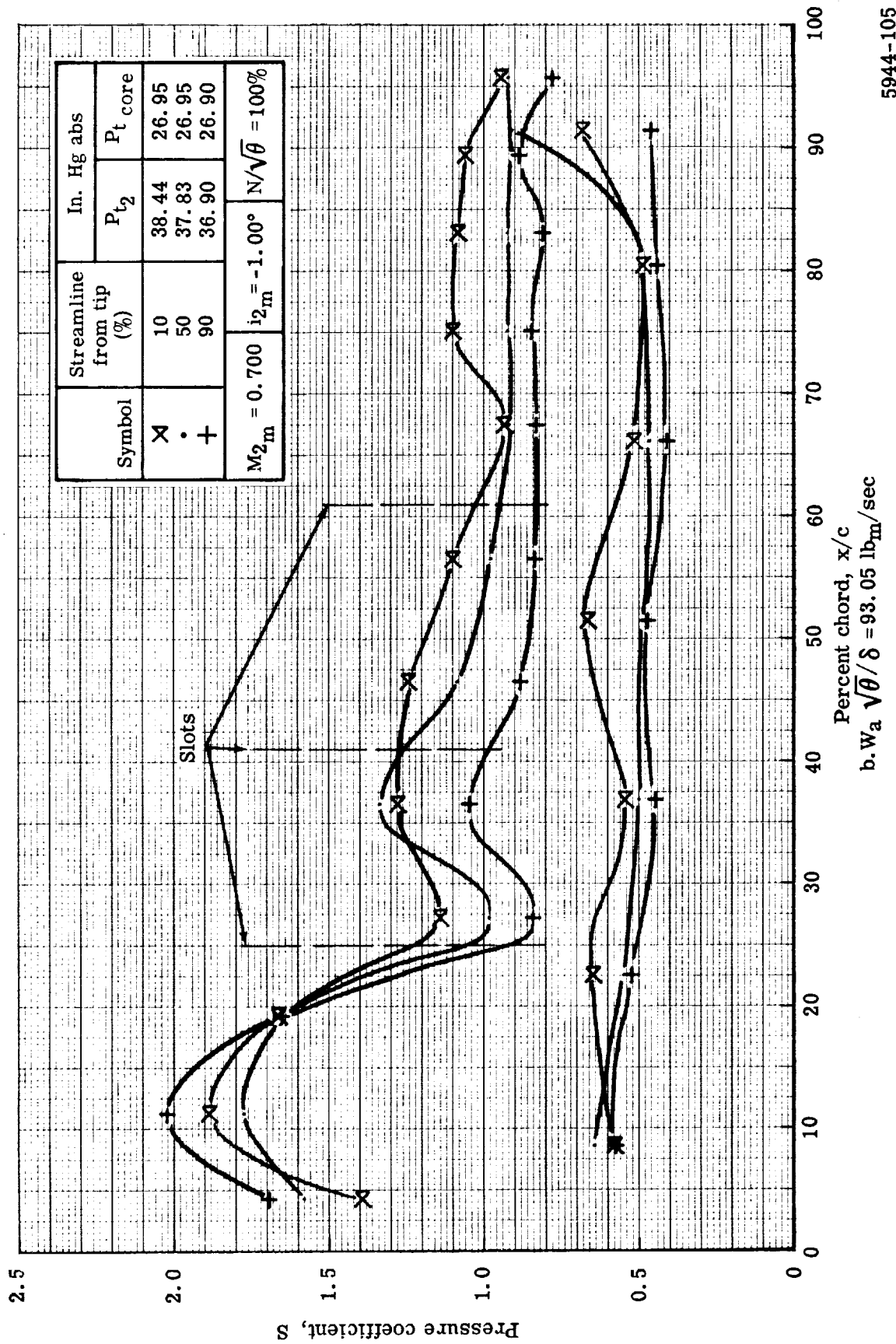


Figure 54. Triple-slotted stator static pressure distribution at 100% speed and zero vane bleed flow rate.

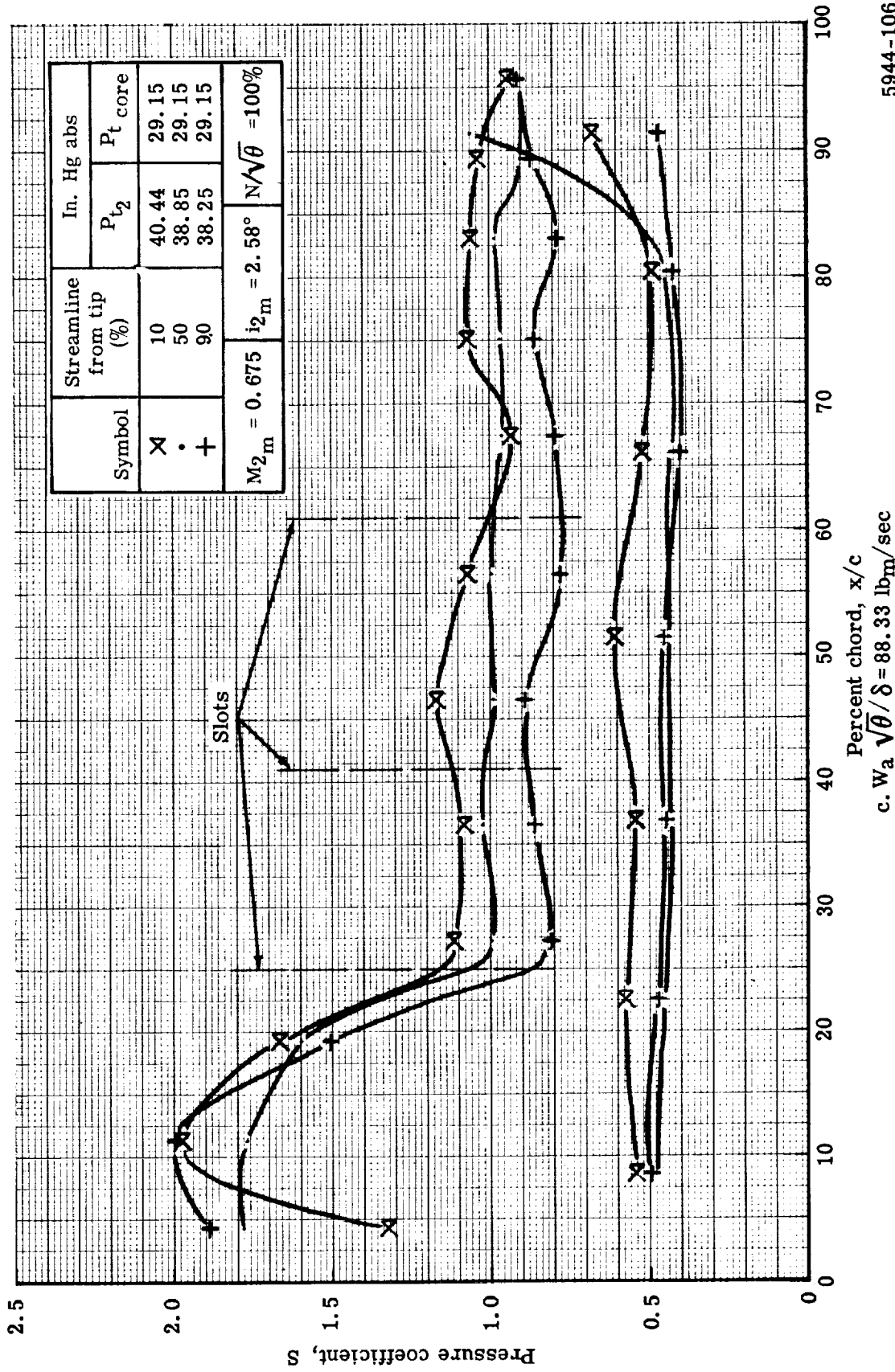


Figure 54. Triple-slotted stator static pressure distribution at 100% speed and zero vane bleed rate.

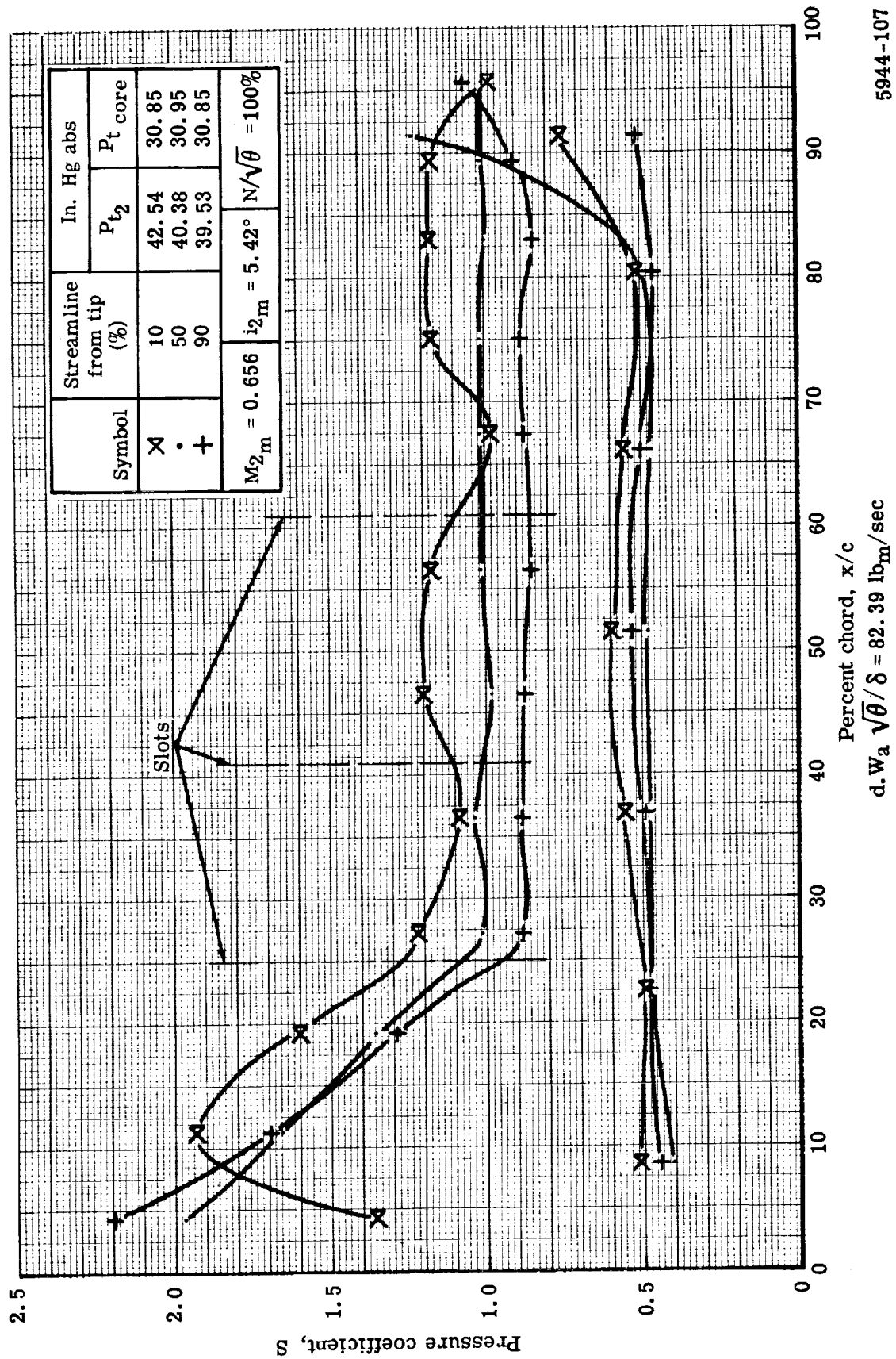


Figure 54. Triple-slotted stator static pressure distribution at 100% speed and zero vane bleed flow rate.

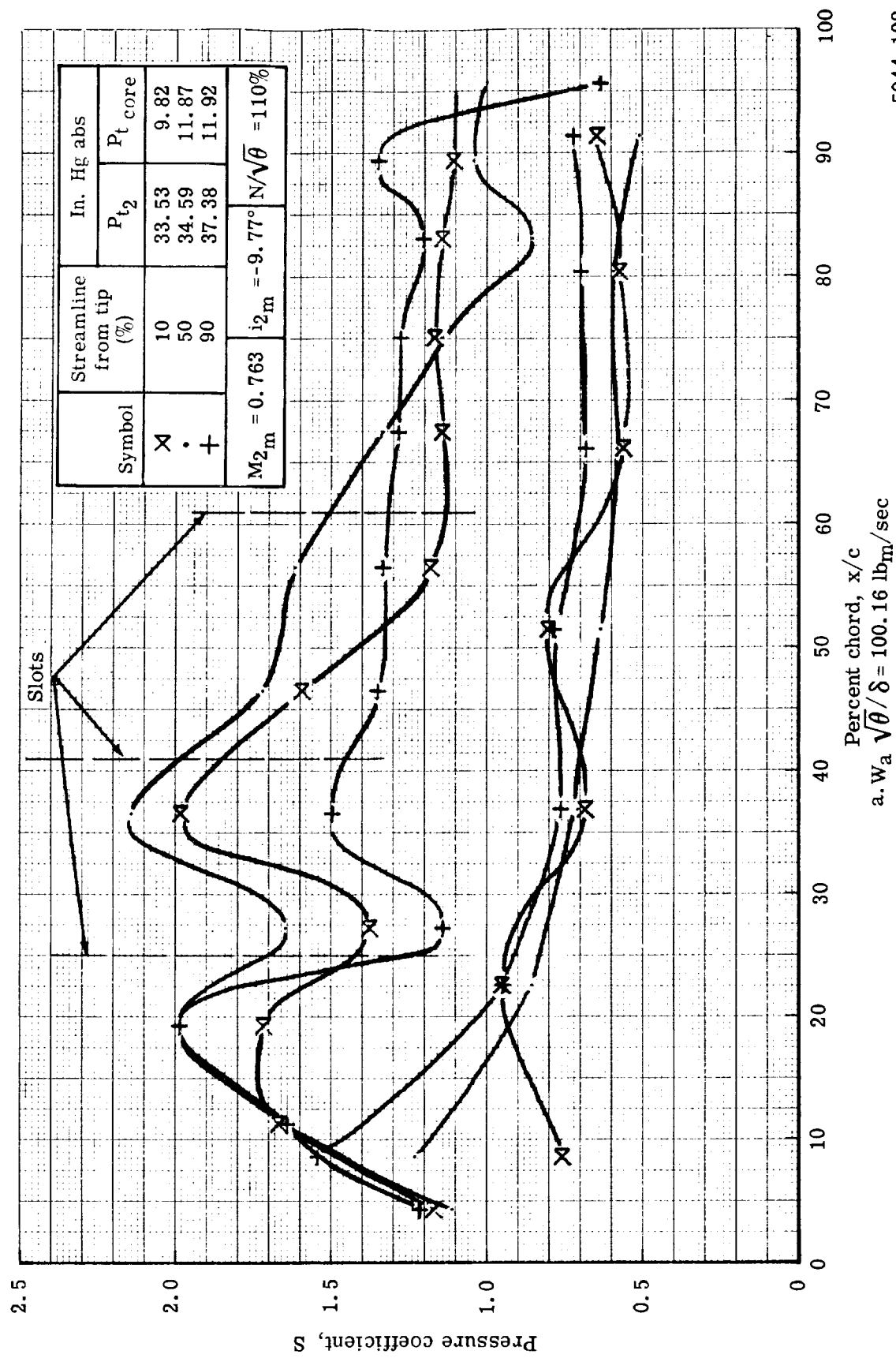


Figure 55. Triple-slotted stator static pressure distribution at 110% speed and vane bleed flow at the optimum rate.

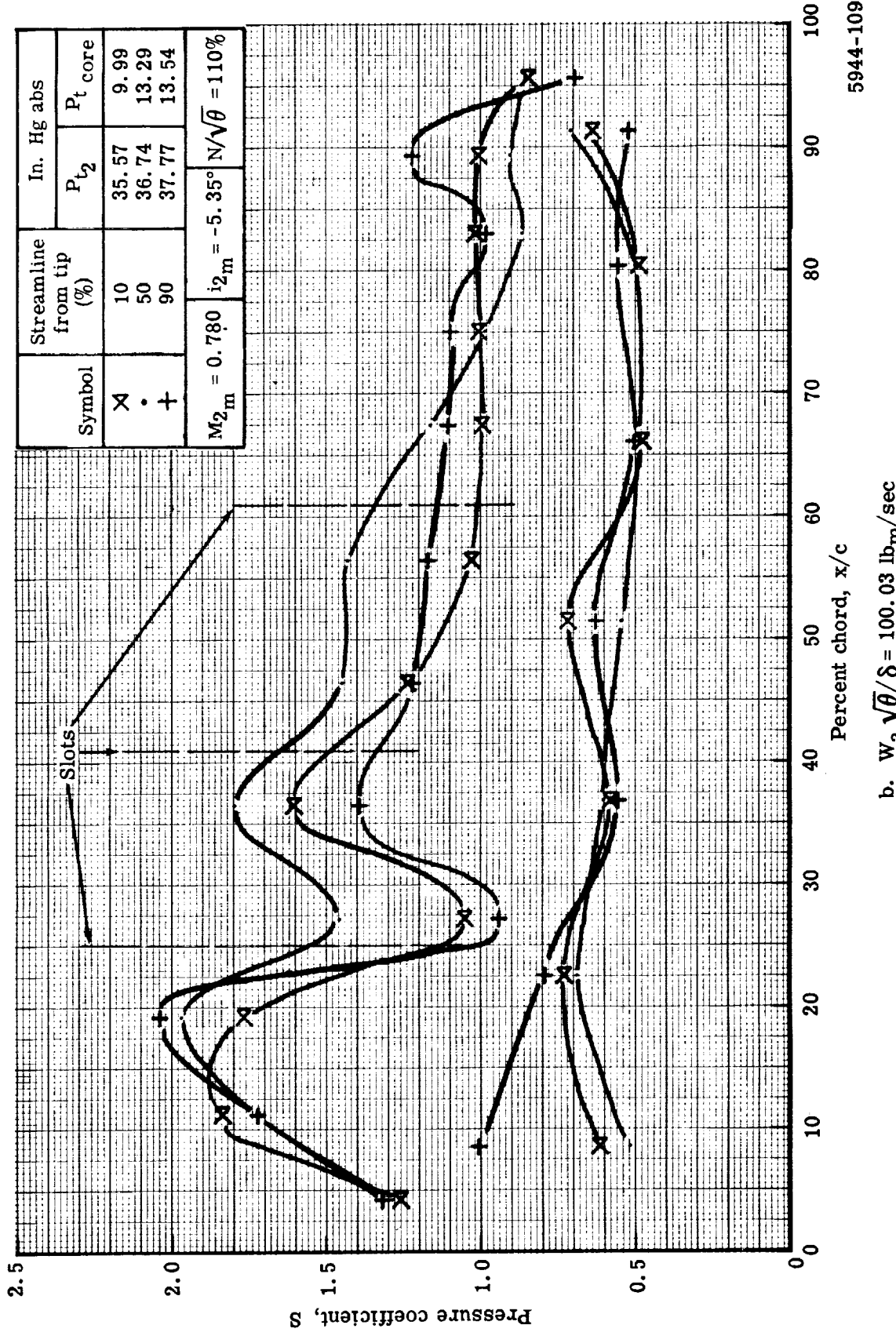


Figure 55. Triple-slotted stator static pressure distribution at 110% speed and vane bleed flow at the optimum rate.

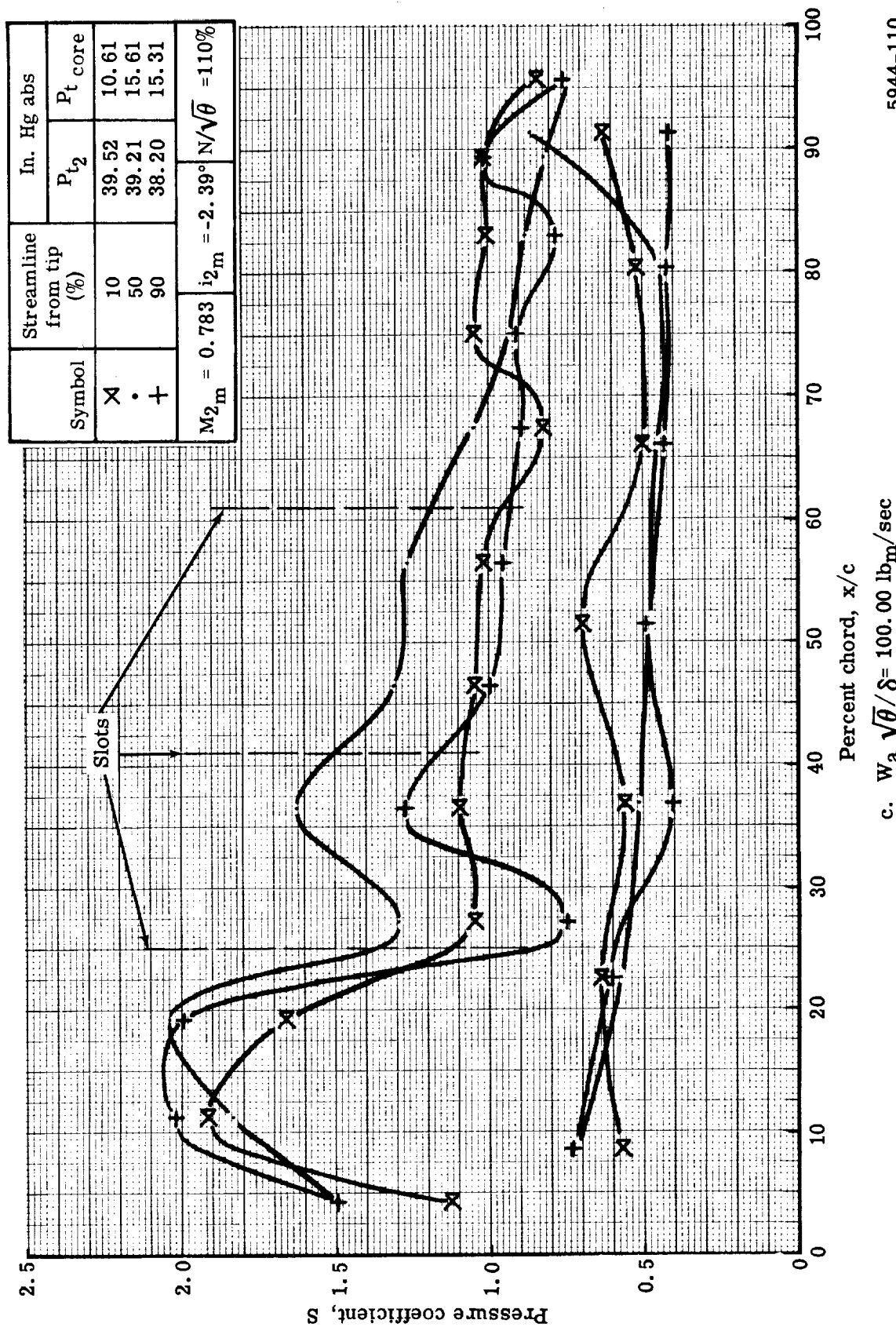


Figure 55. Triple-slotted stator static pressure distribution at 110% speed and vane bleed flow at the optimum rate.

5944-110

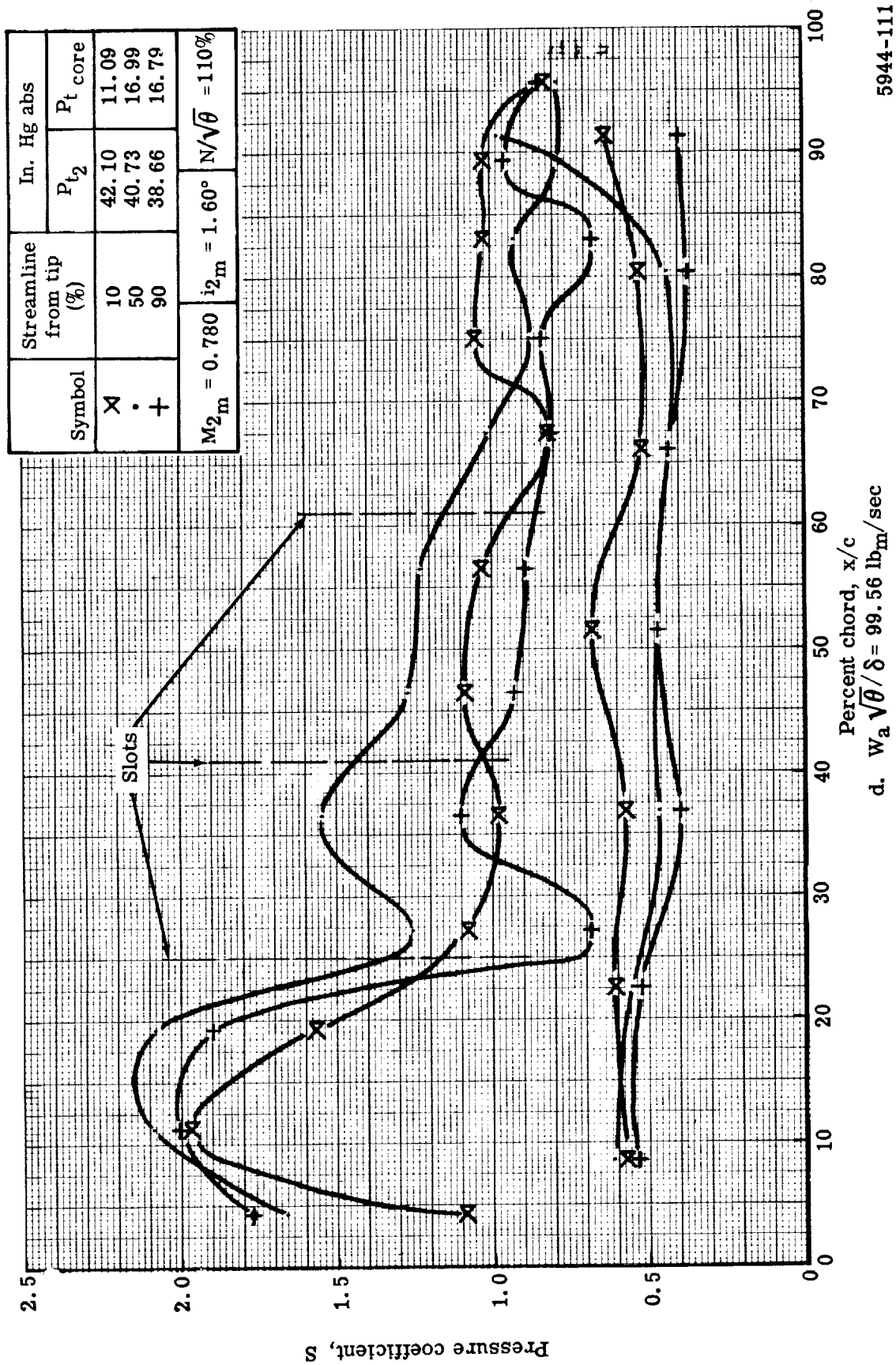


Figure 55. Triple-slotted stator static pressure distribution at 110% speed and vane bleed flow at the optimum rate.

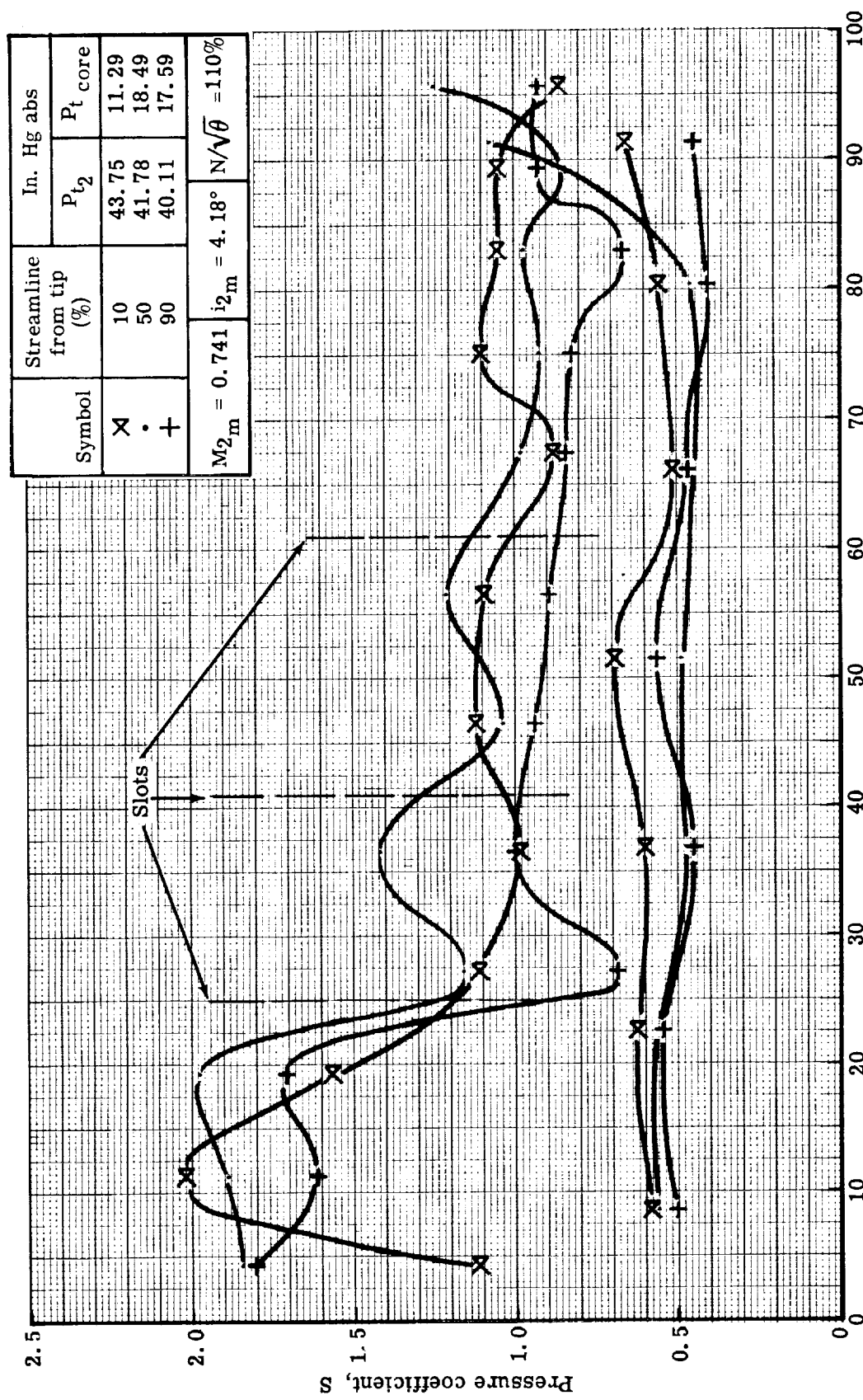


Figure 55. Triple-slotted stator static pressure distribution at 110% speed and vane bleed flow at the optimum rate. 5944-112

137

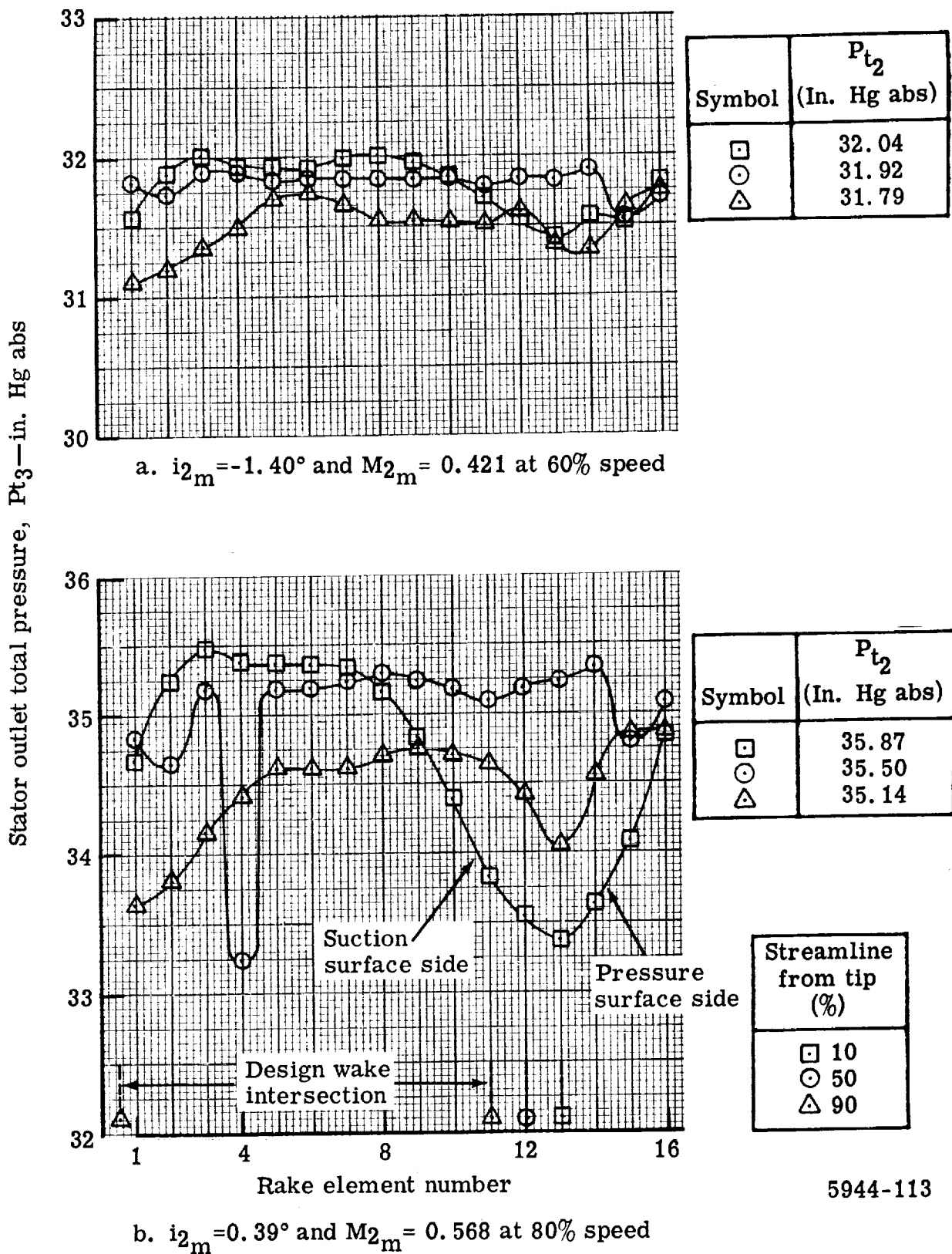


Figure 56. Triple-slotted stator wake surveys with the vane bleed flow at the optimum rate.

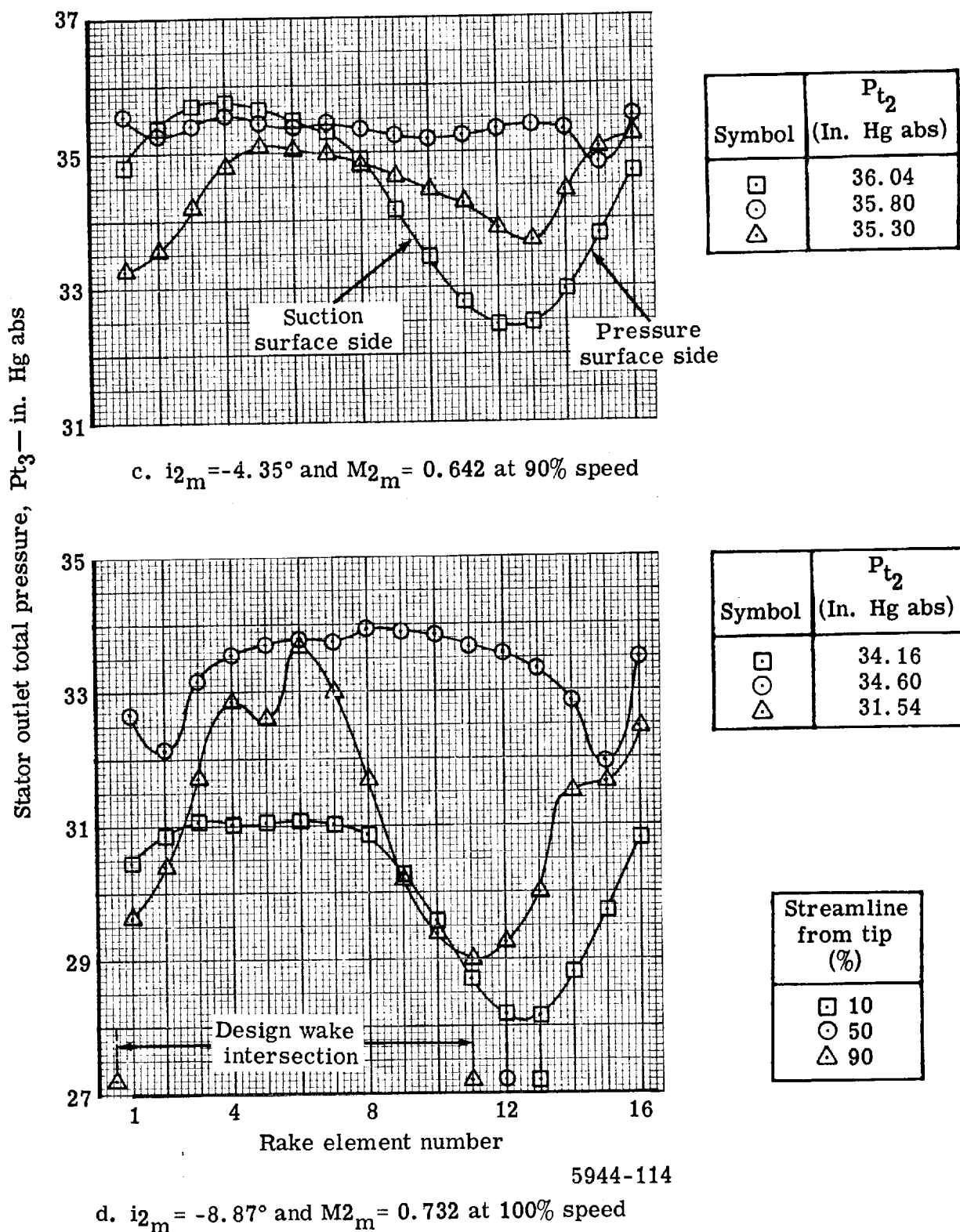


Figure 56. Triple-slotted stator wake surveys with the vane bleed flow at the optimum rate.

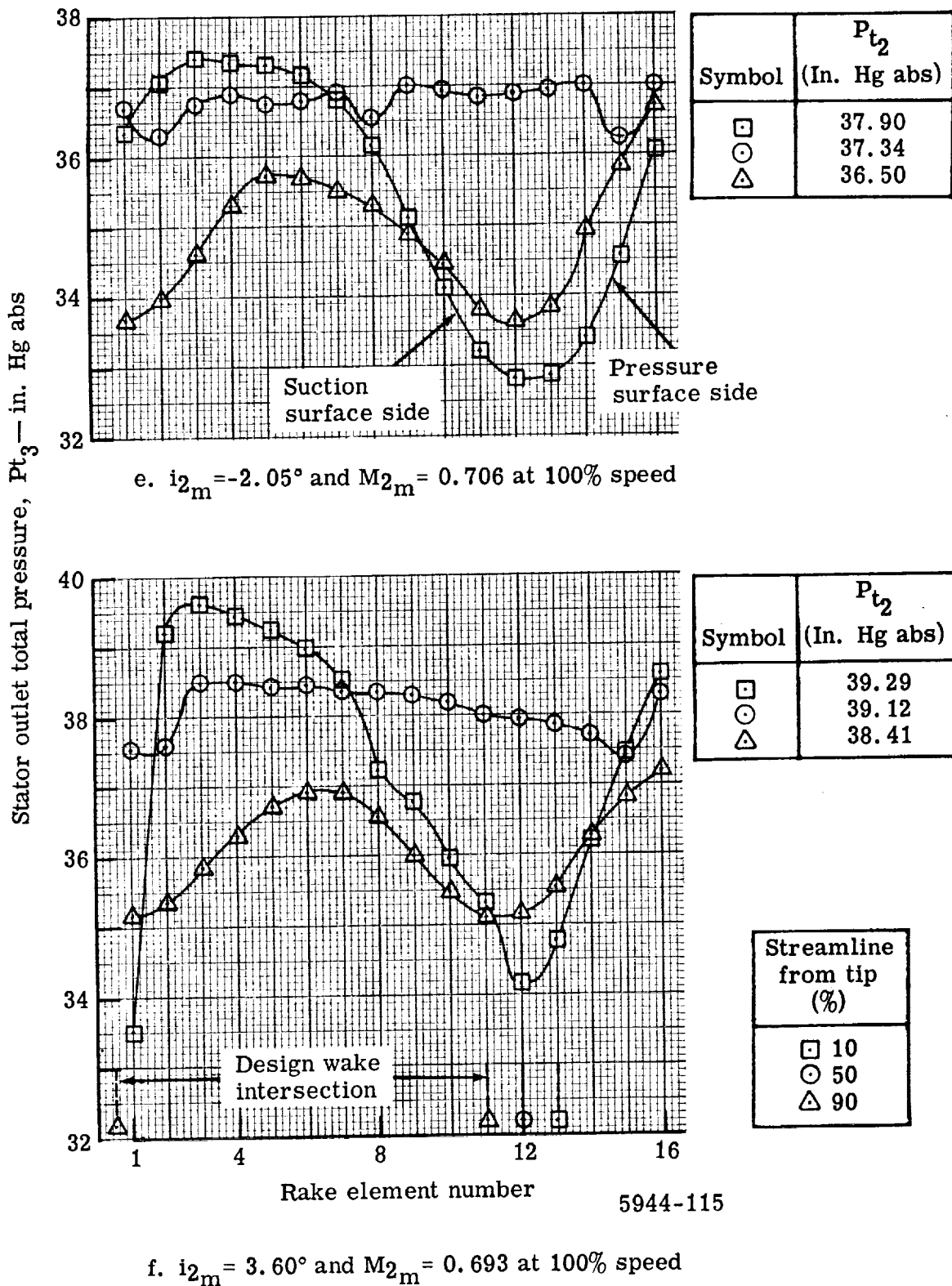
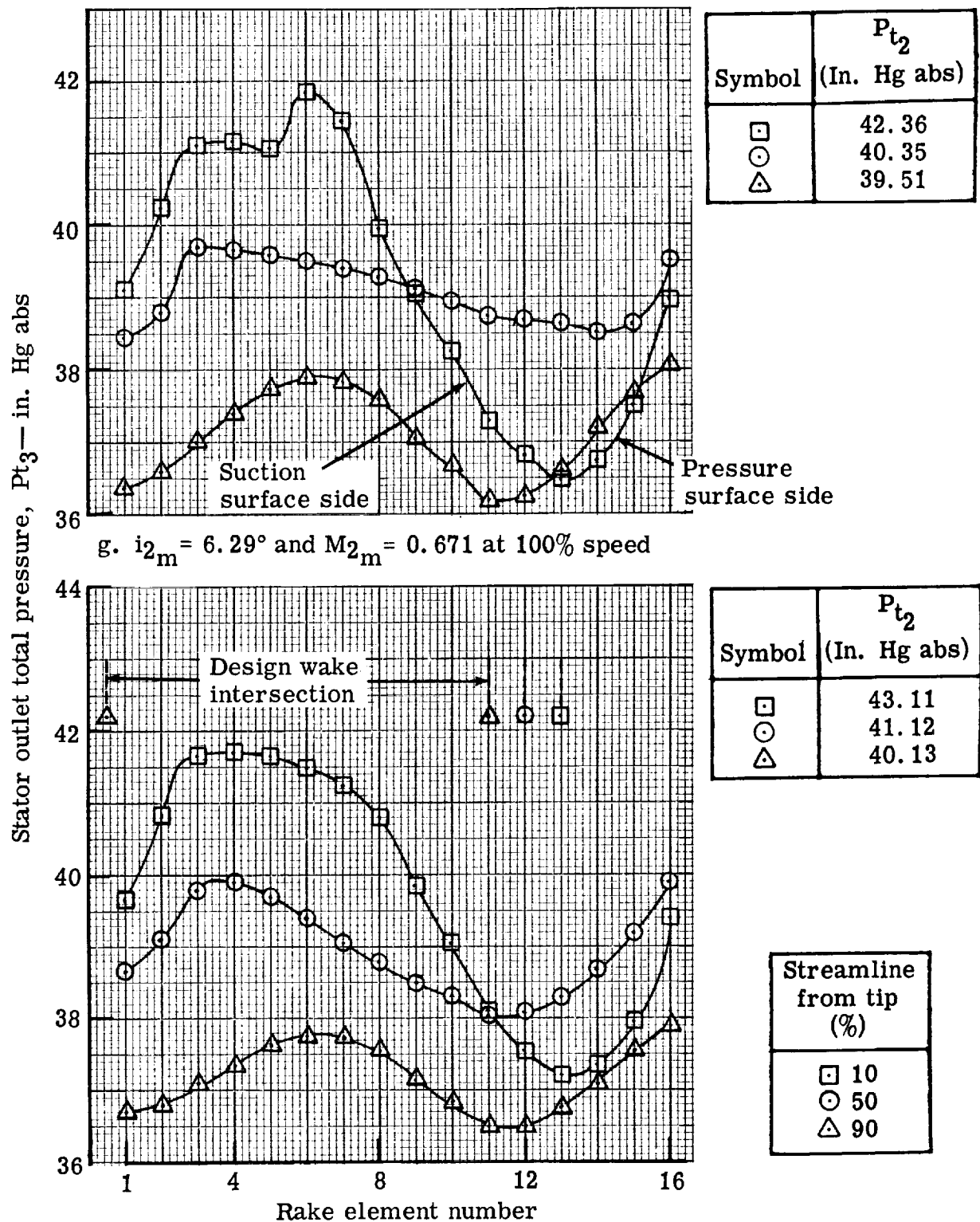


Figure 56. Triple-slotted stator wake surveys with the vane bleed flow at the optimum rate.



5944-116

Figure 56. Triple-slotted stator wake surveys with the vane bleed flow at the optimum rate.

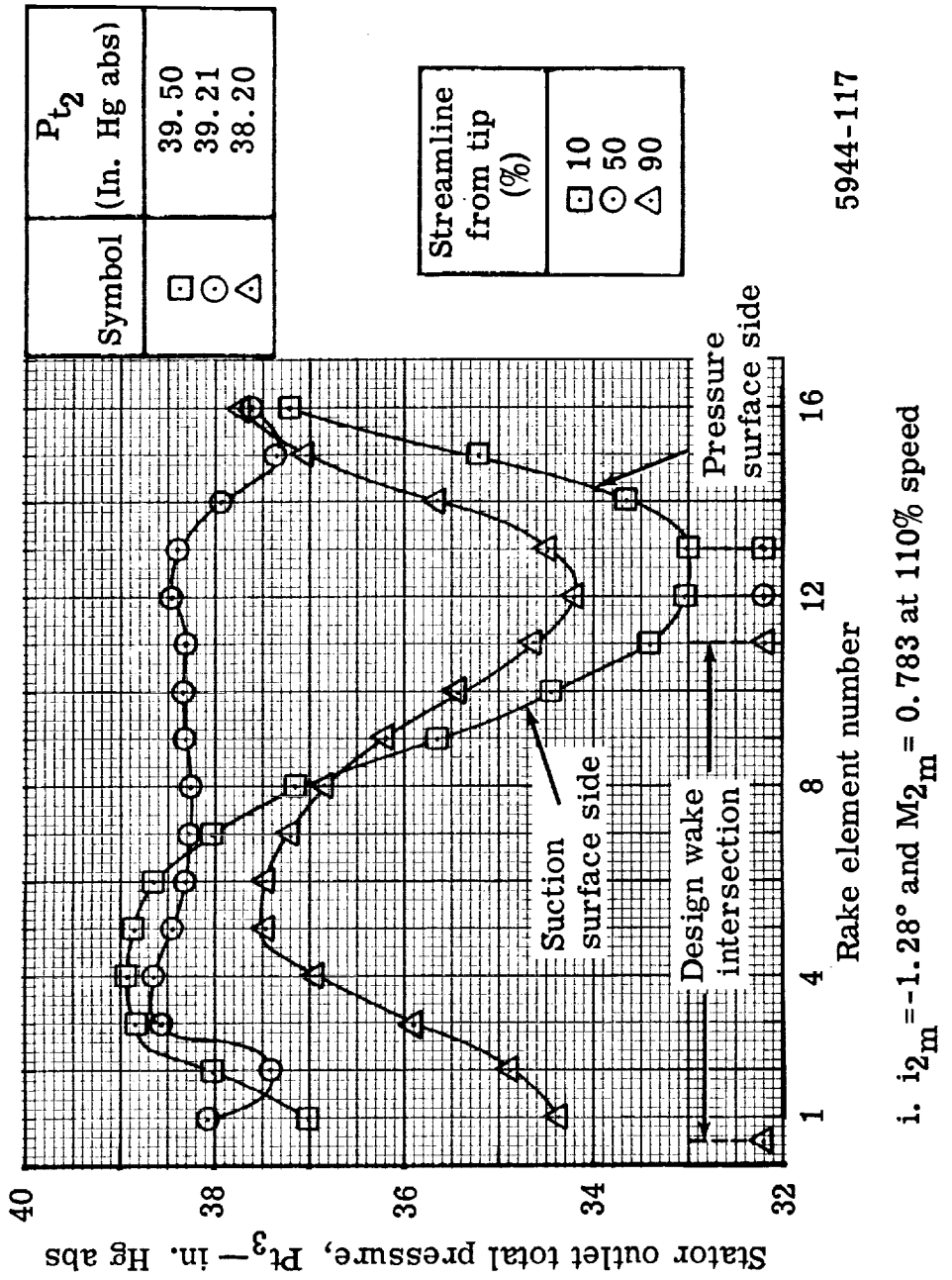


Figure 56. Triple-slotted stator wake surveys with the vane bleed flow at the optimum rate.

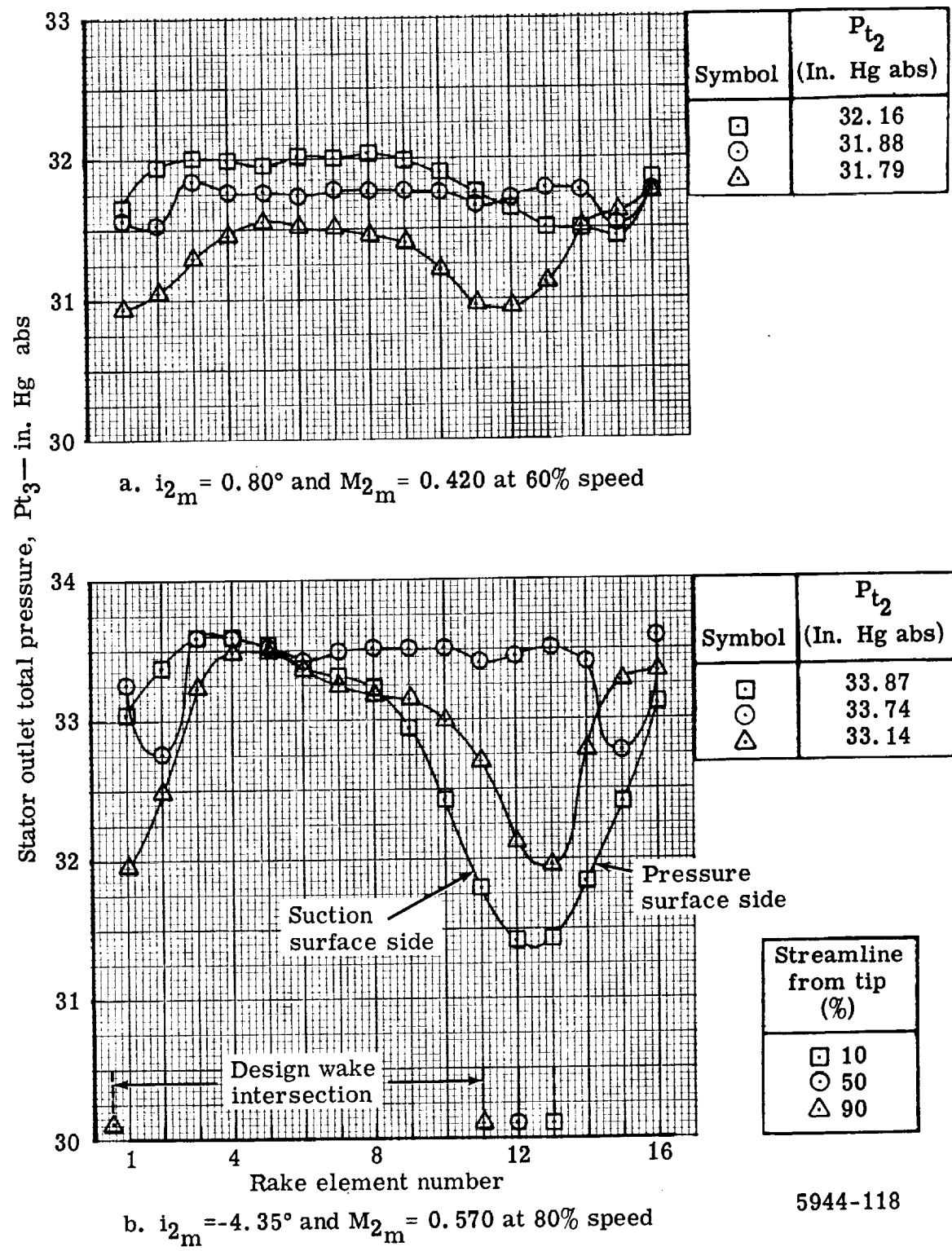


Figure 57. Triple-slotted stator wake surveys with the mean vane bleed flow rate.

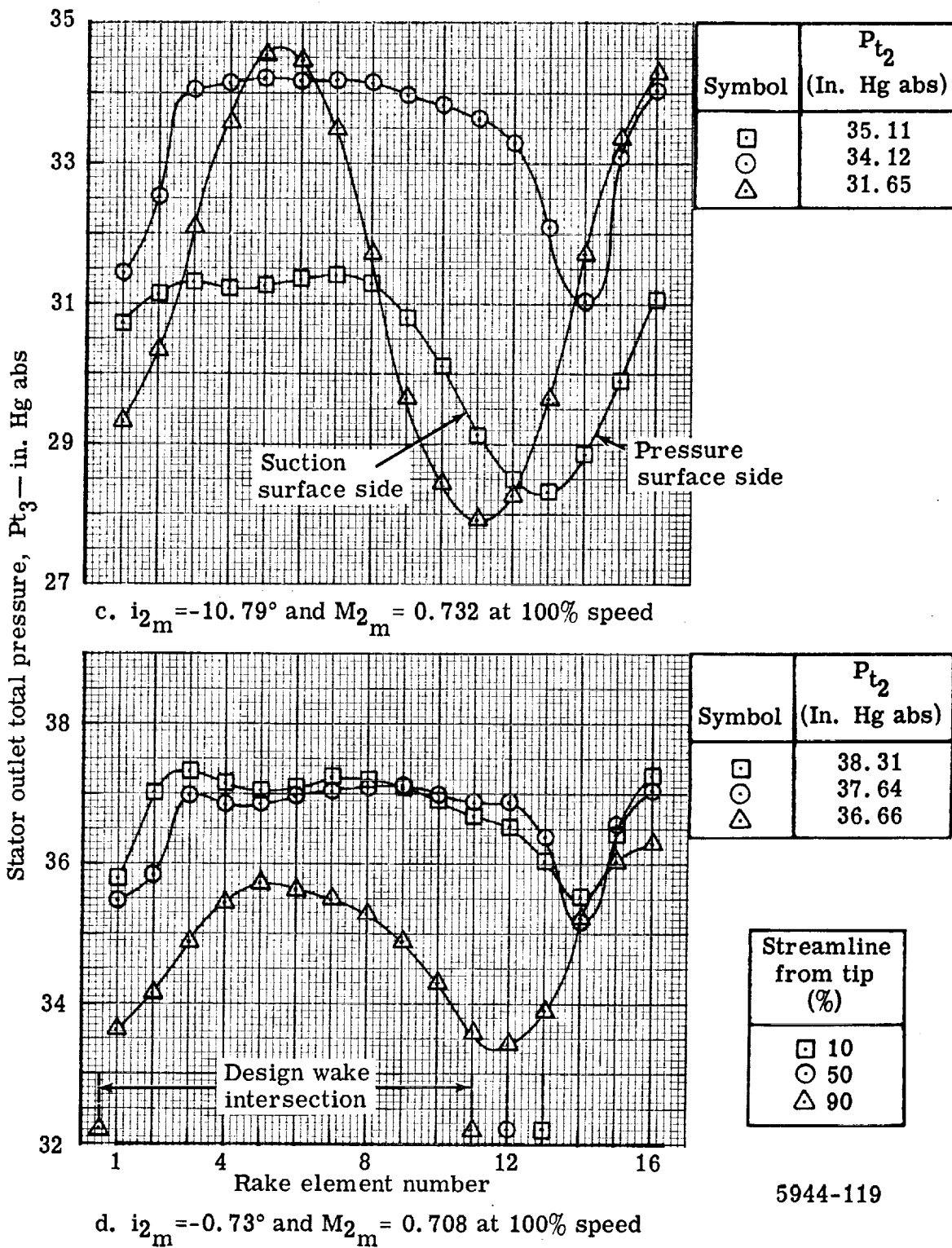


Figure 57. Triple-slotted stator wake surveys with the mean vane bleed flow rate.

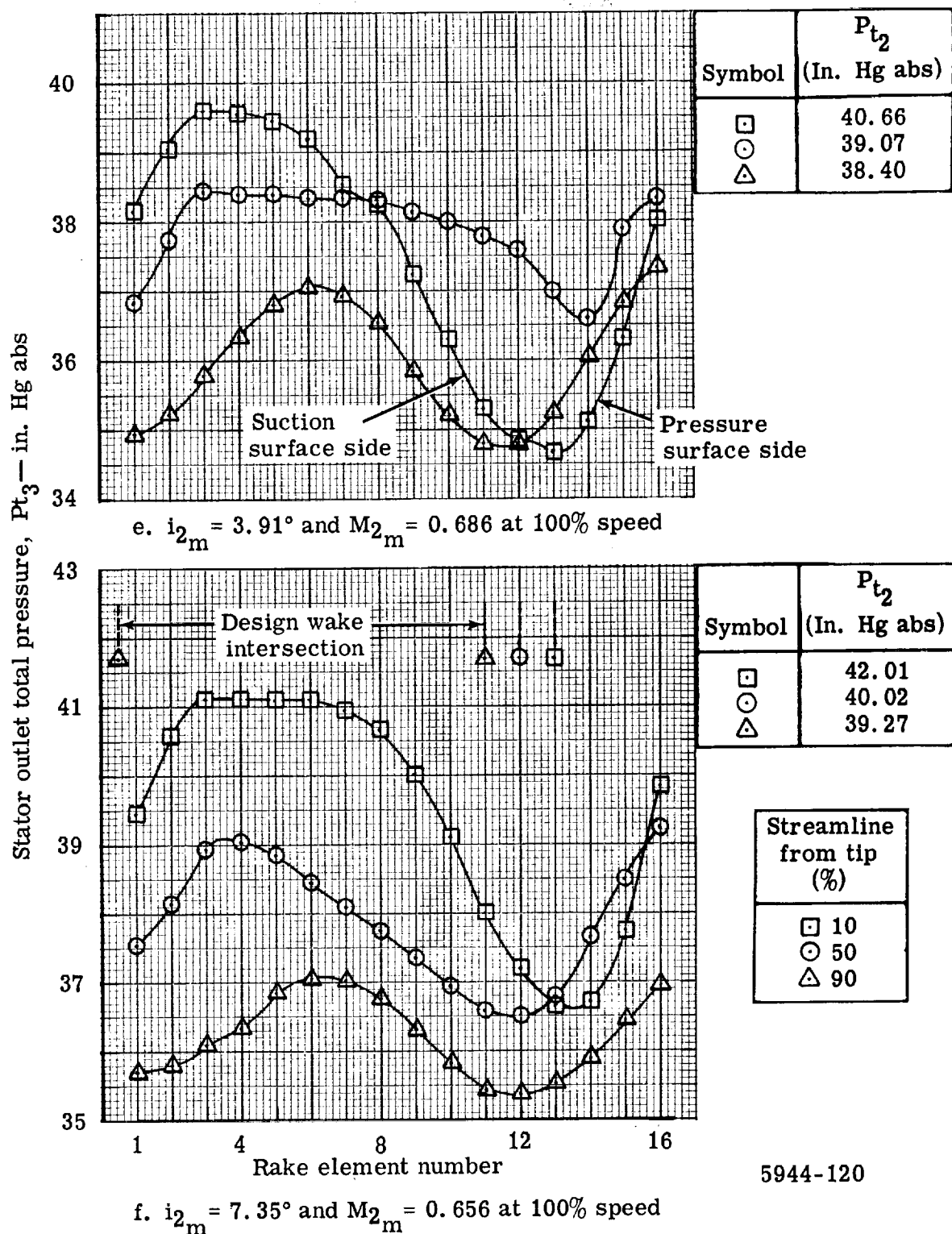


Figure 57. Triple-slotted stator wake surveys with the mean vane bleed flow rate.

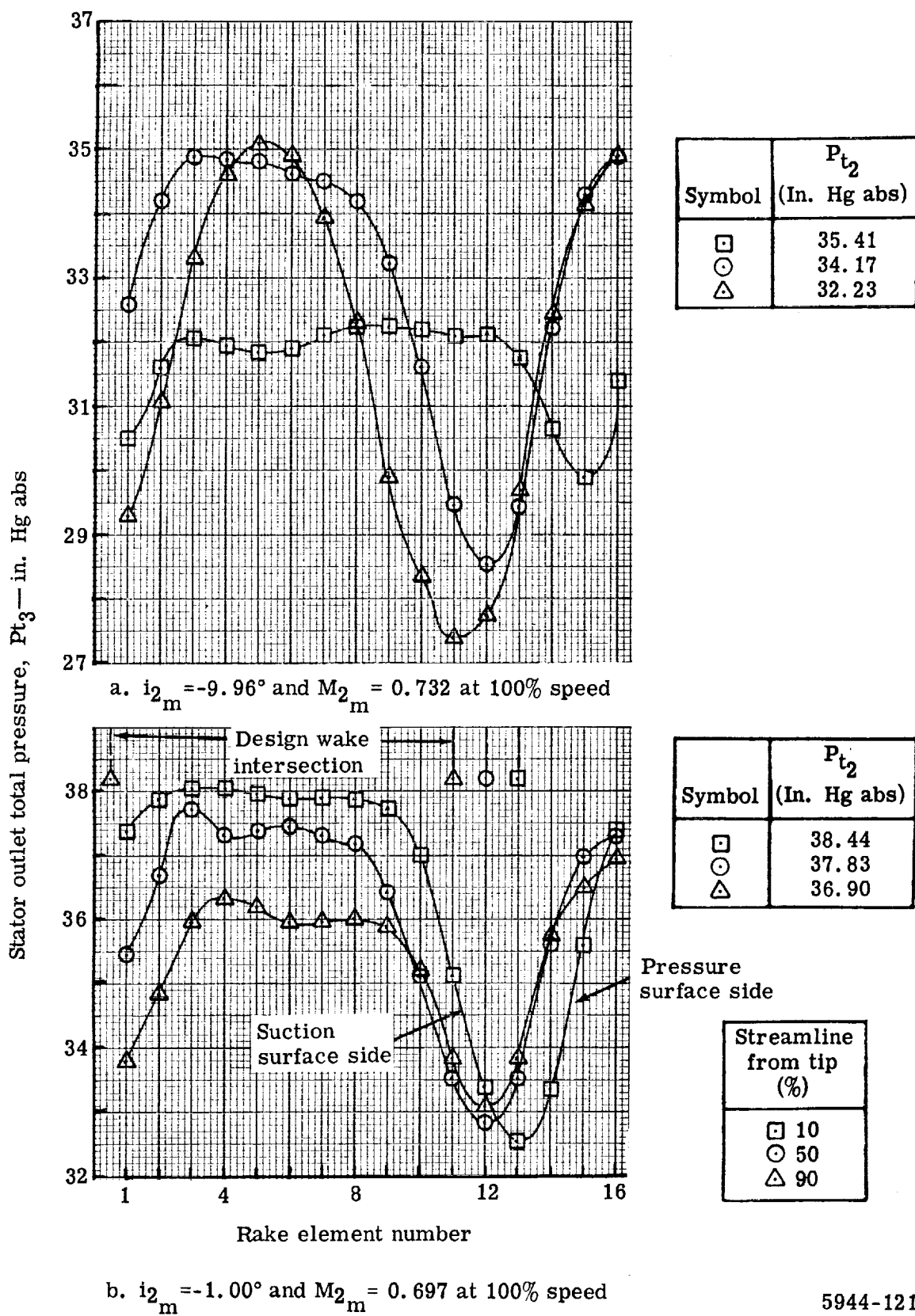


Figure 58. Triple-slotted stator wake surveys with zero vane bleed flow rate.

5944-121

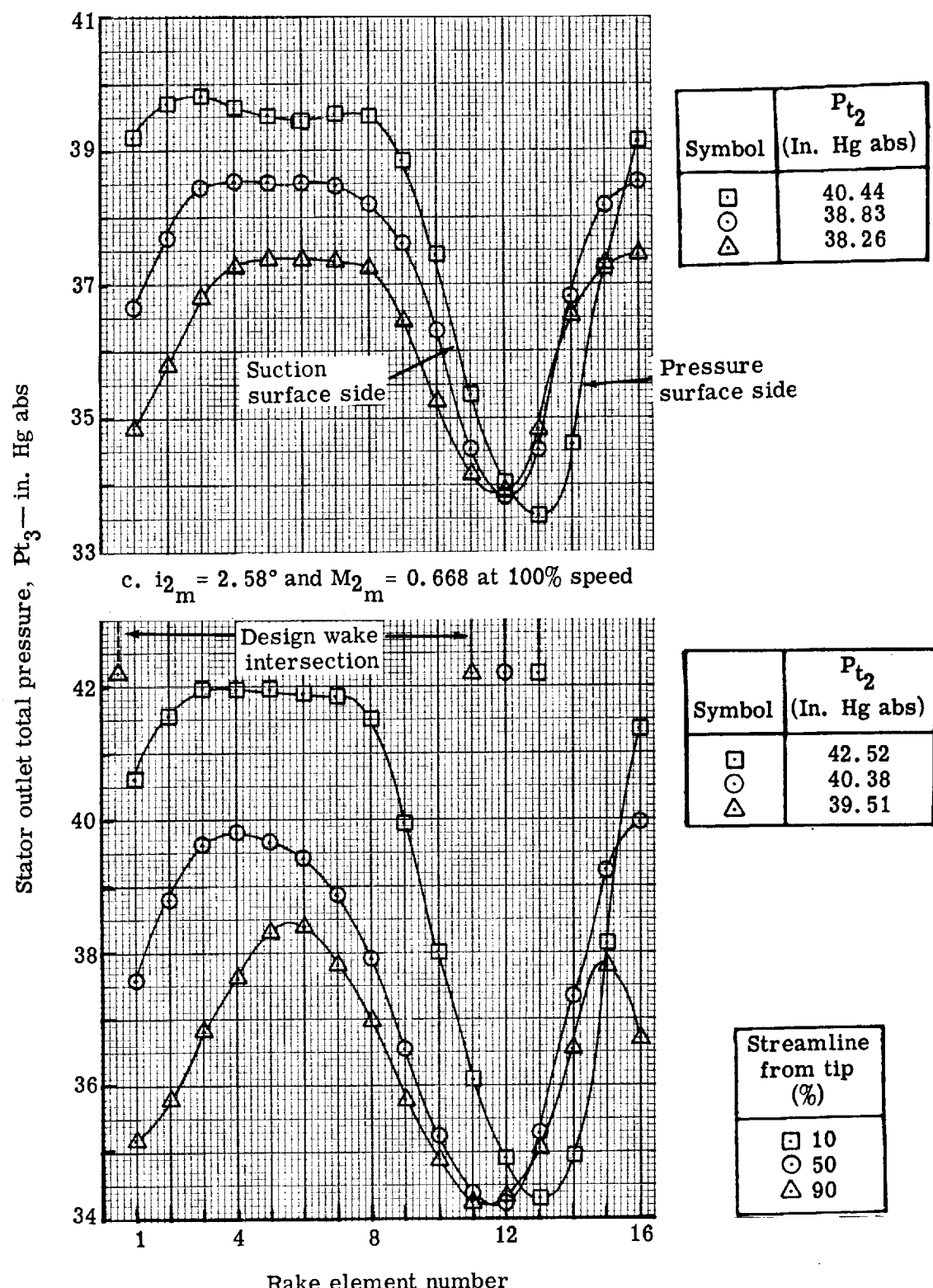


Figure 58. Triple-slotted stator wake surveys with zero vane bleed flow rate.

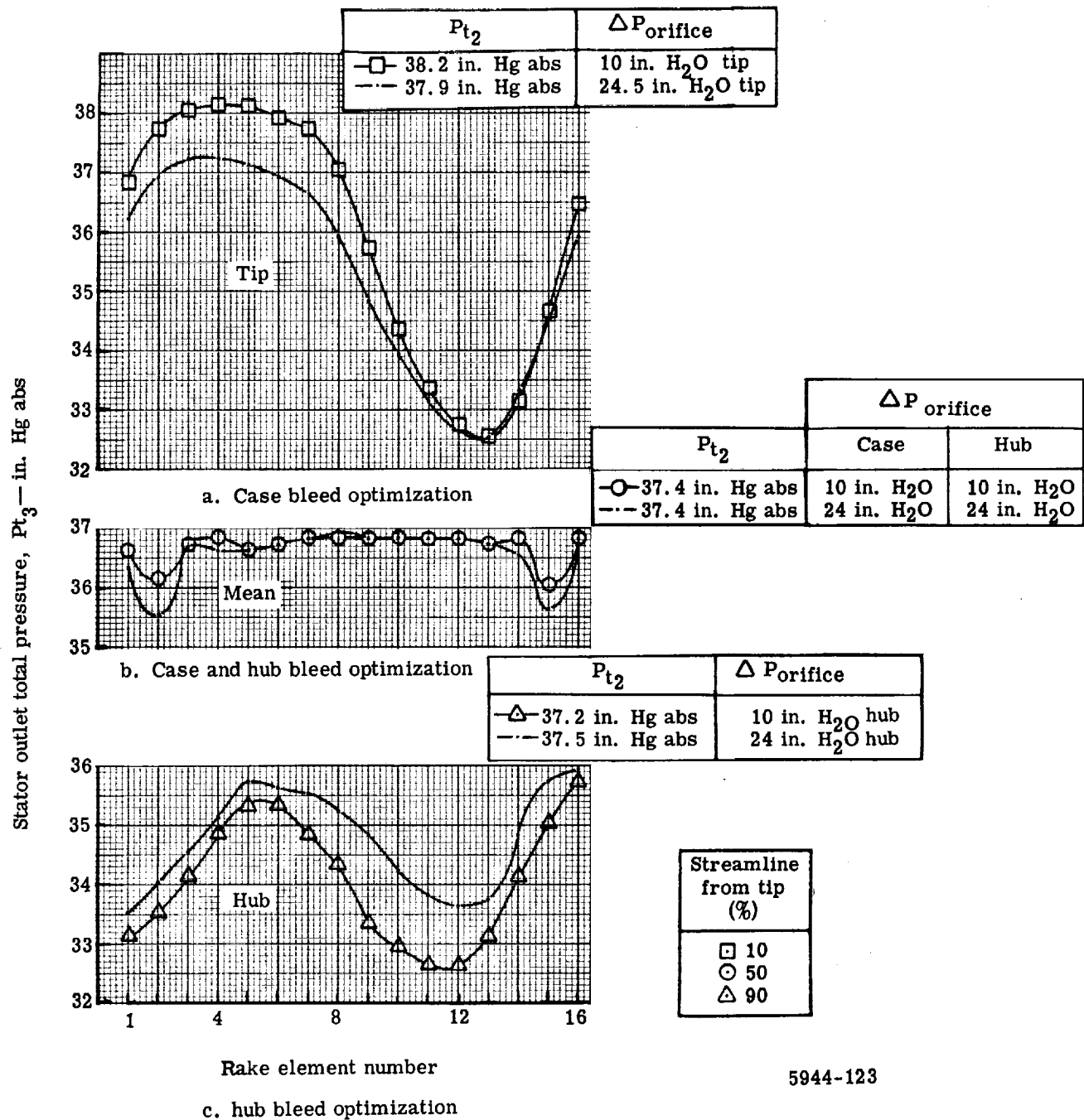


Figure 59. Variation of stator wake at 10, 50, and 90% streamlines from tip during wall bleed optimization.

Table I.
Blade and vane geometry summary.

Blade row	Exit radius (in.)	κ_1 (degrees)	κ_2 (degrees)	$\phi_{(\kappa_1-\kappa_2)}$	c (in.)	$\bar{\sigma}$	t/c	δ° (degrees)	i_{des} (degrees)	a_{des} (degrees)	n
Design inlet guide vane (63-006 series)	10.49	—	—	—	2.733	1.41	0.06	—	—	17.80	—
	11.51	—	—	—	2.733	1.29	0.06	—	—	16.25	—
	12.53	—	—	—	2.733	1.18	0.06	—	—	15.16	34
	13.54	—	—	—	2.733	1.09	0.06	—	—	14.36	—
	14.58	—	—	—	2.733	1.02	0.06	—	—	13.30	—
Rotor blade (double circular arc)	10.97	43.1	9.1	34.0	2.875	1.89	0.078	7.81	0	—	—
	11.86	49.2	21.0	28.2	2.875	1.74	0.052	7.38	0	—	—
	12.76	53.4	31.2	22.2	2.875	1.61	0.039	6.34	0	—	45
	13.65	56.7	39.1	17.6	2.875	1.51	0.033	5.52	0	—	—
	14.54	59.6	44.4	15.2	2.875	1.42	0.032	4.85	0	—	—
	11.02	56.16	-17.80	73.96	3.0	1.65	0.10	17.82	-3	—	—
Stator blade 0.75 DfH (65 series-circular arc meanline)	11.94	54.15	-17.70	71.85	3.0	1.52	0.10	17.70	-3	—	—
	12.84	52.74	-17.75	70.49	3.0	1.41	0.10	17.74	-3	—	—
	13.71	52.12	-18.05	70.17	3.0	1.32	0.10	18.06	-3	—	—
	14.58	50.09	-18.96	69.05	3.0	1.24	0.10	19.03	-3	—	—

Table II.

Rotor incidence at minimum and maximum flow for flow generation rotor and triple-slotted stator stage tests for all three vane bleed flow rates.

Corrected speed (%)	Streamline from tip (%)	Flow generation rotor test (Ref 1)		Triple-slotted stator test at optimum vane bleed		Triple-slotted stator test at mean vane bleed		Triple-slotted stator test at zero vane bleed	
		i_{\max} (stall) (degrees)	i_{\min} (choke) (degrees)	i_{\max} (stall) (degrees)	i_{\min} (choke) (degrees)	i_{\max} (stall) (degrees)	i_{\min} (choke) (degrees)	i_{\max} (stall) (degrees)	i_{\min} (choke) (degrees)
60	10	6.2	-8.0	7.4	-2.8	7.9	-4.3		
	50	6.0	-12.0	7.9	-5.0	7.9	-5.6		
	90	7.6	-13.0	10.4	-5.3	10.6	-5.8		
80	10	5.4	-8.0	6.2	-3.8	5.9	-4.0		
	50	5.4	-7.5	6.4	-5.2	6.7	-5.7		
	90	8.0	-8.0	8.7	-5.8	9.0	-5.8		
100	10	4.0	-3.0	5.5	-2.8	5.0	-2.9	4.9	-2.6
	50	4.0	-4.3	5.7	-3.8	5.3	-4.2	5.7	-3.9
	90	4.7	-5.0	7.8	-3.4	7.7	-4.0	8.0	-3.1

Table III.

Rotating stall results for triple-slotted stator stage test.

Corrected speed (%)	Corrected airflow (lb/sec)	Number of stall cells at streamline from tip 10% 90%	Stall cell rotative speed (% rpm)	Stall cell frequency (cps)	Comment
60	33.3-47.8	1 1	1 28	43 36	Abrupt stall with maximum stresses of 17,800 psi. Hysteresis test.
60	48.5	1 1	1 44	36	Abrupt stall with maximum stresses of 8950 psi. Optimum vane bleed.
60	46.2	1 1	1 27	31	Abrupt stall with maximum stresses of 11,000 psi. Mean vane bleed.
80	64.3	1 1	1 43	37	Abrupt stall with maximum stresses of 12,000 psi. Optimum vane bleed.
80	63.6	1 1	1 43	47	Abrupt stall with maximum stresses of 9800 psi. Mean vane bleed.
90	72.9	-- --	-- --	--	No data available.
100	79.9	1 1	1 45	63	Abrupt stall with maximum stresses of 12,200 psi. Optimum vane bleed.
100	80.1	2 2	2 37	67	Gradual stall with maximum stresses of 12,600 psi. Mean vane bleed.
100	82.0	1 2,4	1 2,4 44 36	61 100,200	Abrupt stall with maximum stresses increasing from 13,590 to 20,600 psi. Zero vane bleed.
110	91.1	-- --	-- --	--	No abrupt stall was observed. Stresses were steady and maximum value of 11,200 psi was recorded.

*The stresses presented in this Table are vibratory stresses. The maximum allowable transient stress and steady-state stress are $\pm 16,900$ psi and $\pm 11,250$ psi, respectively.

Table IVa.

Blade element performance—triple-slotted stator stage with the vane bleed flow at the optimum rate.

BLADE ELEMENT PERFORMANCE (READING 301 LINEAR STATIC PRESSURES)					
PERCENT DESIGN SPEED = 59.96					
CORRECTED WEIGHT FLOW = 66.79					
CORRECTED ROTOR SPEED = 5017.08					
PRESSURE RATIO = 1.0859					
ADIABATIC EFFICIENCY = 78.6054					
ROTOR 1					
STATION 1 - STATION 2					
10	30				
50	70				
90					
DIA 1	29.0150	27.080	25.060	23.020	20.989
DIA 2	29.098	27.302	25.516	23.730	21.944
BETA 1	19.129	21.487	22.511	22.960	24.035
BETA 2	34.044	36.211	39.367	41.302	42.740
BETA(PRI) 1	55.646	52.040	48.358	43.557	39.580
BETA(PRI) 2	48.209	41.345	32.864	23.599	15.595
V 1	371.63	376.15	381.86	380.97	391.03
V 2	425.54	454.53	487.36	519.99	531.75
V 1	351.11	350.01	352.77	357.28	357.12
V 2	350.23	366.74	376.78	390.64	394.95
V-THETA 1	121.78	137.78	146.20	158.77	159.26
V-THETA 2	237.72	268.52	309.13	343.21	366.95
V(PRI) 1	618.77	569.0	530.7	493.0	463.4
V(PRI) 2	526.10	488.5	448.6	426.3	410.0
V(THETA) PRI	509.5	448.6	396.5	339.7	295.2
V(THETA) PR2	392.2	322.17	243.4	170.7	110.2
U 1	631.54	586.41	542.67	498.49	454.49
U 2	629.89	591.22	552.54	513.87	475.19
M 1	0.3906	0.3648	0.3502	0.3587	0.3885
M 2	0.3932	0.4125	0.4427	0.4726	0.4895
M(PRI) 1	0.5670	0.5216	0.4866	0.4524	0.4252
M(PRI) 2	0.4550	0.4450	0.4075	0.3875	0.3732
TURN(PRI)	7.217	10.695	15.474	19.958	23.985
LOSS COEF.	0.1029	0.1251	0.1566	0.2383	0.2418
DIA 3	25.164	27.422	25.672	23.874	22.034
BETA 1	36.211	39.367	41.302	42.740	44.074
BETA 2	-9.067	-9.361	-10.414	-9.830	-10.007
V 2	423.54	454.53	487.36	519.99	537.75
V 3	285.13	305.99	325.75	346.42	366.10
V 2	350.53	366.74	376.78	390.64	394.55
V 2	285.57	305.80	320.38	342.15	354.06
V-THETA 2	237.72	266.52	303.13	343.21	364.55
V-THETA 3	-4.277	-50.42	-56.23	-58.88	-61.21
M 2	0.2832	0.4125	0.4427	0.4726	0.4895
M 3	0.2597	0.2751	0.2934	0.3119	0.3120
TURN	43.151	45.572	46.781	50.309	51.510
LOSS COEF.	0.2119	0.2110	0.2274	0.2116	0.1675
DFAC	0.58.57	0.5824	0.5971	0.5837	0.5638
LOSS PARA.	0.0086	0.0041	0.0095	0.0102	0.0103
INC ID	-17.54	-15.53	-11.33	-12.70	-13.21
DEV	9.933	8.673	7.336	8.613	10.970
CORRECTED WEIGHT FLOW					
UPSTREAM OF ROTOR					
UPSTREAM OF STATOR					
DOWNSTREAM OF STATOR					
66.79					
66.79					
61.83					

Table IVb.

Blade element performance—triple-slotted stator stage with the vane bleed flow at the optimum rate.

BLADE ELEMENT PERFORMANCE (READING 303 LINEAR STATIC PRESSURES)																	
PERCENT DESIGN SPEED = 59.96																	
CORRECTED WEIGHT FLOW = 62.07																	
CORRECTED ROTOR SPEED = 5017.13																	
PRESSURE RATIO = 1.1135																	
ADIABATIC EFFICIENCY = 86.1350																	
ROTOR 1																	
STATION 1 - STATION 2																	
		10	30	50	70	90											
DIA 1	29.150	27.080	25.060	23.020	20.988												
DIA 2	29.088	27.302	25.516	23.730	21.744												
BETA 1	18.823	20.631	22.444	24.588	25.198												
BETA 2	40.459	42.443	44.375	46.298	47.137												
BETA(PRI) 1	58.098	54.587	50.872	46.923	42.537												
BETA(PRI) 2	47.988	41.451	32.688	23.320	14.842												
V 1	342.448	351.44	357.50	358.99	361.87												
V 2	427.51	445.66	477.15	503.41	520.33												
V 2 1	324.16	328.90	330.42	326.43	327.43												
V 2 2	325.28	328.87	341.05	347.81	353.95												
V-THETA 1	110.50	123.83	136.49	149.37	154.06												
V-THETA 2	277.51	300.75	333.69	363.94	381.39												
V(PRI) 1	613.4	567.6	523.6	478.0	444.4												
V(PRI) 2	479.6	436.8	405.2	378.7	360.2												
V(THETA) PRI	520.7	462.6	406.2	349.1	300.4												
V(THETA) PR2	352.5	290.5	218.8	149.9	93.8												
U 1	631.24	586.41	542.67	498.49	454.49												
U 2	629.39	591.22	552.54	513.87	475.19												
STATOR 1	M 1	0.3133	0.3217	0.3273	0.3287	0.3314											
	M 2	0.3850	0.4023	0.4316	0.4556	0.4710											
STATION 2 - STATION 3																	
		NIPR1 1	0.5611	0.5195	0.4794	0.4377	0.4070										
		NIPR1 2	0.4319	0.3961	0.3665	0.3428	0.3315										
		TURN(PRI)	10.800	13.136	18.184	23.604	27.695										
		LOSS COEF.	0.1062	0.1815	0.1960	0.2786	0.3892										
DIA 3	29.164	27.422	25.672	23.574	22.034												
BETA 2	40.459	42.443	44.375	46.298	47.137												
BETA 3	-9.713	-9.537	-8.630	-8.84	EFF	0.7481	0.7737	0.7941	0.7698								
V 2	427.51	445.66	477.15	503.41	520.33	LCS5 PARA.	0.7442	0.7703	0.7909								
V 3	281.05	285.20	299.36	307.06	296.51	INC TO	0.0455	0.0449	0.0506								
VL 2	325.28	328.67	341.05	341.81	353.55	DEV	-1.50	-2.31	-2.83								
VL 3	271.02	265.49	295.22	303.42	292.71		2.198	2.651	1.8888								
V-THETA 2	277.41	303.75	313.69	363.94	381.39	CORRECTED WEIGHT FLOW											
V-THETA 3	-47.42	-46.16	-49.60	-47.13	-47.32												
M 2	0.3850	0.4023	0.4316	0.4556	0.4710	UPSTREAM CF ROTOR			62.07								
M 3	0.2516	0.2592	0.2685	0.2752	0.2657	UPSTREAM OF STATOR			62.07								
TURN	50.172	51.67	53.512	55.128	56.221	DENSTREAM OF STATOR											
LOSS COEF.	0.0375	0.0377	0.0161	0.0213	0.0279												
DFAC	0.6477	0.6444	0.6551	0.6711	0.6791												
LOSS PARA.	0.0168	-0.0114	0.0056	0.0069	0.0098												
INC TO	-1.62	-5.70	-8.32	-7.70	-8.01												
DEV	9.247	8.856	8.213	8.650	8.616												

Table IVc.

Blade element performance—triple-slotted stator stage with the vane bleed flow at the optimum rate.

BLADE ELEMENT PERFORMANCE (READING 302 LINEAR STATIC PRESSURES)		STATION 1 - STATION 2				STATION 1 - STATION 3				CORRECTED WEIGHT FLOW				
		10	30	50	70	90			10	30	50	70	90	
DIA 1	PERCENT DESIGN SPEED = 59.94	29.150	27.080	25.060	23.020	20.988								
CORRECTED WEIGHT FLOW = 56.43		29.088	27.302	25.516	23.730	21.944								
CORRECTED ROTOR SPEED = 3015.07		19.127	20.695	21.147	21.443	23.720								
PRESSURE RATIO = 1.1345		45.227	48.074	50.252	51.622	52.571								
ADIABATIC EFFICIENCY = 86.8148		60.734	57.751	54.675	50.637	47.625								
ROTOR 1														
V 1	313.48	319.138	322.27	327.65	323.30									
V 2	434.31	452.33	467.50	486.37	498.47									
VZ 1	296.18	298.77	298.49	298.39	295.99									
VZ 2	305.89	302.23	298.92	301.97	302.96									
V-THETA 1	102.71	112.87	121.49	134.01	130.05									
V-THETA 2	308.32	316.54	319.44	318.28	315.86									
V (PR) 1	605.9	559.9	516.2	471.4	439.2									
V (PR) 2	443.8	395.2	355.9	329.8	313.2									
V THETA PR1	528.5	473.5	421.2	364.5	324.4									
V THETA PR2	321.6	254.7	193.1	132.6	79.4									
U 1	631.24	586.41	542.67	498.49	454.49									
U 2	629.89	591.22	552.54	513.87	475.19									
STATOR 1														
M 1	0.2862	0.2917	0.2944	0.2964	0.2953									
M 2	0.3894	0.4066	0.4208	0.4369	0.4503									
M (PR) 1	0.5531	0.5114	0.4715	0.4307	0.4012									
M (PR) 2	0.3979	0.3553	0.3204	0.2976	0.2829									
TURN PR1	14.302	17.632	21.813	26.932	32.948									
LOSS COEF.	0.2006	0.1888	0.2254	0.2244	0.2338									
DIFC	0.3879	0.4231	0.4402	0.4402	0.4322									
EFC	0.7809	0.8119	0.8053	0.8291	0.8237									
LCS PARA.	0.7766	0.8082	0.806	0.8259	0.8204									
INCD	0.0688	0.0577	0.0581	0.0586	0.0665									
DEV	1.13	0.85	0.77	0.86	2.62									
VZ 3	272.14	279.65	273.36	267.99	232.55									
V-THETA 2	316.32	336.54	359.44	381.28	399.64									
V-THETA 3	-35.92	-42.35	-42.46	-44.18	-42.74									
M 2	0.3854	0.4066	0.4208	0.4389	0.4503	UPSTREAM OF ROTOR	56.43							
M 3	0.2664	0.2521	0.2470	0.2424	0.2108	UPSTREAM OF STATOR	56.43							
TURN	53.523	56.714	56.082	60.983	62.585	DOWNSTREAM OF STATOR	51.09							
LOSS COEF.	0.0340	0.0233	0.0267	0.0692										
DIFC	0.6551	0.7105	0.7276	0.7515										
LOSS PARA.	0.0584	0.0627	0.0682	0.0096	0.0266									
INCL	-6.85	-4.67	-2.45	-2.38	-3.38									
DEV	10.664	5.398	8.920	8.319	7.386									

Blade element performance—triple-slotted stator stage with the vane bleed flow at the optimum rate.

Table IVd.

BLADE ELEMENT PERFORMANCE (RELATIVE 303 LINEAR STATIC PRESSURES)		STATION 1 - STATION 2				
	PERCENT DESIGN SPEED = 59.88	10	30	50	70	90
CORRECTED WEIGHT FLOW = 52.37						
CORRECTED ROTOR SPEED = 5000.28						
PRESSURE RATIO = 1.1479						
AERODYNAMIC EFFICIENCY = 21.3737						
ROTOR 1						
U1A 1	29.150	27.010	25.060	23.020	20.998	
U1A 2	29.083	27.302	25.516	23.730	21.944	
BETA 1	19.823	21.691	23.244	24.478	24.185	
BETA 2	52.422	54.915	57.409	53.642	59.434	
DELTA(+) 1	63.075	30.363	51.765	52.241	50.439	
DELTA(+) 2	45.046	39.700	30.224	20.148	8.598	
V 1	26.514	28.910	30.117	23.814	29.641	
V 2	44.442	45.151	41.106	48.895	50.115	
VZ 1	268.07	269.37	266.61	264.63	269.10	
VZ 2	271.02	259.45	253.73	253.40	254.35	
V-THETA 1	97.17	107.15	114.51	126.10	124.26	
V-THETA 2	352.21	369.22	356.89	415.82	431.51	
V(PRI) 1	592.0	544.7	493.8	422.8	422.5	
V(PRI) 2	383.0	337.5	294.9	269.9	251.8	
V(THETA PRI)	527.9	473.5	422.8	387.5	329.7	
WHITE 4 PR2	211.5	215.9	150.2	93.0	39.0	
W 1	625.00	530.02	531.31	493.57	450.00	
W 2	322.37	385.38	547.09	508.79	470.50	
W 1	6.2637	6.2637	6.2570	6.2698	6.2729	
W 2	0.4023	0.4102	0.4102	0.4286	0.4318	0.4571
STATION 2 - STATION 3						
M(PRI) 1	0.5447	0.5013	0.4900	0.4686	0.3689	
M(PRI) 2	0.3476	0.3065	0.2863	0.2460	0.2352	
W 10	50	70	90	140	140	
TURB(PRI) 1	13.029	23.603	27.140	31.092	41.142	
LSS CEF	0.1078	0.0607	0.0521	0.0608	0.1055	
EFF P	0.3047	0.3047	0.3047	0.3047	0.3047	
LSS PARA	501.15	501.15	501.15	501.15	501.15	
INCLID	-9.184	-9.184	-9.184	-9.184	-9.184	
DEV	233.72	208.26	208.26	208.26	208.26	
VZ 3	253.40	254.85	254.85	254.85	254.85	
V-THETA 2	241.35	229.37	229.37	229.37	229.37	
V-THETA 3	265.52	150.04	431.51	415.82	415.82	
H 2	-4.436	-4.436	-4.436	-4.436	-4.436	
W 2	-4.436	-4.436	-4.436	-4.436	-4.436	
TURB	0.4102	0.4102	0.4102	0.4102	0.4102	
LSS COEF	0.1162	0.1162	0.1162	0.1162	0.1162	
DFAC	0.1098	0.1098	0.1098	0.1098	0.1098	
LSS PARA	0.4454	0.4454	0.4454	0.4454	0.4454	
INCLID	0.34	0.34	0.34	0.34	0.34	
DEV	10.456	10.456	10.456	10.456	10.456	

Table IVe.

Blade element performance—triple-slotted stator stage with the vane bleed flow at the optimum rate.

BLADE ELEMENT PERFORMANCE READINGS		300 LINEAR STATIC PRESSURES	
PERCENT DESIGN SPEED =	59.88		
CORRECTED WEIGHT FLOW =	49.58		
CORRECTED FOTR SPEED =	5010.33		
PRESSURE RATIO =	1.1511		
ADIABATIC EFFICIENCY =	82.9276		
ROTOR 1			
STATION 1 - STATION 2			
	10	30	50
DIA 1	29.150	27.050	25.060
DIA 2	29.089	27.302	25.516
BETA 1	17.760	19.760	23.257
BETA 2	53.287	54.117	56.487
BETA(PRI) 1	65.383	62.681	58.855
BETA(PRI) 2	45.802	39.266	30.302
V 1	264.68	271.33	283.18
V 2	444.44	458.26	477.51
V 1	252.08	255.35	260.17
V 2	265.69	268.60	263.65
V-THETA 1	80.76	91.73	111.82
V-THETA 2	356.28	371.29	390.13
V(PRI) 1	905.21	556.4	503.0
V(PRI) 2	381.1	346.9	305.4
V(THETA) PRI	550.1	494.3	430.5
V(THETA) PR2	273.2	219.6	154.1
U 1	630.85	596.06	542.34
U 2	629.51	590.86	552.21
M 1	0.2410	0.2471	0.2581
M 2	0.3980	0.4120	0.4301
M(PRI) 1	0.5510	0.5068	0.4384
M(PRI) 2	0.3413	0.3119	0.2751
TURN(PRI)	13.581	23.415	28.553
LSS COEF.	0.1206	0.0460	0.0539
DFAC	0.5315	0.5394	0.5615
EFP	0.8774	0.9362	0.9516
M 3	0.3980	0.4120	0.4301
M 2	0.3413	0.3119	0.2751
TURN	13.581	23.415	28.553
LOSS COEF.	0.1206	0.0460	0.0539
DFAC	0.5315	0.5394	0.5615
LSS PARA.	0.0296	0.0117	0.0159
INC1D	5.78	5.78	5.16
DEV	0.702	0.666	-0.438
CORRECTED WEIGHT FLOW			
DIA 3	27.422	25.672	23.034
BETA 2	54.117	56.248	50.248
BETA 3	-15.176	-6.830	-10.064
V 2	444.44	458.26	477.51
V 3	228.10	249.26	248.67
V 2	265.69	268.60	263.65
VZ 3	220.14	246.90	225.57
V-THETA 2	356.28	371.29	358.13
V-THETA 3	-55.511	-35.20	-29.57
TURN	68.43	62.225	63.317
LOSS COEF.	0.1710	0.2210	0.2034
DFAC	0.8627	0.7942	0.8296
LSS PARA.	0.0362	0.0310	0.0224
INC1G	1.21	1.58	3.79
DEV	3.784	9.923	10.920
			49.58
			49.58
			44.17

Table IVf.

Blade element performance—triple-slotted stator stage with the vane bleed flow at the optimum rate.

STATION 1		STATION 1 - STATION 2						STATION 1 - STATION 2		CORRECTED WEIGHT FLOW	
		10	30	50	70	90					
DIA 1	29.150	27.080	25.060	23.020	20.988	—	501.13	510.03	511.62	512.17	513.80
DIA 2	29.088	27.302	25.516	23.730	21.944	—	782.04	723.70	644.79	590.11	516.37
BETA 1	20.160	22.033	23.793	24.584	24.590	—	204.78	214.94	216.29	216.56	216.83
BETA 2	35.542	37.065	39.848	42.267	43.834	—	376.20	418.24	463.56	495.61	500.50
BETA(PRI) 1	55.710	52.137	48.169	43.757	39.500	—	636.4	650.5	612.7	516.64	518.96
BETA(PRI) 2	46.957	40.533	32.449	23.497	14.978	—	634.3	593.8	556.1	534.4	464.47
V 1	439.06	498.92	507.61	516.64	518.96	—	611.53	652.73	685.22	715.61	742.80
V 2	578.31	611.53	652.73	685.22	715.61	—	459.09	462.48	469.81	472.80	476.03
VZ 1.	459.47	464.47	469.81	472.80	476.03	—	470.56	482.12	501.13	510.03	511.62
VZ 2.	168.55	187.17	204.78	214.94	216.37	—	168.55	187.17	204.78	214.94	216.37
V-THETA 1	336.17	376.20	418.24	463.56	495.61	—	336.17	376.20	418.24	463.56	495.61
V-THETA 2	314.9	375.5	460.97	478.74	481.16	—	314.9	375.5	460.97	478.74	481.16
V(PRI) L	—	0.4518	0.4613	0.4784	0.4816	—	—	0.4518	0.4613	0.4784	0.4816
V(PRI) R	—	0.5235	0.5354	0.5446	0.5551	—	—	0.5235	0.5354	0.5446	0.5551
VTHETA PRI 1	673.3	594.9	518.9	449.9	389.7	—	673.3	594.9	518.9	449.9	389.7
VTHETA PRI 2	503.9	412.2	318.6	221.7	138.1	—	503.9	412.2	318.6	221.7	138.1
U 1	84.882	782.04	723.70	644.79	590.11	—	84.882	782.04	723.70	644.79	590.11
U 2	84.03	788.45	736.87	685.29	633.72	—	84.03	788.45	736.87	685.29	633.72
M 1	—	0.4613	0.4697	0.4784	0.4816	—	—	0.4613	0.4697	0.4784	0.4816
M 2	—	0.5354	0.5446	0.5551	0.5651	—	—	0.5354	0.5446	0.5551	0.5651
STATION 2 - STATION 3		STATION 2 - STATION 3						STATION 2 - STATION 3		STATION 2 - STATION 3	
10	30	50	70	90	—	—	—	—	—	—	—
DIA 3	27.422	25.072	23.874	22.034	—	—	—	—	—	—	—
BETA 2	35.845	35.848	42.267	42.834	—	—	—	—	—	—	—
BETA 3	-7.020	-8.117	-8.630	-7.759	—	—	—	—	—	—	—
V 2	578.31	522.73	689.22	715.61	—	—	—	—	—	—	—
V 3	386.24	456.08	474.70	426.38	—	—	—	—	—	—	—
VZ 2	476.56	482.12	521.13	510.03	516.21	—	476.56	482.12	521.13	510.03	516.21
VZ 3	375.92	416.78	451.49	469.08	422.48	—	375.92	416.78	451.49	469.08	422.48
V-THETA 2	336.17	374.20	418.24	463.56	495.61	—	336.17	374.20	418.24	463.56	495.61
V-THETA 3	-51.20	-21.32	-64.80	-72.87	-57.57	—	-51.20	-21.32	-64.80	-72.87	-57.57
M 2	0.5235	0.5554	0.5844	0.6296	0.6551	—	—	—	—	—	—
M 3	0.3764	0.4093	0.4263	0.3812	0.4263	—	—	—	—	—	—
TURB	44.594	47.566	51.593	51.593	51.593	—	—	—	—	—	—
LCSS CUEF.	0.1619	0.1620	0.0526	0.0573	0.1622	—	—	—	—	—	—
UFAC	0.6157	0.6163	0.5658	0.6377	0.6495	—	—	—	—	—	—
LCSS PARA.	0.0563	0.0299	0.0185	0.0495	0.0604	—	—	—	—	—	—
INCID	-16.54	-14.17	-12.85	-11.73	-12.12	—	-16.54	-14.17	-12.85	-11.73	-12.12
UEV	10.300	10.020	9.633	8.850	10.041	—	—	—	—	—	—
CORRECTED WEIGHT FLOW		CORRECTED WEIGHT FLOW						CORRECTED WEIGHT FLOW		CORRECTED WEIGHT FLOW	
UPSTREAM OF ROTOR		UPSTREAM OF ROTOR						UPSTREAM OF ROTOR		UPSTREAM OF ROTOR	
UPSTREAM OF STATOR		UPSTREAM OF STATOR						UPSTREAM OF STATOR		UPSTREAM OF STATOR	
DOWNSTREAM OF STATOR		DOWNSTREAM OF STATOR						DOWNSTREAM OF STATOR		DOWNSTREAM OF STATOR	
85.30		85.30						85.30		85.30	
80.74		80.74						80.74		80.74	

Table IVg.

Blade element performance—triple-slotted stator stage with the vane bleed flow at the optimum rate.

BLADE ELEMENT PERFORMACE (REACTION)	30%	LINEAR STATIC PRESSURES
PERCENT DESIGN SPEED =	79.90	
CORRECTED WEIGHT FLOW =	78.87	
CORRECTED MOTOR SPEED =	6694.98	
PRESSURE RATIO =	1.2225	
ADIABATIC EFFICIENCY =	99.1339	
ROTUR 1		
STATION 1-- STATION 2		
	10	30
DIA 1	29.150	27.080
DIA 2	29.098	27.302
BETA 1	19.437	21.053
BETA 2	42.819	45.102
BETA(PR) 1	58.379	55.121
BETA(PR) 2	55.665	39.834
V 1	451.25	460.34
V 2	587.00	607.55
VZ 1	425.40	429.61
VZ 2	430.58	428.84
V-THETA 1	150.53	165.37
V-THETA 2	398.97	420.36
V(PRI) 1	811.4	751.3
V(PRI) 2	616.1	558.5
V(THETA) PRI	690.9	516.3
V(THETA) PR2	440.7	432.54
U 1	641.44	791.68
U 2	839.05	788.03
STATOR 1		
STATION 2 -- STATION 3		
	10	30
DIA 3	29.164	25.672
V-THETA 2	45.102	46.963
BETA 2	-11.028	-8.290
H 2	587.00	607.55
V 2	36.779	33.673
VZ 2	430.56	428.84
VZ 3	355.34	384.08
V-THETA 2	398.57	430.36
V-THETA 3	-73.12	-52.23
H 3	0.359	0.545
TURN	54.447	52.861
LOSS COEF.	0.140	0.148
DFAC	0.6613	0.6613
LOSS PARA.	0.0254	0.0241
INC10	-5.26	-7.64
DEV	7.332	10.281
CUMRECTED WEIGHT FLOW		
UPSTREAM OF ROTOR		
DIA 1	20.98	23.020
BETA 1	21.567	22.567
BETA 2	48.963	48.760
BETA(PR) 1	51.700	47.616
BETA(PR) 2	32.286	22.817
V 1	465.79	470.81
V 2	631.79	665.49
VZ 1	428.60	431.33
VZ 2	438.70	442.04
V-THETA 1	176.75	194.85
V-THETA 2	463.25	520.96
V(PRI) 1	535.8	592.45
V(PRI) 2	511.6	475.9
V(THETA) PRI	566.6	459.6
V(THETA) PR2	273.3	213.5
U 1	724.38	664.49
U 2	736.54	633.43
UPSTREAM OF STATOR		
DIA 1	0.4243	0.4343
BETA 1	0.5259	0.5475
H 1	0.7474	0.6925
TURN(PR1)	1.2.714	1.5.287
LOSS COEF.	0.1423	0.0897
DFAC	0.4150	0.4243
EFF P	0.5259	0.5475
EFF	0.7474	0.6925
LGS PARA.	0.0351	0.0227
INC10	-1.22	-1.78
DEV	0.565	1.034
DOWNSTREAM OF STATOR		
DIA 1	0.3702	0.3827
BETA 1	0.8298	0.8969
H 1	0.8245	0.8938
TURN	0.0351	0.0227
LOSS COEF.	0.1423	0.0897
DFAC	0.6613	0.6613
LOSS PARA.	0.0241	0.0214
INC10	-5.26	-5.26
DEV	7.332	7.945
CUMRECTED WEIGHT FLOW		
DIA 1	20.98	23.020
BETA 1	21.567	22.567
BETA 2	48.963	48.760
BETA(PR) 1	51.700	47.616
BETA(PR) 2	32.286	22.817
V 1	465.79	470.81
V 2	631.79	665.49
VZ 1	428.60	431.33
VZ 2	438.70	442.04
V-THETA 1	176.75	194.85
V-THETA 2	463.25	520.96
V-THETA 3	516.3	475.9
H 1	58.473	59.749
TURN	52.861	55.259
LOSS COEF.	0.140	0.148
DFAC	0.6613	0.6613
LOSS PARA.	0.0254	0.0241
INC10	-5.26	-5.26
DEV	7.332	7.945

Blade element performance—triple-slotted stator stage with the vane bleed flow at the optimum rate.

Table IVh.

STATION 1 - STATION 2									
	10	30	50	70	90				
PERCENT DESIGN SPCEU = 19.37						LINELAR STATIC PRESSURE(S)			
CORRECTED WEIGHT IN LIN = 7.540									
CORRECTED ROTOR SPECIE = 30.208									
ROT.SQUARE RATIO = 1.2429									
AERODYNAMIC EFFICIENCY = 40.1052									
KUTUK 1									
	10	30	50	70	90				
JIA 1	27.150	27.040	25.060	23.020	20.986				
JIA 2	29.058	27.302	25.316	23.750	21.944				
JETIA 4	20.165	21.643	21.739	25.232	25.157				
JETIA 2	49.623	51.338	53.087	56.010	56.193				
BELIA(PRI) 1	50.582	37.516	54.457	50.508	46.687				
BELIA(PRI) 2	45.304	39.543	31.549	22.479	11.959				
V 1	416.222	42.320	42.206	43.616	435.37				
V 2	357.20	302.09	624.52	642.25	662.76				
VL 1	390.71	392.50	389.50	394.07					
VL 2	380.38	276.14	375.09	368.29	371.59				
V-THETA 1	143.48	157.25	171.32	182.08	185.03				
V-THETA 2	47.34	470.14	479.33	526.17	548.79				
V(PRI) 1	753.0	731.6	670.1	614.9	572.3				
V(PRI) 2	540.8	497.3	440.1	393.6	379.3				
V-THETA PRI	390.1	317.1	545.3	473.2	415.1				
V-THETA PRI	386.4	310.6	230.3	154.4	78.7				
V 1	833.55	774.20	716.59	656.26	600.15				
V 2	831.77	750.70	729.53	678.56	627.49				
STATION 1									
	10	30	50	70	90	TURB(PRI)			
N 1	0.383.0	0.379.7	0.364.9	0.354.9	0.343.2	0.403.2	0.404.3		
N 2	0.530.5	0.546.3	0.563.3	0.584.6	0.606.1				
M(PRI) 1	0.733*	0.676.3	0.621.9	0.571.0	0.531.3				
M(PRI) 2	0.498.5	0.644.7	0.609.5	0.563.9	0.527.3				
STATION 2 - STATION 3									
	10	30	50	70	90	LSS(GEF)			
DIA 2	27.054	27.046	23.874	22.034	20.935	0.0.0404	0.0.0364	0.0.0337	
BELIA 2	51.050	53.087	55.698	57.740	59.715	0.437.6	0.400.0	0.382.4	
BELIA 3	-11.572	-10.459	-10.064	-11.283	-10.907	0.965.3	0.912.9	0.911.1	0.941.3
V 2	567.40	564.02	562.02	561.75	565.91A	0.920.0	0.907.1	0.770.1	0.931.4
V 2	567.45	562.02	562.02	561.75	565.91A	0.920.0	0.907.1	0.770.1	0.931.4
VL 2	376.14	375.05	368.29	371.59	371.59	0.905.0	0.895.5	0.821.3	
VL 3	386.39	386.39	386.39	386.39	386.39	0.905.0	0.895.5	0.821.3	
V-THETA 2	447.34	470.14	495.33	528.17	546.79	0.905.0	0.895.5	0.821.3	
V-THETA 3	-67.42	-49.76	-48.76	-30.31	-58.86				
N 2	0.531.2	0.545.8	0.555.4	0.565.0	0.575.6				
N 3	0.230.4	0.214.3	0.210.5	0.228.0	0.235.0				
TURB(GEF)	17.427	17.026	17.74	27.081	UPSTREAM OF STATOR	7.4.50			
LSS(GEF)	0.160.6	0.157.8	0.155.9	0.155.1	0.155.2				
LEAF	0.173.5	0.173.7	0.174.3	0.174.1	0.174.2				
LOSS PARA	0.0.0.14	0.0.0.17	0.0.0.19	0.0.0.21	0.0.0.24	DOWNSTREAM OF STATOR	68.48		
INCIG	-6.60	-6.60	-6.60	-6.60	-6.60				
DEV	0.930.0	12.151	5.011	7.616	6.117				

Table IVi.

Blade element performance—triple-slotted stator stage with the vane bleed flow at the optimum rate.

	BLADE ELEMENT PERFORMANCE (READING :10)			LINEAR STATIC PRESSURE)		
	PERCENT DESIGN SPEED	= 79.33				
CORRECTED WEIGHT FLOW =	0.9.68					
CORRECTED ROTOR SPEED = 6687.37						
PRESSURE RATIO = 1.0263						
ADIABATIC EFFICIENCY = 07.6551						
ROTOR 1						
	STATION 1 - STATION 2			STATION 1		
	10	30	50	70	90	
DIA 1	29.150	27.050	25.060	23.020	20.984	
DIA 2	29.088	27.302	25.216	23.720	21.944	
BETA 1	20.103	24.181	23.018	25.319	24.827	
BETA 2	5.0.140	5.0.201	5.7.145	5.0.665	5.0.700	
DELTA (P/R) 1	02.644	35.287	50.558	53.174	49.776	
DELTA (P/R) 2	45.212	39.473	31.873	20.630	9.453	
V 1	386.47	395.97	405.01	402.35		
V 2	392.79	606.85	620.28	640.73	659.75	
V 3	352.92	367.41	366.46	364.20	365.12	
V 4	355.00	345.63	336.51	335.63	332.37	
V-THETA 1	1.3.0.3	1.49.67	160.24	172.35	168.96	
V-THETA 2	47.0.30	47.0.40	521.06	522.65	567.62	
V(P/R) 1	789.8	725.0	600.7	607.3	565.5	
V(P/R) 2	504.8	446.5	390.2	359.7	338.0	
V(THETA) P/R 1	701.5	625.4	527.0	486.5	431.7	
V(THETA) P/R 2	358.2	382.6	209.2	126.7	58.+	
J 1	1.54.31	775.06	717.35	658.86	600.70	
J 2	83.54	781.42	730.30	679.13	628.07	
	STATION 1			STATION 2		
	M 1	M 2	M 3	M 4	M 5	
M(R/R) 1	0.7308	0.6714	0.6175	0.5630	0.5234	
M(R/R) 2	0.4939	0.4037	0.3593	0.3270	0.3060	
M(R/R) 3	0.3593	0.3270	0.3060	0.2813		
LSS 1	17.432	20.214	24.786	32.544		
LSS 2	1.002	0.925	0.855	0.685	0.0872	
LSS 3	0.3671	0.3104	0.3733			
LSS 4	0.5330	0.5487	0.5055	0.5882	0.6013	
LSS 5	0.4037	0.3593	0.3270	0.3060		
LSS 6	0.3060					
	STATION 3 - STATION 4			CORRECTED WEIGHT FLOW		
	10	30	50	70	90	
DIA 3	25.664	27.422	23.072	22.634	21.674	0.5145
BETA 2	5.0.40	5.0.45	5.0.70	5.0.75	5.0.80	0.5443
BETA 3	-18.104	-5.126	-9.713	-10.239	LFF	0.9520
V 4	25.60.12	24.0.23	6.0.93	6.59.75	LSS PARAB.	0.9452
V 5	20.0.29	3.0.0.41	3.20.0.04	24.7.47	LNG 10	0.0162
VZ 2	355.00	293.0.3	316.0.21	330.63	336.37	0.0224
VZ 3	28.0.43	21.0.54	159.63	317.42	242.53	1.254
V-THETA 2	474.30	42.0.30	52.0.05	52.0.62		
V-THETA 3	-9.0.21	-2.0.57	-61.0.45	-54.2.3	-43.0.99	
H 2	0.13.0	0.0.47	0.26.2	0.0.0.13	UPSTREAM OF ROTOR	69.08
H 3	0.20.0	0.28.4	0.2.04.2	0.0.0.01	UPSTREAM OF STATOR	69.08
TURN	71.242	61.0.47	64.15.5	62.0.25	0.9.533	
LSS COEF.	0.20.5	0.13.4	0.0.49.7	0.0.0.13	J.0.1412	
DFAC	0.0.730	0.0.664	0.0.7.74	0.0.6.69	J.0.0.59	
LSS PANAL	0.0.750	0.0.512	0.0.0.75	0.0.4.03	0.0.4.03	
INCIC	1.0.5	3.0.14	4.0.44	3.0.75		
DEV	0.0.870	0.0.714	1.0.730	1.0.567	1.0.070	

Table IVj.

Blade element performance—triple-slotted stator stage with the vane bleed flow at the optimum rate.

BLADE ELEMENT PERFORMANCE, READING: 307 LINEAR STATIC PRESSURES									
	PERCENT DESIGN SPEED = 79.82	CORRECTED WEIGHT FLOW = 67.15	CORRECTED ROTOR SPEED = 6678.21	PRESSURE RATIO = 1.2961	ADIABATIC EFFICIENCY = 94.459%	ROTOR 1	S T A T I O N 1 - S T A T I O N 2	S T A T I O N 10	S T A T I O N 30
DIA 1	29.150	27.080	25.060	23.020	20.988				
DIA 2	29.088	27.302	25.516	23.730	21.944				
BETA 1	19.625	20.983	22.747	24.755	23.848				
BETA 2	52.540	54.348	56.071	57.493	58.070				
BETA(PR) 1	63.918	61.419	58.450	55.017	51.908				
BETA(PR) 2	46.717	39.183	31.539	21.853	9.940				
V 1	372.29	377.11	382.84	396.95	385.44				
V 2	601.19	611.76	628.00	646.42	668.41				
VZ 1	351.10	352.09	353.07	351.39	352.53				
VZ 2	365.65	356.57	350.53	347.49	344.55				
V-THETA 1	123.92	135.08	148.03	162.03	155.84				
V-THETA 2	477.21	497.10	521.07	545.31	572.76				
V(PR) 1	798.6	735.9	674.8	612.9	571.4				
V(PR) 2	514.6	460.0	411.3	374.4	349.8				
V(PI) 1	717.2	666.3	575.0	502.2	469.7				
V(PI) 2	362.1	290.6	211.1	139.4	60.4				
U 1	861.05	781.33	723.05	664.19	605.56				
U 2	839.27	787.74	736.20	694.67	633.14				
M 1	0.3408	0.3454	0.3507	0.3546	0.3532				
M 2	0.5329	0.5455	0.5621	0.5804	0.6015				
M(PD) 1	0.7311	0.6140	0.5882	0.5612	0.5236				
M(PD) 2	0.4560	0.4102	0.3681	0.3360	0.3148				
TURNP(K)	19.201	22.234	26.910	33.164	41.968				
LCS COEF.	18.824	0.1231	0.1235	0.1512	0.1700				
DFAC	0.5125	0.5344	0.5541	0.5733	0.5653				
EFF	0.9359	0.8942	0.9067	0.8992	0.8933				
BETA 3	29.164	25.672	23.874	22.036	20.956				
BETA 2	52.260	54.348	58.071	57.493	58.070				
V 2	-23.251	-7.400	-6.072	-5.713	-10.069				
V 3	601.19	611.76	628.00	646.62	668.41				
V 2	302.15	305.29	346.71	424.34	236.75				
V 2	365.65	356.57	350.53	347.49	344.55				
VZ 2	276.61	306.71	340.85	418.26	233.11				
V-THETA 2	477.21	497.10	521.07	545.31	572.76				
V-THETA 3	-115.28	-35.83	-36.26	-71.59	-41.37				
M 2	0.5328	0.5455	0.5621	0.5804	0.6015				
M 3	0.2621	0.479	0.3013	0.3144	0.2077				
TURN	75.791	61.748	62.143	67.206	69.036				
LCS COEF.	0.2381	0.1684	0.0674	-0.3142	0.1577				
DFAC	0.8959	0.8251	0.6662	0.6557	0.9234				
LCS PARA.	0.6879	0.6629	0.0336	-0.1177	0.0469				
INCIE	0.46	0.21	3.37	3.49	3.02				
DEV	-4.291	10.640	11.678	7.567	7.736				
						C O R R E C T E D W E I G H T F L O W			

Table IVk.

Blade element performance—triple-slotted stator stage with the vane bleed flow at the optimum rate.

BLADE ELEMENT PERFORMANCE (READING 311 LINEAR STATIC PRESSURE)		STATION 1 - STATION 2					
		10	30	50	70	90	
FREQUENT DESIGN SPEED = 87.87							
CORRECTED WEIGHT FLUX = 92.05							
CORRECTED FURTHER SPEED = 1516.78							
PRESSURE RATIO = 4.01e3							
ADIABATIC EFFICIENCY = 75.9211							
ACTION 1							
U1A 1	29.150	27.060	25.060	23.020	20.980		
U1A 2	29.038	27.302	25.516	23.730	21.944		
U1A 4	20.345	22.129	24.376	25.149	25.542		
U1A 5	35.361	37.670	40.034	41.510	42.193		
U1A(PK) 1	55.991	22.260	43.125	43.775	39.527		
U1A(PK) 2	47.901	49.677	33.178	24.676	16.512		
V1	256.65	553.50	563.81	571.55	574.15		
V2	621.54	675.21	717.43	726.91	738.62		
V4	305.59	312.72	513.55	515.17	518.03		
V5	515.03	535.45	549.31	568.17	571.25		
V-THETA 1	187.61	208.50	232.70	23.3.48	24.7.56		
V-THETA 2	365.49	417.18	461.48	501.60	536.46		
V(PK) 1	904.0	637.7	769.7	712.3	671.6		
V(PK) 2	708.2	700.0	656.3	620.6	597.8		
V-THETA PK1	749.7	362.4	573.3	451.9	427.4		
V-THETA PK2	570.0	460.2	359.2	25.0.6	16.9.3		
J 1	937.50	870.93	805.96	740.35	675.00		
J 2	935.51	878.07	620.23	763.19	705.75		
STATION 1							
H 1	0.5059	0.5195	0.5268	0.5379	0.5400		
H 2	0.5772	0.6246	0.6625	0.7014	0.7282		
H(PK) 1	0.8480	0.7863	0.7232	0.6698	0.6317		
H(PK) 2	0.7021	0.6493	0.6060	0.5751	0.5537		
STATION 2 - STATION 3							
LSS COEF.	0.1375	0.0938	0.0791	0.0696	0.0559		
LSS COEF.	0.1375	0.0938	0.0791	0.0696	0.0559		
DIA 3	25.672	23.034	0.614	0.2209	0.2368	0.2217	0.2129
BETA 2	46.034	41.610	43.198	0.7682	0.8581	0.8977	0.9246
BETA 3	-14.005	-7.620	-6.300	0.7623	0.8542	0.8947	0.9233
V 3	631.54	717.43	756.51	0.0325	0.0232	0.0190	0.0135
V 4	42.023	346.13	436.45	1PC.U	-3.61	-5.56	-6.13
V 2	215.02	235.45	247.31	564.07	571.25		-5.67
V 3	407.72	47.30	213.16	522.87	433.35		
V-THETA 2	36.045	41.786	46.048	50.640	53.640		
V-THETA 3	-101.73	-10.185	-71.510	-57.91	-51.91		
M 2	0.5712	0.5446	0.4622	0.7114	0.7282		
M 3	0.3767	0.4422	0.4436	0.4710	0.4710		
TURN	49.370	46.940	41.872	45.210	50.0.28		
LOSS COEF.	0.1516	0.0533	0.0516	0.0507	0.0534		
DFAC	0.6517	0.5235	0.5250	0.6697	0.6697		
LOSS PARA.	0.6591	0.6085	0.6123	0.6670	0.6670		
INCID	-16.72	-14.617	-14.677	-12.19	-12.75		
DEV	4.951	3.020	5.811	10.280	10.970		
CORRECTED WEIGHT FLUX							
UPSTREAM OF STATOR							
87.81							
F							

Blade element performance—triple-slotted stator stage with the vane bleed flow at the optimum rate.

Table IV1.

DESIGN ELEMENT PERFORMANCE (REALING = 217 LINEAR STATIC PRESSURE)		PERCENT DESIGN SPEED = 89.65	
CORRECTED MACH FLOW = 0.717		CORRECTED ALTER SP.EU = 7517.81	
PRESSURE RATIO = 1.2782		ALIAS STATIC EFFICIENCY = 36.2702	
STATION 1 — STATION 2		RUTER 1	
		10	50
		70	70
Beta 1	23.150	21.020	25.040
Beta 2	29.038	23.302	23.020
Beta 3	15.816	21.632	23.730
Beta 4	15.816	21.632	23.730
Beta 5	44.963	46.300	25.356
Beta 6	51.262	52.019	24.034
Beta 7	42.763	35.985	49.710
Beta 8	50.542	51.234	23.381
V 1	0.7326	0.7326	51.948
V 2	0.7623	0.7623	70.244
V 3	0.7623	0.7623	73.076
V 4	46.617	46.617	67.725
V-Theta 1	171.447	137.332	473.84
V-Theta 2	461.02	492.51	23.77
V(Pr)	901.09	833.03	525.00
V(Pr)	0.665	0.625	525.00
V(Theta) Pr1	716.68	586.82	604.40
V(Theta) Pr2	474.07	395.07	205.76
J 1	913.27	371.04	23.77
J 2	913.27	371.04	74.62
N 1	0.4707	0.4733	760.06
P	0.5905	0.6177	51.202
STATION 2 — STATION 3		RUTER 2	
J 0	30	90	90
Beta 1	27.642	22.674	20.572
Beta 2	44.000	40.647	39.007
Beta 3	-11.623	-10.604	0.5072
Beta 4	0.3322	0.2905	1.243
Beta 5	35.652	35.000	24.25
V 1	46.037	46.726	46.037
V 2	35.701	37.475	35.701
V-Theta 1	46.302	46.000	37.55
M 2	6.394	6.394	6.394
N 3	0.3396	0.3377	0.3396
TURB	6.6119	5.942	2.31
LSS COEF.	0.1059	0.1059	0.1059
DEFL	0.1059	0.1059	0.1059
LSS PARA.	0.0252	0.0194	0.0091
INCAC	-1.041	-5.24	0.0222
Dev	1.0735	10.646	8.850

CORRECTED WEIGHT FLOW

Table IVm.

Blade element performance—triple-slotted stator stage with the vane bleed flow at the optimum rate.

BLADE ELEMENT PERFORMANCE (RELATING TO 100%)		LINEAR STATIC PRESSURES					
PERCENT DESIGN SPEED = 59.03							
CORRECTED WEIGHT FLOW = 81.38							
CORRECTED RELATIVE SPEED = 75.60.12							
PRESSURE RATIO = 1.3.10							
ADJUSTABLE EFFICIENCY = 86.752							
RUNNER 1		STATION 1 - STATION 2					
		10	30	50	70	90	
VIA 1		29.150	27.353	25.030	23.020	20.346	
VIA 2		29.048	27.302	25.546	23.750	21.944	
DETA 1		20.538	22.402	23.755	25.710	26.174	
VZ 1		49.235	52.195	54.657	58.815	57.233	
DETA 2		60.754	57.335	54.796	50.505	47.312	
DETA 3		49.420	39.226	31.862	21.452	11.711	
V 1		40.237	41.746	47.222	47.977	47.324	
V 2		67.784	67.915	63.706	72.6794	73.320	
VZ 1		43.653	43.619	43.513	43.148	42.262	
VZ 2		41.693	41.632	40.521	40.844	40.037	
V-THEIA 1		162.37	176.15	190.63	207.94	203.43	
V-THEIA 2		500.48	515.63	269.58	60.134	62.153	
V(PR) 1		48.64	51.202	751.3	68.43	63.92	
V(PR) 2		60.83	53.74	47.77	43.83	40.86	
VTHEIA PR1		713.5	691.2	613.9	531.1	470.4	
VTHEIA PR2		433.4	339.9	250.6	160.5	82.9	
U 1		935.85	369.39	304.56	73.9.05	67.3.31	
U 2		933.86	876.52	819.18	761.84	704.50	
STATION 1		M 1	0.4311	0.4550	0.4416	0.4472	0.4455
		M 2	0.5930	0.6159	0.6363	0.6541	0.6750
STATION 2 - STATION 3		M(PR) 1	0.5264	0.7604	0.7011	0.6388	0.5967
		M(PR) 2	0.5484	0.4873	0.4320	0.4009	0.3742
AC 20		TURB(PR)	15.335	13.757	22.9.24	29.457	35.671
		LOSS CUF.	0.0644	0.0211	0.0346	0.0384	0.0716
VIA 3		27.054	27.466	22.634	20.460	20.5137	
DETA 2		49.232	52.195	57.233	61.702	60.9513	
DETA 3		-1.0.2.65	-0.4.53	-0.1.84	-10.1.62	0.9704	
V 2		63.784	67.915	73.9.20	80.609	84.5433	
V 3		-0.7.69	-1.0.61	-1.7.4.27	-28.9.32	1.012	
VZ 2		46.635	21.6.26	40.0.07	0.329	1.10	
VZ 3		347.98	375.87	322.49	269.47	284.23	
V-THEIA 2		21.6.10	21.6.10	20.9.28	60.34	62.1.58	
V-THEIA 3		-1.1.5.11	-1.6.2.0	-1.5.3.3	-59.74	-54.03	
M 2		0.330	0.6125	0.6143	0.6641	0.6769	
M 3		0.225	0.3347	0.3343	0.3356	0.3356	
TURB		6.5.2.9	3.6.5.4	3.6.5.37	6.5.5.5	JPSTKLR LF STATOR	81.58
LOSS CUF.		0.162	0.1644	0.0118	0.0660	0.1412	
DFAC		0.6136	0.6136	0.6137	0.6867	0.6867	
LOSS PARAB.		0.6.2.0	0.6.1.0	0.6.1.0	1.22	0.0183	
INCLD		-0.0.25	11.358	11.358	1.96	1.28	
DEV		-0.0.25	11.358	11.358	0.456	7.036	
CORRECTED WEIGHT FLOW							
16.18							

Blade element performance—triple-slotted stator stage with the vane bleed flow at the optimum rate.

Table IVn.

BLADE ELEMENT PERFORMANCE (RELATIVE LINEAR STATIC PRESSURES)	
PISTON DESIGN SPEED = 320,000	CORRECTED RELATIVE FLOW = 79.43
CORRECTED RELATIVE SPEED = 1514.08	
PRESSURE RATIO = 1.02267	
ADIABATIC EFFICIENCY = 0.74053	
ROTOR 1	
STATION 1 - STATION 2	
	10 30 50 70 90
JIA 1	29.150
JIA 2	29.030
DETA 1	29.000
DETA 2	21.793
DETA (PS) 1	6.4099
DETA (PS) 2	4.5103
V 1	4.4352
V 2	2.0278
V 3	4.1212
V 4	410.52
V-THERM 1	1.2632
V-THERM 2	2.1132
V-PSI 1	0.8400
V-PSI 2	2.5622
VH-1A PSI 1	180.4
VH-1A PSI 2	412.9
U 1	9.2048
U 2	5.3449
U 3	0.4126
STATION 2 - STATION 3	
	10 30 50 70 90
DETA 1	-2.6154
DETA 2	-2.6153
DETA 3	-2.6152
DETA 4	-2.6151
DETA 5	-6.4078
DETA 6	20.6282
DETA 7	410.652
DETA 8	31.0330
DETA 9	3.0687
DETA 10	31.0330
DETA 11	2.1132
DETA 12	2.1132
DETA 13	2.1132
DETA 14	2.1132
DETA 15	2.1132
DETA 16	2.1132
DETA 17	2.1132
DETA 18	2.1132
DETA 19	2.1132
DETA 20	2.1132
DETA 21	2.1132
DETA 22	2.1132
DETA 23	2.1132
DETA 24	2.1132
DETA 25	2.1132
DETA 26	2.1132
DETA 27	2.1132
DETA 28	2.1132
DETA 29	2.1132
DETA 30	2.1132
DETA 31	2.1132
DETA 32	2.1132
DETA 33	2.1132
DETA 34	2.1132
DETA 35	2.1132
DETA 36	2.1132
DETA 37	2.1132
DETA 38	2.1132
DETA 39	2.1132
DETA 40	2.1132
DETA 41	2.1132
DETA 42	2.1132
DETA 43	2.1132
DETA 44	2.1132
DETA 45	2.1132
DETA 46	2.1132
DETA 47	2.1132
DETA 48	2.1132
DETA 49	2.1132
DETA 50	2.1132
DETA 51	2.1132
DETA 52	2.1132
DETA 53	2.1132
DETA 54	2.1132
DETA 55	2.1132
DETA 56	2.1132
DETA 57	2.1132
DETA 58	2.1132
DETA 59	2.1132
DETA 60	2.1132
DETA 61	2.1132
DETA 62	2.1132
DETA 63	2.1132
DETA 64	2.1132
DETA 65	2.1132
DETA 66	2.1132
DETA 67	2.1132
DETA 68	2.1132
DETA 69	2.1132
DETA 70	2.1132
DETA 71	2.1132
DETA 72	2.1132
DETA 73	2.1132
DETA 74	2.1132
DETA 75	2.1132
DETA 76	2.1132
DETA 77	2.1132
DETA 78	2.1132
DETA 79	2.1132
DETA 80	2.1132
DETA 81	2.1132
DETA 82	2.1132
DETA 83	2.1132
DETA 84	2.1132
DETA 85	2.1132
DETA 86	2.1132
DETA 87	2.1132
DETA 88	2.1132
DETA 89	2.1132
DETA 90	2.1132
DETA 91	2.1132
DETA 92	2.1132
DETA 93	2.1132
DETA 94	2.1132
DETA 95	2.1132
DETA 96	2.1132
DETA 97	2.1132
DETA 98	2.1132
DETA 99	2.1132
DETA 100	2.1132
COPRECITED MASTERTABLE	
	10 30 50 70 90
USS 1	0.5621
USS 2	0.5621
USS 3	0.5621
USS 4	0.5621
USS 5	0.5621
USS 6	0.5621
USS 7	0.5621
USS 8	0.5621
USS 9	0.5621
USS 10	0.5621
USS 11	0.5621
USS 12	0.5621
USS 13	0.5621
USS 14	0.5621
USS 15	0.5621
USS 16	0.5621
USS 17	0.5621
USS 18	0.5621
USS 19	0.5621
USS 20	0.5621
USS 21	0.5621
USS 22	0.5621
USS 23	0.5621
USS 24	0.5621
USS 25	0.5621
USS 26	0.5621
USS 27	0.5621
USS 28	0.5621
USS 29	0.5621
USS 30	0.5621
USS 31	0.5621
USS 32	0.5621
USS 33	0.5621
USS 34	0.5621
USS 35	0.5621
USS 36	0.5621
USS 37	0.5621
USS 38	0.5621
USS 39	0.5621
USS 40	0.5621
USS 41	0.5621
USS 42	0.5621
USS 43	0.5621
USS 44	0.5621
USS 45	0.5621
USS 46	0.5621
USS 47	0.5621
USS 48	0.5621
USS 49	0.5621
USS 50	0.5621
USS 51	0.5621
USS 52	0.5621
USS 53	0.5621
USS 54	0.5621
USS 55	0.5621
USS 56	0.5621
USS 57	0.5621
USS 58	0.5621
USS 59	0.5621
USS 60	0.5621
USS 61	0.5621
USS 62	0.5621
USS 63	0.5621
USS 64	0.5621
USS 65	0.5621
USS 66	0.5621
USS 67	0.5621
USS 68	0.5621
USS 69	0.5621
USS 70	0.5621
USS 71	0.5621
USS 72	0.5621
USS 73	0.5621
USS 74	0.5621
USS 75	0.5621
USS 76	0.5621
USS 77	0.5621
USS 78	0.5621
USS 79	0.5621
USS 80	0.5621
USS 81	0.5621
USS 82	0.5621
USS 83	0.5621
USS 84	0.5621
USS 85	0.5621
USS 86	0.5621
USS 87	0.5621
USS 88	0.5621
USS 89	0.5621
USS 90	0.5621
USS 91	0.5621
USS 92	0.5621
USS 93	0.5621
USS 94	0.5621
USS 95	0.5621
USS 96	0.5621
USS 97	0.5621
USS 98	0.5621
USS 99	0.5621
USS 100	0.5621
COPRECITED MASTERTABLE	
	10 30 50 70 90
USS 1	0.5621
USS 2	0.5621
USS 3	0.5621
USS 4	0.5621
USS 5	0.5621
USS 6	0.5621
USS 7	0.5621
USS 8	0.5621
USS 9	0.5621
USS 10	0.5621
USS 11	0.5621
USS 12	0.5621
USS 13	0.5621
USS 14	0.5621
USS 15	0.5621
USS 16	0.5621
USS 17	0.5621
USS 18	0.5621
USS 19	0.5621
USS 20	0.5621
USS 21	0.5621
USS 22	0.5621
USS 23	0.5621
USS 24	0.5621
USS 25	0.5621
USS 26	0.5621
USS 27	0.5621
USS 28	0.5621
USS 29	0.5621
USS 30	0.5621
USS 31	0.5621
USS 32	0.5621
USS 33	0.5621
USS 34	0.5621
USS 35	0.5621
USS 36	0.5621
USS 37	0.5621
USS 38	0.5621
USS 39	0.5621
USS 40	0.5621
USS 41	0.5621
USS 42	0.5621
USS 43	0.5621
USS 44	0.5621
USS 45	0.5621
USS 46	0.5621
USS 47	0.5621
USS 48	0.5621
USS 49	0.5621
USS 50	0.5621
USS 51	0.5621
USS 52	0.5621
USS 53	0.5621
USS 54	0.5621
USS 55	0.5621
USS 56	0.5621
USS 57	0.5621
USS 58	0.5621
USS 59	0.5621
USS 60	0.5621
USS 61	0.5621
USS 62	0.5621
USS 63	0.5621
USS 64	0.5621
USS 65	0.5621
USS 66	0.5621
USS 67	0.5621
USS 68	0.5621
USS 69	0.5621
USS 70	0.5621
USS 71	0.5621
USS 72	0.5621
USS 73	0.5621
USS 74	0.5621
USS 75	0.5621
USS 76	0.5621
USS 77	0.5621
USS 78	0.5621
USS 79	0.5621
USS 80	0.5621
USS 81	0.5621
USS 82	0.5621
USS 83	0.5621
USS 84	0.5621
USS 85	0.5621
USS 86	0.5621
USS 87	0.5621
USS 88	0.5621
USS 89	0.5621
USS 90	0.5621
USS 91	0.5621
USS 92	0.5621
USS 93	0.5621
USS 94	0.5621
USS 95	0.5621
USS 96	0.5621
USS 97	0.5621
USS 98	0.5621
USS 99	0.5621
USS 100	0.5621

Blade element performance—triple-slotted stator stage with the vane bleed at the optimum rate.

Table IVo.

BLADE ELEMENT PERFORMANCE (READING)		PERCENT DESIGN SPEED = 39.08		LINEAR STATIC PRESSURES	
CORRECTED WEIGHT FLUX = 75.90		CORRECTED ROTOR SPEED = 7520.13		PRESSURE RATIO = 1.3449	
ADIABATIC EFFICIENCY = 84.6334					
STATION 1 - STATION 2		ROTOR 1		ROTOR 2	
		10	30	50	70
DIA 1	29.150	27.080	25.050	23.020	20.983
DIA 2	29.098	27.302	25.516	21.944	
DIA 1	21.367	22.570	24.637	25.933	24.891
DIA 2	53.049	57.233	59.246	51.359	63.077
ULTRAPR 1	62.992	69.303	57.431	53.758	50.225
ULTRAPR 2	43.305	49.950	32.737	22.212	28.547
V 1	426.25	425.30	438.53	455.35	443.39
V 2	682.74	675.70	691.34	709.21	736.51
V 3	396.16	401.96	396.61	400.51	402.65
V 4	412.22	355.74	352.46	335.94	324.29
V-THETA 1	155.17	157.07	182.81	154.76	186.35
V-THETA 2	549.00	508.24	594.75	622.45	656.24
V-PK1	378.1	311.4	740.5	677.5	633.3
V-PK2	200.5	479.9	419.1	368.2	338.0
VINELA PK1	782.4	704.8	654.0	488.9	
VINELA PK2	388.5	210.0	226.9	144.6	50.2
J 1	933.62	371.67	80.64	741.16	675.13
J 2	933.52	879.02	321.52	734.02	706.51
STATION 1		STATION 2		STATION 3	
M 1	0.3973	0.4000	0.4071	0.4137	0.4123
M 2	0.6131	0.6072	0.6076	0.6076	0.6076
M(PK) 1	0.8140	0.7551	0.6874	0.6265	0.5885
M(PK) 2	0.8065	0.6412	0.3281	0.3316	0.3074
N 1	1.0637	1.0947	24.64	31.147	41.971
N 2	1.0637	1.0947	24.64	31.147	41.971
N 3	1.0637	1.0947	24.64	31.147	41.971
N 4	1.0637	1.0947	24.64	31.147	41.971
N 5	1.0637	1.0947	24.64	31.147	41.971
N 6	1.0637	1.0947	24.64	31.147	41.971
N 7	1.0637	1.0947	24.64	31.147	41.971
N 8	1.0637	1.0947	24.64	31.147	41.971
N 9	1.0637	1.0947	24.64	31.147	41.971
N 10	1.0637	1.0947	24.64	31.147	41.971
CORRECTED WEIGHT FLUX		UPSTREAM OF ROTOR		UPSTREAM OF STATOR	
LSS GUEF	0.1631	0.1631	0.1631	0.1631	0.1631
DEAL	0.6659	0.6723	0.6723	0.6723	0.6723
LSS PAKA	0.1007	0.1013	0.1013	0.1013	0.1013
INCIE	0.6512	0.6512	0.6512	0.6512	0.6512
DEV	-7.531	7.516	24.550	30.524	-0.153

Table IVp.

Blade element performance—triple-slotted stator stage with the vane bleed flow at the optimum rate.

	BLADE ELEMENT PERFORMANCE	HEADING	297	LINEAR STATIC PRESSURES ¹
	PERCENT DESIGN SPEED	=	95.81	
CORRECTED WEIGHT FLOW =	96.55			
CORRECTED ROTOR SPEED =	3351.43			
PRESSURE RATIO =	1.2164			
ADIABATIC EFFICIENCY =	56.3649			
ROTOR 1				
			10	30
			50	70
			90	
DIA 1	29.150	27.080	25.060	23.020
DIA 2	29.088	27.302	25.916	23.730
BETA 1	21.689	23.123	24.934	25.616
BETA 2	38.483	+0.955	43.729	45.138
BETA(P) ₁	56.748	53.366	49.450	45.501
BETA(P) ₂	50.800	+1.452	32.325	41.032
V 1	590.00	600.99	611.76	619.48
V 2	604.91	746.57	803.44	623.63
VZ 1	548.23	552.71	554.74	851.25
VZ 2	520.48	533.83	580.58	595.16
V-THETA 1	218.05	236.01	257.90	275.78
V-THETA 2	413.76	489.35	555.38	598.04
V(PR) 1	999.8	926.3	853.3	785.9
V(PR) 2	823.5	752.3	687.1	649.5
V(THETA PR1)	936.1	743.3	556.7	582.33
V(THETA PR2)	638.2	498.0	367.4	596.64
U 1	1054.18	979.32	905.27	275.90
U 2	1051.94	949.35	922.76	607.16
M 1	0.5486	0.5594	0.5701	745.5
M 2	0.5991	0.6774	0.7221	625.1
STATOR 1				
DIA 1	0.9296	0.8822	0.7952	186.4
M(PR) 2	0.7420	0.6826	0.6260	0.7720
TURN(P) ₁	5.948	11.914	17.124	0.5725
LOSS COEF.	0.1835	0.1362	0.1368	23.681
DFAC	0.2462	0.2753	0.2958	0.1603
EFF P	0.6835	0.8061	0.8479	0.1556
EFF	0.6755	0.8000	0.8425	0.2807
LOSS PARA.	0.0409	0.0337	0.0359	0.2673
INC10	-2.95	-3.53	-4.25	0.8550
DEV	5.700	2.652	1.525	-3.97
CORRECTED WEIGHT FLOW				
V-THETA 2	-59.49	-55.38	598.04	501.16
V-THETA 3	-56.46	-67.40	-73.20	-117.22
H 2	0.5951	0.6714	0.7320	0.7757
H 3	0.2551	0.4419	0.5333	0.5327
TURN	51.987	47.750	50.180	52.158
LOSS COEF.	0.1751	0.1551	0.0477	0.2137
DFAC	0.6092	0.6073	0.5259	0.6815
LUSI PARA.	0.6884	0.6918	0.0167	0.0290
INC10	-12.50	-11.14	-8.97	0.0627
DEV	5.156	11.210	11.299	-10.45
				3.959

Table IVq.

Blade element performance—triple-slotted stator stage with the vane bleed flow at the optimum rate.

BLADE ELEMENT PERFORMANCE (READING 296)		LINEAR STATIC PRESSURES					
		10	30	50	70	90	
PERCENT DESIGN SPEED	= 99.81						
CORRECTED WEIGHT FLOW	= 94.13						
CORRECTED ROTOR SPEED =	8350.77						
PRESSURE RATIO	= 1.3562						
ADIABATIC EFFICIENCY	= 95.9856						
ROTOR 1							
		STATION 1 - STATION 2					
DIA 1	29.150	27.080	25.060	23.020	20.984		
DIA 2	29.088	27.302	25.516	23.730	21.944		
BETA 1	20.774	22.606	20.873	26.056	26.119		
BETA 2	46.902	48.940	50.652	52.270	54.154		
BETA(PR) 1	57.775	54.814	51.030	45.452	42.926		
BETA(PR) 2	45.493	39.961	32.440	23.370	14.530		
V 1	573.68	378.34	567.80	595.78	595.28		
V 2	738.23	757.11	784.65	813.37	82.8.31		
V L 1	535.39	533.90	535.28	535.25	534.49		
V 2	504.33	497.30	497.48	497.73	483.01		
V-THETA 1	203.48	222.31	247.23	261.70	26.06		
V-THETA 2	539.11	570.86	606.78	643.30	668.59		
V(PR) 1	1005.9	926.5	867.49	782.6	729.9		
V(PR) 2	719.4	648.8	589.5	542.2	499.0		
V THETA PR1	851.0	757.2	659.3	571.0	497.1		
V THETA PR2	513.1	416.7	316.2	215.1	125.2		
U 1	1054.44	979.56	906.49	835.70	759.19		
U 2	1052.13	922.98	858.38	793.77			
M 1	0.5324	0.5369	0.5462	0.5541	0.5536		
M 2	0.6569	0.6781	0.7064	0.7359	0.7482		
M(PR) 1	0.9334	0.8002	0.7880	0.7279	0.6788		
M(PR) 2	0.6402	0.5811	0.5307	0.4906	0.4526		
TURN(PK) J	12.282	14.353	18.590	23.482	28.396		
LOSS COEF.	0.0811	0.0453	0.0414	0.0378	0.0373		
LOSS COEF.	0.0811	0.0453	0.0414	0.0378	0.0373		
DIA 3	29.164	27.422	25.672	22.034			
BETA 2	46.940	50.552	52.270	54.154			
BETA 3	-15.010	-6.641	-7.400	-6.184			
V 2	738.23	757.11	784.65	813.37			
V 3	437.31	450.44	480.41	450.52			
V 2	504.33	457.30	497.48	497.73			
V 2	422.38	447.42	460.38	444.75			
V-THETA 2	535.11	510.88	606.78	643.30			
V-THETA 3	-113.26	-52.09	-62.39	-71.91	-103.66		
M 2	0.6509	0.6781	0.7064	0.7359	0.7482		
M 3	0.2789	0.3327	0.4240	0.3937	0.3238		
TURN	61.919	55.581	58.052	61.454	70.329		
LOSS COEF.	0.1784	0.1292	0.0533	0.0535	0.1344		
UFAC	0.7625	0.7151	0.6325	0.7337	0.8317		
LUSS PARA.	0.6923	0.6483	0.0166	0.0259	0.0390		
INCID	-5.17	-3.20	-2.05	-1.13	-1.80		
DEV	3.950	11.395	1C.350	8.496	1.625		
CORRECTED WEIGHT FLOW							
UPSTREAM OF ROTOR							
UPSTREAM OF STATOR							
DOWNSTREAM OF STATOR							
94.13							
94.13							
89.14							

Table IVr.

Blade element performance—triple-slotted stator stage with the vane bleed flow at the optimum rate.

BLADE ELEMENT PERFORMANCE (READING 298 LINEAR STATIC PRESSURES)		PERCENT DESIGN SPEED = 99.83			
CORRECTED WEIGHT FLOW =	88.55				
CORRECTED ROTOR SPEED =	8353.13				
PRESSURE RATIO =	1.4017				
ADIABATIC EFFICIENCY =	84.3338				
STATION 1 - STATION 2					
		10	30	50	70
DIA 1	29.150	27.080	25.060	23.020	20.988
DIA 2	29.088	27.302	25.516	23.730	21.944
BETA 1	20.821	22.629	23.657	25.548	24.625
BETA 2	49.880	52.507	54.882	57.082	58.074
BETA(PR) 1	60.570	57.775	54.487	50.643	47.123
BETA(PR) 2	47.723	41.601	32.953	24.162	12.532
V 1	52.446	53.021	53.849	54.423	54.441
V 2	714.71	741.03	775.70	793.08	822.59
V2.1	490.21	489.39	493.24	491.02	494.90
V2.2	460.55	451.04	446.23	430.99	435.74
V-THETA 1	186.42	204.01	216.08	234.71	226.04
V-THETA 2	546.56	587.96	630.50	665.75	697.60
V(PRI) 1	997.6	917.8	849.1	776.3	727.3
V(PRI) 2	884.6	603.2	531.8	475.4	446.0
V(THETA PR1)	868.9	776.4	691.2	598.7	533.0
V(THETA PR2)	506.5	400.5	289.3	193.3	96.8
U 1	1055.33	980.39	901.25	833.40	759.94
U 2	1053.09	988.42	923.76	859.10	794.45
M 1	0.4861	0.4897	0.4977	0.5033	0.5025
M 2	0.6288	0.6553	0.6925	0.7114	0.7398
M(PRI) 1	0.9210	0.8476	0.7848	0.7161	0.6726
M(PRI) 2	0.6023	0.5334	0.4747	0.4237	0.4012
TURN(PR)	1.2.847	1.6.173	2.1.535	2.6.481	3.4.581
LOSS COEF.					
DFAC	0.1410	0.1423	0.0588	0.0583	0.0588
EFFP	0.4418	0.4780	0.5186	0.5387	0.5430
EFF	0.8619	0.8740	0.9514	0.9569	0.9379
EFF	0.8543	0.8672	0.9488	0.9546	0.9365
LOSS PARA.	0.0336	0.0351	0.0151	0.0151	0.0239
INC ID	0.97	0.97	0.79	0.84	2.12
DEV	2.623	2.801	2.153	3.462	3.842
CORRECTED WEIGHT FLOW					
N 1					
10	30	50	70	90	
DIA 3	29.164	25.672	23.874	22.034	
BETA 2	49.880	54.882	57.082	58.074	
BETA 3	-18.632	-7.210	-10.239	-18.104	
V 2	714.71	775.70	793.08	822.59	
V 3	422.48	447.28	462.81	372.84	
VZ 2	460.55	451.04	446.23	430.99	
VZ 3	400.34	445.22	439.31	366.91	
V-THETA 2	546.56	587.96	634.50	665.75	
V-THETA 3	-134.98	-42.90	-55.58	-66.28	
N 2	0.6228	0.6553	0.6925	0.7114	
N 3	0.3623	0.3865	0.3837	0.3222	
TURN	68.512	58.011	62.092	67.321	
LOSS COEF.	0.1290	0.6726	0.0874	0.1375	
DFAC	0.7918	0.7172	0.7419	0.8317	
LOSS PARA.	0.0491	0.0272	0.0305	0.0443	
INC ID	-2.20	0.37	2.18	3.08	
DEV	0.328	12.536	1.0.540	7.441	
					0.304

Table IVs.

Blade element performance—triple-slotted stator stage with the vane bleed flow at the optimum rate.

BLADE ELEMENT PERFORMANCE (REALINE 315 LINEAR STATIC PRESSURES)	
PERCENT DESIGN SPEED = 99.74	CORRECTED WEIGHT FLOW = 6.647
CORRECTED ROTOR SPEED = 3345.31	
PRESSURE RATIO = 1.04175	
AJABATIC EFFICIENCY = 77.8701	
STATION 1 - STATION 2	
	10 30 50 70 90
BLA 1	29.150 27.083 25.050 23.020 20.983
BLA 2	29.055 27.302 25.316 23.730 21.944
BLA 1	21.368 22.812 24.630 26.119 25.092
o-T ₁	22.141 27.473 30.374 32.307 34.037
o-T ₂ (PK)	1 63.470 30.360 57.656 54.297 51.121
o-T ₁ (PK)	2 45.292 41.502 36.625 29.926 15.043
V 1	45.711 47.702 44.312 45.534 46.480
V 2	74.322 73.615 73.829 73.018 77.138
V _L 1	434.491 439.711 439.16 437.22 439.05
V _L 2	423.29 395.55 358.78 341.2 337.70
V-INETA 1	171.71 134.9 201.34 214.37 205.59
V-INETA 2	60.613 52.06 64.525 67.181 69.354
V(PK) 1	972.5 997.3 921.5 749.2 699.5
V(PK) 2	904.0 531.4 447.1 325.0 349.7
V-INETA PR1	870.1 762.3 695.3 508.4 566.5
V-INETA PR2	430.3 354.3 265.7 174.3 90.0
J 1	104.134 927.5 895.6 802.75 750.12
J 2	1034.6 975.79 911.90 848.12 784.29
STATION 1	
M 1	0.4365 0.4443 0.4500 0.4537 0.4515
M 2	0.3233 0.6170 0.6119 0.6108 0.5967
M(PK) 1	0.9062 0.6323 0.7052 0.6980 0.6516
M(PK) 2	0.5345 0.4743 0.4008 0.3466 0.3158
STATION 2 - STATION 3	
L0	30 50 70 90
L0	17.901 13.773 21.351 27.371 36.079
L1	0.1399 0.0755 0.0712 0.0748 0.0890
L1A 3	25.134 27.042 25.472 25.054 22.054
BETA 2	55.191 51.495 45.324 64.627 67.207
BETA 3	-12.363 -11.250 -12.143 -12.176 LFF
V 2	13.645 7.30.25 750.18 71.38 LSS PATA
V 3	452.42 4.6.72 351.43 300.42 261.01 INCID
V 2	42.23 352.35 239.78 242.22 357.10 UEV
V 2	42.20 33.25 33.43 293.10 251.91 LSS CUEF
V-INETA 2	60.613 64.06 64.25 67.281 693.54 CORRECTED WEIGHT FLOW
V-INETA 3	-154.43 62.63 62.64 -52.91 -53.20 -56.33 UPS STREAM OF Rotor
H 2	0.653 0.570 0.615 0.658 0.0567 UPS STREAM OF STATOR
M 3	0.3910 0.3101 0.370 0.207 0.2266 UPS STREAM OF STATOR
TURB	75.059 69.220 69.225 75.150 75.213 UPS STREAM OF STATOR
LSS COEF	0.2605 0.2625 0.2632 0.2532 f
WFL	0.8916 0.7657 0.8151 0.9114 0.9004 f
LSS PARA	0.0465 0.0474 0.0403 0.0444 0.0400 f
INCID	3.11 5.35 8.24 9.01 8.09 f
DEV	-0.903 6.757 9.6454 5.637 2.624 f

Table IVt.

Blade element performance—triple-slotted stator stage with the vane bleed flow at the optimum rate.

BLADE ELEMENT PERFORMANCE (CREATING)		PERCENT DESIGN SPEED = 96.49		LINEAR STATIC PRESSURES	
CORRECTED WEIGHT FLOW = 85.00		CORRECTED MOTOR SPEED = 3241.45			
PRESSURE RATIO = 1.4192		ADIASTATIC EFFICIENCY = 33.6063			
ROTOR 1		STATION 1 - STATION 2			
		10	30	50	70
VIA 1	24.150	27.050	25.060	23.020	20.988
VIA 2	29.026	27.302	25.510	23.730	21.944
DETA 1	21.305	22.946	24.442	26.119	25.480
DETA 2	53.226	56.014	58.994	61.355	62.826
DETA(PR) 1	61.853	58.964	56.069	52.335	49.033
DETA(PR) 2	44.651	39.304	35.525	30.858	13.249
V 1	434.80	504.02	506.89	513.12	510.33
V 2	745.64	733.02	746.17	766.11	786.54
VZ 1	460.35	464.14	461.46	460.72	460.69
VZ 2	446.98	414.59	384.37	366.31	359.21
V-THETA 1	131.39	136.09	209.73	253.89	219.54
V-THETA 2	596.06	629.09	639.55	670.59	699.72
V(PR) 1	975.9	900.2	826.7	754.0	702.7
V(PR) 2	628.3	540.4	471.1	407.1	369.0
VTHETA PR1	630.6	171.4	685.9	596.9	530.3
VTHETA PR2	441.6	346.7	272.4	177.5	84.3
U 1	104.84	967.36	895.66	827.75	750.12
U 2	1035.62	975.79	911.96	843.12	784.29
STATOR 1					
M 1	0.4611	0.4700	0.4728	0.4784	0.4762
M 2	0.3636	0.6750	0.6711	0.3305	0.7129
STATION 2 - STATION 1					
M(PR) 1	0.3093	0.8395	0.7712	0.7037	0.5557
M(PR) 2	0.5564	0.4962	0.4237	0.3678	0.3345
TURN(PR)	17.02	19.066	20.744	26.477	35.785
LSSS CULF	0.1005	0.0447	0.0479	0.0472	0.0684
UFAC	0.9117	0.9229	0.9011	0.9672	0.9574
EFFP	0.5553	0.5836	0.6181	0.6401	
DIA 3	49.164	47.444	46.674	46.034	
DETA 2	53.26	56.04	56.94	62.826	
V 2	-26.479	-6.264	-6.451	-16.656	
V 3	746.6	753.6	746.17	786.54	
VZ 2	428.24	437.67	444.22	397.22	
VZ 3	446.28	414.59	384.37	366.31	
V 1	405.65	435.05	424.53	355.21	
V-THETA 2	55.616	62.65	61.52	29.63	
V-THETA 3	-165.45	-41.92	-47.66	-62.49	
M 2	0.4636	0.6756	0.6711	0.6645	
M 3	0.3152	0.3819	0.3707	0.3627	
LURN	75.405	64.113	65.442	71.543	
LSSS COEF.	0.2672	0.1508	0.1119	0.1776	
UFAC	0.8437	0.7555	0.7523	0.6599	
LSSS PARA.	0.0219	0.0738	0.0251	0.0571	
INCIC	4.15	4.47	4.29	7.25	
DEV	-3.219	12.536	11.259	7.092	
CORRECTED WEIGHT FLOW					
UPSTREAM OF ROTOR					
UPSTREAM OF STATOR					
DOWNSTREAM OF STATOR					
DOWNSTREAM OF FLOW					
HOT RATE					

Table IVu.

Blade element performance—triple-slotted stator stage with the vane bleed flow at the optimum rate.

BLADE ELEMENT PERFORMANCE (READING 218 LINEAR STATIC PRESSURES)		STATION 1 - STATION 2				
		10	30	50	70	90
PERCENT DESIGN SPEED =	105.63					
CORRECTED WEIGHT FLOW =	100.16					
CORRECTED ROTOR SPEED =	1172.91					
PRESSURE RATIO =	1.02446					
AOLABATIC EFFICIENCY =	60.7729					
ROTOR 1						
STATION 1 - STATION 2						
DIA 1	29.150	27.040	23.060	23.020	20.983	
DIA 2	29.098	27.302	25.310	23.730	21.944	
BELA 1	20.754	22.002	24.042	25.720	24.695	
BELA 2	20.941	38.719	42.930	45.800	45.974	
BETA(PR) 1	53.550	54.159	51.533	47.053	43.396	
BETA(PR) 2	43.344	35.760	26.119	14.031		
V 1	0.0530	0.28590	0.3165	0.4301	0.63346	
V 2	7.3562	7.7543	8.5585	8.7768	9.4920	
V 2 1	5.0203	5.9120	5.1868	5.7931	5.8480	
V 2 2	59.395	0.0201	6.0540	6.1189	6.5939	
V-THETA 1	21.4643	24.1552	28.16	27.904	26.491	
V-THETA 2	44.7443	48.503	64.921	68.271		
V(PR) 1	1.0861	1.0102	0.6002	0.3003	0.04048	
V(PR) 2	91.17	64.09	74.61	68.15	68.1	
V-THETA PR1	9.2740	0.189	72.32	32.4	552.9	
V-THETA PR2	0.9110	284.1	410.0	300.0	176.6	
U 1	114.147	10.0041	981.03	901.43	821.35	
U 2	1139.04	1059.10	998.17	929.23	859.29	
STATOR 1						
M 1	0.5722	0.6065	0.6010	0.5106	0.6112	
M 2	0.6766	0.7142	0.7613	0.8134	0.8876	
M(PR) 1	1.0269	0.9586	0.3735	0.8074	0.7633	
M(PR) 2	0.8319	0.7745	0.0361	0.6316	0.6346	
TURN(PR)	9.252	10.164	15.272	20.334	28.416	
LSS. CUEF.	0.1902	0.1655	0.1788	0.1947	0.0840	
DIA 3	23.164	23.422	23.874	22.034	0.2443	0.2730
BELA 4	36.921	33.719	46.520	42.800	45.974	EFF P
BELA 3	-11.628	-7.020	-8.420	-8.023	-9.252	0.7089
V 2	74.252	66.043	67.68	64.950	65.800	0.7521
V 3	4.855	1.111	550.88	603.46	615.03	0.6990
V 2 2	59.95	6.501	605.40	611.89	655.89	0.0437
V 2 3	415.07	54.675	557.15	608.03	687.96	LOSS COEF.
V-THETA 2	44.743	46.03	563.18	629.21	682.71	DEAC
V-THETA 3	-56.58	-67.3	-87.07	-92.52	-179.76	LSS. PARA.
M 2	0.4786	0.1142	0.763	0.8134	0.8676	TURN
M 3	0.4345	0.4937	0.5408	0.5503	0.4600	LOSS COEF.
TURN	48.619	45.735	51.226	54.452	66.196	UPSTREAM OF STATOR
LOSS COEF.	0.1929	0.0989	0.0259	0.0917	0.3128	UPSTREAM OF RUTOR
DEAC	0.6371	0.5580	0.5457	0.5682	0.7267	DOWNSTREAM OF STATOR
LOSS PARA.	0.0759	0.0470	0.0131	0.0296	0.0887	ANGLE
ANGLE	-12.09	-12.42	-9.77	-8.20	-9.98	DEV
DEV	7.332	11.020	9.454	9.028	-2.423	
CORRECTED WEIGHT FLOW						
100-16						
96.45						

Table IVv.

Blade element performance—triple-slotted stator stage with the vane bleed flow at the optimum rate.

BLADE ELEMENT PERFORMANCE (READING 345)		LINEAR STATIC PRESSURES					
PERCENT DESIGN SPEED = 105.80							
CORRECTED WEIGHT $\bar{W}_{LCW} = 100.01$							
CORRECTED ROTOR SPEED = 987.15							
PRESSURE RATIO = 1.4076							
ADIABATIC EFFICIENCY = 80.1455							
ROTOR 1							
STATION 1 = STATION 2							
		10	30	50	70	90	
UIA 1	29.150	27.040	25.070	23.100	20.930		
UIA 2	29.088	27.302	25.510	23.730	21.944		
BETA 1	21.379	22.637	23.950	25.314	24.745		
OCTA 2	43.533	50.073	51.424	51.822	52.505		
BETA(PK) 1	58.229	55.025	51.308	47.102	42.196		
BETA(PK) 2	45.858	37.713	21.643	22.326	14.857		
V 1	64.182	653.42	360.27	674.40	679.04		
V 2	33.270	30.126	900.06	930.90	945.13		
V L 1	597.05	607.81	608.36	609.70	616.69		
V L 2	223.39	553.78	561.24	580.77	575.30		
V-THETA 1	233.97	256.13	270.55	283.39	284.23		
V-THETA 2	626.22	660.48	703.05	735.18	749.87		
V(PK) 1	11.351	1.351.6	974.0	397.4	845.9		
V(PK) 2	754.0	720.7	659.2	626.7	595.2		
V-THETA PK1	965.0	961.7	760.2	653.5	579.0		
V-THETA PK2	570.2	496.5	495.9	240.9	152.7		
U 1	1198.98	111.34	1030.75	946.84	463.27		
U 2	1196.42	112.47	1049.51	976.05	902.59		
STATION 1							
M 1	0.5791	0.5403	0.6027	0.6107	0.6151		
M 2	0.7161	0.7643	0.7676	0.8200	0.8321		
M (PK) 1	1.0241	0.9560	0.8810	0.8125	0.7663		
M (PK) 2	0.6229	0.5132	0.5509	0.5241			
STATION 2 = STATION 3							
		7C	90				
U 10	30	7C	90				
UIA 3	27.422	25.072	23.674	22.034			
UIA 2	30.073	31.414	31.642	22.365			
BETA 3	-17.225	-7.020	-8.250	-10.000			
V 2	51.570	46.128	51.000	51.090			
V 3	50.302	50.312	50.603	51.120			
V L 2	553.39	524.78	261.64	580.77			
V L 3	475.42	455.51	552.20	511.75			
V-THETA 2	6.552	7.020	7.135	7.187	CORRECTED WEIGHT FLOW		
V-THETA 3	-146.24	-25.64	-65.0	-74.62	-123.08		
H 2	0.7161	0.7449	0.7810	0.8212	0.8748	100.01	
H 3	0.4107	0.4208	0.4579	0.4730	0.5051	0.0203	
TURB	0.3129	0.3063	0.2953	0.2857	0.2757	100.01	
LOSS_GEF	0.1174	0.1497	0.0955	0.1201	0.1296	-1.30	
UFAL	0.7721	0.7310	0.6853	0.7307	0.8065	96.21	
LOSS_PARA	0.0586	0.0560	0.0474	0.0585	0.0776	LOSS INLET FLOW	
INCLD	-2.35	-2.07	-1.42	-2.31	-3.45		
DEV	1.732	1.1210	1.0750	0.384	1.500		

Table IV w.

Blade element performance—triple-slotted stator stage with the vane bleed flow at the optimum rate.

BLADE ELEMENT PERFORMANCE (READING 344)		LINEAR STATIC PRESSURES!		
PERCENT DESIGN SPEED = 100.00				
CORRECTED WEIGHT FLOW = 99.56				
CORRECTED MOTOR SPEED = 9194.52				
PRESSURE RATIO = 1.4513				
ADIABATIC EFFICIENCY = 82.3806				
MOTOR 1				
STATION 1 - STATION 2		10	30	50
		70	70	90
DIA 1	29.150	27.080	25.060	23.020
DIA 2	29.098	27.302	25.516	23.730
BETA 1	21.628	22.766	24.022	24.129
BETA 2	51.252	52.689	54.299	55.637
BETA(PRI) 1	58.251	54.916	51.732	47.490
BETA(PRI) 2	43.977	37.845	31.396	13.645
V 1	640.98	655.26	658.64	668.83
V 2	864.57	886.81	898.39	925.78
VZ 1	595.76	604.22	601.59	603.35
VZ 2	541.12	537.54	524.25	496.55
V-THETA 1	236.22	253.56	260.13	288.63
V-THETA 2	674.28	705.33	729.56	764.21
V(PRI) 1	1132.2	1051.3	971.3	692.9
V(PRI) 2	752.0	680.7	614.2	563.8
V(THETA) PRI	962.4	840.3	762.6	658.2
V(THETA) PZ2	522.1	417.6	320.0	211.8
U 1	1198.98	1113.84	1030.75	946.84
U 2	1196.43	1122.97	1049.51	902.59
M 1	0.5787	0.5925	0.5958	0.6057
M 2	0.7379	0.7447	0.7795	0.8085
M(PRI) 1	1.0223	0.9506	0.8787	0.7425
M(PRI) 2	0.6418	0.5870	0.5329	0.4924
TURN(PRI)	1.4-273	1.7-072	20.336	25.423
LOSS COEF.	0.13377	0.0870	0.0731	0.0685
DFAC	0.4731	0.4914	0.5075	0.5105
EFF P	0.8696	0.9206	0.9374	0.9468
EFF	0.8608	0.9155	0.9336	0.8959
LOSS PARA.	0.0349	0.0227	0.0192	0.0335
INC10	-1.35	-1.98	-1.97	-1.46
DEV	-1.122	-0.955	0.596	1.368
CORRECTED WEIGHT FLOW				
UPSTREAM OF ROTOR		99.56		
UPSTREAM OF STATOR		99.56		
DOWNSTREAM OF STATOR		94.37		
TURN	64.428	59.329	61.130	44.467
LOSS COEF.	0.2538	0.2005	0.1485	0.1420
DFAC	0.1228	0.7480	0.7185	0.7986
LOSS PARA.	0.0984	0.0750	0.0295	0.0405
INC10	-0.63	0.55	1.60	1.64
DEV	3.784	11.399	10.920	-1.361

Table IVx.

Blade element performance—triple-slotted stator stage with the vane bleed flow at the optimum rate.

BLADE ELEMENT PERFORMANCE (READING 343 LINEAR STATIC PRESSURES)		STATION 1 - STATION 2						STATION 1 - STATION 2					
		10	30	50	70	90			10	30	50	70	90
PERCENT DESIGN SPEED	= 109.79												
CORRECTED WEIGHT FLOW	= 96.76												
CORRECTED ROTOR SPEED	= 9105.74												
PRESSURE RATIO	= 1.4489												
ADIABATIC EFFICIENCY	= 81.6128												
ROTOR 1													
DIA 1	29.150	27.080	25.060	23.020	20.988								
DIA 2	29.086	27.302	25.516	23.730	21.944								
BETA 1	21.509	22.646	23.832	25.310	25.104								
BETA 2	52.511	54.123	56.880	59.522	60.918								
BETA(PR) 1	59.577	56.576	53.093	49.264	45.539								
BETA(PR) 2	45.004	40.180	34.964	27.265	16.570								
V 1	613.64	623.63	634.52	640.03	639.90								
V 2	852.00	859.12	859.25	867.68	884.84								
V2 1	570.91	575.55	580.41	578.59	579.43								
V2 2	516.53	503.48	469.50	440.09	430.08								
V-THETA 1	224.99	240.12	256.38	273.02	271.54								
V-THETA 2	676.04	696.12	719.65	747.79	773.28								
VIPRI 1	1127.4	1044.9	966.5	886.6	827.3								
V(PR) 2	733.4	659.0	572.9	495.1	448.7								
VTHETA PR1	972.2	872.1	772.8	671.8	590.4								
VTHETA PR2	518.6	425.2	328.3	226.8	128.0								
U 1	1197.20	1112.18	1029.22	945.44	861.98								
U 2	1194.65	1121.30	1047.95	974.60	901.25								
M 1	0.5528	0.5624	0.5729	0.5782	0.5780								
M 2	0.7238	0.7370	0.7411	0.7515	0.7682								
NIPRI 1	1.0157	0.9423	0.8726	0.8009	0.7473								
NIPRI 2	0.6220	0.5653	0.4941	0.4288	0.3895								
TURN(PR)	1.4.573	1.6.393	1.8.129	2.1.999	2.8.970								
LOSS COEFF.	0.1191	0.0547	0.0540	0.0714	0.1209								
DFAC	0.4914	0.5105	0.5483	0.5842	0.6032								
EFFP	0.8937	0.9528	0.9596	0.9442	0.9174								
LOSS PARA.	0.8861	0.9496	0.9528	0.9429	0.9126								
INC10	-0.029	0.0138	0.0136	0.0180	0.0302								
DEV	-0.02	-0.32	-0.61	-0.54	0.54								
STATOR 1													
STATION 2 - STATION 3													
10	30	50	70	90									
DIA 3	27.422	25.672	23.874	22.034									
BETA 2	54.123	56.880	59.322	60.918									
BETA 3	-5.693	-6.830	-11.425	-21.110									
V 2	852.00	859.12	867.68	884.84									
V 3	484.31	492.59	511.35	399.77	347.61								
V 2 2	516.53	503.48	469.50	440.09	430.08								
V 2 3	486.13	490.16	513.68	391.61	324.28								
V 2 3	676.04	696.12	719.65	747.79	773.28								
V-THETA 2	-124.08	-48.87	-61.53	-79.40	-125.19								
M 2	0.7238	0.7411	0.7515	0.7682	0.7850								
M 3	0.3986	0.4091	0.4324	0.3224	0.2887								
TURN	67.355	59.816	63.710	70.977	82.028								
LOSS COEFF.	0.2887	0.2297	0.157	0.224	0.2074								
DFAC	0.8087	0.7534	0.7176	0.8510	0.9139								
LOSS PARA.	0.1121	0.0861	0.0404	0.0649	0.0585								
INC10	C-43	1.98	4.18	5.32	4.97								
DEV	4.116	12.347	10.920	6.225	-3.310								
CORRECTED WEIGHT FLOW													
UPSTREAM OF ROTOR													96.76
UPSTREAM OF STATOR													96.76
DOWNSTREAM OF STATOR													91.39

Table Va.

Blade element performance—triple-slotted stator stage with the mean vane bleed flow rate.

BLADE ELEMENT PERFORMANCE (READINGS)		LINEAR STATIC PRESSURES)		
PERCENT DESIGN SPEED	= 59.89	10	30	50
CORRECTED WEIGHT FLOW	= 66.21	70	70	90
CORRECTED ROTOR SPEED = 5010.75				
PRESSURE RATIO = 1.05902				
ADIABATIC EFFICIENCY = 05.5103				
ROTORS 1				
STATION 1 - STATION 2				
		10	30	50
BETA 1	29.150	27.080	25.060	23.020
DIA 2	29.088	27.302	25.516	23.730
BETA 1	20.449	21.810	23.393	21.944
BETA 2	31.555	34.821	37.202	40.106
BETA(PK) 1	55.008	51.764	48.347	43.769
BETA(PK) 2	48.720	41.080	36.099	31.393
V 1	370.38	381.43	392.85	388.93
V 2	425.03	457.77	486.94	510.81
V 2 1	347.08	354.13	351.38	352.06
V 2 2	362.13	375.80	387.85	395.29
V-THETA 1	125.28	141.71	152.01	165.24
V-THETA 2	222.43	261.39	294.42	332.93
V(PK) 1	914.5	372.02	528.7	481.6
V(PK) 2	549.0	503.2	468.4	436.5
V-THETA PR1	507.0	449.4	395.0	337.3
V-THETA PR2	412.5	334.6	292.6	185.1
U 1	636.33	591.14	547.04	502.51
U 2	634.97	595.99	551.00	479.02
STATOR 1				
M 1	0.3362	0.3465	0.3478	0.3534
M 2	0.3817	0.4122	0.4590	0.4666
M(PK) 1	0.5177	0.5197	0.4431	0.4152
M(PK) 2	0.4930	0.4530	0.4223	0.3940
LSS COEF.	0.8888	10.084	14.248	13.679
TURN(PK)	0.0666	0.0666	0.0784	0.0873
DIA 3	27.442	25.672	23.574	22.024
BETA 2	34.382	37.202	40.106	41.322
BETA 3	-8.256	-8.652	-6.830	-5.504
V 2	425.03	451.07	466.54	516.81
V 3	303.06	317.43	325.84	345.93
V 2 2	362.16	375.80	387.35	395.29
V 2 3	300.06	316.9	330.04	342.48
V-THETA 2	216.43	261.39	254.02	232.93
V-THETA 3	-46.61	-46.09	-50.22	-41.14
M 2	0.3817	0.4122	0.4383	0.4666
M 3	0.2705	0.2982	0.3089	0.2961
TURN	40.386	43.117	45.655	46.536
LSS COEF.	0.0063	0.0219	0.0212	0.0112
DEFL.	0.539d	0.553d	0.563d	0.573d
LSS PARA.	0.0007	0.0014	0.0122	0.0214
INCID	-26.52	-17.32	-15.20	-13.89
DEV	10.130	9.744	9.098	10.650

Table Vb.

Blade element performance—triple-slotted stator stage with the mean vane bleed flow rate.

BLADE ELEMENT PERFORMANCE (READING)		PERCENT DESIGN SPEED = 59.92	LINEAR STATIC PRESSURES	
CORRECTED WEIGHT FLOW = 61.11				
CORRECTED ROTOR SPEED = 5013.15				
PRESSURE RATIO = 1.1151				
ADIABATIC EFFICIENCY = 90.7205				
MOTOR 1			STATION 1 - STATION 2	
			10	30
			50	70
			90	
DIA 1	29.150	27.080	25.060	23.020
DIA 2	29.088	27.302	25.516	23.730
BETA 1	20.369	21.810	23.339	25.138
BETA 2	41.537	43.205	45.140	46.422
BETA(PR) 1	57.995	55.121	51.799	47.151
BETA(PR) 2	47.151	41.771	33.570	43.464
V 1	344.26	346.96	349.86	356.83
V 2	431.85	446.12	473.16	498.66
V 1	322.73	322.13	321.11	323.10
V 2	323.25	325.16	333.76	343.74
V-THETA 1	119.83	128.71	138.88	151.61
V-THETA 2	286.36	305.42	335.39	361.25
V(PRI) 1	508.9	563.3	519.2	444.7
V(PRI) 2	475.3	436.0	400.6	277.8
V-THETA(PR) 1	516.4	462.1	408.0	350.8
V-THETA(PR) 2	348.5	290.4	221.5	156.7
U 1	636.20	591.02	546.93	502.41
U 2	634.95	595.87	556.89	517.91
M 1	0.3122	0.3147	0.3174	0.3239
M 2	0.3186	0.4002	0.4251	0.4487
M 3	0.5522	0.5109	0.4711	0.4328
M(PRI) 1	0.4255	0.3911	0.3399	0.3284
M(PRI) 2	0.3085	0.3059	0.3039	0.3026
TURN(PR)	10.844	13.350	18.229	22.853
LOSS COEF.	0.0144	0.0616	0.0626	0.0795
DFAC	0.3166	0.3266	0.3288	0.3236
LSS COEF.	0.0144	0.0616	0.0626	0.0795
EFF	0.9153	0.9264	0.9276	0.9242
EFFP	0.9896	0.9166	0.9276	0.9242
LSS PARA.	0.0178	0.0152	0.0163	0.0206
INCID	-1.61	-1.78	-1.90	-1.54
DEV	2.051	2.911	2.770	3.801
STATION 2 - STATION 3				
10	30	50	70	90
DIA 3	27.642	25.672	23.674	22.034
BETA 2	43.05	45.146	46.422	47.151
BETA 3	-8.830	-6.656	-5.266	-4.451
V 2	42.045	446.12	473.16	498.66
V 3	251.31	294.15	300.92	307.03
V 2	323.25	325.10	323.76	343.74
V 3	291.79	293.05	257.67	204.22
V-THETA 2	284.36	305.42	325.39	361.25
V-THETA 3	-45.04	-42.73	-43.40	-41.45
M 2	0.3866	0.4002	0.4251	0.4487
M 3	0.2641	0.2533	0.2676	0.2732
TURN	50.307	51.501	52.436	54.162
LOSS COEF.	0.6446	0.0112	0.0236	0.0336
DFAC	0.6203	0.6302	0.6457	0.6626
LSS PARA.	0.0177	0.0042	0.0092	0.0484
INCID	-16.54	-6.93	-7.56	-7.58
DEV	10.130	9.744	9.434	9.521
CORRECTED WEIGHT FLOW				
				56.88
				11.349

Table Vc.

Blade element performance—triple-slotted stator stage with the mean vane bleed flow rate.

BLADE ELEMENT PERFORMANCE (READING)		339	LINEAR STATIC PRESSURES			
PERCENT DESIGN SPEED =		59.92				
CORRECTED WEIGHT FLOW =		55.28				
CORRECTED ROTOR SPEED =		5013.52				
PRESSURE RATIO =		1.1364				
ADIABATIC EFFICIENCY =		83.6557				
ROTOR 1						
STATION 1 - STATION 2						
	10	30	50	70		
DIA 1	29.150	27.080	25.060	23.070		
DIA 2	29.088	27.302	25.516	23.730		
BETA 1	20.241	21.745	23.709	25.134		
BETA 2	49.898	51.790	53.495	55.688		
DETA(PR) 1	69.903	58.079	55.372	51.368		
DETA(PR) 2	45.722	39.972	32.927	23.237		
V 1	313.18	317.56	316.58	317.61		
V 2	465.44	456.96	468.44	486.38		
V 2.1	293.84	294.96	289.86	287.54		
V 2.2	286.93	282.65	278.67	282.32		
V-THETA 1	108.35	117.65	127.30	134.90		
V-THETA 2	340.71	359.05	376.53	390.79		
V(PR) 1	604.2	550.9	510.1	466.7		
V(PR) 2	411.0	368.8	332.0	307.2		
V-THETA PR1	528.0	473.5	419.7	357.6		
V-THETA PR2	294.3	236.9	180.5	121.2		
U 1	630.33	591.14	547.04	502.51		
U 2	630.97	595.99	557.00	518.01		
M 1	0.2835	0.2775	0.2866	0.2876		
M 2	0.3974	0.4336	0.4195	0.4367		
M(PR) 1	0.5470	0.5051	0.4619	0.4226		
M(PR) 2	0.3667	0.3298	0.2973	0.2755		
TURN(PR)	15.180	18.108	22.446	28.731		
LOSS COEF.	0.0136	0.0150	0.0553	0.0617		
DEAC	0.4462	0.4788	0.4930	0.4917		
EFFP	0.9131	0.9405	0.9476	0.9507		
EFF	0.9113	0.9394	0.9469	0.9497		
LSS PARA.	0.0181	0.0159	0.0142	0.0161		
INC10	1.30	1.18	1.61	2.17		
DEV	0.622	1.0172	2.127	2.557		
V2.3	237.61	237.55	230.77	230.77		
V-THETA 2	340.71	359.05	376.53	412.24		
V-THETA 3	-36.33	-38.44	-39.15	-28.42		
H 2	0.3974	0.4086	0.4145	0.4511		
N 3	0.2566	0.2588	0.2492	0.2908		
TURN	57.108	51.572	62.147	66.123		
LOSS COEF.	0.0604	0.0466	0.0402	0.0394		
DEAC	0.6852	0.6551	0.7204	0.7155		
LSS PARA.	0.0115	0.0140	0.0142	0.0168		
INC10	-2.18	-0.22	0.19	-0.65		
DEV	11.750	10.400	9.613	10.100		

55.28

55.28

55.28

55.28

55.28

55.28

55.28

55.28

55.28

55.28

55.28

55.28

55.28

55.28

55.28

55.28

55.28

55.28

55.28

55.28

55.28

55.28

55.28

55.28

55.28

55.28

55.28

55.28

55.28

55.28

55.28

55.28

55.28

55.28

55.28

55.28

55.28

55.28

55.28

55.28

55.28

55.28

55.28

55.28

55.28

55.28

55.28

55.28

55.28

55.28

55.28

55.28

55.28

55.28

55.28

55.28

55.28

55.28

55.28

55.28

55.28

55.28

55.28

55.28

55.28

55.28

55.28

55.28

55.28

55.28

55.28

55.28

55.28

55.28

55.28

55.28

55.28

55.28

55.28

55.28

55.28

55.28

55.28

55.28

55.28

55.28

55.28

55.28

55.28

55.28

55.28

55.28

55.28

55.28

55.28

55.28

55.28

55.28

55.28

55.28

55.28

55.28

55.28

55.28

55.28

55.28

55.28

55.28

55.28

55.28

55.28

55.28

55.28

55.28

55.28

55.28

55.28

55.28

55.28

55.28

55.28

55.28

55.28

55.28

55.28

55.28

55.28

55.28

55.28

55.28

55.28

55.28

55.28

55.28

55.28

55.28

55.28

55.28

55.28

55.28

55.28

55.28

55.28

55.28

55.28

55.28

55.28

55.28

55.28

55.28

55.28

55.28

55.28

55.28

55.28

55.28

55.28

55.28

55.28

55.28

55.28

55.28

55.28

55.28

55.28

55.28

55.28

55.28

55.28

55.28

55.28

55.28

55.28

55.28

55.28

55.28

55.28

55.28

55.28

55.28

55.28

55.28

55.28

55.28

55.28

55.28

55.28

55.28

55.28

55.28

55.28

55.28

55.28

55.28

55.28

55.28

55.28

55.28

55.28

55.28

55.28

55.28

55.28

55.28

55.28

55.28

55.28

55.28

55.28

55.28

55.28

55.28

55.28

55.28

55.28

55.28

55.28

55.28

55.28

55.28

55.28

55.28

55.28

55.28

55.28

55.28

55.28

55.28

55.28

55.28

Table Vd.

Blade element performance—triple-slotted stator stage with the mean vane bleed flow rate.

BLADE ELEMENT PERFORMANCE (REACTIONS 338 LINEAR STATIC PRESSURES)	
PERCENT DESIGN SPEED =	59.91
CORRECTED WEIGHT FLOW =	49.10
CORRECTED ROTOR SPEED = 5012.70	
PRESSURE RATIO = 1.1491	
AERODYNAMIC EFFICIENCY = 92.3914	
ROTOR 1	
STATION 1 - STATION 2	
	10 30 50 70 90
DIA 1	29.150
DIA 2	29.098
BETA 1	20.425
BETA 2	57.404
BETA(PR) 1	65.126
BETA(PR) 2	47.410
V 1	208.45
V 2	444.58
V 3	251.24
V 4	239.50
V-THETA 1	94.56
V-THETA 2	314.56
V(PR) 1	597.3
V(PR) 2	353.9
V(THETA) PR1	541.9
V(THETA) PR2	260.5
U 1	636.45
U 2	635.10
STATUR 1	N L
STATION 2 - STATION 3	
	10 30 50 70 90
DIA 3	29.164
BETA 2	57.457
BETA 3	-16.24
V 2	444.58
V 3	227.65
V 4	239.50
V 5	218.24
V-THETA 2	374.50
V-THETA 3	-64.75
H 2	0.3944
H 3	0.1397
TUEN	73.929
LUES COEF.	0.1977
DFAC	0.8848
LOSS PARA.	0.0761
INCID	5.32
DEV	2.436
CORRECTED WEIGHT FLOW	
H 2	0.4045
H 3	0.1885
TUEN	0.219
LUES COEF.	0.1055
DFAC	0.7575
LOSS PARA.	0.0761
INCID	5.36
DEV	2.436
	UPSTREAM OF ROTOR
	UPSTREAM OF STATOR
	DOWNSTREAM OF STATOR

Blade element performance—triple-slotted stator stage with the mean vane bleed flow rate.

Table Ve.

BLADE ELEMENT PERFORMANCE (HEADIN ₀ = 3.51 LINEAR STATIC PRESSURE)		STATION 1 - STATION 2					
		10	30	50	70	90	
DIA 1	PERCENT DESIGN SPEED = 79.88	29.150	27.080	25.060	23.020	20.988	
DIA 2	CORRECTED WEIGHT FLOW = 84.76	29.088	27.302	25.316	23.730	21.944	
BETA 1	CORRECTED ROTOR SPEED = 60.833, 9.3	20.808	21.719	23.542	25.385	26.102	
BETA 2	PRESSURE RATIO = 1.1577	33.633	30.644	38.806	41.426	42.533	
BETA(PR) 1	AUTOMATIC EFFICIENCY = 31.7874	55.825	52.304	48.453	42.879	39.222	
BETA(PR) 2		47.660	40.394	33.196	29.254	16.502	
V 1		48.502	49.433	501.57	509.20	513.54	
V -		57.505	61.056	64.433	661.40	708.21	
V ₁		451.551	459.23	459.83	460.03	461.17	
V ₂		478.76	439.49	502.12	510.92	518.92	
V-THETA 1		171.59	1d2.93	200.34	218.30	223.94	
V-THETA 2		318.50	364.11	403.78	450.85	476.06	
V(PR) 1		803.8	751.0	693.3	638.2	595.3	
V(PR) 2		704.2	644.6	600.0	560.4	541.2	
V(HETA PR1)		605.0	394.3	518.9	442.4	376.4	
V(HETA PR2)		516.3	419.5	328.5	230.2	153.7	
U 1		836.60	777.19	719.22	660.67	602.35	
U 2		834.82	783.56	732.31	681.05	629.79	
M 1		0.4486	0.4596	0.4666	0.4740	0.4792	
M 2		0.5244	0.5386	0.5915	0.6277	0.6501	
STATION 2 - STATION 3	M(PR) 1	0.7466	0.7482	0.6450	0.5941	0.5544	
	M(PR) 2	0.6421	0.5902	0.5508	0.5162	0.4996	
10	30	50	70	90	TURN(PR)	8.668	
					LSS CUF*	0.0557	0.0203
					DFAC	0.0850	0.0191
DIA 3	V-THETA 2	27.462	25.072	22.034	DFAC	0.1692	0.2187
BETA 2	BETA 3	36.644	30.604	41.426	EFFP	0.8503	0.9117
BETA 3	-6.4951	-6.261	-6.072	EFF	0.8477	0.9097	
V 2	517.05	610.06	444.33	LSS PARA	0.0204	0.0139	
V 3	351.54	442.64	455.69	INCID	-3.77	-4.60	
V2	476.79	486.45	502.12	UEV	2.060	1.794	
V2	396.02	440.57	462.57				
V-THETA 2	316.50	344.11	403.78	450.85	476.06	CORRECTED WEIGHT FLOW	
V-THETA 3	-41.660	-48.385	-50.52	-57.96			
M 2	0.5244	0.5610	0.6277	0.6501	UPSTREAM OF ROTOR	81.78	
M 3	0.570	0.4004	0.4206	0.4317	0.3774		
TURN	40.884	42.495	43.495	47.458	50.472	UPSTREAM OF STATOR	
LSS COEF*	0.1358	0.1665	0.0415	0.0440	0.1719	T	
DFAC	0.5623	0.5262	0.5276	0.5357	0.6332	DOWNSTREAM OF STATOR	
LSS PARA*	0.0542	0.0145	0.0208	0.0514		81.13	
INCID	-16.50	-15.42	-13.90	-12.57	-13.42		
DEV	12.059	11.779	11.105	11.608	9.861		

Table Vf.

Blade element performance—triple-slotted stator stage with the mean vane bleed flow rate.

BLADE ELEMENT PERFORMANCE (REACTION = .332)		LINEAR STATIC PRESSURES	
PERCENT DESIGN SPEED = 79.83			
CORRECTED WEIGHT FLOW = 78.08			
CORRECTED ROTOR SPEED = 6079.65			
PRESSURE RATIO = 1.0202			
ADIABATIC EFFICIENCY = 91.631			
ROTOR 1			
		10	30
		50	70
		90	
STATION 1 - STATION 2			
		10	30
		50	70
		90	
DIA 1	29.150	27.080	25.060
DIA 2	.9.083	.27.302	.25.516
BETA 1	20.874	22.069	23.346
BETA 2	44.223	46.339	48.347
BETA(PK) 1	59.558	55.439	52.131
BETA(PK) 2	45.889	40.103	32.034
V 1	443.12	430.10	454.63
V 2	580.02	599.40	625.02
VZ 1	414.04	417.12	416.46
VZ 2	415.66	413.82	415.40
V-THETA 1	157.69	158.12	182.34
V-THETA 2	404.53	433.53	467.01
V(PN) 1	753.7	745.2	674.4
V(PN) 2	597.2	541.0	492.2
V(THETA) PK1	577.2	506.7	535.6
V(THETA) PK2	428.3	348.5	264.0
U 1	835.07	715.77	717.91
U 2	833.30	742.13	730.97
A 1	0.4106	0.4175	0.4218
A 2	0.5252	0.5449	0.5697
M(PK) 1	0.7358	0.6829	0.6295
M(PK) 2	0.5408	0.4918	0.4486
TURB PK1	12.669	12.386	14.697
LOSS CURF.	0.0528	0.0287	0.0311
DFAC	0.3580	0.3804	0.3974
EFF-P	0.9326	0.9305	0.9664
LICS PARA.	0.0130	0.0073	0.0081
IMD	-1.04	-1.04	-1.57
DEV	0.789	1.303	1.634
CORRECTED WEIGHT FLOW			
DIA 3	29.164	27.422	25.672
BETA 2	46.223	46.329	43.347
BETA 3	-9.713	-6.630	-10.520
V 2	580.02	555.40	615.02
V 3	362.53	396.70	400.99
VZ 2	415.66	413.82	415.40
VZ 3	358.32	337.98	338.15
V-THETA 2	404.53	431.53	447.01
V-THETA 3	-61.33	-46.47	-47.69
H 2	0.5222	0.5449	0.5097
H 3	0.32219	0.2446	0.3592
TURB	53.916	53.165	53.178
LOSS COEF.	0.1010	0.0760	0.0460
DFAC	0.6538	0.6495	0.6480
LICS PARA.	0.0637	0.0284	0.0161
IMCID	-7.66	-5.80	-4.35
DEV	11.210	10.920	11.039

Table Vg.

Blade element performance—triple-slotted stator stage with the mean vane bleed flow rate.

BLADE ELEMENT PERFORMANCE (READING 335 LINEAR STATIC PRESSURES)												
PERCENT DESIGN SPEED	79.77											
CORRECTED WEIGHT FLUX	71.95											
CORRECTED Rotor Speed	5674.57											
PRESSURE RATIO	1.4570											
AERODYNAMIC EFFICIENCY	34.2553											
ROTOR 1												
STATION 1 - STATION 2												
	10	30	50	70	90							
DIA 1	29.150	27.060	25.060	23.020	20.938							
DIA 2	29.038	27.302	25.516	23.730	21.944							
BETA 1	20.426	22.305	23.847	25.509	25.302							
BETA 2	41.925	52.973	55.289	56.530	56.834							
BETA(PR) 1	61.561	53.917	55.823	56.016	56.370							
BETA(PR) 2	43.406	32.596	32.659	21.702	12.287							
V 1	401.53	+11.55	416.03	-42.72	422.36							
V 2	590.27	612.20	624.90	655.71	656.90							
V 4 1	361.14	381.61	380.57	380.42	381.84							
V 2 2	383.87	368.56	355.24	361.07	364.35							
V-THETA 1 1	142.23	124.22	168.07	182.01	160.51							
V-THETA 2	456.77	438.76	513.59	540.15	518.58							
V(PR) 1	802.0	755.2	677.4	618.1	574.8							
V(PR) 2	246.8	476.4	422.7	388.6	372.9							
THETA PR1	705.2	633.0	560.4	487.2	429.0							
THETA PR2	389.3	304.9	226.1	143.7	79.4							
U 1	847.42	787.29	728.52	689.21	610.14							
U 2	445.61	793.39	741.77	699.85	631.93							
M 1	0.3769	0.3747	0.3788	0.3842	0.3946							
M 2	0.5236	0.5449	0.5576	0.5856	0.5978							
M(PR) 1	0.7296	0.6756	0.6169	0.5631	0.5236							
M(PR) 2	0.4897	0.4259	0.3772	0.3476	0.3342							
TUR(NPR)	16.16	17.32	23.162	30.314	36.385							
LSS COEF.	0.0251	0.0474	0.0774	0.1070	0.0003							
DFAC	0.4571	0.4792	0.5266	0.5922	0.5130							
EFFP	0.9311	0.9055	0.9588	0.9483	0.9339							
EFF	0.9283	0.9046	0.9574	0.9464	0.9337							
LSS PARA.	0.0160	0.0069	0.0122	0.0187	0.0255							
INC10	1.35	2.02	2.12	2.22	3.37							
DEV	0.306	0.756	1.059	1.002	2.587							
STATION 1												
STATION 2 - STATION 3												
	10	30	50	70	90							
DIA 3	29.164	27.422	23.072	23.074	<2.034							
BETA 2	49.925	52.773	55.265	56.530	56.884							
BETA 3	-12.315	-6.830	-6.830	-7.020	-7.020							
V 2	-56.027	612.20	624.90	654.71	666.90							
V 3	341.73	365.07	330.19	291.39	INC10							
V2 2	383.87	368.66	355.64	361.07	364.35							
V2 3	322.86	366.47	357.916	327.84	259.43							
V-THETA 2	456.77	488.10	513.05	546.15	558.58							
V-THETA 3	-12.318	-4.342	-4.342	-39.27	-31.55							
M 2	0.2972	0.2740	0.5419	0.5576	0.5504							
N 3	0.0272	0.1737	0.0934	0.1129	0.1618							
TURN	0.4564	0.4537	0.4594	0.4618	0.4650							
LSS COEF.	0.0081	0.0081	0.0081	0.0081	0.0081							
DFAC	0.7833	0.7312	0.7449	0.7661	0.7156							
LSS PARA.	0.0081	0.0081	0.0081	0.0081	0.0081							
INC10	11.210	10.520	10.850	10.850	10.850							
STATION 2												
CORRECTED WEIGHT FLUX												
	10	30	50	70	90							
UPSTREAM OF ROTOR												
UPSTREAM OF STATOR												
DOWNSTREAM OF STATOR												
ROTOR 2												
CORRECTED WEIGHT FLUX												
	10	30	50	70	90							
UPSTREAM OF STATOR												
DOWNSTREAM OF STATOR												
ROTOR 3												
CORRECTED WEIGHT FLUX												
	10	30	50	70	90							
UPSTREAM OF STATOR												
DOWNSTREAM OF STATOR												

Table Vh.

Blade element performance—triple-slotted stator stage with the mean vane bleed flow rate.

BLADE ELEMENT PERFORMANCE (READING 334 LINEAR STATIC PRESSURES)		ROTOR 1					
	FRECENT DESIGN SPEED = 79.71	STATION 1 - STATION 2			STATION 1 - STATION 2		
		10	30	50	70	90	
DIA 1	29.150	27.480	25.060	23.020	20.988		
DIA 2	29.088	27.302	25.516	23.730	21.944		
BETA 1	20.148	22.664	24.029	25.629	25.490		
BETA 2	55.371	57.057	59.435	60.744	61.179		
BETA(PRI) 1	66.433	61.469	58.759	55.516	51.902		
BETA(PRI) 2	46.111	40.352	33.236	23.109	10.336		
V 1	35.99	376.85	379.42	382.02	384.32		
V 2	595.96	607.66	618.77	635.77	659.06		
VZ 1	343.59	348.76	346.54	344.44	346.91		
VZ 2	338.66	330.45	314.66	310.71	317.71		
V-THETA 1	126.06	142.78	154.50	165.24	165.39		
V-THETA 2	490.39	509.95	532.79	554.67	577.42		
V(PRI) 1	796.1	730.2	668.2	608.4	562.2		
V(PRI) 2	488.2	433.6	376.2	337.8	323.0		
V(THETA PRI) 1	718.2	641.5	571.3	501.5	442.5		
V(THETA PRI) 2	352.1	280.8	206.2	132.6	58.1		
U 1	864.24	784.28	725.78	666.70	607.95		
U 2	842.44	790.71	738.99	687.26	655.54		
M 1	0.3332	0.3433	0.3457	0.3481	0.3503		
M 2	0.5267	0.5404	0.5517	0.5682	0.5901		
STATION 2 - STATION 3		M(PRI) 1	0.7248	0.6052	0.6038	0.5544	0.5124
10	30	M(PRI) 2	0.4317	0.3856	0.3354	0.3019	0.2892
		TURN(PRI)	18.322	21.117	25.572	32.407	41.536
DIA 3	29.164	27.422	25.672	23.874	22.034		
BETA 4	55.371	57.057	60.449	61.179	62.449		
BETA 3	-60.623	-67.406	-66.451	-70.400	-71.539		
V 2	55.250	60.666	61.077	63.577	65.066		
V 3	332.27	355.67	352.44	350.63	354.34		
VZ 2	330.43	314.66	310.71	317.71	324.71		
VZ 3	311.00	345.73	350.21	304.08	251.90		
V-THETA 2	490.39	505.55	512.79	524.67	537.42	CORRECTED WEIGHT FLOW	
V-THETA 3	-14.62	-4.42	-9.60	-19.43	-35.13		
M 2	0.5267	0.5404	0.5517	0.5682	0.5901	UPSTREAM OF ROTOR	65.89
M 3	0.4317	0.3856	0.3354	0.3019	0.2892	UPSTREAM OF STATOR	65.89
TURN	73.254	64.627	62.886	60.144	58.118	DOWNSTREAM OF STATOR	
LSS COEF.	0.2133	0.342	0.1153	0.1697	0.2056		
UFAL	0.6302	0.6446	0.7357	0.7233	0.6549	DOWNSTREAM OF STATOR	61.26
LSS PARA.	0.6323	0.5202	0.5270	0.5387	0.5098		
INCIC	3.25	4.54	6.73	6.74	2.23		
DEV	-1.263	10.454	11.269	10.280	9.881		

Table Vi.

Blade element performance—triple-slotted stator stage with the mean vane bleed flow rate.

BLADE ELEMENT PERFORMANCE (REAUIN, 1947)		BLADE STATIC PRESSURES			
PRESENT DESIGN SPEED = 99.40	UNSLICED WEIGHT FLOW = 99.9	10	30		
UNSLICED WEIGHT FLOW = 99.21					
PRESSURE RATIO = 1.3240					
AUTOMATIC EFFICIENCY = 93.295					
ROTOR 1					
STATION 1 - STATION 2		STATION 1 - STATION 2			
10	30	50	70		
V ₁	29.150	27.080	25.060	23.020	20.980
J _{1A} 1	29.933	27.302	25.516	23.730	21.944
J _{1A} 2	29.933	27.302	25.516	23.730	21.944
V _{1A} 1	21.034	21.513	24.151	25.637	25.373
V _{1A} 2	30.000	37.048	41.506	44.414	44.310
S _{1A} (P.) 1	30.310	31.510	49.850	45.781	41.503
S _{1A} (P.) 2	30.310	32.841	42.841	32.841	16.133
V ₂	26.550	29.543	60.359	60.359	61.027
V ₂	66.124	78.644	79.645	83.809	87.076
V _L 1	54.539	50.018	55.103	54.868	55.009
V _L 2	29.493	27.411	59.424	56.965	62.503
V-THETA 1	21.660	22.871	26.708	26.132	26.284
V-THETA 2	31.660	44.835	53.330	53.330	60.825
V(PR) 1	93.04	42.56	85.47	13.58	740.5
V(PR) 2	87.07	163.2	707.3	657.1	678.0
V(HTA) PR1	3.35	74.43	653.4	253.9	491.3
V(HTA) PR2	2.55	23.67	38.20	25.61	130.3
U 1	104.744	373.06	600.47	827.17	754.16
U 2	104.524	931.03	316.86	852.63	788.51
U 3	104.524	931.03	316.86	852.63	788.51
A 1	0.5935	0.6637	0.7321	0.7715	0.8032
A 2	0.5935	0.6637	0.7321	0.7715	0.8032
R(PN) 1	0.7341	0.8664	0.9012	0.9779	0.9949
R(PN) 2	0.7535	0.7155	0.7035	0.6331	0.5938
U(DNTR)	0.7155	0.7155	0.7155	0.7155	0.7155
LSS CTR	0.1394	0.1636	0.1189	0.1323	0.0635
STATION 1					
STATION 2 - STATION 3					
10	20	30	40	90	
DIA 3	2.20.154	2.20.742	2.20.174	2.20.34	2.20.942
BETA 2	3.6.00.3	4.6.50.3	4.4.0.1.9	4.4.0.3.1.0	4.4.0.4.4
BETA 3	-2.0.45.1	-2.0.30.3	-2.0.71.3	-1.6.3.2.0	1.6.3.2.1
V 2	0.21.65	1.70.4.1.2	1.70.6.7.4	1.70.6.7.4	1.70.6.7.4
V 3	-2.1.3.3	5.25.0.5.6	5.14.5.1.0	5.17.7.2.9	5.23.3.3.2
V _L 2	2.4.6.3.3	5.19.4.1.1	5.34.2.2.4	5.6.6.6.5	6.2.3.0.6
V _L 3	2.16.3.0	5.16.5.0.1	5.16.5.0.1	5.09.12	5.06.95
V-THETA 2	2.5.2.3.3	4.4.0.0.5	3.9.0.0	2.0.0.2.3	0.08.0.0
V-THETA 3	-2.5.2.3.3	-2.0.0.2.1	-2.2.0.0	-2.7.4.1	-4.4.0.7.2
M 2	0.5.5.5	1.6.6.6.7	0.7.7.2.1	0.7.7.1.5	0.3.3.5.2
M 3	0.4.4.3.3	0.4.7.0.8	0.5.5.7	0.5.5.7	0.4.5.5.3
TURB	4.4.0.7.7	4.4.0.4.5	4.7.1.3.4	5.4.1.2.7	5.0.6.5.9
LSS CTR	0.18.0	0.18.0	0.18.4.1	0.18.5.9	0.18.5.9
UFAL	0.2.2.2.2	0.2.2.7.4	0.2.2.7.4	0.2.2.7.4	0.2.2.7.4
LSS PARA	0.2.2.2.2	0.2.2.7.4	0.2.2.7.4	0.2.2.7.4	0.2.2.7.4
INCIE	-1.6.0.3	-1.6.1.5	-1.6.7.5	-9.9.29	-11.64
DEV	10.465	11.585	11.887	7.567	1.450
CORRECTED WEIGHT FLOW					
UPSTREAM OF ROTOR					
JPS STREAM OF STATOR					
UNSLICED WEIGHT FLOW					

Table Vj.

Blade element performance—triple-slotted stator stage with the mean vane bleed flow rate.

Table V_k.

Blade element performance—triple-slotted stator stage with the mean vane bleed flow rate.

DESIGN ELEMENT PERFORMANCE (READING = 240 LINEAR STATIC PRESSURE'S)		STATION 1 - STATION 2					
		10	30	50	70	90	
PERCENT DESIGN SPEED =	99.59						
CORRECTED WEIGHT FLOW =	88.34						
CORRECTED ROTOR SPEED =	3357.68						
PRESSURE RATIO =	1.4951						
ADIABATIC EFFICIENCY =	.940457						
POINT 1							
U _{1A} 1	27.150	27.080	25.350	23.020	20.988		
U _{1A} 2	27.088	27.302	25.216	23.730	21.944		
U _{1A} 1	21.259	22.323	24.034	25.250	25.430		
U _{1A} 2	21.523	54.658	56.014	58.643	59.696		
DETA(P ₁) 1	60.649	57.827	54.556	51.006	47.078		
DETA(P ₁) 2	44.491	39.748	33.577	24.351	12.540		
V ₁ 1	51.878	52.620	53.250	53.516	23.8.81		
V ₁ 2	75.020	75.6.9	76.3.6	78.3.14	80.8.71		
V ₂ 1	49.358	48.6.74	48.6.47	48.4.93	48.6.61		
V ₂ 2	42.6.78	43.7.6	42.0.12	40.7.52	40.6.38		
V-THERM 1	188.14	196.51	217.55	223.71	231.37		
V-THERM 2	287.30	0.17.47	63.7.48	66.8.76	69.8.22		
V(PK) 1	986.6	914.1	828.9	770.7	714.5		
V(PK) 2	634.3	569.5	504.8	447.3	418.1		
VINT(TA) PR1	839.9	773.7	683.5	595.0	523.2		
VINT(TA) PK2	458.9	376.2	279.9	184.4	90.8		
U 1	1046.07	973.55	901.02	827.67	756.61		
U 2	1049.34	931.63	917.42	855.20	788.99		
U 3	1048.25	948.19	949.02	0.4993	0.5019		
A 2	0.086	0.0775	0.0662	0.7076	0.7337		
A (PK) 2	0.0714	0.0516	0.0711	0.6857			
TURK(PK)	1.0.1.3	0.5814	0.5097	0.4537	0.4041	0.3790	
LSS CUF	1.0.1.3	1.0.0.79	20.884	26.655	34.538		
U _{1A} 3	27.049	27.0572	27.0724	27.0826	27.0826	0.5726	
DETA 2	54.622	55.234	55.656	56.155	56.666	0.9530	0.9720
DETA 3	44.612	45.311	46.356	47.350	48.351	0.9504	0.9705
V 2	73.624	73.340	73.14	68.73	63.54	0.0144	0.0157
V 3	54.604	49.617	47.656	37.6.52	31.7.55	1.0.15	0.0.15
V ₂ 2	44.670	45.606	46.614	40.7.52	40.0.08	0.6V	0.66
V ₂ 3	45.622	45.667	45.677	37.2.19	31.4.70	0.948	2.677
V-THERM 2	61.167	61.167	61.167	57.76	59.0.12		
V-THERM 3	-5.2.44	-5.2.44	-5.2.44	-5.2.44	-5.2.44		
U 2	0.0.0.0	0.0.0.0	0.0.0.0	0.0.0.0	0.0.0.0		
U 3	0.3.1.9	0.3.3.2	0.3.3.2	0.2.2.9	0.2.1.6		
TURK	0.0.0.0	0.0.0.0	0.0.0.0	0.0.0.0	0.0.0.0		
LSS CUF	0.0.0.0	0.0.0.0	0.0.0.0	0.0.0.0	0.0.0.0		
UFL	0.0.0.0	0.0.0.0	0.0.0.0	0.0.0.0	0.0.0.0		
LSS PAKA	0.0.0.0	0.0.0.0	0.0.0.0	0.0.0.0	0.0.0.0		
INCID	-0.0.0.0	-0.0.0.0	-0.0.0.0	-0.0.0.0	-0.0.0.0		
WAV	0.0.0.0	0.0.0.0	0.0.0.0	0.0.0.0	0.0.0.0		
CONNECTED WEIGHT FLOW							
UPSTREAM OF RULER							
JOURNAL STREAM CF STATOR							
d = 74							

Blade element performance—triple-slotted stator stage with the mean vane bleed flow rate.

Table VI.

BLADE ELEMENT PERFORMANCE (RADIAL)		LINEAR STATIC PRESSURES		
		10	30	50
PERCENT DESIGN SPAN =	95.75			
CORRECTED WEIGHT FLOW =	83.05			
CORRECTED WEAVER SPELLO = 6.466.25				
PRESSURE RATIO = 1.04130				
AERODYNAMIC EFFICIENCY = 100.5593				
ROTOR 1		STATION 1 - STATION 2		
		10	30	50
VIA 1	25.130	27.080	25.060	23.020
VIA 2	29.058	27.302	25.516	23.730
BETA 1	20.969	22.393	24.064	25.438
BETA 2	54.925	50.791	60.043	61.794
BETA(PK) 1	63.238	60.440	57.665	54.054
BETA(PK) 2	46.159	41.875	37.379	27.398
V 1	47.539	484.08	487.31	493.18
V 2	737.34	739.46	735.27	737.56
VZ 1	442.10	447.57	444.85	444.63
VZ 2	423.79	404.99	367.09	359.20
V-THETA 1	159.25	164.41	198.94	216.56
V-THETA 2	60.515	61.669	63.07	65.70
V(PK) 1	963.3	907.4	834.2	757.4
V(PK) 2	912.0	543.3	642.0	601.6
V-THETA PK1	678.3	189.4	702.2	613.2
V-THETA PK2	442.1	263.1	260.5	163.6
U 1	1048.20	973.77	901.13	827.77
U 2	1045.97	931.75	917.53	855.30
STATOR 1		STATION 2 - STATION 3		
M 1	0.4378	0.4481	0.4512	0.4559
M 2	0.4590	0.4570	0.4539	0.4593
M(PK) 1	0.9039	0.8400	0.7396	0.7017
M(PK) 2	0.5397	0.4832	0.4121	0.3615
LSS CIEF.	0.1185	0.0585	0.0557	0.0550
LSS CIEF.	0.1185	0.0585	0.0557	0.0550
DIA 3	25.109	27.462	23.874	22.034
BETA 2	24.273	25.751	26.794	26.487
BETA 3	-10.054	-5.421	-5.007	-17.150
V 2	737.54	739.49	735.67	777.56
V 3	49.654	49.74	31.35	311.55
VZ 2	42.519	40.455	35.05	326.11
VZ 3	49.529	49.866	368.76	297.07
V-THETA 2	60.613	61.057	61.707	685.62
M 2	-6.647	-2.105	-2.024	-51.25
H 3	9.0205	9.6570	9.5523	9.7511
TIN	94.337	93.523	93.387	93.235
LSS CIEF.	0.4210	0.4242	0.4254	0.4255
LSS CIEF.	0.4210	0.4242	0.4254	0.4255
LSS PAR.	0.0735	0.0754	0.0764	0.0774
INCID	4.053	7.075	7.715	5.564
DEV	11.583	11.743	10.630	-5.272

Table VIa.

Blade element performance—triple-slotted stator stage with zero vane bleed flow rate.

BLADE ELEMENT PERFORMANCE (INCHES)		LINEAR STATIC PRESSURES)	
		10	30
PERCENT DESIGN SPEED =	99.76		
CORRECTED WEIGHT FLUX =	96.63		
CORRECTED WOTLK SPEC = 0.94667			
PRESSURE RATIO =	1.12248		
ADIABATIC EFFICIENCY = 102.418			
ROTOR 1			
STATION 1 - STATION 2			
		50	70
		90	
DIA 1	29.150	27.060	25.060
DIA 2	29.063	25.516	23.730
BELA 1	20.943	26.209	24.214
BELA 2	35.643	29.942	42.765
DETA (P ₁) 1	26.904	49.001	44.333
DETA (P ₁) 2	30.610	44.249	32.555
V 1	57.051	39.135	59.955
V 2	52.096	75.034	79.321
V 2.1	54.123	24.634	54.717
V 2.2	52.873	25.655	532.51
V-THEIA 1	60.114	226.030	246.007
V-THEIA 2	39.329	474.07	236.038
V(PK) 1	49.02	41.03	347.7
V(PK) 2	83.04	75.51	69.09
VTH-TA PK1	832.3	739.3	647.5
VTH-TA PK2	64.09	493.0	371.5
U 1	1039.12	565.081	830.58
U 2	1037.21	973.53	309.86
H 1	0.3640	0.5375	0.5055
H 2	0.0004	0.6755	0.5205
H(PK) 1	0.5372	0.3006	0.7323
H(PK) 2	0.7591	0.6440	0.6378
TURN(P ₁)	6.0336	1.0108	1.0120
LESS GWF.	0.1333	0.1088	0.1088
DIA 3	25.164	27.46	25.672
BELA 4	36.043	39.942	44.153
DETA 2	-8.339	-10.633	-12.524
V 2	65.653	123.314	73.21
V 3	51.575	51.624	55.716
V 2	56.873	206.03	505.05
V 2.3	51.354	115.07	294.00
V-THEIA 2	33.248	41.407	53.638
V-THEIA 3	-75.73	-55.36	-7.16
H 2	0.4608	0.6755	0.723
H 3	0.4608	0.2221	0.591
TURN	42.412	42.844	43.156
LESS COEF.	0.6523	0.6762	0.1071
DFAC	0.6950	0.6855	0.5134
LSS. FARA.	0.6210	0.6285	0.0747
INCIC	-1.644	-1.620	-5.95
DEV	10.130	12.157	1.1295
CORRECTED WEIGHT FLOW			
N 2	0.6075	0.723	0.7380
N 3	0.4608	0.2221	0.591
TURN	42.412	42.844	43.156
LESS COEF.	0.6523	0.6762	0.1071
DFAC	0.6950	0.6855	0.5133
LSS. FARA.	0.6210	0.6285	0.0747
INCIC	-1.644	-1.620	-5.95
DEV	10.130	12.157	1.1295
UNSTEADY FLOW STATUS			
			92.51

Table VIb.

Blade element performance—triple-slotted stator stage with zero vane bleed flow rate.

DIAM. ELEMENT PERFORMANCE (RATINGS)		32.5° LINEAR STATIC PRESSURES		
PERCENT DESIGN SPEED = 99.74				
CORRECTED MACH FLOW = 92.05				
CORRECTED ROTOR SP. FLU. = 0.45034				
PRESSURE RATIO = 1.03652				
ADIABATIC EFFICIENCY = 0.93052				
ROTOR 1				
STATION 1 - STATION 2				
		10	30	
		50	70	
		90		
VIA 1	29.150	27.030	25.060	23.020
VIA 2	29.006	27.362	25.516	23.730
VIA 4	29.745	22.306	21.544	21.944
BETA 2	47.0444	49.352	51.761	52.407
BETA(PK) 1	58.925	50.777	52.048	54.391
BETA(PK) 2	45.999	40.073	33.110	44.584
V 1	54.238	55.223	56.263	56.645
V 2	718.55	735.02	761.77	798.72
V 3	507.67	511.18	515.31	508.17
V 2	493.96	478.51	472.12	466.45
V-THETA 1	192.32	299.72	228.83	246.67
V-THETA 2	529.30	587.65	597.63	626.24
V(PK) 1	963.5	908.9	631.9	649.3
V(PK) 2	994.6	531.3	563.6	493.2
VIA 1, PK1	8.624	751.5	630.7	507.3
VIA 2, PK2	503.42	411.4	301.9	214.1
V 1	1034.71	501.24	886.53	817.12
V 2	1032.51	939.12	905.72	842.32
STATION 1	0.5120	0.5216	0.5229	0.5340
STATION 2 - STATION 3	0.6504	0.6699	0.6772	0.7186
VIA 1, PK1	0.9276	0.6560	0.7919	0.7220
VIA 2, PK2	0.0332	0.5754	0.5159	0.4713
TURB(PK) 1	12.925	15.104	18.938	23.661
LSS. LSF. 1	0.0138	0.0138	0.0138	0.0138
DFAC	0.4103	0.4239	0.4505	0.4605
EFF 0	0.9438	0.9805	0.9785	0.9705
EFF 1	0.9407	0.9558	0.9714	0.9691
LSS. PARA. 1	0.0127	0.0035	0.0051	0.0095
INCLD 1	-0.66	-1.12	-1.65	-1.51
DFAC	0.6248	0.6267	0.899	2.310
LSS. PARA. 0	0.0542	0.0494	0.0323	0.0190
INCLD	-0.654	-0.715	-0.559	-1.36
DEV	12.888	11.968	12.246	0.225
CULRECTED WEIGHT FLOW				
H 2	0.6204	0.6059	0.6172	0.7186
H 3	0.4453	0.4281	0.4173	0.3917
TURB	2.0510	5.5444	2.7605	4.4833
LSS. CUEF.	0.1303	0.1647	0.1368	0.1120
DFAC	0.6248	0.6267	0.6262	0.6263
LSS. PARA.	0.0542	0.0494	0.0494	0.0323
INCLD	-0.654	-0.715	-0.559	-1.36
DEV	12.888	11.968	12.246	0.225

Table VIc.

Blade element performance—triple-slotted stator stage with zero vane bleed flow rate.

BLADE ELEMENT PERFORMANCE (READING 25)		LINEAR STATIC PRESSURES		
PERCENT DESIGN SPEED =	.99.07			
CORRECTED WEIGHT FLOW =	46.35			
CORRECTED REFLICK SPEED = 8,339.11				
PRESSURE RATIO = 1.4011				
AERODYNAMIC EFFICIENCY = .94.2347				
RUTUR 1				
STATION 1 - STATION 2				
	10	30	50	
	10	30	50	
U ₁	27.150	27.080	25.030	22.020
U _{1A} 1	25.083	27.302	25.216	23.730
U _{1A} 2	20.866	22.577	23.302	25.947
U _{1A} 3	51.072	23.376	25.282	58.028
U _{1A(PK)} 1	60.529	27.764	54.581	50.456
U _{1A(PK)} 2	42.462	40.353	34.826	25.052
V ₁	517.315	523.213	529.30	535.74
V ₁ _z	733.330	744.777	747.98	747.53
V ₂ _z	493.97	433.13	483.50	481.74
V ₂ _z	460.76	441.47	426.00	424.77
V-THE _{1A} 1	186.50	206.38	214.46	234.41
V-THE _{1A} 2	570.46	600.05	614.82	648.86
V _{PR} 1	9.83-7	905.8	835.0	759.9
V _{PR} 2	636.9	270.0	519.0	468.9
V _{THE_{1A}} PR1	836.4	760.1	680.4	567.6
V _{THE_{1A}} PR2	468.3	376.9	296.6	198.5
U ₁	1040.95	937.613	994.89	822.05
U ₁ _z	1038.73	974.36	911.18	847.40
M ₁	0.4335	0.4891	0.4950	0.5014
M ₂	0.6532	0.6697	0.6754	0.7031
M _{PK} 1	0.9191	0.8446	0.7609	0.7111
M _{PK} 2	0.2870	0.5206	0.4086	0.4251
TURN(PK)	1.5467	1.7446	1.9755	1.7467
STATION 1				
STATION 2 - STATION 3				
	10	30	50	70
	10	30	50	90
LOS ₂ CULF.	0.0333	0.0380	0.0277	0.0617
DFAC	0.4713	0.5034	0.5196	0.5284
EFF P	0.9296	0.9556	0.9602	0.9551
EFF	0.9254	0.9536	0.9280	0.9527
LUS ₂ PARA.	0.0181	0.0197	0.0120	0.0159
INC ID	0.033	0.035	0.088	0.086
UEV	0.363	1.553	4.026	4.352
VL ₃	5146.46	492.94	433.96	412.64
V-THE _{1A} 2	570.46	406.05	649.86	677.03
V-THE _{1A} 3	570.46	-50.79	-56.70	-160.24
M ₂	0.6532	0.6697	0.6754	0.7031
M ₃	0.4331	0.4111	0.3771	0.3671
TURN	57.523	55.59	62.492	72.750
LOSS COEF.	0.1718	0.1525	0.1886	0.1400
DFAC	0.6377	0.6639	0.5914	0.7731
LOSS PARA.	0.0042	0.0573	0.0414	0.0694
INC ID	-1.01	1.54	2.58	2.08
DEV	12.509	12.157	10.540	1.680
COPRECTED WEIGHT FLOW				
UPSTREAM OF RUTUR				88.33
UPSTREAM OF STATOR				68.33
UPSTREAM OF STATOR				84.34

Table VI d.

Blade element performance—triple-slotted stator stage with zero vane bleed flow rate.

ELEMENT ELEMENT PERFORMANCE (KTRACIN, 2.24 LINEAR STATIC PRESSURE)		ROTOR 1					
		10	30	50	70	40	STATION 1 - STATION 2
PERCENT DESIGN SPEED =	92.73	29.150	27.080	25.000	23.020	20.993	
CORRECTED WEIGHT FLUX =	32.59	29.083	27.302	25.216	23.730	21.944	
CORRECTED ROTOR SPEED =	3344.37	29.143	26.613	23.754	21.910	24.971	
PRESSURE RATIO =	1.04375	2.3866	2.20467	2.067	1.9261	2.0825	
ADIABATIC EFFICIENCY = 30.450		6.3457	6.1273	5.8105	5.6519	51.435	
STATION 1 - STATION 2		V 1	46.022	41.365	36.997	27.045	16.446
V 2		731.34	724.33	729.83	734.22	480.17	
V2 1		437.06	434.30	430.70	436.77	432.28	
V2 2		421.26	416.31	385.45	401.67		
V-THETA 1		105.28	177.32	192.18	211.21	202.71	
V-THETA 2		590.66	604.98	619.75	661.33	661.89	
V(PR) 1		477.4	900.3	826.5	749.0	638.2	
V(PR) 2		620.1	556.2	482.0	407.2	418.9	
VTHETA PR1		874.2	766.6	701.7	609.9	546.0	
VTHETA PR2		446.9	366.9	290.4	185.1	118.9	
U 1		1039.80	905.96	893.91	821.14	748.03	
U 2		1037.59	973.88	910.18	846.47	748.76	
STATION 1		M 1	0.4356	0.4372	0.4450	0.4511	0.4430
M 2		0.6489	0.6559	0.6550	0.6807	0.7024	
STATION 2 - STATION 3		M(PR) 1	0.9109	0.8392	0.7709	0.6690	0.5514
M(PR) 2		0.5911	0.4976	0.4338	0.3675	0.3792	
TURB(PR)		17.414	19.613	21.108	27.473	34.949	
LOSS COEF.		0.1105	0.0439	0.0498	0.0674	0.0998	
DIA 3		29.164	27.422	25.372	24.874	22.034	
BETA 2		55.466	55.467	58.120	61.261	58.825	
V2 3		-114.93	-12.666	-16.524	-20.755	-22.714	
V 2		731.34	734.38	729.83	734.23	735.54	
V 3		545.88	521.07	439.94	390.37	355.60	
V2 2		431.26	416.21	385.65	362.65	401.67	
V2 3		536.21	505.00	421.77	365.04	320.02	
V-THETA 2		59c.66	604.98	619.75	601.33	639.09	
V-THETA 3		-167.00	-114.30	-125.13	-118.34	-137.31	
H 2		0.6569	0.6569	0.6566	0.6607	0.6724	
H 3		0.4758	0.4564	0.3847	0.3407	0.3100	
TURN		05.148	68.123	14.665	E2.616	31.539	
LOSS COEF.		0.1811	0.1444	0.1894	0.2236	0.190	
DFAC		0.4353	0.6567	0.7501	0.8291	0.8537	
LOSS PARA.		0.0713	0.0538	0.0639	0.0684	0.0610	
INCID		1.79	3.33	5.42	7.26	2.87	
DEV		7.677	5.364	1.226	-3.075	-4.914	
CORRECTED WEIGHT FLOW							
82.39							
82.39							
78.26							



DISTRIBUTION LIST

1. NASA-Lewis Research Center
21000 Brookpark Road
Cleveland, Ohio 44135
Attention:

Report Control Office	MS 5-5	1
Technical Utilization Office	MS 3-19	1
Library	MS 60-3	2
Fluid System Components Division	MS 5-3	1
Pump and Compressor Branch	MS 5-9	6
A. Ginsburg	MS 5-3	1
M. J. Hartmann	MS 5-9	1
W. A. Benser	MS 5-9	1
D. M. Sandercock	MS 5-9	1
L. J. Herrig	MS 7-1	1
T. F. Gelder	MS 5-9	1
C. L. Ball	MS 5-9	1
L. Reid	MS 5-9	1
J. H. DeFord	MS 77-3	2
S. Lieblein	MS 54-6	1
C. L. Meyer	MS 60-4	1
J. H. Povolny	MS 60-4	1
A. W. Goldstein	MS 7-1	1
J. J. Kramer	MS 7-1	1
W. L. Beede	MS 5-3	1
C. H. Voit	MS 5-3	1
J. H. Childs	MS 60-4	1
B. Lubarsky	MS 3-5	1
E. Bailey	MS 5-9	1
2. NASA Scientific and Technical Information Facility
P.O. Box 33
College Park, Maryland 20740
Attention: NASA Representative 6
3. FAA Headquarters
800 Independence Ave., S.W.
Washington, D.C. 20553
Attention: Brig. General J. C. Maxwell 1
F. B. Howard 1
4. NASA Headquarters
Washington, D.C. 20546
Attention: N. F. Rekos (RAP) 1

5. U.S. Army Aviation Materiel Laboratory
Fort Eustis, Virginia
Attention: John White 1
6. Headquarters
Wright-Patterson AFB, Ohio 45433
Attention: J. L. Wilkins, SESOS 1
S. Kobelak, APTP 1
R. P. Carmichael, SESSP 1
7. Department of Navy
Bureau of Weapons
Washington, D. C. 20525
Attention: Robert Brown, RAPP14 1
8. Department of Navy
Bureau of Ships
Washington, D. C. 20360
Attention: G. L. Graves 1
9. NASA-Langley Research Center
Technical Library
Hampton, Virginia 23365
Attention: Mark R. Nichols 1
John V. Becker 1
10. Boeing Company
Commercial Airplane Division
P. O. Box 3991
Seattle, Washington 98124
Attention: C. J. Schott MS80-66 1
11. Douglas Aircraft Company
3855 Lakewood Boulevard
Long Beach, California 90801
Attention: J. E. Merriman 1
Technical Information Center C1-250
12. Pratt & Whitney Aircraft
Florida Research & Development Center
P. O. Box 2691
West Palm Beach, Florida 33402
Attention: R. A. Schmidtke 1
H. D. Stetson 1
J. M. Silk 1
B. A. Jones 1

- | | | |
|-----|--|-------------|
| 13. | Pratt & Whitney Aircraft
400 Main Street
East Hartford, Connecticut
Attention: J. A. Fligg
A. W. Stubner
M. J. Keenan | 1
1
1 |
| 14. | Allison Division, GMC
Department 8894, Plant 8
P.O. Box 894
Indianapolis, Indiana 46206
Attention: J. N. Barney
Library | 1
1 |
| 15. | Northern Research and Engineering
219 Vassar Street
Cambridge 39, Massachusetts
Attention: R. A. Novak | 1 |
| 16. | General Electric Company
Flight Propulsion Division
Cincinnati 15, Ohio
Attention: L. H. Smith H-50
Technical Information Center N-32 | 1
1 |
| 17. | General Electric Company
1000 Western Avenue
West Lynn, Massachusetts
Attention: L. H. King - Bldg. 2-40
Dr. C. W. Smith
Library, Bldg. 2-40M | 1
1 |
| 18. | Curtiss-Wright Corporation
Wright Aeronautical
Woodridge, New Jersey
Attention: S. Lombardo | 1 |
| 19. | AiResearch Manufacturing Company
402 South 36th Street
Phoenix, Arizona 85034
Attention: Robert O. Bullock | 1 |
| 20. | AiResearch Manufacturing Company
8951 Sepulveda Boulevard
Los Angeles, California 90009
Attention: Linwood C. Wright | 1 |

21. Union Carbide Corporation
Nuclear Division
Oak Ridge Gaseous Diffusion Plant
P.O. Box "P"
Oak Ridge, Tennessee 37830
Attention: R. G. Jordan 1
22. Avco Corporation
Lycoming Division
550 South Main Street
Stratford, Connecticut
Attention: Clause W. Bolton 1
23. Continental Aviation & Engineering Corp.
12700 Kercheval
Detroit, Michigan 48215
Attention: Eli H. Benstein 1
24. Solar Division, International Harvester Co.
2200 Pacific Highway
San Diego, California 92112
Attention: P. A. Pitt 1
25. Goodyear Atomic Corporation
Box 628
Piketon, Ohio
Attention: C. O. Langebrake 1
26. Iowa State University of Science and Technology
Ames, Iowa 50010
Attention: Professor George K. Serovy
Dept. of Mechanical Engineering 1
27. Hamilton Standard Division of United Aircraft
Corporation
Windsor Locks, Connecticut
Attention: Mr. Carl Rohrbach
Head of Aerodynamics and Hydrodynamics 1
28. Westinghouse Electric Corporation
Small Steam and Gas Turbine Engineering B-4
Lester Branch
P.O. Box 9175
Philadelphia, Pennsylvania 19113
Attention: Mr. S. M. DeCorso 1

29. J. Richard Joy
Supervisor, Analytical Section
Williams Research Corporation
P.O. Box 95
Walled Lake, Michigan 1
30. Raymond S. Poppe
Building 541, Dept. 80-91
Lockheed Missile and Space Company
P.O. Box 879
Mountain View, California 94040 1
31. James D. Raisbeck
The Boeing Company
224 N. Wilkinson
Dayton, Ohio 45402 1
32. James Furlong
Chrysler Corporation
Research Office
Dept. 9000
P.O. Box 1118
Detroit, Michigan 48231 1
33. Elliott Company
Jeannette, Pennsylvania 15644
Attention: J. Rodger Schields
Director-Engineering 1
34. California Institute of Technology
Pasadena, California 91109
Attention: Professor Duncan Ronnie 1
35. Massachusetts Institute of Technology
Cambridge, Massachusetts 02139
Attention: Professor Jack Kerrebrock 1
36. General Electric Company
Flight Propulsion Division
Cincinnati, Ohio 45215
Attention: Mr. Marlen Miller, H-50 1
37. Union Carbide Corporation
Nuclear Division
Oak Ridge, Tennessee 37830
Post Office Box P
Attention: Donald W. Burton, K-1001, K-25 1

